HYDROGEN BONDING

IN

SEGMENTED

BLOCK COPOLYMERS

PROEFSCHRIFT

ter verkrijging van
de graad van doctor aan de Universiteit Twente,
op gezag van de rector magnificus,
prof. dr. W.H.M. Zijm,
volgens besluit van het College van Promoties
in het openbaar te verdedigen
op donderdag 16 februari om 15.00 uur

door

Gerard Jan Eduard Biemond

geboren op 30 juli 1976
te Zevenaar

Dit proefschrift is goedgekeurd door:

Promotor: prof. dr. J.Feijen

Assistant promotor: dr. R.J. Gaymans

Cover: Morphology of a polymer, as described in this thesis, measured by Atomic Force Microscopy. The front of this thesis is a phase image and the back of the thesis is the height image of a PTMO-T6A6T polymer surface. The actual size of the cover image is 1 μm^2 (=$1x10^{-12}$ m^2).

Cover design by: Ype van der Zypp & Edwin Biemond

Voorwoord

"Don't cry because it's over. Smile because it happened"

Met veel plezier kijk ik terug op mijn promotie tijd. Het waren 4 mooie jaren, waarin ik een hoop heb geleerd. Dit proefschrift was niet tot stand gekomen zonder de hulp van een aantal mensen.

Als eerste wil ik mijn assistent-promotor Reinoud Gaymans bedanken. Jij hebt mij de mogelijkheid gegeven om te promoveren. De samenwerking heb ik als prettig ervaren, ik kon je altijd iets vragen en meestal kreeg ik een direct antwoord terug. Veel dank ben ik tevens verschuldigd aan mijn promotor Prof. Feijen. Uw inzicht, correcties en discussies heb ik zeer op prijs gesteld.

Uiteraard mag ik mijn twee afstudeerders, Gustaaf Bock en Kai Braspenning niet vergeten om te bedanken. Gustaaf, jouw werk aan de T6A6T polymeren heeft ertoe geleid dat mijn proefschrift hoofdzakelijk op T6A6T is gebaseerd. Jammer dat je niet in dit vak verder bent gegaan. Kai, jij bent een ster in het synthetiseren van polyurethanen. Jouw werk heeft veel vragen opgeroepen maar de meeste daarvan zijn uiteindelijk opgelost. Dit prachtige stuk werk is beschreven in hoofdstuk 8 en 9 en de resultaten zijn deels opgenomen in een patent.

De STEP collega's bedank ik voor hun gezelligheid en discussies. Debby, Wilco, Martijn, Josien, Gustaaf, Kai, Jan, Marloes, Mark, Arun, Debasish, Kasper en Niels. De gezellige uitjes zoals de BBQ's, thema etentjes, triatlons, oliebollen bakken en menig borrel zijn een leuke afleiding geweest van het werk. In het bijzonder bedank ik mijn collega Debby. Zeer bewonderenswaardig dat jij het 5 jaar hebt uitgehouden om met mij een kantoor te delen. Sorry voor de soms Robbie-, vrouw-, en konijn onvriendelijke opmerkingen. Ik wens je veel succes met de laatste loodjes aan jouw proefschrift. I thank my post-doc colleagues, Arun and Debasish, for the pleasant disturbance during the period of writing my thesis. Very respectable that you leave your native country to do research in the STEP group. Alle collega's van de RBT, PBM en MPT groepen bedank ik voor de gezelligheid bij de koffietafel en op het lab.

De mooie AFM plaatjes, die tevens de omslag van dit proefschrift sieren, zijn met uiterste precisie opgenomen door Hetty. Bedankt voor het opnemen van menig AFM plaatje. Jij bent de beste in vezels op het beeldscherm toveren. Wim Bras wil ik bedanken voor de mogelijkheid om geavanceerde temperatuursafhankelijke SAXS/WAXS metingen te doen bij het ESRF in Grenoble. De introductie en begeleiding van Guido Heunen heeft het mogelijk gemaakt dat wij de metingen "zelfstandig" konden uitvoeren. De metingen (dag en nacht) zijn uitgevoerd met de hulp van Debby en Wilco. Een loodzware maar unieke ervaring. Het onderzoek naar de polyurethanen (H8&H9) was niet mogelijk geweest zonder de unieke prepolymeren van Crompton Corporation. Chris Maupin bedank ik voor de medewerking en de levering van deze prepolymeren.

Speciale dank gaat uit naar Wilco, jij hebt laten zijn hoe onderzoek op het lab echt uitgevoerd moet worden. Ik heb veel geleerd van jouw adviezen en meningen die standaard beginnen met "Onzin!". Debby en Kai, het is een eer om jullie als paranimfen te hebben. Alvast bedankt voor de zware taak die jullie moeten uitvoeren op het podium.

Eén middagpauze per week werd er fanatiek gezaalvoetbald. Jaren ben ik met plezier teamcoach geweest ondanks dat ik het minste verstand van voetbal heb. De "vaste" sterspelers Ype, Kai, Niels K., Wilco, Mark, Joost (KK), Niels S., Kasper, Gerard, Luuk, Kuno en vele invallers, bedankt voor jullie inzet. 4 jaar konden jullie op mijn keeperstalent vertrouwen, er gingen namelijk altijd wel een paar ballen langs mij in het net. Ook het volleyballen, klaverjassen en tafeltennissen hebben menig middagpauze opgewaardeerd.

Dit alles was niet mogelijk geweest zonder de steun van mijn ouders. Door jullie heb ik de mogelijkheid gehad om te studeren en mij verder te ontwikkelen. De meeste steun in de periode van mijn promotie heb ik van mijn lieve Anneliese gehad. Je snapt niet waarom een meting kan mislukken maar als ik daarom chagrijnig thuis kwam dan had jij altijd bemoedigende woorden. Zonder jouw steun en liefde weet ik niet of het boekje wel was afgekomen. Sorry voor de keren dat ik "ietsje" later thuis was omdat ik nog één meting moest doen. Mochten wij paarden en koeien op ons bergpad tegenkomen dan kunnen wij die samen zeker overwinnen. Ik heb je lief.

Edwin

CONTENTS

CHAPTER 1

SEGMENTED BLOCK COPOLYMERS: GENERAL INTRODUCTION

Introduction

Thermoplastic elastomers (TPE's) are melt-processable materials that show elastomeric properties at their service temperature[1,2]. TPE's possess many rubber-like properties like softness, flexibility and elasticity but in contrast to conventional rubbers have the advantage of being melt processable. These materials can be melt processed repeatedly as the physical crosslinks are thermally reversible[1,2].

The TPE industry covers about 1% of the total polymer consumption and is a growing part of the polymer industry[3,4]. The global TPE consumption is expected to be 2.15 million metric ton in 2006 with a turnover of $10 billion[5,6]. The TPE market is forecast to grow with 7% yearly due to the replacement of conventional rubbers and to new applications[3,5,6]. The global TPE market is mainly concentrated in developed countries like US, Western Europe and Japan. However, many developing countries, particularly in Asia, are rapidly expanding their positions in TPE's[5,6].

The first work on thermoplastic elastomers was based on plasticized poly(vinyl chloride) (PVC) discovered in 1926[7], later marketed by Goodrich under the trade name Koroseal. In 1937 Prof. Dr. Otto Bayer and co-workers of German I.G. Farben Industrie applied the reaction between isocyanates and alcohols to synthesise polyurethane fibres which could compete with nylon[8]. The elastomeric properties of these polyurethane materials were recognised by Dupont and ICI and the materials were soon produced on an industrial scale (Lycra 1959). In the 1960's, other block copolymers such as PC/Polyether were found to have elastomeric properties. Anionic polymerisation introduced in the 1950's, led to the development of styrenic tri-block copolymers (SBC) that were commercialised by Shell Chemical Company (now Kraton) in 1965[1,9]. In 1970, the polyether ester elastomers (TPE-E) were developed and became commercially available in 1972 as Hytrel (Dupont) and in

1975 as Arnitel (Akzo Plastics, now DSM) and later others followed[1,6]. It was not until 1980 that thermoplastic elastomers based on polyamide (TPE-A) like Pebax (Atochem) and Vestamid-E (Creanova) were developed and produced[1,6,10].

TPE's can be divided in three main groups of which the styrenic tri-block copolymers (SBC's) is the largest group. The second largest group is elastomeric blends: thermoplastic olefins (TPO) and thermoplastic vulcanisates (TPV)[1,3,6,10]. The last group consist of segmented block copolymers (TPU, TPE-E, TPE-A) that became more and more important over the last years[3,5].

Table 1.1: Expected European TPE consumption and growth for 2005[1,3].

		Approx. consumption (10^3 ton)	Average growth (%/year)
I	SBC	226	3
II	TPO	172	8
	TPV	59	16
III	TPU	79	5
	TPE-E	30	15
	TPE-A	10	20
	Total	576	7

TPE's are used in a broad range of applications like for example cushions, mattresses, footwear, automotive and all kind of soft touch materials[1,2]. In Europe, TPE's are mostly used in the automotive industry followed by footwear and bitumen modification (Figure 1.1)[3].
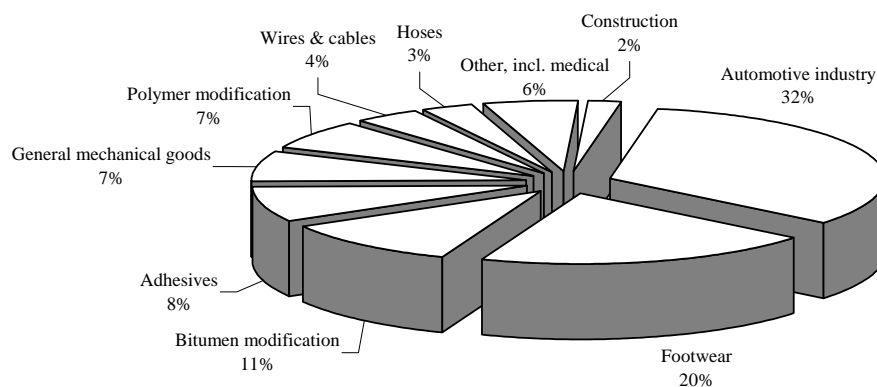

Figure 1.1: Applications of TPE's in Europe [3]

The important commercial TPE's are listed in Table 1.2 with the commercial name and company that produces the polymer.

Table 1.2: Important commercial thermoplastic elastomeric segmented block copolymers.

	Commercial name	Company
TPE-E	Arnitel, Hytrel, Riteflex, Pibiflex	DSM, Dupont, Ticona, Enichem
TPE-A	Pebax, Vestamid-E, Grilon/Grilamid	Atochem, Creanova, EMS-Chemie
TPU	Desmopan, Elastollan, Estane, Pellethane	Bayer, Elastogran, Noveon, DOW

Segmented block copolymers

Segmented block copolymers or multi-block copolymers consist of alternating crystallisable rigid segments and flexible soft segments[1,2]. The flexible segments form the continuous amorphous soft phase with a low T_g, which gives the material low temperature flexibility. The rigid segments can phase separate by crystallisation and form lamellae in the low T_g phase, acting as physical crosslinks, giving the material dimensional stability and solvent resistance.
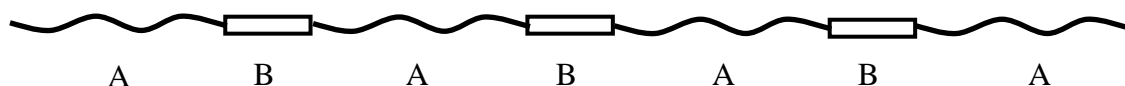

Figure 1.2: Representation of a segmented block copolymer; A, flexible segment; B, rigid segment.

The rigid segments in segmented block copolymers are normally fast crystallising segments, such as esters and amide groups. Also, urea and urethane groups are well-know for their ability to self-associate via hydrogen bonding. Thermoplastic elastomers with ester, amide and urethane groups are discussed below in more detail.

TPE-E[1,6,10]

Most polyester based multi-block copolymers are prepared by polycondensation reactions of a poly(ether) diol with a mixture of a terephthalate ester and a low molecular weight diol. The rigid segments have a random length distribution. Most commercial TPE-E's have poly(butylene terephthalate) (PBT) as the rigid segment and poly(ethylene oxide) (PEO),

poly(tetramethylene oxide) (PTMO) or poly(propyleneglycol) (PPG) as flexible segment. The properties of TPE-E can vary from soft to hard by changing the concentration of the rigid segment.

TPE-A[1,6,10]

Thermoplastic polyamide elastomers consist of alternating flexible polyether segments and rigid polyamide segments. The polyamide can be partially aromatic or aliphatic but commercial TPE-A's are derived from aliphatic polyamide. TPE-A's are characterised by their excellent toughness, flexibility at low temperature, chemical resistance and elastic recovery. The properties of the segmented block copolymers can be varied by changing the block length of the flexible and rigid segments. Commercial TPE-A's are Pebax, Vestamid and Grilon/Grilamide (Table 1.2). TPE-A's are more chemically resistant than TPE-E's[1].

Thermoplastic polyurethanes (TPU)[1,11,12]

Thermoplastic polyurethanes (TPU's) are linear copolymers that can be synthesised with a long-chain diol, diisocyanate and a chain extender. The long-chain diol can either be a polyester or a polyether. Several diisocyanates can be used but the commercially most important are diphenyl-4,4'-diisocyanate (MDI) and toluene diisocyanate (TDI). The chain extender is usually a low molecular weight component; diol or diamine. Important commercial segmented polyurethanes are Desmopan (Bayer), Elastollan (Elastogran) and Pellethane (DOW). Polyurethanes form a versatile class of polymers which are used in all kind of applications like cushions, mattresses, footwear and foams. A disadvantage of polyurethanes is their low thermal stability at temperatures above 180 °C[11,13].

Morphology

The morphology of segmented block copolymers is determined by the phase separation between flexible and rigid segments. Phase separation can occur by liquid-liquid demixing or crystallisation. TPE's that phase separate by crystallisation have a morphology that comprises a soft phase with dispersed crystalline lamellae (Figure 1.3) [1,6]. The lamellae are built up of rigid segments that crystallise perpendicular to the length of the lamellae (phase B), as proposed by Cella[14,15]. Some rigid segments that do not crystallise mix with the amorphous segments (A). This incomplete phase separation leads to an increase in glass transition temperature of the soft phase and is typically seen in TPE-E's.
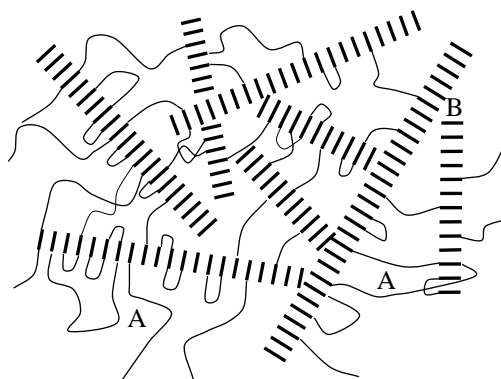
Figure 1.3: Schematic diagram of the two phase morphology of segmented copolymers with rigid segments as proposed by Cella: A) amorphous phase; B) crystalline lamellae.

Phase separation by liquid-liquid demixing is due to thermodynamic incompatibility between the segments. Especially in polyurethanes the flexible and rigid urea/urethane segments are known to phase separate by liquid-liquid demixing, followed by partially crystallisation of the rigid segments[1,11,12]. The resulting morphology is complex and consists of liquid-liquid demixed hard phase (non crystallised and partially crystalline), non crystallised rigid segments dispersed in the soft phase and crystalline rigid segments in the polyether phase.

Uniform rigid segments

An important parameter affecting the properties of segmented block copolymers is the segment length distribution of the rigid segments. Commercially available segmented block copolymers normally have a random length distribution of the rigid segment. The properties of segmented block copolymers can be improved by using uniform rigid segments. For example, polyurethanes with uniform rigid segments have a better phase separation of the rigid and flexible segments resulting in a narrow glass transition and a high degree of crystallinity compared to polyurethanes with random rigid segments[16-19]. Also, the properties of polyether(ester amide)s (PEEA) with uniform rigid amide segments were studied[20-25]. The uniform rigid amide segments crystallise nearly complete. PEEA's with uniform rigid segments have a high degree of crystallinity, low T_g, temperature independent rubbery plateau, a relatively high and sharp melting temperature and are transparent. Segmented block copolymers with uniform rigid segments have a two-phase morphology almost without any rigid segment dissolved in the soft phase. Copolymers with uniform rigid ester segments cannot be synthesised as the ester segments loose their uniformity due to transesterfication reactions that occur at high temperatures. The examples mentioned above,

show that uniform rigid segments compared to random rigid segments clearly improve the properties of segmented block copolymers.

Research aim

The aim of the research, described in this thesis, is to study the synthesis and mechanical and elastic properties of segmented block copolymers based on poly(tetramethylene oxide) (PTMO) flexible segments and uniform rigid segments. Uniform amide segments are used as rigid segments. The effect of type and concentration of amide segment on the thermal and mechanical properties of these copolymers is studied. The mechanical properties are related to the morphology of the copolymers. Other parameters studied are the influence of hydrogen bonding in the amide segments and the effect of the polydispersity of the amide segments in segmented block copolymers. The concept of using uniform amide segments is also applied to segmented polyurethanes to improve the thermal and mechanical properties.

Outline of this thesis

This thesis consists of 9 chapters concerning the research on poly(tetramethylene oxide) based segmented block copolymers with uniform rigid segments.

The synthesis and thermal properties of different uniform tetra-amide units that are used as crystallisable segments in the copolymers in this project are described in **Chapter 2**. The structure of the tetra-amide is varied from aromatic to more aliphatic. The tetra-amide units are synthesised in two steps to ensure the uniformity.

In **Chapter 3** segmented block copolymers with varying concentrations of uniform rigid segment are studied for their thermal and mechanical properties and structure-property relationship.

Chapter 4 describes the elastic properties of segmented block copolymers with uniform rigid segments as a function of temperature and time. Tensile and relaxation experiments show how the elastic behaviour depends on temperature.

The thermal and mechanical properties of segmented block copolymers based on PTMO and different tetra-amide segments is described in **Chapter 5**.

The next chapter, **Chapter 6**, describes the influence of the uniformity of the rigid segments on the polymer properties. Polymers with uniform, polydisperse and random rigid segments are studied.

In **Chapter 7**, the influence of hydrogen bonding in rigid segments is studied. The synthesis of segmented block copolymers with non hydrogen bonding rigid segments is discussed and the properties are compared with analogous segmented block copolymers which have hydrogen bonding rigid segments (from chapter 5).

In the last two chapters, polyurethanes with uniform rigid segments are investigated. The influence of different isocyanate endcappers on the properties of segmented polyurethanes is discussed in **Chapter 8**. Finally, in **Chapter 9**, the influence of different chain extenders in polyurethanes with uniform rigid segments on the polymer properties is discussed. The type and length of chain extender is varied and the properties of the resulting polyurethanes are studied.

References

1. Holden, G., Legge, N.R., Quirk, R.,.Schroeder, H.E., *'Thermoplastic elastomers'*, Hanser Publisher, Second Ed. Munich (1996).

2. Holden, G., *'Understanding thermoplastic elastomers'*, Carl Hanser, Munich (2000).

3. Dufton, P., *'Thermoplastic elastomers'*, Rapra technology LTD, Shawbury (2001).

4. *Nachrichten aus der chemie* **3**, (2003).

5. http://www.freedoniagroup.com/pdf/1553smwe.pdf

6. Fakirov, S., Yamakawa, H., *'Handbook of condensation thermoplastic elastomers'*, Wiley-VCH, New York (2005).

7. Semon, W. L.,Patent, 1933, U.S.patent 1,929,453

8. Bayer, O. to I. G. Farben,Patent, 1937, German patent 728,981

9. http://www.kraton.com/tl_warehouse/technical_literature/docs/AN%20INTRO%20TO%20KRATON.pdf

10. Bhowmick, A.K., Stephens, H.L., *'Handbook of elastomers'*, Marcel Dekker, 2nd New York (2001).

11. Szycher, M., *'Szycher's handbook of polyurethanes'*, Boca Raton: CRC Press LLC, (1999).

12. Thomson, T., *'Polyurethanes as speciality chemicals "principles and applications"'*, CRC press, Boca Raton (2005).

13. Lattimer, R.P., Williams, R.C., *J. Analyt. Appl. Pyrol.* **63**, 85-104 (2002).

14. Cella, R.J.J., *J. Polym. Sci. : Symp. no. 47* (1973).

15. Cella, R.J.J., Wiley, 2 New Yrok (1977).

16. Allegrezza, A.E., Seymour, R.W., Ng, H.N., Cooper, S.L., *Polymer* **15**, 433-440 (1974).

17. Harrel, L.L., *Macromolecules* **2**, 607-612 (1969).

18.   Heijkants, R.G.J.C., *'Polyurethane scaffolds as meniscus reconstruction materials'*, Ph.D. Thesis, University of Groningen (2004).

19.   Versteegen, R.M., *'Well-defined Thermoplastic Elastomers'*, Ph.D. Thesis, University of Eindhoven (2003).

20.   Gaymans, R.J., Dehaan, J.L., *Polymer* **34**, 4360-4364 (1993).

21.   Hutten van, P.F., Mangnus, R.M., Gaymans, R.J., *Polymer* **34**, 4193-4202 (1993).

22.   Krijgsman, J., Husken, D., Gaymans, R.J., *Polymer* **44**, 7573-7588 (2003).

23.   Niesten, M.C.E.J., *'Polyether based segmented copolymers with uniform aramid units'*, Ph.D. Thesis, University of Twente (2000).

24.   Schuur van der, J.M., *'Poly(propylene oxide) based segmented blockcopolymers'*, Ph.D. Thesis, University of Twente (2004).

25.   Lips, P.A.M., *'Aliphatic segmented poly(ester amide)s based on symmetrical bisamide-diols'*, Ph.D. Thesis, University of Twente (2005).

CHAPTER 2

SYNTHESIS AND CHARACTERISATION OF UNIFORM TETRA-AMIDE UNITS

Abstract

The synthesis and characterisation of bisester tetra-amide units with varying length and composition that can be used in the copolymerisation for segmented block copolymers were studied. The bisester tetra-amide units were prepared from aliphatic diamines with $x = (CH_2)_n$ (n = 4 - 10), dimethyl terephthalate (T) and or dimethyl adipate (A). The first step was the synthesis of the diamine-diamide xTx and xAx. The second step was the reaction of the diamine-diamide with methyl phenyl terephthalate to the TxTxT and TxAxT-dimethyl segment. The structure of the tetra-amide units was confirmed with NMR and MALDI-TOF. The melting and crystallisation behaviour was studied with DSC, FT-IR and WAXS. The melting temperature of these units increases with decreasing x and the melting temperatures of TxTxT are approximately 50 °C higher than the corresponding TxAxT units.

Introduction

Currently, there is interest in crystallisable amide segments in segmented block copolymers[1-6]. Segmented block copolymers consist of alternating crystallisable and amorphous segments. The melting temperature of the crystalline segments in these block copolymer depends on the type and size of the crystallisable segment and the type and concentration of the amorphous phase[3,7].

The properties of the copolymers also depend on the size distribution of the crystallisable segments. If the crystallisable segments have a regular structure and are uniform, then crystallisation is fast and the degree of crystallisation is high[8-11]. In polyether(ester amide) copolymers, uniform crystallisable amide segments result in fast crystallisation, a sharp melting transition, low compression set and no decrease of the modulus in the plateau region[2,4-6,12,13]. Short amide containing units are of interest to use in copolymers as these units have a good thermal stability and side reactions like transamidation reactions and exchange between ester groups hardly takes place[14].

Suitable starting compounds for preparing copolymers with uniform crystallisable amide segments are bisester-diamides, bisester tetra-amides and bisester hexa-amides[2,6,13].

In earlier research, polymers with diamide segments have been studied[1,2,4,15-20]. These diamides have relatively low melting temperatures. Higher melting temperatures can be obtained by using bisester tetra-amides, TxTxT[13,21,22]. The tetra-amides form thicker lamellae compared with diamides. Subsequently, the melting temperature of the polymers is higher and crystallites are more resistant to deformation[13]. Hexa-amide units have also been used for the preparation of segmented copolymers but problems were encountered limiting the polymerisation reaction[13].

The structure and regularity of the rigid segments are of importance for the crystallisation behaviour. For example, Van der Schuur[13] compared amide containing segments based on para and meta substituted phenylene rings in copolymers. Segments containing para substituted segments crystallise rapidly while meta substituted segments were almost unable to crystallise.

Research aim

The aim of this research is to study the synthesis and properties of crystallisable bisester tetra-amide units that can be used for the preparation of segmented block copolymers. The bisester tetra-amides units were synthesised from aliphatic diamines and esters of terephthalate and/or dimethyl adipate. The bisester tetra-amide units were analysed by NMR, MALDI-TOF, FT-IR and WAXS and the thermal properties were studied by DSC.

Experimental

Materials: 1,4-Diaminobutane, 1,6-diaminohexane, 1,8-diaminodecane, dimethyl terephthalate (DMT), N-methyl-2-pyrrolidone (NMP), phenol, dimethyl adipate and a 0.5 M sodium methoxide solution in methanol were purchased from Aldrich and used as received. Methyl-(4-chlorocarbonyl) benzoate (MCCB) was obtained from Dalian (no.2 Organic Chemical Works P.R.O.C.).

Synthesis of methyl phenyl terephthalate (MPT)[13,22]**:** To a solution of methyl-(4-chlorocarbonyl) benzoate (MCCB) (794 g, 4 mol) in toluene (600 ml) at 75 °C in a round bottomed flask with nitrogen inlet and a reflux condenser an excess of phenol (580 g, 6 mol) was slowly added. The reaction was carried out for 5 h at 75 °C and the condensation product hydrochloric acid (HCl) was passed through a sodium hydroxide solution (164 g, 4.1 mol) to neutralise the acid gas. The product was filtered hot and washed three times with water to remove the phenol (yield 80%). The product was recrystallised from methanol at 60 °C (125 g/l).The resulting product melted at 114 °C with a melting enthalpy of 135 J/g, corresponding with literature. The purity of the product estimated from the NMR spectrum was 99%.

Synthesis of TxTxT-dimethyl[22]**:** T6T6T-dimethyl, T8T8T-dimethyl, T10T10T-dimethyl were synthesised from dimethyl terephthalate (DMT), methyl phenyl terephthalate (MPT) and 1,6-hexamethylenediamine (HMDA), 1,8-octamethylenediamine (OMDA) or 1,10-decamethylenediamine (DMDA) respectively. The synthesis of T6T6T-dimethyl is given as an example.

T6T6T-dimethyl: DMT (45 gram, 0.23 mol) was added to an excess amount of 1,6-hexanediamine (250 gram, 2.15 mol) in a round bottomed flask with a nitrogen inlet, mechanical stirrer and a reflux condenser. The reaction mixture was heated to 80 °C and 6T6-diamine started to precipitate. After 2 h at 80 °C, the reaction mass was nearly solid and 500 ml toluene was added to allow stirring. After 16 h reaction at 80 °C, the reactor was cooled and the product was collected by filtration. The crude 6T6 was washed two times with hot toluene (80 °C) and two times with diethyl ether to remove the excess of 1,6-hexanediamine. The purity as determined by NMR[22] was 71% (Equation 2.2). The 6T6 was recrystallised using hot butyl acetate (25 g/l) and the purity as determined by NMR was found to be 98% (Equation 2.1) with a yield of 40%. ^{1}H-NMR (TFA-*d*): δ 7.98 (s, 4H, terephthalic H), δ 6.6-7.0 (s, 4H, NH$_2$ endgroups), δ 3.69 (t, 4H, CH$_2$ HMDA amide side), δ 3.31 (s, 4H, CH$_2$ HMDA amine side), δ 1.85 (t, 8H, 2nd and 5th CH$_2$ HMDA), δ 1.58 (s, 8H, 3rd and 4th CH$_2$ HMDA).

A mixture of recrystallised 6T6-diamine (18.1 g, 0.05 mol) and MPT (38.5 g, 0.15 mol) was dissolved in 500 ml NMP in a dry 1000 ml flask and stirred for 16 h at 120 °C. The reaction product was cooled and then collected on a no.4 glass filter and washed with NMP, toluene and acetone consecutively. The TxTxT-dimethyl units were characterised using NMR, MALDI-TOF and DSC.

Synthesis of TxAxT-dimethyl: T4A4T-dimethyl and T6A6T-dimethyl were synthesised from dimethyl adipate, MPT and 1,4-butanediamine or 1,6-hexanediamine respectively. The synthesis of T6A6T is given as an example.

T6A6T-dimethyl: 1,6-diaminohexane (500 g, 4.3 mol), was melted in a round bottomed flask and dimethyl adipate (53 g, 0.3 mol) was added. Sodium methoxide (6 ml of a 0.5 M solution in methanol) was added as a catalyst. The reaction was performed at 75 °C for 16 h. After cooling, the product was collected over a no. 4 filter and washed twice with diethyl ether. The purity determined with NMR was 85% (Equation 2.2). 6A6 was recrystallised from hot 1,4-dioxane (16 g/l) at 100 °C. After recrystallisation with a yield of 63% the purity was 98% (Equation 2.1). With DSC the T_m was determined at 183 °C with a ΔH_m of 33 J/g. ^{1}H-NMR (TFA-*d*): δ 6.80 (s, 4H, NH_2 endgroups), δ 3.56 (d, 4H, CH_2 HMDA amide side), δ 3.28 (s, 4H, CH_2 HMDA amine side), δ 2.77 (s, 4H, 1st and 4th CH_2 adipate), δ 1.90 (t, 8H, 2nd and 5th CH_2 HMDA), δ 1.74 (d, 2nd and 3rd CH_2 adipate), δ 1.54 (s, 8H, 3rd and 4th CH_2 HMDA). A mixture of 6A6-diamine (34 g, 0.1 mol) and MPT (77 g, 0.3 mol) was dissolved in 1 l NMP and heated to 120 °C. The reaction was kept at 120 °C for 16 h. After cooling, the reaction product was collected on a glass filter and washed with NMP, toluene and acetone consecutively. The TxAxT-dimethyl units were characterised using NMR, MALDI-TOF and DSC.

^{1}**H-NMR:** NMR spectra were recorded using a Bruker AC 300 spectrometer at 300 MHz. Deuterated trifluoro acid (TFA-*d*) was used as a solvent.

MALDI-TOF (matrix assisted laser desorption ionization time-of-flight): Mass spectroscopy was performed using a voyager-DE-RP MALDI-TOF mass spectrometer (applied biosystem / perseptive biosystems, INC., Framingham, MA, USA) equipped with delayed extraction. Mass spectra were obtained in reflection mode with a 337 nm UV nitrogen laser producing 3 ns pulses. Samples were dissolved in 10 μl of trifluoracetic acid and 30 μl water / acetonitrile solution (50/50 molar). 1 mg dihydroxybenzoic acid (DHB) was added to the solution as the matrix. One μl of the solution was placed on a gold 100-well plate. The solvent was evaporated and the plate was transferred to the mass spectrometer.

DSC: DSC spectra were recorded on a Perkin Elmer DSC apparatus, equipped with a PE7700 computer and TAS-7 software. Dried samples of 5 - 10 mg were heated to approximately 30 °C above the melting temperature and subsequently cooled, both at a rate of 20 °C/min. The maximum of the peak in the heating scan was taken as the melting temperature. The first heating scan was used to determine the melting peak and enthalpy of the sample. The first cooling curve was used to determine the crystallisation temperature, which was taken as the onset of crystallisation.

FT-IR: Infrared transmission spectra were recorded using a Nicolet 20SXB FTIR spectrometer with a resolution of 4 cm^{-1}. Samples were prepared by pressing pellets of dry KBr together with some sample. Temperature dependent FT-IR spectra were recorded at temperatures between room temperature and 300 °C under a helium flow. The degree of crystallinity was estimated with the following equations.

$$X_c \ FT\text{-}IR = \frac{Crystalline\ amide\ peak}{Amorphous + Crystalline\ amide\ peak} = \frac{\lambda_{25°C(1630cm^{-1})}}{a \times \lambda_{25°C(1670cm^{-1})} + \lambda_{25°C(1630cm^{-1})}} \quad (Equation\ 2.1)$$

With λ_T = height of absorption band at temperature T (°C)

The height of the amorphous and crystalline amide peak are related by factor a, which can be calculated according to;

$$a = \frac{decrease\ of\ crystalline\ peak\ {}_{(25°C - melt)}}{increase\ of\ amorphous\ peak\ {}_{(25°C - melt)}} = \frac{\lambda_{25°C(1630cm^{-1})} - \lambda_{melt(1630cm^{-1})}}{\lambda_{melt(1670cm^{-1})} - \lambda_{25°C(1670cm^{-1})}}$$

Synchotron WAXS: Wide angle X-ray scattering (WAXS) experiments were performed at the Dutch-Belgium (DUBBLE) beamline, BM26 at the European Synchotron Radiation Facility (ESRF, Grenoble). The wavelength of the beam was 1.2 Å. A one dimensional WAXS detector was used and a 2θ-range of 9.3 - 70° was measured. Temperature dependent profiles were recorded using a remote controlled LINKAM DSC stage.

Results and discussion

Bisester tetra-amide units were prepared for use as starting compounds in the synthesis of segmented block copolymers. Two types of bisester tetra-amides units were synthesised, TxTxT-dimethyl and TxAxT-dimethyl (Figure 2.1).
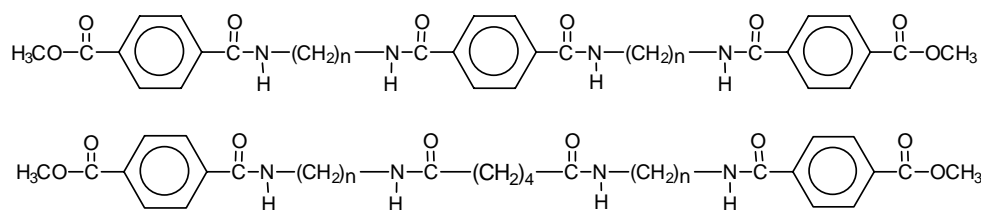

Figure 2.1: Structure TxTxT-dimethyl with x = (CH$_2$)$_n$ with n = 6, 8, 10 and TxAxT-dimethyl with n = 4, 6.

Synthesis of TxTxT-dimethyl

Bisester tetra-amide units were synthesised in two steps. The first step was the synthesis of xTx-diamine (Table 2.1)[5,22]. In this synthesis a molar excess of 8 times diamine was used to limit the formation of longer blocks. The reaction between dimethyl terephthalate and the diamine is fast and a catalyst is not needed. After some time toluene was added to keep

stirring of the reaction mixture possible. The reaction product was filtered and washed with diethylether to remove the free diamine. A white powder was obtained with a yield of 88%. The purity of the product was estimated by NMR spectroscopy (Equation 2.2) and the results are given in Table 2.1. The xTx units were recrystallised from hot n-butyl acetate to further improve the purity (>98%). The purity was calculated from the ^{1}H-NMR integral ratio of CH_2 amide side (c) to CH_2 amine side (d) (Figure 2.2).

$$\text{Purity of xTx or xAx} = \left(2 - \frac{Integral\ CH_2\ amide\ side}{Integral\ CH_2\ amine\ side} \right) \times 100\% \ (\%) \qquad (Equation\ 2.2)$$
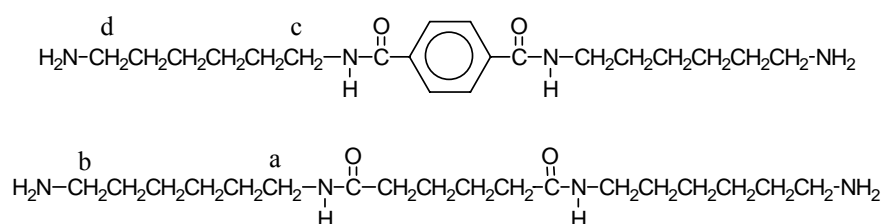

Figure 2.2: Structure of 6T6-diamine and 6A6-diamine.

Table 2.1: Properties of xTx-diamine and xAx-diamine.

	After synthesis		After recrystallisation			
	Yield (%)	Purity (%)	Yield (%)	Purity (%)	T_m (°C)	ΔH (J/g)
6T6-diamine	88	71	40	98	201	250[a] / 135
8T8-diamine	90	86	43	98	191	197[a] / 80
10T10-diamine	85	83	50	98	175	183[a] / 70
4A4-diamine	83	86	40	99	183	330[a] / 42
6A6-diamine	85	85	63	98	180	290[a] / 33

[a] *melting enthalpy of the 1st heating run*

The melting temperature of xTx-diamine decreases with increasing diamine length, x. The diamine-diamide extenders have a very high melting enthalpy at the first heating run but the crystallisation enthalpy and melting enthalpy of the second heating run are much lower. This difference is probably due to degradation or instability of the diamine-diamide unit. The diamine-diamide extenders do not appear to be stable in their melts.

TxTxT-dimethyl is synthesised from xTx-diamine and methyl phenyl terephthalate (MPT) in an NMP solution. The phenyl group of MPT is a better leaving group than the methyl group

and reacts faster, so further reaction is limited. Starting from a uniform xTx-diamide unit and MPT a uniform bisester tetra-amide unit is obtained without further purification (Figure 2.1).

Bisester tetra-amides characterised by MALDI-TOF

The molecular weight of reaction products above 200 g·mol^{-1} can be analysed with MALDI-TOF. In this way impurities can be measured.
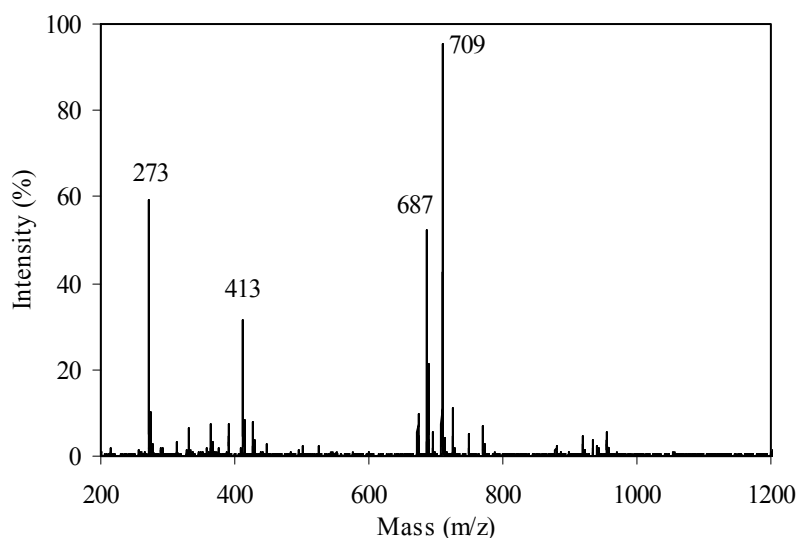

Figure 2.3: MALDI-TOF spectrum of T6T6T-dimethyl.

In the MALDI-TOF spectra of T6T6T-dimethyl four main peaks are visible. The first two peaks at 273 and 413 are known peaks from dihydroxybenzoic acid that was used as a matrix. These peaks do not appear if another matrix was used. The peaks at 687 and 709 can be ascribed to mass+H and mass+Na corresponding to a mass of 686 g·mol^{-1}, which is the molecular weight of T6T6T-dimethyl. Peaks corresponding to other fractions are less than 3% intensity and can be neglected. According to MALDI-TOF measurements the T6T6T-dimethyl is rather pure. It can be assumed that the concentrations of T6T-dimethyl and T6T6T6T- dimethyl are small. Similar MALDI-TOF results were obtained for the other bisester tetra-amides and impurities were not observed.

^{1}H-NMR

The molecular structure of TxTxT-dimethyl was analysed by ^{1}H-NMR (Figure 2.4). The spectrum of T6T6T-dimethyl (Figure 2.4) with chemical shifts and peak assignment (Table 2.2) is given as an example.
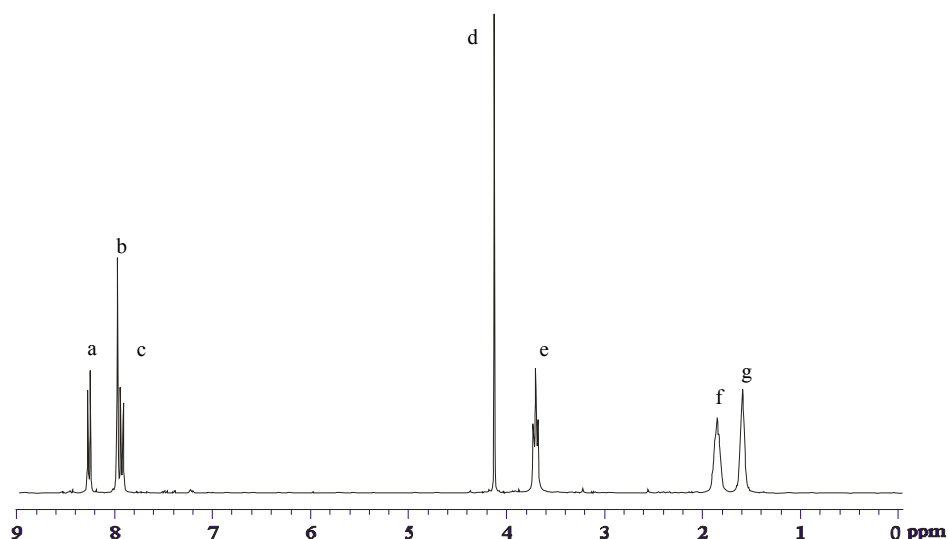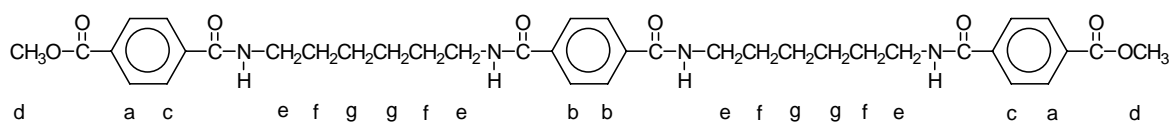
Figure 2.4: NMR spectrum T6T6T-dimethyl.

Figure 2.5: Peak assignments of protons of T6T6T-dimethyl.

Table 2.2: Chemical shifts δ and assignment of protons of TxTxT-dimethyl.

	Chemical shift (ppm)	T6T6T integral	T8T8T integral	T10T10T integral	Type
a	8.2-8.3	4.00	4.00	4.00	Doublet
b	7.95	4.34	4.20	3.93	Singlet
c	7.9-8.0	3.93	4.10	4.29	Doublet
d	4.1	6.02	5.99	5.83	Singlet
e	3.7	8.50	8.75	8.26	Singlet
f	1.85	8.81	9.15	8.73	Singlet
g	1.60	8.71	18.08	25.53	Singlet

The integral values of the peaks are close to the calculated values and correspond with data from literature[13,23]. The purity of the TxTxT units can be determined from the ester to amide ratio assuming that no TxT is present. The uniformity of the rigid units is important as it affects the properties of the segmented copolymers. To estimate the purity of the TxTxT-dimethyl units the integrals of the terephthalic protons are compared (Equation 2.3).

$$\text{Purity TxTxT} - \text{dimethyl} = \left(2 - \frac{b+c}{2a} \right) \times 100\% \qquad (\%) \qquad \qquad (Equation\ 2.3)$$

Table 2.3: Properties of tetra-amide units.

Bisester tetra-amide	M_w (g/mol)	Yield (%)	Purity (%)	T_m (°C)	T_c (°C)	ΔH_m (J/g)	ΔH_c (J/g)
T6T6T	686	80	97	303	284:259	170	113
T8T8T	742	86	96	275	253;184	184	141
T10T10T	789	84	97	244	221;184	126	103
T4A4T	611	80	99	287	261	161	120
T6A6T	667	83	98	255	235	138	111

The calculated purity of the bisester tetra-amides is an indication that the units are uniform.

Synthesis of TxAxT-dimethyl

The bisester tetra-amides TxAxT have an adipate acid group in the middle of the unit, instead of a terephthalic group (Figure 2.1). The adipate group in the tetra-amide unit was employed to lower the melting temperature[14].

The synthesis route for TxAxT-dimethyl is similar to the synthesis of TxTxT-dimethyl. The uniform TxAxT-dimethyl units were synthesised in two steps. The xAx-diamine unit was synthesised via a reaction of dimethyl adipate and an excess of diamine to decrease the chance of forming oligoamides. The diamines have either 4 or 6 methylene groups.

Although an excess of diamine was used, longer blocks were also formed. The diamine-diamides were purified by re-crystallisation (yield 40 - 60%). After recrystallisation of the diamine-diamide the purity of the units was, according to Equation 2.2, above 98%. The melting temperatures of the 4A4- and 6A6-diamine-diamide units were respectively 180 °C and 183 °C (Table 2.1). The melting enthalpies are lower compared with the melting enthalpies of xTx-diamine. TxAxT-dimethyl was synthesised from xAx-diamine and methyl phenyl terephthalate (MPT) (Table 2.3).

^{1}H-NMR

The crude xAx contained some longer blocks (77% purity, Equation 2.2) and was recrystallised (yield 40 - 60%, purity 98%). Second, the xAx-diamine was reacted with methyl phenyl terephthalate (MPT), resulting in uniform TxAxT-dimethyl units. The phenyl

ester is far more reactive compared with the methyl ester of MPT so further reaction is therefore limited.

The purity of the bisester-tetra-amides was determined by ^{1}H-NMR. In Figure 2.6 the ^{1}H-NMR spectrum is given for T6A6T and the peak assignments are listed in Table 2.4.
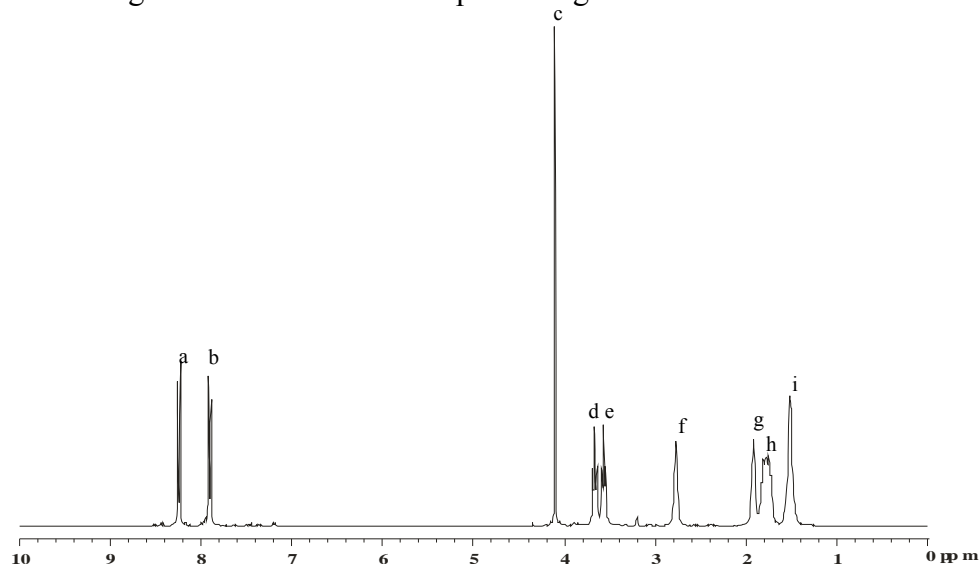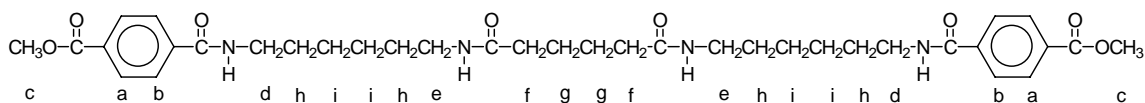

Figure 2.6: NMR spectrum T6A6T-dimethyl.

Figure 2.7: Peak assignments of protons of T6A6T-dimethyl.

Table 2.4: Chemical shifts and assignment of protons of T6A6T-dimethyl.

	Chemical shift (ppm)	T6A6T integral	T4A4T integral	Type
a	8.2-8.3	4.00	4.00	Doublet
b	7.8-8.0	4.04	4.04	Doublet
c	4.1	6.02	6.11	Singlet
d	3.7-3.8	4.12	4.12	Triplet
e	3.6-3.7	4.08	4.09	Triplet
f	2.7-2.8	4.07	4.05	Singlet
g	1.92	4.24	4.09	Singlet
h	1.78	8.25	8.5	Multiplet
i	1.53	8.42	-	Triplet

The ratio of aliphatic amide ester CH_2 (e) over the aromatic amide ester CH_2 group (d) is an indication for the purity of the rigid segment. In case of a pure product this ratio is 1.0. In our

sample the ratio was 0.99 and thus the purity was 98% (Table 2.3). T6A6T-dimethyl had a melting temperature of 255 °C and a ΔH_m of 138 J/g.

Bisester tetra-amides characterised by DSC

The melting and the crystallisation behaviour of the different rigid units were evaluated with DSC. The heating curves for five bisester tetra-amides are shown in Figure 2.8a.
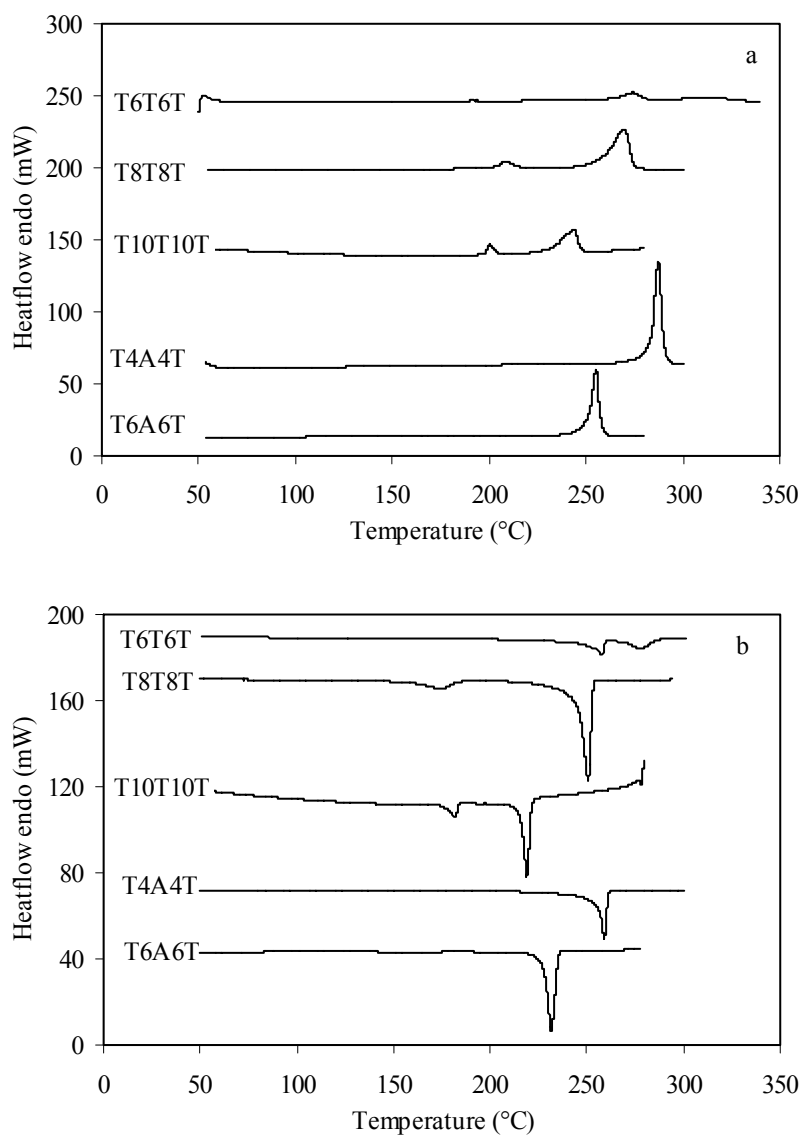

Figure 2.8: DSC traces of different tetra-amide units: a) heating run b) cooling run.

T6T6T-dimethyl shows the highest melting temperature. The melting temperature can be decreased by increasing the length of the aliphatic amine x or by replacing the central terephthalic group by an adipic group (Figure 2.9, Table 2.3). The decrease in melting

19

temperature between T6T6T and T6A6T, by replacing a terephthalate group with an adipate group, is about 50 °C. These results are analogous to the difference in melting temperature of nylon-6,T (T_m = 371 °C)[24] and nylon-6,6 (T_m = 256 °C)[14].

The cooling curves (Figure 2.8) of T6T6T, T8T8T and T10T10T show two crystallisation peaks. The first crystallisation peak is very close to the melting temperature (ΔT = 20 - 26 °C). The second transition of the double crystallisation behaviour is believed to be due to a change in crystalline structure of the amide phase, as is more often observed in polyamides[5,25-28]. The T4A4T and the T6A6T have only one crystallisation temperature.
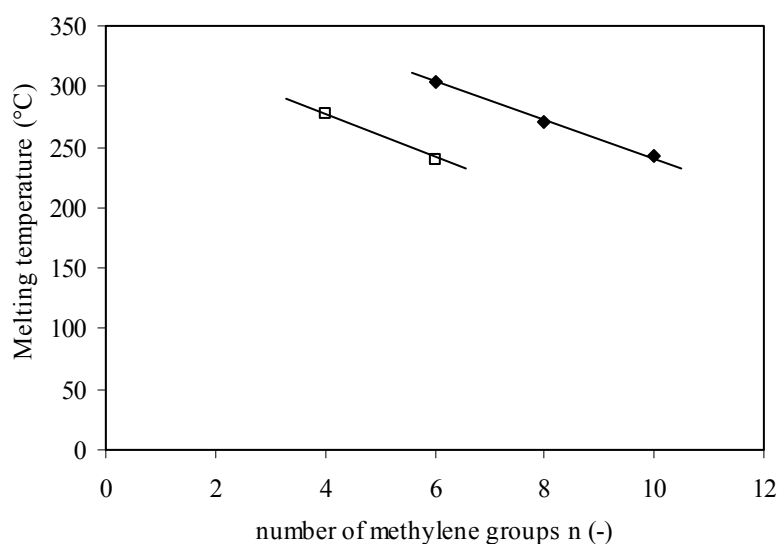

Figure 2.9: Melting temperatures of tetra-amide units as a function of even number of methylene groups (n): □, TxAxT-dimethyl; ♦, TxTxT-dimethyl.

Infrared

Temperature dependent infrared spectra were recorded to study the crystallinity of the T6A6T-dimethyl units. The IR spectrum of T6A6T is given (Figure 2.10) and relevant bands are in the region 1600-1700 cm^{-1} (amide I), 1700-1750 cm^{-1} (ν C=O ester) and 3200-3500 cm^{-1} (ν N-H).

The crystallinity of the amide groups in the T6A6T-dimethyl units as a function of temperature was studied by infrared spectroscopy (Figure 2.11). Especially the amide I band at 1630 - 1640 cm^{-1} and the νNH at 3300 cm^{-1} are temperature sensitive. At room

temperature, the amide I region (ν C=O crystalline state) showed two strong peaks, one of the aliphatic amide (1640 cm^{-1}) and the other of the aromatic amide band (1630 cm^{-1})[29]
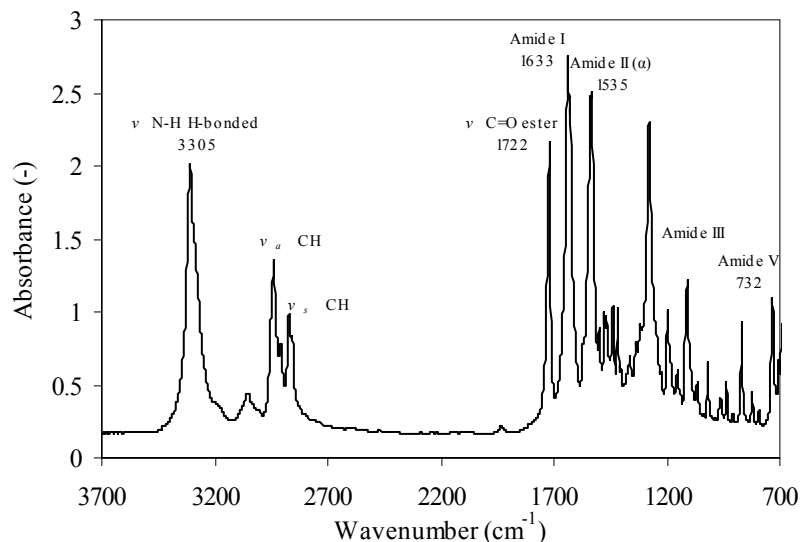
Figure 2.10: FT-IR spectrum of T6A6T at 25 °C.

At high temperatures, close to the melting temperature these peaks disappear and a broad peak at 1670 cm^{-1} (ν C=O amorphous) was formed. The ν N-H band at 3300 cm^{-1} also decreased with temperature and a small broad peak at 3400 cm^{-1} was formed corresponding with non hydrogen bonded N-H groups. A peak at 3320 cm^{-1} was present above 260 °C, which suggests that association of H-bonded assemblies was still present in the melt.

Figure 2.11: Temperature dependent FT-IR spectra of T6A6T-dimethyl recorded at different temperatures: ■ 25 °C; □, 260 °C.

21

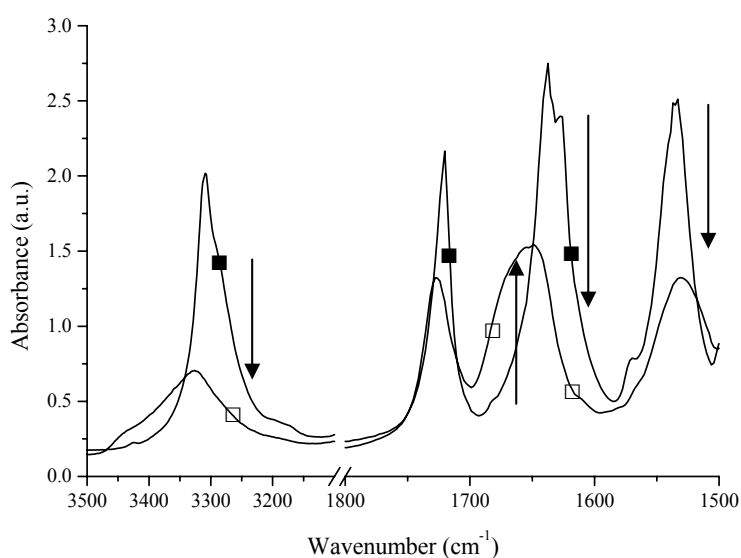From the FT-IR scan at different temperatures the ratio of ester (1720 cm^{-1}) to crystalline aromatic amide (1630 cm^{-1}) was calculated. Comparing the ratio of ester and the amide absorbance gives insight in the stability and recoverability of the crystallinity of the amide units. The baseline was subtracted from the peak absorbance. A ratio of 1 was expected for fully crystallised units. The ratio is almost one and decreases at the melting temperature of the T6A6T-dimethyl segment when the peak of the crystalline amide decreases (Figure 2.12a). The ratio is in accordance with the expected ratio and this means that the crystallinity is nearly 100%.

A way to calculate the crystallinity of the T6A6T-dimethyl is to compare the peak of the crystalline aromatic amide at 1630 cm^{-1} with the peak of amorphous amide at 1670 cm^{-1}. From the ratio of these two peaks the crystallinity was plotted versus the temperature (Figure 2.12b). A crystallinity of 83% at room temperature was calculated, which decreases just before the melting temperature. Upon cooling, the crystallinity strongly increases and completely recovers. The cooling curve is near to the heating curve (Figure 2.12).
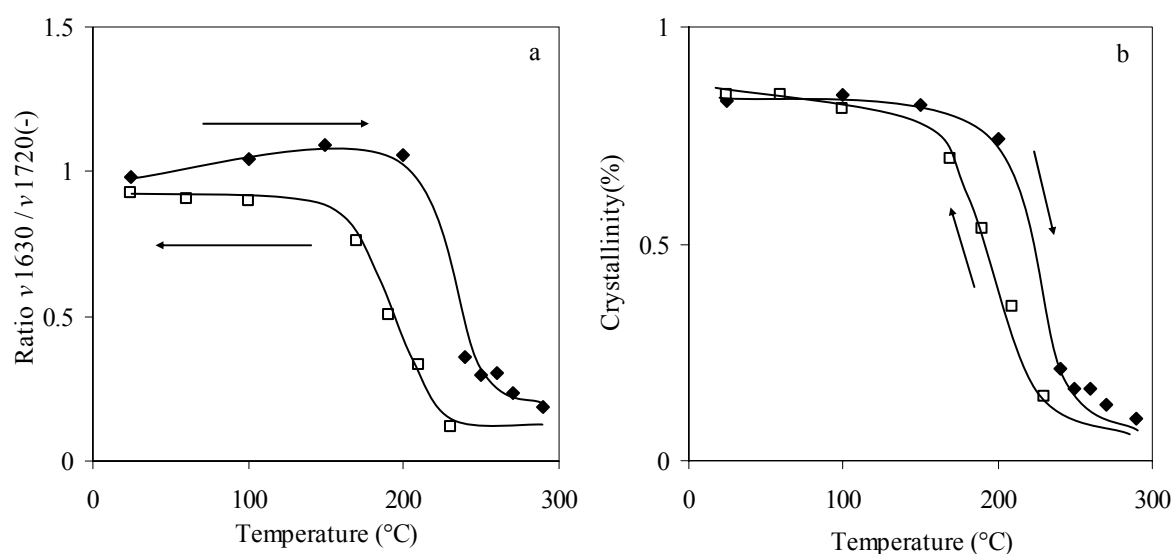
Figure 2.12: a) Peak ratio of crystalline amide (1630 cm^{-1}) to ester (1730 cm^{-1}) for T6A6T at different temperatures: ♦, heating; □, cooling; b) Crystallinity of T6A6T calculated from IR bands at 1630 and 1670 cm^{-1} ; ♦, heating; □, cooling.

WAXS

With wide angle X-ray scattering (WAXS) the diffraction patterns of the different bisester tetra-amides were measured (Figure 2.13). The diffraction patterns look similar to earlier results[22].
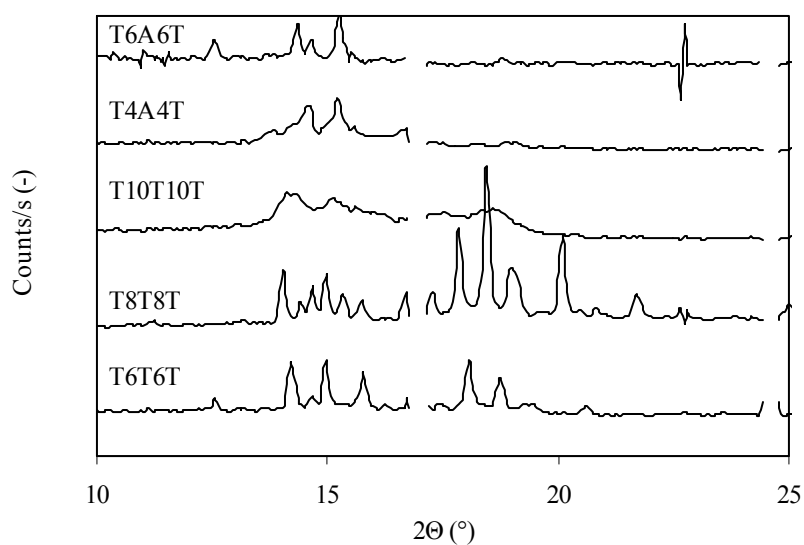
Figure 2.13: WAXD spectrum of different TxTxT-dimethyl units and different TxAxT-dimethyl units.

For T6A6T-dimethyl the WAXS spectrum was also studied as a function of temperature (Figure 2.14). Upon increasing the temperature the peak at 13° shifts to lower angles while the peaks at 15° shift to higher angles. Above the melting temperature of T6A6T-dimethyl (280 °C) no peaks were observed, indicating that in the melt no liquid crystalline order was present.
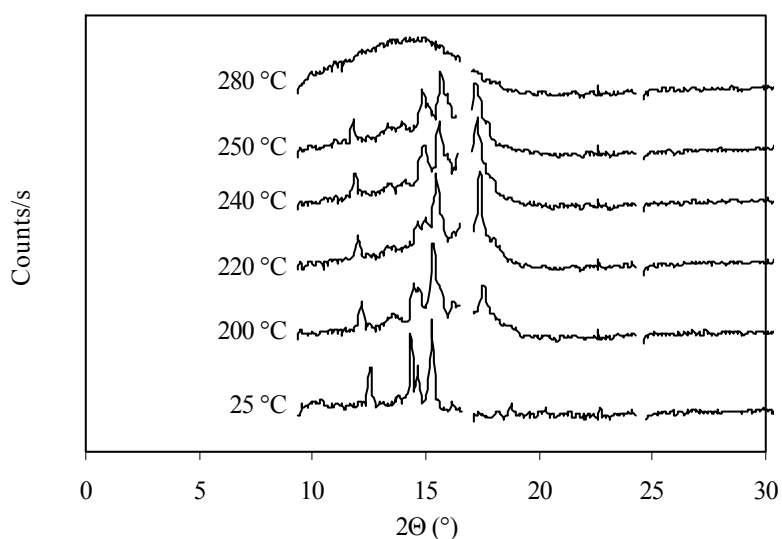
Figure 2.14: WAXS patterns for T6A6T-dimethyl for increasing temperatures.

Conclusions

Bisester tetra-amide TxTxT-dimethyl units and TxAxT-dimethyl units with x = $(CH_2)_n$ and n = 4 - 10 can be synthesised in a two step synthesis. The first step is the synthesis of the diamine-diamide segment, followed by recrystallisation to obtain a diamine-diamide with high purity. By reacting the diamine-diamide with methyl phenyl terephthalate bisester tetra-amides were prepared with a high purity.

The purity of the units was confirmed using NMR and MALDI-TOF. Using DSC the melting and crystallisation behaviour was studied. The bisester tetra-amide units have high melt temperatures (240 - 303 °C) and upon cooling, the uniform units crystallise rapidly. According to the temperature dependent FT-IR results the crystallinity at room temperature is high and the material completely melts at the melting temperature. However, a peak at 3320 cm^{-1} suggests that hydrogen bonding is still present in the melt. The WAXS data show a change in crystalline cell dimensions with temperature. At temperatures above the melting temperature of the tetra-amide segment no ordering in the melt was observed.

References

1. Bennekom van, A.C.M., Gaymans, R.J., *Polymer* **38**, 657-665 (1997).
2. Bouma, K., Wester, G.A., Gaymans, R.J., *J. Appl. Polym. Sci.* **80**, 1173-1180 (2001).
3. Holden, G., Legge, N.R., Quirk, R.,.Schroeder, H.E., *'Thermoplastic elastomers'*, Hanser Publisher, Second Ed. Munich (1996).
4. Hutten van, P.F., Mangnus, R.M., Gaymans, R.J., *Polymer* **34**, 4193-4202 (1993).
5. Krijgsman, J., Husken, D., Gaymans, R.J., *Polymer* **44**, 7573-7588 (2003).
6. Niesten, M.C.E.J., Feijen, J., Gaymans, R.J., *Polymer* **41**, 8487-8500 (2000).
7. Flory, P.J., *Trans. Faraday Soc.* 848 (1955).
8. Miller, J.A. *et al.*, *Macromolecules* **18 (1)**, (1985).
9. Allegrezza, A.E., Seymour, R.W., Ng, H.N., Cooper, S.L., *Polymer* **15**, 433-440 (1974).
10. Harrel, L.L., *Macromolecules* **2**, 607-612 (1969).
11. Ng, H.N., *Polymer* **14**, 255-261 (1973).
12. Gaymans, R.J., Dehaan, J.L., *Polymer* **34**, 4360-4364 (1993).
13. Schuur van der, J.M., *'Poly(propylene oxide) based segmented block copolymers'*, Ph.D. Thesis, University of Twente (2004).
14. Kohan, M.I., *'Nylon Plastics Handbook'*, Hanser, (1995).
15. Bouma, K., Lohmeijer, J.H.G.M., Gaymans, R.J., *Polymer* **41**, 2719-2725 (2000).

16.   Gaymans, R.J., *Abstracts of Papers of the American Chemical Society* **214**, 297-MSE (1997).

17.   Gaymans, R.J., Bennekom van, A.C.M., *Abstracts of Papers of the American Chemical Society* **214**, 155-OLY (1997).

18.   Serrano, P.J.M., van Bennekom, A.C.M., Gaymans, R.J., *Polymer* **39**, 5773-5780 (1998).

19.   Brisson, J., Brisse, F., *Macromolecules* **19**, 2632 (1986).

20.   Cicero, i L., Di Gregotio, F., and Platone, E.,Patent1970US 1,365,962

21.   Husken, D., Krijgsman, J., Gaymans, R.J., *Polymer* **45**, 4837-4843 (2004).

22.   Krijgsman, J., Husken, D., Gaymans, R.J., *Polymer* **44**, 7043-7053 (2003).

23.   Krijgsman, J., *'Segmented copolymers based on poly(2,6-dimethyl-1,4,phenylene ether)'*, Ph.D. Thesis, University of Twente (2002).

24.   Morgan, P.W., Kwolek, S.L., *Macromolecules* **8**, (1975).

25.   Hirschinger, J., Miura, H., Gardner, K.H., English, A.D., *Macromolecules* **23**, 2153-2169 (1990).

26.   Todoki, M., Kawaguchi, T., *Journal of Polymer Science, Polymer Physics Edition* **15**, 1067-1075 (1977).

27.   Li, W.H., Yan, D.Y., Zhang, G.S., Huang, Y., *Polymer international* **52**, 1905-1908 (2003).

28.   Stapert, H.R., *'Environmentally degradable polyesters, poly(ester-amide)s and poly(ester-urethane)s'*, Ph.D. Thesis, University of Twente (1998).

29.   Dechant, J., *'Ultrarot-spektroskopische Untersuchungen an Polymeren'*, Maxim Gorki, Berlin (1972).

CHAPTER 3

POLYETHER BASED SEGMENTED COPOLYMERS
WITH UNIFORM T6A6T-DIMETHYL SEGMENTS

Abstract

Poly(tetramethylene oxide) based poly(ether-ester-amide)s (PEEA's) having uniform tetra-amide segments were synthesised. The tetra-amide segment (T6A6T) is based on adipic acid (A), terephthalic acid (T) and hexamethylene diamine (6). These segmented copolymers were made by polycondensation of polyether segments and tetra-amide segments. In the copolymers, the concentration of the tetra-amide segment was varied between 3% and 44%. The polymers were characterised by DSC and temperature dependent FT-IR, SAXS and DMTA. The mechanical properties of the polymers were evaluated by compression set and tensile set measurements.

The amide segments form crystalline ribbons with a high aspect ratio in a polyether matrix. The crystallinity of the tetra-amide segments in the copolymers was about 80%. The glass transition temperatures of the PTMO phase are low (-65 to -70 °C). The rubber modulus in the plateau region of the copolymers is almost temperature independent. With increasing content of crystallisable segment in the copolymer, the rubber modulus at room temperature increases from 1 to 102 MPa. This strong increase in modulus with amide content can be approximated using a model for fibre reinforced polymers. The melting temperatures of the copolymers decrease with increasing ether content and this can be explained by the solvent effect proposed by Flory.

Introduction

Thermoplastic elastomers (TPE's) are melt-processable materials that show elastomeric behaviour at their service temperature. A special kind of TPE's are segmented copolymers that consist of alternating crystallisable rigid segments and flexible segments[1]. The rigid segments can crystallise in lamellae dispersed in the low T_g phase. These crystallites function as physical crosslinks that give the material dimensional stability and solvent resistance. The low T_g soft phase forms the continuous phase and gives the material low temperature flexibility. The T_g of the soft phase depends on the glass transition of the flexible segment, the segment length between physical crosslinks and the amount of dissolved rigid segment[1]. Between the glass transition temperature and the melting temperature the copolymer shows elastic behaviour. For a wide rubbery plateau, the T_g of the soft phase should be low and the T_m of the hard phase high.

It has been found that the properties of segmented copolymers depend on the uniformity of the crystallisable segment. The effect of uniform crystallisable segments has been studied both on polyurethanes[2-5] and polyamides[6-13]. These studies showed that polymers with uniform crystallisable segments crystallise fast, have a relatively high modulus, a temperature independent rubbery plateau and that these polymers also have a high elasticity and high fracture strains.

Poly(tetramethylene oxide) (PTMO) is often used as flexible soft phase as it has a low T_g, good hydrolytic stability and good reactivity[14]. Segmented copolymers with PTMO flexible segments and uniform crystallisable segments containing amide segments were studied before[7,9-11,15,16]. Niesten[11] studied copolymers with uniform aramid diamide units (TΦT). High molecular weight PTMO segments were obtained by extending $PTMO_{1000}$ with terephthalate groups. The amide content was changed from 22 to 3% and with that the modulus decreased from 44 to 1.5 MPa. The TΦT-dimethyl units have a high melting temperature of 371 °C, which is too high for a melt polymerisation.

Krijgsman[7,9,17] studied similar segmented copolymers based on $PTMO_{1000}$ extended with terephthalate groups to different lengths (3000 – 10,000 g·mol^{-1}) and uniform tetra-amide units (T6T6T). The T6T6T segment concentration was changed from 16 - 5 wt% and with

that the modulus changed from 15 to 3 MPa. Segmented copolymers with tetra-amide segments have even better elastic properties compared with copolymers with diamide segments[12,18]. The T6T6T-dimethyl unit has a high melting temperature of 306 °C. The melting temperatures of these two different amide units (TΦT and T6T6T) are above 300 °C, making melt synthesis difficult as degradation of the PTMO occurs above 250 °C[19]. Furthermore, the melting temperatures of the copolymers based on T6T6T are high resulting in too high processing temperatures. Therefore it would be interesting to study copolymers based on a tetra-amide segment combined with a lower melting temperature of the tetra-amide.

Research aim

In this chapter the synthesis and properties of PTMO-T6A6T segmented copolymers are discussed. The crystallisable segment of uniform length is the tetra-amide T6A6T (Figure 3.1) based on adipic acid (A), terephthalic acid (T) and hexamethylene diamine (6). In these copolymers the PTMO length is varied from 650 to 20,000 g·mol^{-1} and with that the concentration of the tetra-amide segment from 44% to 2.7 wt%. The morphology of the polymers was studied using AFM, TEM and SAXS and the crystallisation was studied with DSC and FT-IR. The thermal mechanical behaviour was studied with DMTA and the elastic behaviour with compression set and tensile set measurements.
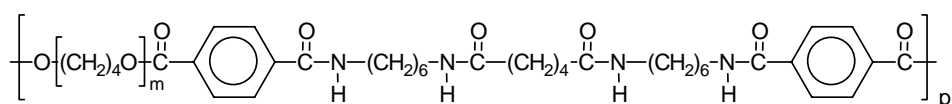
Figure 3.1: Polymer structure of PTMO-T6A6T.

Experimental

Materials: Dimethyl terephthalate (DMT), N-methyl-2-pyrrolidone (NMP), phenol, terephthaloylchloride, toluene and a 0.5 M sodium methoxide solution in methanol were purchased from Aldrich and used as received. Tetra-isopropyl orthotitanate (Ti(i-OC$_3$H$_7$)$_4$) was purchased from Aldrich and was diluted with m-xylene (0.05 M). m-Xylene was purchased from Merck. Poly(tetramethylene oxide) (PTMO) 632 was a gift from Bayer. PTMO with a molecular weight of 1000, 1400, 2000 and 2900 g·mol^{-1} were a gift from Dupont. Irganox 1330 was obtained from CIBA. Synthesis of 6A6 and T6A6T-dimethyl was performed as described before[20]

Synthesis of diphenyl terephthalate (DPT)[11,12,17]: Terephthaloylchloride (220 g, 1.1 mol) was added slowly to phenol (258 g, 2.8 mol) at 100 °C in a round bottomed flask with nitrogen inlet reflux condenser and a mechanical stirrer. The reaction was carried out for 3 h at 100 °C and the condensation product hydrochloric acid (HCl) was passed through sodium hydroxide solution in water (90 g, 2.2 mol) to neutralize the acid gas. In time the reaction mixture partly solidifies. The cooled product was collected by filtration over a no.4 glass filter and washed three times with water and two times with warm ethanol (65 °C) to remove the phenol (yield 85%). The resulting product melted at 206 °C, corresponding with literature[12,18].

Solution/melt polymerisation of PTMO$_x$-T6A6T: The polymerisation of PTMO$_{1000}$ with T6A6T-dimethyl is given as an example. The polymerisation was carried out in a 250 ml stainless steel reactor with a nitrogen inlet and magnetic coupling stirrer. The reactor was charged with PTMO$_{1000}$ (50 g, 0.05 mol), T6A6T-dimethyl (33.3 g, 0.05 mol), 100 ml NMP, 1 wt% Irganox 1330 (based on PTMO) and catalyst solution (5 ml of 0.05 M Ti(i-OC$_3$H$_7$)$_4$ in m-xylene) under nitrogen flow. The stirred reaction mixture was heated in 30 min to 180 °C, in subsequently 2 h to 250 °C and maintained at 250 °C for 2 h. Subsequently, the pressure was carefully reduced (P<20 mbar) to distil off the NMP and then further reduced (P<0.3 mbar) for 1 h. After this, the reactor was cooled slowly, maintaining the low pressure. The copolymers were transparent and tough materials. ^{1}H-NMR (TFA-*d*): δ 8.35 (d, 4H, terephthalate H ester side), δ 8.00 (d, 4H, terephthalate amide side), δ 4.6 (s, 4H, CH$_2$ PTMO, ester side), δ 3.88 (m, 52H, CH$_2$ PTMO ether side), δ 2.87 (t, 4H, 1st and 4th CH$_2$ methyl adipate), δ 2.07 (t, 8H, CH$_2$ PTMO, ester side), δ 1.91 (s, 48H, CH$_2$ PTMO) + δ 1.9 (d, 4H, 2nd and 3rd CH$_2$ methyl adipate), δ1.78 (s, 8H, 2nd and 5th CH$_2$ amine), δ 1.63 (s, 8H, 3rd and 4th CH$_2$ amine).

Melt polymerisation of PTMO$_x$-T6A6T: The same setup was used as described above. The reactor was charged with PTMO$_{2900}$ (50 g, 0.017 mol), T6A6T-dimethyl (11.48 g, 0.017 mol), 1 wt% Irganox 1330 (based on PTMO) and catalyst solution (2 ml of 0.05 M Ti(i-OC$_3$H$_7$)$_4$ in m-xylene) under nitrogen flow. The initial reaction temperature was 260 °C, 10 °C higher than the melting temperature of the bisester tetra-amide unit. After 0.5 h the tetra-amide unit was melted and the reaction temperature was lowered to 250 °C. This temperature was maintained for 4 h. Subsequently, the pressure was reduced to (P<20 mbar) and then further reduced to (P<0.3 mbar) for 1 h. Finally, the reactor was cooled slowly maintaining the low pressure. The copolymers were transparent and tough.

Solution/melt polymerisation of PTMO$_x$-T6A6T starting from 6A6/DPT: The same setup was used as described above. The reactor was charged with PTMO$_{1400}$ (50 g, 0.036 mol), DPT (17 g, 0.054 mol), 1 wt% Irganox 1330 (based on PTMO) and catalyst solution (0.9 ml of 0.05 M Ti(i-OC$_3$H$_7$)$_4$ in m-xylene) under nitrogen flow. After 2 h of reaction at 220 °C a solution of 6A6-diamine (6.11 g, 0.018 mol) in 50 ml NMP was added to the reactor. The temperature was raised to 250 °C and maintained for 2 h. Subsequently, the pressure was carefully reduced (P<20 mbar) to distil off the NMP and then further reduced (P<0.3 mbar) for 60 min. Finally, the reactor was cooled slowly maintaining the low pressure. The copolymers were yellowish coloured and tough.

Viscometry: The inherent viscosity was measured at a concentration of 0.1 g/dl in a mixture of phenol/1,1,2,2-tetrachloroethane (1:1 molar ratio) at 25 ºC using a capillary Ubbelohde type 1B.

DSC: DSC spectra were recorded on a Perkin Elmer DSC apparatus, equipped with a PE7700 computer and TAS-7 software. Dried samples of 5 - 10 mg were heated to approximately 30 °C above the melting temperature and subsequently cooled, both at a rate of 20 °C/min. The maximum of the peak in de heating scan was taken as the melting temperature. The second heating scan was used to determine the melting peak and enthalpy of the sample. The first cooling curve was used to determine the crystallisation temperature, which was taken as the onset of crystallisation. The degree of crystallinity was calculated from the melting enthalpy of the polymer and the melting enthalpy of the bisester tetra-amide.

FT-IR: Infrared transmission spectra were recorded using a Nicolet 20SXB FTIR spectrometer with a resolution of 4 cm^{-1}. Samples measured at room temperature were prepared by adding a droplet of a polymer solution in HFIP (1 g/l) on a pressed KBr pellet. Solution cast polymer films (0.05 g/ml in HFIP) of <10 μm thick placed in-between two KBr pellets were used for temperature dependent FT-IR recorded at temperatures between room temperature and 210 °C under a helium flow. The degree of crystallinity of the rigid segments in the polymers (X_c) was estimated with the following equations.

$$X_c \, FT\text{-}IR = \frac{Crystalline \; amide \; peak}{Amorphous + Crystalline \; amide \; peak} = \frac{\lambda_{25°C(1630\,cm^{-1})}}{a \times \lambda_{25°C(1670\,cm^{-1})} + \lambda_{25°C(1630\,cm^{-1})}} \quad (Equation \; 3.1)$$

With λ_T = height of absorption band at temperature T (°C)

The height of the amorphous and crystalline amide peak are related by factor a, which can be calculated according to;

$$a = \frac{decrease \; of \; crystalline \; peak \, _{(25°C-melt)}}{increase \; of \; amorphous \; peak \, _{(25°C-melt)}} = \frac{\lambda_{25°C(1630\,cm^{-1})} - \lambda_{melt(1630\,cm^{-1})}}{\lambda_{melt(1670\,cm^{-1})} - \lambda_{25°C(1670\,cm^{-1})}}$$

AFM: AFM measurements were carried out with a Nanoscope IV controller (Veeco) operating in tapping mode. The AFM was equipped with a J-scanner with a maximum size of 200 μm^2. Si-cantilevers (Veeco) were used to obtain height and phase images. The amplitude in free oscillation was 5.0 V. The operating setpoint value (A/A_0) was set to relatively low values of 0.70. Scan sizes were 1-3 μm^2 to obtain the best contrast. Solvent cast samples of ~20 μm thick were prepared from a 3 wt% solution in TFA.

SAXS: Small angle X-ray scattering (SAXS) experiments were performed at the Dutch-Belgium (DUBBLE) beamline, BM26 at the European Synchotron Radiation Facility (ESRF) in Grenoble. The wavelength of the beam was 1.2 Å. A two dimensional SAXS detector was used and a q-range of 0 - 1.8 nm^{-1} was measured. Temperature dependent profiles were recorded using a remote controlled LINKAM DSC stage at a heating and cooling rate of 10 °C/min. The background was subtracted from the intensity. The two dimensional SAXS intensity was azimuthally integrated to obtain the scattering pattern as a function of q = 2 sin θ/λ.

DMTA: Samples (70x9x2 mm) for the DMTA were prepared on an Arburg H manual injection moulding machine. The test samples were dried in vacuum at 50 °C for 24 h before use. DMTA spectra were recorded with a Myrenne ATM3 torsion pendulum at a frequency of 1 Hz and 0.1% strain. The storage modulus G' and the loss modulus G'' were measured as a function of temperature. The samples were cooled to -100 °C and subsequently heated at a rate of 1 °C/min. The glass transition was determined as the peak in the loss modulus. The flow temperature (T_{flow}) is defined as the temperature where the storage modulus reaches 1 MPa. The start of the rubbery plateau, the intercept of the tangents, is called the flex temperature (T_{flex}). The decrease in storage modulus of the rubbery plateau with increasing temperature is quantified by ΔG', which is calculated from:

$$\Delta G' = \frac{G'_{(Tflex)} - G'_{(Tflow-50°C)}}{G'_{25°C}} \times \frac{1}{\Delta T} \qquad (°C^{-1}) \qquad \qquad (Equation\ 3.2)$$

ΔT is described as the temperature range: (T_{flow}-50 °C) - T_{flex}.

Compression set: Samples for compression set were cut from injection moulded bars. The compression set was measured at room temperature according to ASTM 395 B standard. After 24 h the compression was released. After relaxation for half an hour, the thickness of the samples was measured. The compression set was taken as the average of four measurements. The compression set is defined as:

$$Compression\ set = \frac{d_0 - d_2}{d_0 - d_1} \times 100\% \qquad (\%) \qquad \qquad (Equation\ 3.3)$$

With: d_0 = thickness before compression (mm)
        d_1 = thickness during compression (mm)
        d_2 = thickness after 0.5 h relaxation (mm)

Tensile test: Stress-strain curves were obtained using injection moulded bars with a thickness of 2.2 mm, cut to dumbbell (ISO 37 type 2), using a Zwick Z020 universal tensile machine equipped with a 500 N load cell. The strain was measured with extensometers. Standard tensile test were performed in three-fold according to ISO 37 at a strain rate of 0.4 s^{-1} (test speed of 60 mm/min).

Tensile set: Cyclic stress-strain experiments were conducted with injection-moulded bars with a thickness of 2.2 mm cut to dumbbells (ISO 37 type 2). A Zwick Z020 universal tensile machine equipped with 500N load cell was used to measure the stress as a function of strain of each loading and unloading cycle at a strain rate of 0.4 s^{-1} (test speed of 60 mm/min). The strain of each loading-unloading cycle was increased (stair-case loading) and the tensile set of the strain increment was determined as a function of the applied strain. The incremental tensile set (TS) was calculated from the following relation (Equation 3.4):

$$Tensile\ set = \frac{\Delta \varepsilon_{remaining}}{\Delta \varepsilon_{cycle}} = \frac{\varepsilon_{r,cycle(i)} - \varepsilon_{r,cycle(i-1)}}{\Delta \varepsilon_{cycle}} \times 100\% \qquad (\%) \qquad \qquad (Equation\ 3.4)$$

With: $\varepsilon_{r,cycle(i)}$ = remaining strain at the end of cycle i

        $\varepsilon_{r,cycle(i-1)}$ = remaining strain at the end of the preceding cycle i-1.

Immediately after the stress was zero, a new cycle was started. The strain of the first cycle was 20% and for each following cycle the strain was increased with 40%.

Results and discussion

Copolymers based on T6A6T-dimethyl and PTMO or PTMO extended with terephthalate groups were synthesised via a polycondensation reaction. The T6A6T-dimethyl segment was synthesised prior to the polymerisation[20].
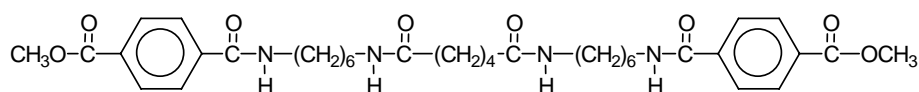

Figure 3.2: Structure of T6A6T-dimethyl.

T6A6T-dimethyl has a melting temperature of 255 °C and a melting enthalpy of 137 J/g.

Polymerisation method

Melt polymerisation

The copolymers were prepared by reacting the methyl ester endgroups of T6A6T-dimethyl with the hydroxyl endgroups of the PTMO segment. In a melt polymerisation the bisester tetra-amide unit has to melt and mix with the PTMO. Thus, the initial temperature during polymerisation needs to be about ~10 °C higher than the melting temperature of the bisester tetra-amide unit (255 °C). An initial polymerisation temperature of 260 °C was used and once the reaction was going the polymerisation temperature was lowered to 250 °C for further reaction. A problem of a high polymerisation temperature is degradation of the polyether segment[19]. The melt synthesised copolymer with ~15% T6A6T was transparent and only slightly coloured. The inherent viscosity of this copolymer was high, the rubber modulus at room temperature was 6 MPa and melting temperature was 150 °C. The CS was 14%, which is high for a copolymer with a low modulus (Table 3.1).

Solution/melt polymerisation

It was thought that the properties of the melt synthesised copolymers could be further improved by using a solvent in the initial part of the polymerisation. NMP was used to dissolve T6A6T-dimethyl and the reaction temperature was kept low. When the rigid

segment is incorporated in the copolymer, its melting temperature decreases and the reaction can be continued in the melt at 250 °C. In this way, copolymers with higher inherent viscosities were obtained than with melt polymerisation. Probably less degradation occurred as the polymerisation temperature during the reaction was low. The copolymers had a high T_{flow}, a high rubber modulus and a low compression set (Table 3.1).

Table 3.1: Synthesis method PTMO-T6A6T (~15% T6A6T).

	Polymerisation type	η_{inh}	T_g	$G'_{25 °C}$	$\Delta G'$ *10^{-3}	T_{flow}	CS	Transparency
		(dl/g)	(°C)	(MPa)	(°C^{-1})	(°C)	(%)	
T6A6T-dimethyl + PTMO$_{2900}$	Melt	2.1	-71	6	3.7	150	14	Transparent
T6A6T-dimethyl + PTMO$_{2900}$	Solvent/melt	3.5	-70	9	1.8	175	7	Transparent
6A6 + (DPT + PTMO$_{1400}$)$_{3060}$	Solvent/melt	1.6	-60	8	4.1	165	14	Opaque

Solution/melt polymerisation starting with 6A6

A disadvantage of using bisester tetra-amides for the preparation of the copolymer is the synthesis of the tetra-amide prior to the polymerisation. Synthesis of the bisester tetra-amide unit takes two steps and in between a recrystallisation step. A shorter route for the preparation of the copolymer is to first react PTMO with DPT which leads to extension and endcapping of the PTMO (DPT-PTMO$_x$-T-PTMO$_x$-DPT). Subsequently the extended PTMO was reacted with 6A6. In this way the rigid blocks will be formed in situ. The final ratio of DPT:PTMO:6A6 was 3:2:1. This ratio minimises the formation of longer amide segments. In this reaction we used PTMO$_{1400}$ which gave in the copolymer a PTMO extended with DPT to a segment length of 3060 g·mol^{-1} (PTMO$_{1400}$-T)$_{3060}$.
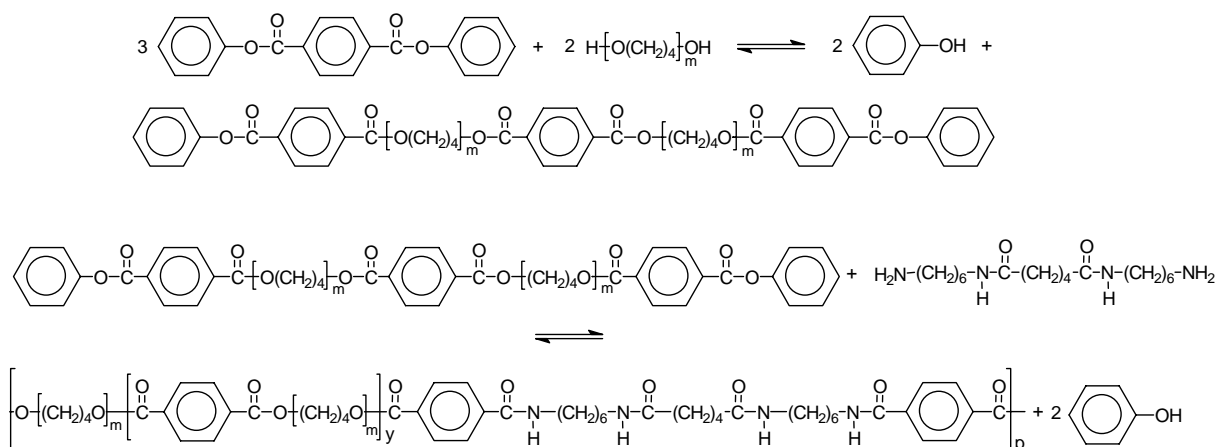

Figure 3.3: Extension and endcapping of PTMO with DPT followed by the polymerisation with 6A6.

The inherent viscosity of the polymer prepared from $PTMO_{1400}$-T and 6A6 was somewhat lower than the inherent viscosity of the segmented copolymers made with $PTMO_{2900}$ and uniform T6A6T-dimethyl (Table 3.1). The polymers were lightly coloured and were not transparent. The rubber modulus and melting temperature are lower and the compression set was higher compared with the solution/melt polymerisation.

PTMO-T6A6T copolymers can be well prepared via the three routes discussed above. However, the copolymers synthesised by the solution/melt route had the best properties. Therefore this route was also used for the synthesis of the copolymers discussed in the next section.

PTMO-T6A6T copolymers

In segmented copolymers with crystallisable segments of uniform length a change in PTMO length has a direct effect on the amide content[7,9-11,15,16]. Two series of copolymers were made; one with PTMO segments of different length (650 - 2900 g·mol^{-1}) and one with $PTMO_{1000}$ extended with DMT (4000 - 20,000 g·mol^{-1}). Using both approaches, copolymers could be synthesised with tetra-amide content varying from 44 to 2.7 wt % (Table 3.2). The $PTMO_x$-T6A6T segmented copolymers with PTMO length of 650 - 2900 g·mol^{-1} had high inherent viscosities, which increased with $PTMO_x$ segment length.

The second copolymer series, $(PTMO_{1000}$-T$)_x$-T6A6T had segment lengths x of 4000 - 20,000 g·mol^{-1}. In this way the tetra-amide content of the copolymers was varied from 11 to only 2.7 wt%. The inherent viscosities of the polymers of this series are somewhat lower than of series 1.

The copolymers of both series were transparent in the melt, so melt phasing did not occur. At room temperature the segmented copolymer with a PTMO length of 650 g·mol^{-1} (series 1) was opaque and all other copolymers were transparent. All the copolymers were easily injection mouldable.

Table 3.2: Some properties of PTMO$_x$-T6A6T copolymers.

	T6A6T	η_{inh}	T_m	ΔH_m	T_c	T_m-T_c	X_c DSC	X_c FT-IR
	(wt%)	(dl/g)	(°C)	(J/g)	(°C)	(°C)	(%)	(%)
T6A6T-dimethyl	100	-	255	138	235	20	-	-
Series 1								
PTMO$_{650}$	43.8	1.8	200	55	176	24	95	87
PTMO$_{1000}$	34.2	2.5	191	40	165	26	93	92
PTMO$_{1400}$	27.1	1.5	188	31	156	28	90	89
PTMO$_{2000}$	21.1	2.9	183	27	164	19	93	86
PTMO$_{2900}$	15.7	3.5	-	-	-	-	-	86
Series 2								
(PTMO$_{1000}$-T)$_{4000}$	11.9	1.7	-	-	-	-	-	85
(PTMO$_{1000}$-T)$_{6000}$	8.3	1.7	-	-	-	-	-	89
(PTMO$_{1000}$-T)$_{8000}$	6.4	1.5	-	-	-	-	-	93
(PTMO$_{1000}$-T)$_{10,000}$	5.2	1.8	-	-	-	-	-	81
(PTMO$_{1000}$-T)$_{20,000}$	2.7	1.8	-	-	-	-	-	92

DSC

The melting and crystallisation behaviour of the segmented copolymers was evaluated using DSC (Table 3.2). For polymers with a low concentrations of crystallisable segment (<16%) no melt and crystallisation peaks related to the rigid block were observed. The melting enthalpy and melting temperature decrease with decreasing amount of rigid segment. The difference between the melting peak and the onset of the crystallisation peak, the so-called undercooling, is only 20 degrees. This means that crystallisation is extremely fast. The degree of crystallinity can be calculated using the melting enthalpy of the pure T6A6T (138 J/g)[12,18]. For these segmented copolymers the crystallinity is high, 80 - 90%.

FT-IR

FT-IR is a helpful tool for studying the crystallinity of the amide groups in polymers. The carbonyl and amide bands depend on the strength of the hydrogen bonds (Figure 3.4). Temperature dependent infrared was used to study the crystallinity as a function of temperature and particular the transition of carbonyl groups from the crystalline state to the amorphous state (Figure 3.5).
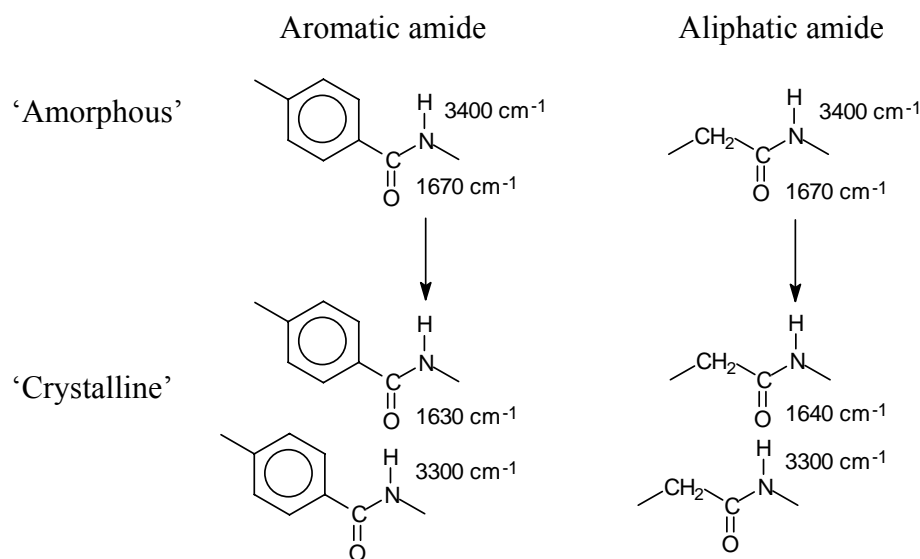
Aromatic amide   Aliphatic amide

'Amorphous'

'Crystalline'

Figure 3.4: Infrared absorption bands of aromatic and aliphatic amide[21,22].

The amide I band is of interest, as this band is sensitive to the amorphous or crystalline state. For the C=O groups in the crystalline state, two peaks are observed at 1630 cm^{-1} (aromatic) and 1640 cm^{-1} (aliphatic) amide[21,22]. The amorphous amide C=O groups give a broad peak at 1670 cm^{-1}.
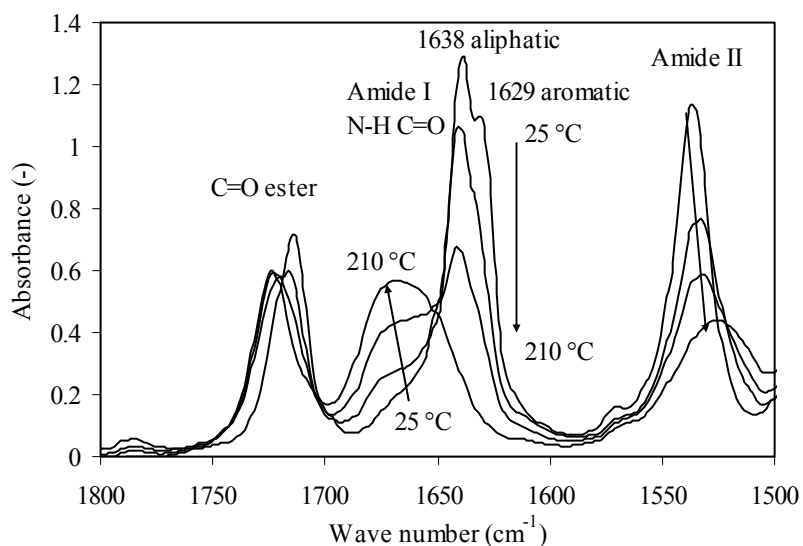
Figure 3.5: Temperature dependent FT-IR spectra of PTMO$_{1000}$-T6A6T (T$_m$ = 191 °C): 25, 160, 190 and 210 °C.

The crystalline amide I peaks (1630 and 1640 cm^{-1}) are high up to the melting temperature of the copolymer (Figure 3.5). Upon melting, the intensity of these peaks decreases, while at the same time the intensity of the peak at 1670 cm^{-1} of amorphous C=O groups increases. The ratio of these crystalline and amorphous amide peaks gives an indication of the crystallinity of the polymer (Equation 3.1). An absolute calculation of the crystallinity was already done for Nylon-6,6 and proved to be linear with the density of the polymer[23]. In Figure 3.6 the crystallinity of PTMO$_{1000}$-T6A6T is given as a function of the temperature in a heating and a cooling cycle. The crystallinity of the T6A6T segment in the copolymer was high (92%) at room temperature and remained high to 150 °C. At 170 °C, just before the melting temperature, a sharp decrease in crystallinity was observed. At temperatures above the melting temperature still some crystallinity of the T6A6T segments was observed. This is possibly due to a small fraction of longer amide segments in the copolymer, which have a higher melting temperature. The cooling cycle shows a similar path as the heating curve and the crystallinity recovered completely.
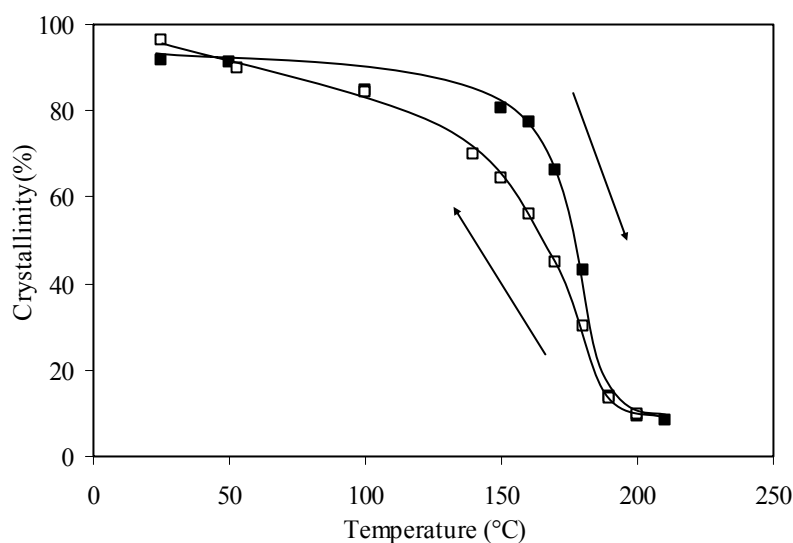
Figure 3.6: Crystallinity as a function of temperature for PTMO$_{1000}$-T6A6T: ■, heating curve; □, cooling curve.

For the copolymers of series 1 and 2 the FT-IR at room temperature was studied (Figure 3.7). When PTMO is extended with DMT (series 2) the ester content in the polymer increases resulting in an increase of the peak at 1720 cm^{-1}[20]. For series 1 the ester to amide ratio is always the same. The crystallinity of the copolymers was calculated comparing the ratio of the crystalline amide (1630 cm^{-1}) and amorphous amide (1670 cm^{-1}) peaks by using

Equation 3.1. The factor 'a' in this equation is the peak height ratio of the amide in the melted state and crystalline state of $PTMO_{1000}$-T6A6T and it was assumed that this ratio is constant for all PTMO lengths.
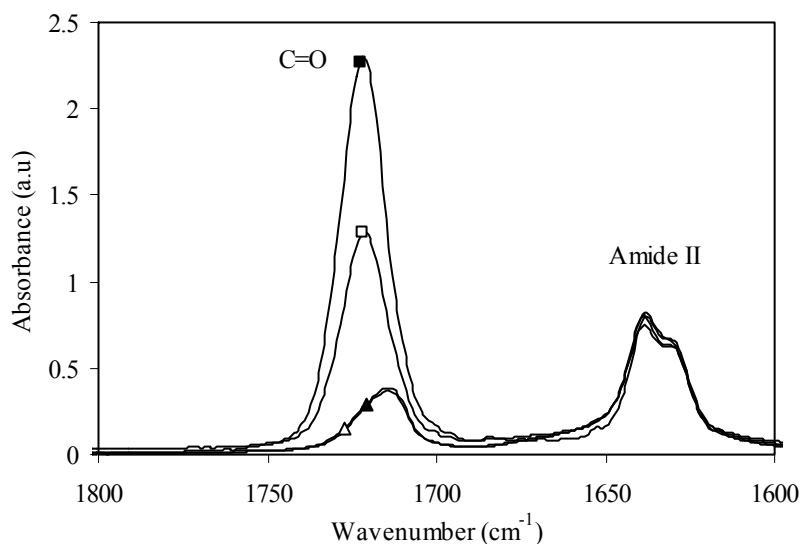

Figure 3.7: FT-IR 1600 - 1800 cm^{-1} for: Δ, PTMO$_{1000}$-T6A6T: ▲, PTMO$_{2000}$-T6A6T; □, (PTMO$_{1000}$-T)$_{4000}$-T6A6T; ■, (PTMO$_{1000}$-T)$_{8000}$-T6A6T.

It is realised that the calculated degree of crystallinity is not very accurate but it is a good estimation. The so determined crystallinities of the copolymers were high (Table 3.2) and even for the segmented copolymers with just 2 - 5% of crystallisable segment a high degree of crystallinity of the hard segments was found. The crystallinities determined in this way correspond well with those determined by DSC (Table 3.2).

AFM

The morphology of the copolymers was studied by AFM. In the AFM phase image the difference between the hard and soft phase can be distinguished and the white ribbons are the T6A6T crystallites. The thickness of the ribbon is expected to be the extended length of T6A6T, about 3.7 nm. From the AFM image an average thickness of the ribbons of ~4 - 5 nm was measured. This thickness is an indication because with the AFM tip dimensions the thickness can not be measured accurately. In Figure 3.8 the length of a crystalline ribbon is up to 1 μm. The total length of a ribbon can not be measured with AFM as only the morphology at the surface is measured while ribbons can bend out of the surface. TEM

measurements of similar copolymers revealed a ribbon length of 1000 - 5000 nm[12]. Therefore, the aspect ratio of the crystalline ribbons is expected to be about 200 - 1000.

2 µm
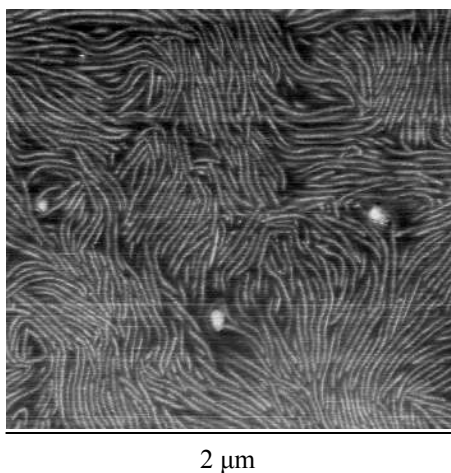
Figure 3.8: AFM phase image of (PTMO$_{1000}$)$_{20,000}$-T6A6T solution cast on a silicon wafer.

SAXS

Small-angle X-ray scattering (SAXS) has been used to investigate the morphology of the segmented block copolymers. With temperature dependent SAXS the copolymer PTMO$_{1000}$-T6A6T was studied in a heating and cooling scan. For the heating scan, the scattering intensity I(q) is plotted versus the scattering vector q (nm) (Figure 3.9). The background was subtracted from the intensity. The first maximum in the SAXS curve is from the scattering of the beam. The second maximum of q is related to the interdomain spacing (L).

Figure 3.9: SAXS curves of PTMO$_{1000}$-T6A6T (T$_m$ = 191°C) for increasing temperatures.

The domain spacing was calculated using Equation 3.5.

$$L = \frac{2\pi}{q} \qquad \text{(nm)}$$

(Equation 3.5)

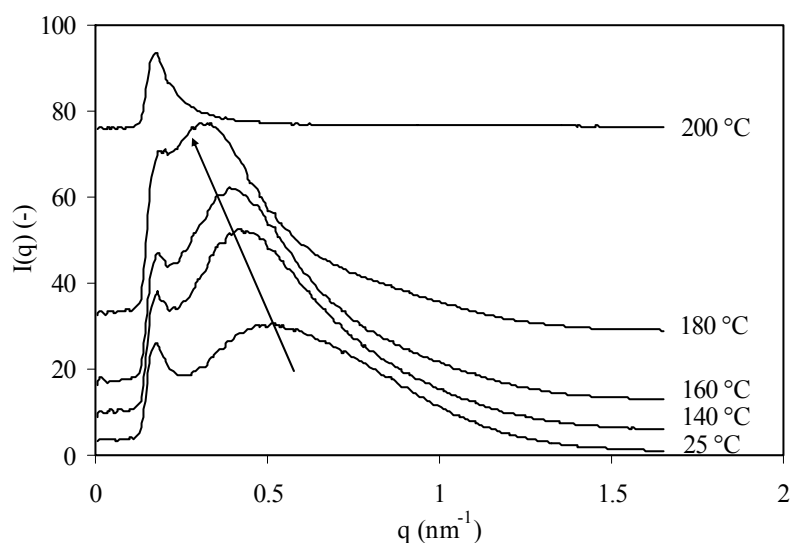The domain spacing (L) of $PTMO_{1000}$-T6A6T at 25 °C was 12 nm and slightly increased upon heating (Figure 3.10). This is because uniform segments were used and these all melt at one temperature.
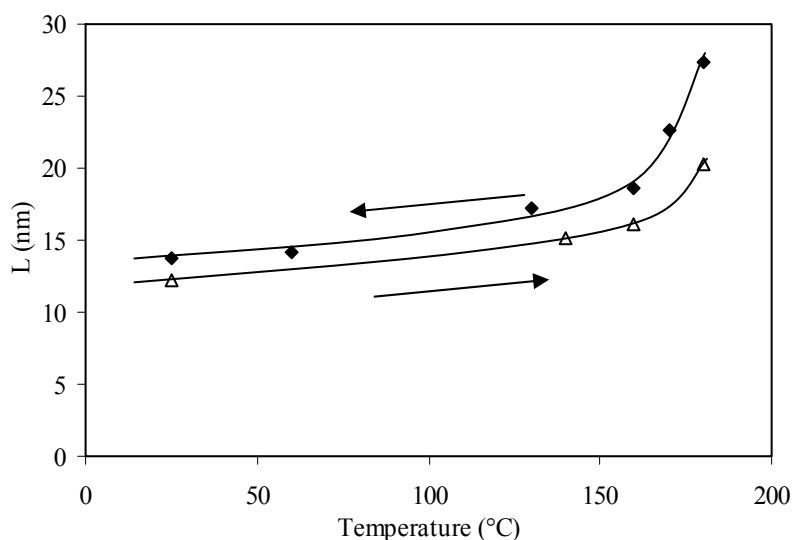
Figure 3.10: Domain spacing for $PTMO_{1000}$-T6A6T versus temperature: Δ, heating; ♦, cooling.

Above the melting temperature of the segmented copolymer there was no long range order, which is an indication that no crystalline order was present in the melt. Upon cooling, the domain spacing nearly returned to the starting value. The domain spacing of the cooling curve is close to the heating curve, confirming the high rate of crystallisation. A similar fast crystallisation rate was also reported for other copolymers with uniform crystallisable segments[24,25].

The lamellar thickness can be determined from the SAXS data with the linear correlation function (Equation 3.6 and 3.7). This function is based on a two phase lamellar morphology and is obtained by a cosine transformation and Riemann integration of the SAXS data[26]. It is assumed that the crystalline domains are stacked periodically.

$$\gamma(r) = \frac{1}{Q} \int_0^\infty I(q) * q^2 (\cos 2\pi r q) dq \qquad \textit{(Equation 3.6)}$$

$$Q = \int_0^\infty I(q) * q^2 dq \qquad \textit{(Equation 3.7)}$$

With   Q: invariant (-)

I(q): scattering intensity (-)

q: scattering vector (nm^{-1})

r: radius (nm)

The calculated correlation function shows a typical graph corresponding well to literature[24,25].
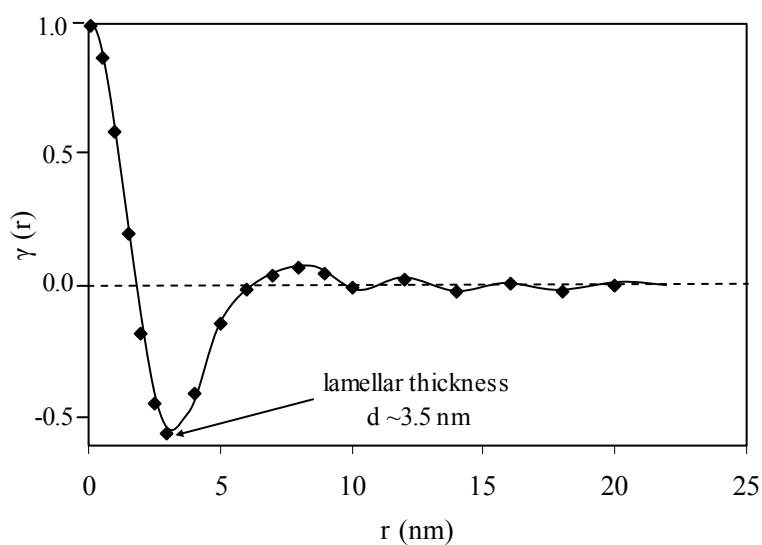

Figure 3.11: Correlation function for PTMO$_{1000}$-T6A6T.

The minimum in the linear correlation function reveals for PTMO$_{1000}$-T6A6T a lamellar thickness of ~3.5 nm at room temperature. A similar value was obtained for PTMO$_{2000}$-T6A6T (Table 3.3). The calculated lamellar thickness corresponds well with the extended length of the T6A6T segments, which is 3.7 nm (Figure 3.8).
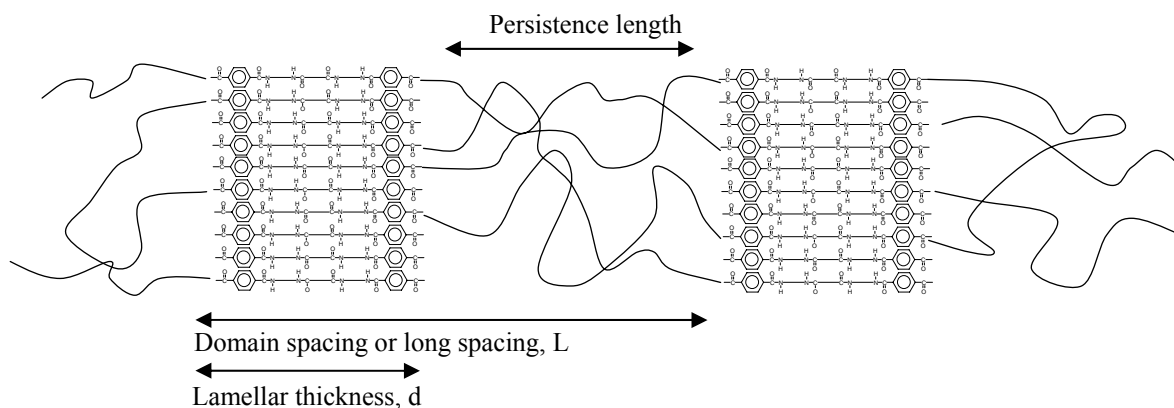
Figure 3.12: Schematic representation of the morphology of a segmented copolymer with uniform crystallisable segments.

With the longer $PTMO_{2000}$ segments the lamellar thickness did not change but the lamellar spacing (L) increased. The determined morphology dimensions are given in Table 3.3.

Table 3.3: Long spacing, lamellar thickness and amorphous domain thickness for $PTMO_{1000}$-T6A6T and $PTMO_{2000}$-T6A6T.

	q_{max} (nm^{-1})	Long spacing, L (nm)	Lamellar thickness, d (nm)	Persistence length (L-d) (nm)
$PTMO_{1000}$-T6A6T	0.51	12.2	3.5	8.7
$PTMO_{2000}$-T6A6T	0.42	15.1	3.5	11.6

The persistence length of PTMO in the copolymer was calculated by subtracting the lamellar thickness from the long spacing (Table 3.3, Figure 3.12). The persistence length of a polymer increases with the square root of the length of a polymer chain. An increase from $PTMO_{1000}$ to $PTMO_{2000}$ in the segmented copolymer increases the persistence length with the square root of the segment length. Assuming the persistence length of 8.7 nm for $PTMO_{1000}$-T6A6T is correct, a persistence length of 12.3 nm for $PTMO_{2000}$ was calculated, which is close to the measured value.

DMTA

Series 1: PTMO$_x$-T6A6T

Thermal mechanical properties of these polymers were studied using DMTA and the storage modulus and loss modulus versus temperature were determined (Figure 3.13). Three

transitions are present: the glass transition of the soft phase, the melting transition of the PTMO and the melting transition of T6A6T. A glass transition of an amorphous T6A6T phase, expected at about 125 °C, was not observed. The T_g of the soft phase of PTMO$_x$-T6A6T increases from -70 °C for PTMO$_{2900}$ and PTMO$_{2000}$ to -45 °C for PTMO$_{650}$. This increase in T_g is due to the increase of the density of physical crosslinks[27]. The low T_g values for PTMO$_{2900}$ and PTMO$_{2000}$ based polymers indicates that the concentration of T6A6T segments in the polyether phase is very low.

Table 3.4: DMTA properties of PTMO$_x$-T6A6T with varying molecular weight of PTMO.

	T6A6T (%)	T_g (°C)	T_{flex} (°C)	G'$_{25 °C}$ (MPa)	T_{flow} (°C)	ΔG' *10^{-3} (°C^{-1})
Series 1						
PTMO$_{650}$	43.8	-45	35	102	200	5.0
PTMO$_{1000}$	34.2	-60	-15	51	185	4.9
PTMO$_{1400}$	27.1	-65	0	30	180	4.0
PTMO$_{2000}$	21.1	-70	10	20	180	2.9
PTMO$_{2900}$	15.7	-70	20	9	175	1.8
Series 2						
(PTMO$_{1000}$-T)$_{4000}$	11.9	-63	5	8	165	2.1
(PTMO$_{1000}$-T)$_{6000}$	8.3	-63	10	6	160	0.7
(PTMO$_{1000}$-T)$_{8000}$	6.4	-62	15	4	150	0.7
(PTMO$_{1000}$-T)$_{10,000}$	5.2	-60	15	3	150	1.7
(PTMO$_{1000}$-T)$_{20,000}$	2.7	-62	15	1.6	130	1.8

The flex temperature (T_{flex}) is the start of the rubber plateau and varies from -15 till 35 °C. The T_{flex} is particularly low for PTMO$_{1000}$-T6A6T. For shorter PTMO length PTMO$_{650}$-T6A6T the T_{flex} is increased by the higher T_g due to the increased network density. For a longer PTMO length the T_{flex} is influenced by the crystallisation of PTMO segments. PTMO segments with a molecular weight above 1400 g·mol^{-1} can crystallise[14]. This crystalline phase will melt at approximately ~0 °C, giving a shoulder after the T_g and increasing the T_{flex} to 5 - 10 °C.

The copolymers have a rubber modulus that is almost temperature independent and this is typical for copolymers with crystallisable segments of uniform length[2,4,28]. The stability of the rubber modulus at increasing temperature is quantified with ΔG' (Equation 3.2, Table 3.4). A high value of ΔG' indicates a modulus that strongly depends on temperature. The ΔG'-values decrease slightly with longer PTMO length and this may be due to a less-

developed phase separation. The uniform segments in these copolymers form lamellae with a uniform thickness, which lead to a well defined flow temperature. These flow temperatures correspond well with the melt temperatures measured with DSC (Table 3.2).
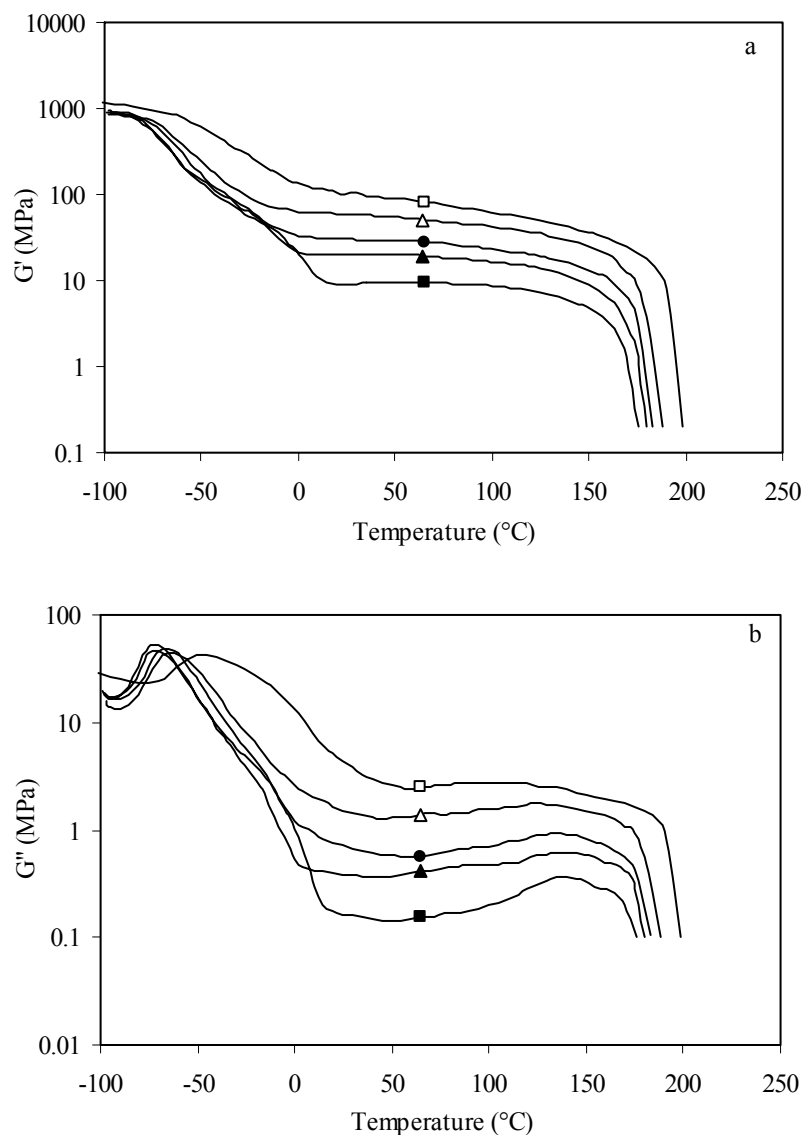
Figure 3.13: a) Storage modulus and b) loss modulus as a function of temperature for PTMO$_x$-T6A6T with varying molecular weight of PTMO: □, 650 g·mol^{-1}; Δ, 1000 g·mol^{-1}; ●, 1400 g·mol^{-1}; ▲, 2000 g·mol^{-1}; ■, 2900 g·mol^{-1}.

Series 2 (PTMO$_{1000}$-T)$_x$-T6A6T

A second polymer series, (PTMO$_{1000}$-T)$_x$-T6A6T with uniform T6A6T and PTMO$_{1000}$-T with length x of 4000 - 20,000 g·mol^{-1} was synthesised. The mechanical properties of (PTMO$_{1000}$-T)$_x$-T6A6T are listed in Table 3.4 and shown in Figure 3.14. The values of the

T_g's for $PTMO_{1000}$ from series 1 and $(PTMO_{1000}-T)_x$ from series 2 are similar, suggesting that the extension of PTMO with terephthalate has little effect on the T_g or phase separation. All polymers of the second series have an almost temperature independent rubber modulus over a wide temperature range. Even very low concentrations of T6A6T (2.7%) in the segmented copolymer give already a rubber plateau and a flow temperature of 130 °C.
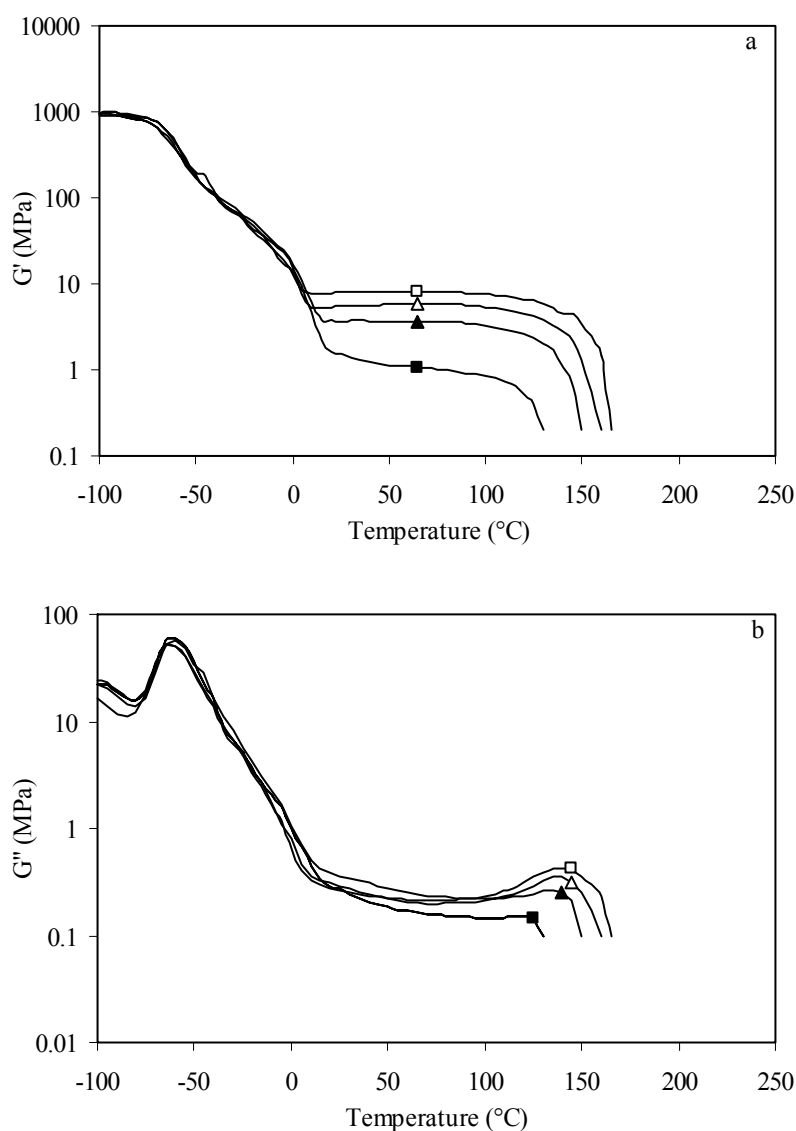
Figure 3.14: a) Storage modulus and b) loss modulus as a function of temperature for varying x of $(PTMO_{1000}-T)x-T6A6T$: □, 4000 g·mol^{-1}; Δ, 6000 g·mol^{-1}; ▲, 10,000 g·mol^{-1}; ■, 20,000 g·mol^{-1}.

The DMTA spectra of the polymers of series 1 and 2 show the effect of varying PTMO length or amide percentage on the rubber modulus as a function of temperature. The rubber plateau of all copolymers is fairly constant, as is the case with other polymers with

crystallisable segments of uniform length[2,4,28]. $G'_{25\,°C}$ of these polymers increases strongly with increasing amide content (Figure 3.15). This can be explained by the increasing concentration of crystallites and the aspect ratio of these crystallites (Figure 3.8)[12].

Many models, e.g. Wegner, Cox or Guth-Smallwood, describe the modulus as a function of filler content[1,29-31]. A model describing the change in modulus as a function of crystalline content and aspect ratio is that of Halpin-Tsai[12,29]. Halpin-Tsai describes the elastic modulus of a fibre composite for randomly oriented fibres as a function of fibre content and aspect ratio. In this calculation it was assumed that the crystallinity of the amide segments was 88%. The following parameters were used for the calculation of the modulus as a function of aspect ratio and filling content of rigid segment. The calculation can be found in the appendix of reference[12].

Table 3.5: Parameters used for the Halpin-Tsai model.

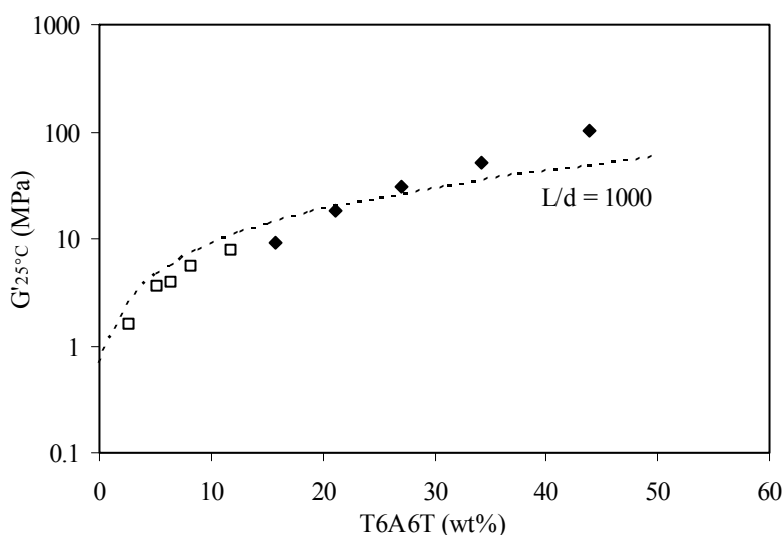| E_s:	modulus matrix, extrapolated from Figure 3.15	2.1 MPa
$E_{//}=E_\perp$:	$E_\perp$ of Kevlar®[32]	5000 MPa
L/D:	Aspect ratio (TEM), [12]	1000
v_s:	Poisson ratio PTMO[32]	0.5
v_c:	Poisson ratio (Kevlar)[32]	0.35

Figure 3.15: Storage modulus versus amide %: ♦, series 1, PTMO$_x$-T6A6T; □, series 2, (PTMO$_{1000}$-T)$_x$-T6A6T; ----Halpin-Tsai relation L/d = 1000.

The Halpin-Tsai model (dotted line) with a E-modulus for the crystallites of 5 GPa and an aspect ratio of 1000 fits reasonably well to the experimental results[12,25,29]. Composite moduli increase with increasing aspect ratio of the fibre and with increasing fibre filler content. A high aspect ratio of the crystallites is therefore advantageous.

The flow temperatures of the T6A6T segments in the copolymers are sharp and decrease with increasing PTMO length. This lowering in the flow temperature can be explained with the solvent effect, as proposed by Flory[33]. This equation is based on the assumption that the solution is ideal. The change in flow temperature can be related to the change in the molar fraction of the crystalline segment, X_A.

$$\frac{1}{T_m} - \frac{1}{T_m^0} = -\left(\frac{R}{\Delta H_f}\right) \ln X_A \qquad \text{(Equation 3.8)}$$

This equation is valid if the molar volumes of both segments are about the same. In that case, X_A is not only a molar fraction but also a weight fraction. A straight line can be fitted through the points of Figure 3.16, indicating that the melting depression of the crystalline segments can be well described by the Flory equation.

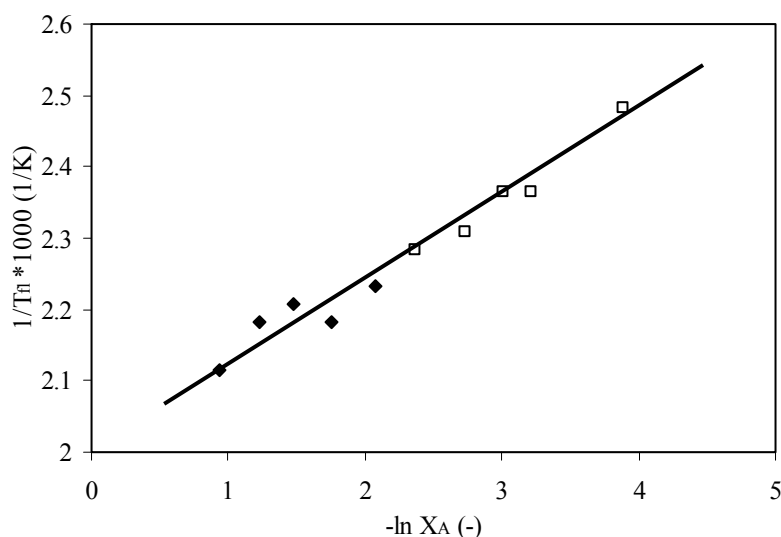*Figure 3.16: $1/T_{flow}$ versus $\ln X_A$: ♦, series 1, $PTMO_x$-T6A6T; □, series 2, $(PTMO_{1000}$-T$)_x$-T6A6T.*

The intercept at y = 2.0144 is at a flow temperature of 224 °C. The lowering of the melting temperature of the copolymers seems thus to be due to the solvent effect of the PTMO phase.

Compression set

A standard method to measure the elasticity of polymers is the compression set test. A lower compression set refers to more elastic behaviour. The compression set was measured for both series (Table 3.6). In earlier research, Krijgsman[9] also found compression set values below 10% for low moduli segmented copolymers with uniform tetra-amide segments. Normally, the compression set decreases for polymers with decreasing modulus, as is the case for series 1 (Figure 3.17). When the crystalline content is lower, there is less plastic deformation. The second series shows the opposite effect, the compression set slightly increases for decreasing moduli. These results suggest that very low crystallisable segment contents do not enhance the elastic properties further. Apparently, if the concentration of tetra-amide is low, the physical crosslink density becomes to low to respond effectively to the deformation during the compression set. This minimum was also observed for $(PTMO_{1000}\text{-}T)_x\text{-}T\Phi T$ segmented copolymers[11,16]. The CS values are low compared to segmented copolymers in general[1].
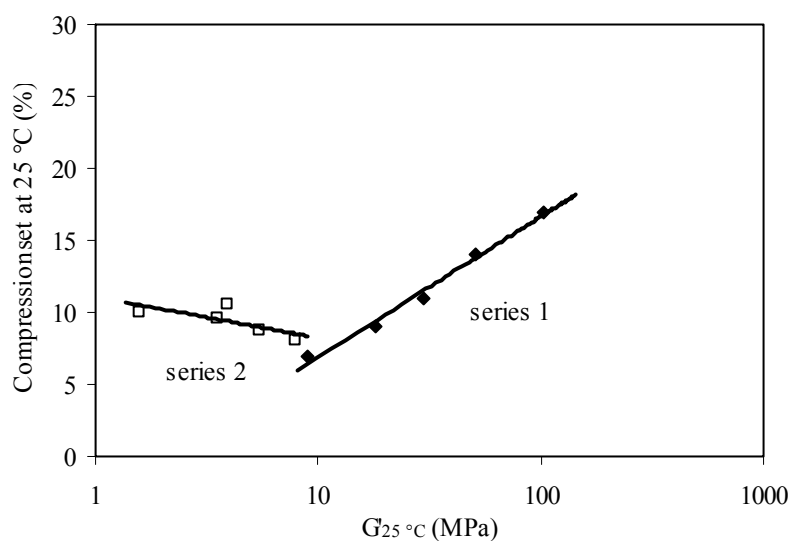
Figure 3.17: $CS_{25\%}$ at 25 °C as a function of modulus: ♦, series 1, $PTMO_x\text{-}T6A6T$; □, series 2, $(PTMO_{1000}\text{-}T)_x\text{-}T6A6T$.

Tensile set

The elastic behaviour of TPE's is often quantified by a compression set test. A disadvantage of the compression test is that it is a one-point test, only indicating a measure of the elasticity using one compression. A test that gives more insight in the elastic behaviour of polymers as a function of strain is the cyclic tensile set test. The strain of each loading-unloading cycle

was increased (staircase loading) and the tensile set (TS) of the strain increment was determined as a function of the applied strain. In Figure 3.18 the tensile set is plotted versus the strain. A lower tensile set value corresponds with a more elastic response of the polymer.
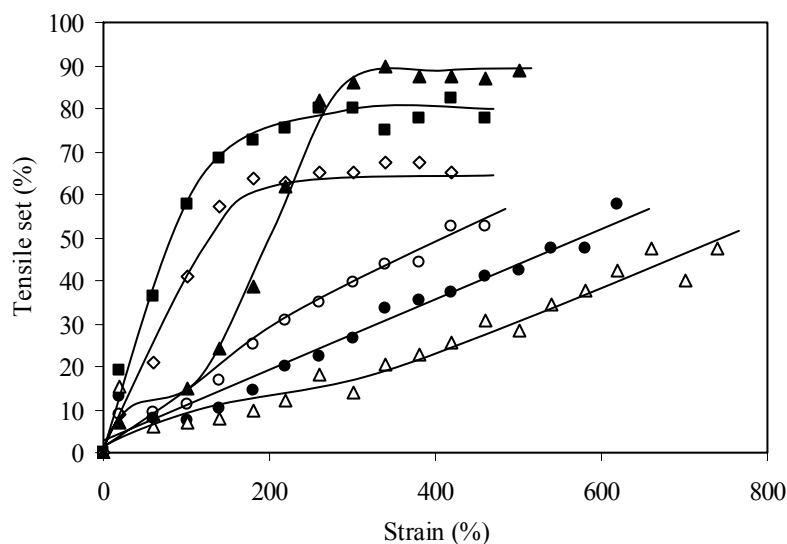
Figure 3.18: Tensile set as a function of the applied strain: ■, PTMO$_{650}$-T6A6T; ◊, PTMO$_{1400}$-T6A6T; ▲, PTMO$_{2900}$-T6A6T; o, (PTMO$_{1000}$-T)$_{4000}$-T6A6T; ●, (PTMO$_{1000}$-T)$_{6000}$-T6A6T; Δ, (PTMO$_{1000}$-T)$_{10,000}$-T6A6T.

Up to 200% strain, the TS-values of the polymers increase with increasing strain. This increase is stronger with increasing amount of tetra-amide. For copolymers with a high amount of tetra-amide, the TS seem to level off at high strains. The strong upswing for PTMO$_{2900}$-T6A6T at 200% strain is caused by strain induced crystallisation of the long PTMO segments. Crystallisation of PTMO negatively influences the elasticity of the polymer. For copolymer series 2, the crystallisation of PTMO segments was diminished by using a small terephthalate extender, which breaks up the regularity of the chains and prevents crystallisation[7,9,10,16]. This results in low TS values even at high strains. For copolymers with a lower tetra-amide content the TS increases less steep. The increase in TS is probably caused by the break up of lamellae. For copolymers with a high content of tetra-amide this break up of lamellae takes place at lower strains.

A typical value is the TS at 50% strain (TS$_{50\%}$) (Table 3.6). The TS$_{50\%}$ decreases with decreasing tetra-amide content and thus also with decreasing modulus (Table 3.6, Figure 3.19). The harder materials have considerable higher TS$_{50\%}$ values. The strong upswing is probably caused by the fact that the polymers with a higher modulus have a yield point

below 50% strain. The plastic deformation is much higher above the yield point where lamellae are broken up.
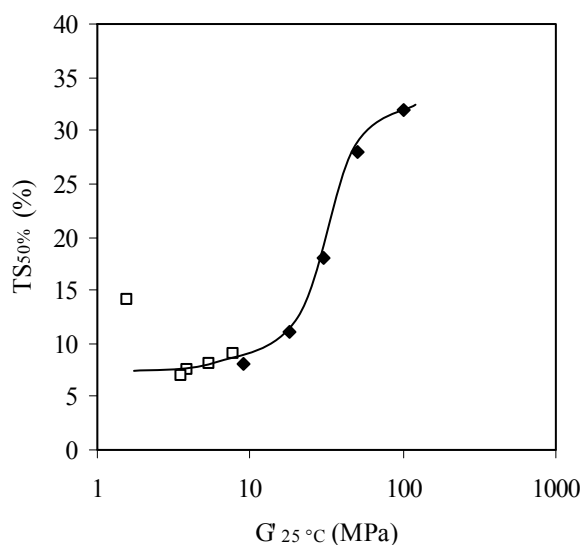
Figure 3.19: $TS_{50\%}$ as a function of modulus: series 1; ♦, $PTMO_x$-T6A6T and series 2; □, $(PTMO_{1000}$-T$)_x$-T6A6T.

Tensile testing

Tensile properties of the segmented block copolymers were studied using injection moulded bars cut to dumbbells (ISO37 s2) (Figure 3.20, Table 3.6). The stress-strain curves are typical for thermoplastic elastomeric materials.
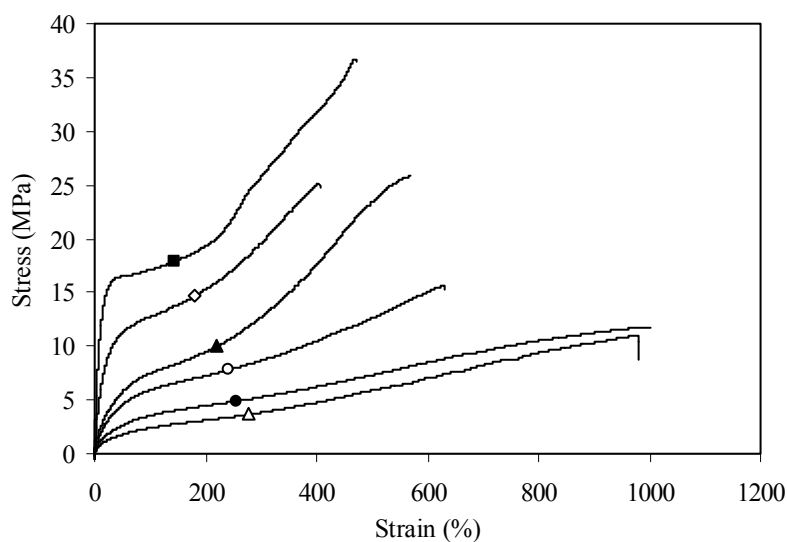
Figure 3.20: Tensile test: ■, $PTMO_{650}$-T6A6T; ◊, $PTMO_{1400}$-T6A6T; ▲, $PTMO_{2900}$-T6A6T; O, $(PTMO_{1000}$-T$)_{4000}$-T6A6T; ●, $(PTMO_{1000}$-T$)_{6000}$-T6A6T; Δ, $(PTMO_{1000}$-T$)_{10,000}$-T6A6T.

At small deformations the stress increases linearly with the strain (Hooke's Law)[34]. Above the yield strain the stress gradually increases. At higher strains, strain hardening can take place. The E-modulus increases strongly with the concentration of tetra-amide segment as was also the case with the G'-modulus (Figure 3.15) and can be described with the Halpin-Tsai model[29].

The yield strain is generally considered as the highest strain of a material where deformation is mainly elastic[35]. For elastic materials it is important that the yield strain is high so that high strains can be applied without plastic deformation. In these series of segmented copolymers, the yield stress and yield strain both depend linearly on the content of tetra-amide in the copolymer (Figure 3.21b, c). In semi-crystalline polymers the yield stress depends on the crystallinity and the crystal thickness in the segmented copolymer[35]. As in these two series uniform lamellae are used, the yield stress is determined by the crystallisable segment content. Combining the results of the modulus and the yield stress as a function of amide content, the log E-modulus depends linearly on the yield stress.

Table 3.6: Tensile properties of PTMO$_x$-T6A6T copolymers: series 1, PTMO$_x$-T6A6T; series 2, (PTMO$_{1000}$-T)$_x$ - T6A6T.

	Tetra-amide (%)	E-modulus (MPa)	ε_{yield} (%)	σ_{yield} (MPa)	ε_b (%)	σ_b (MPa)	CS $_{25\,°C}$ (%)	TS$_{50\%}$ (%)
Series 1								
PTMO$_{650}$	43.8	311	25	16	471	37	17	32
PTMO$_{1000}$	34.2	133	29	12	593	37	14	28
PTMO$_{1400}$	27.1	87	42	11	407	25	11	18
PTMO$_{2000}$	21.1	46	49	9	476	29	9	11
PTMO$_{2900}$	15.7	29	66	6	568	26	7	8
Series 2								
(PTMO$_{1000}$-T)$_{4000}$	11.9	24	69	5	632	15	13	9
(PTMO$_{1000}$-T)$_{6000}$	8.3	17	75	3	1000	12	9	8
(PTMO$_{1000}$-T)$_{8000}$	6.4	13	72	2.5	848	8	10	7.5
(PTMO$_{1000}$-T)$_{10,000}$	5.2	11	77	2	980	9	10	7
(PTMO$_{1000}$-T)$_{20,000}$	2.7	3	110	1.3	872	11	9	14

At higher strains there is an upsweep in the stress-strain curve due to strain hardening. This effect is stronger for segmented copolymers with lower PTMO length. The strain hardening for PTMO$_{2000}$ and PTMO$_{2900}$ is due to strain crystallisation of these PTMO segments. Strain

hardening is strongly influenced by the molecular weight of the copolymer[10,36]. The fracture strains, using cut dumbbells, did easily reach strains above 400% and the series 2 copolymers, with lower moduli, did reach strains up to 1000%.

Spun fibres of similar segmented copolymers easily reached strain at breaks over 1000%[10,15].
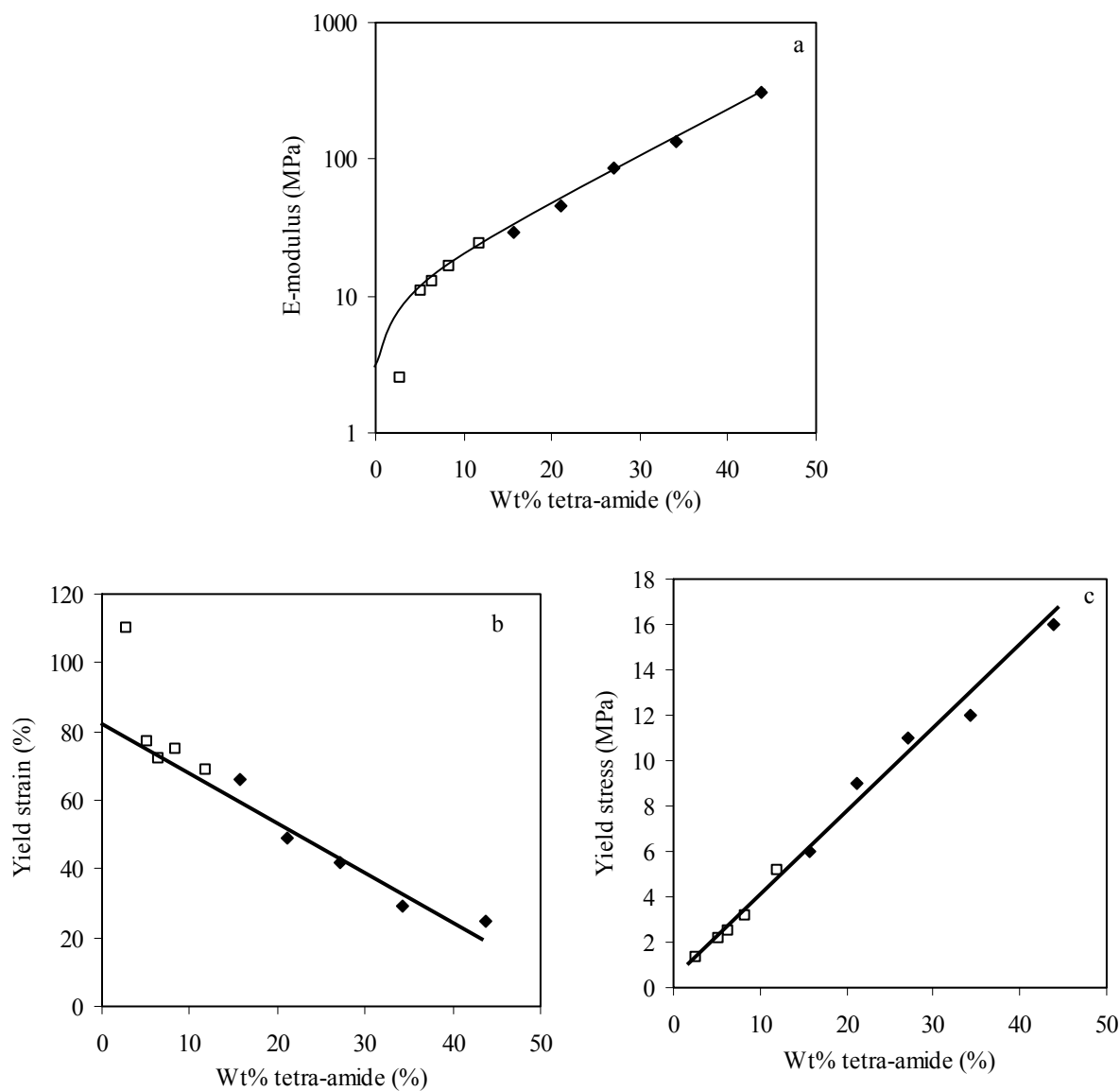

Figure 3.21: Dependence of a) E-Modulus b) yield strain and c) yield stress on the crystallisable segment content T6A6T in the segmented copolymers of series 1: ♦, PTMOx-T6A6T and series 2; □, (PTMO1000-T)x-T6A6T.

Conclusions

Three synthesis routes for segmented block copolymers based on PTMO and tetra-amide units were studied. Polymers were synthesised by a melt polymerisation, a combined solvent/melt polymerisation and a synthesis route starting with PTMO, 6A6-diamine and DPT. All routes resulted in polymers with high molecular weight. $PTMO_x$-T6A6T copolymers prepared from solution/melt had the best properties like a lower CS and a higher G'. Therefore this route was used for the syntheses of series 1 and 2.

In these series the length of the PTMO segment was changed from 650 - 20,000 g·mol^{-1} and thereby the concentration of tetra-amide segments was decreased from 44 to 2.7 wt%. The crystallinity of the T6A6T segments in the copolymers was studied with DSC and FT-IR. The crystallinities obtained by FT-IR correspond well with those obtained by DSC. The crystallinity of the T6A6T segments in the copolymers was on average 88%. The crystallinity measured with FT-IR remained high up to the melting temperature of the copolymer. Upon cooling the crystallinity of the rigid segments was close to the crystallinity of the heating curve, indicating fast crystallisation of the tetra-amide segments.

The long-spacing as a function of temperature and PTMO length was determined with SAXS. The long-spacing in the segmented polymers hardly changed up to the melting temperature, indicating the presence of stable lamellae. After cooling from the melt, the L-spacing as a function of temperature was only slightly different as determined during heating. The crystallite thickness was found to be 3.5 nm, which is close to the extended length of the T6A6T segment. The persistence length increased with the square root of the amorphous segment length.

The copolymers have a T_g at -70 °C, indicating good phase separation of the ether and amide segments. The amide segments formed crystallites with a nano-ribbon shape with a thickness of 4 nm and several μm long. The modulus of the rubbery plateau is almost temperature independent. The modulus at room temperature increases strongly (1 - 102 MPa) with amide content and this increase can be modelled with the Halpin-Tsai model. The model fits reasonably well when using an aspect ratio of the nano ribbons (L/d) of 1000. The melting

temperature decreases with decreasing concentration of tetra-amide and this can be explained by the solvent effect as proposed by Flory.

The elastic behaviour of these segmented copolymers was evaluated with compression set and tensile set tests. Compression set measurements at room temperature showed values below 20% that decrease for lower concentration of tetra-amide segment. For concentrations of tetra-amide lower than 16%, the compression set slightly increases, indicating that a minimum amount of tetra-amide is necessary. The tensile set data indicate a more elastic behaviour for polymers with lower content of tetra-amide. Tensile experiments showed a linear increase in yield stress and a linear decrease in yield strain with increasing tetra-amide segment content.

References

1. Holden, G., Legge, N.R., Quirk, R.,.Schroeder, H.E., *'Thermoplastic elastomers'*, Hanser Publisher, Second Ed. Munich (1996).
2. Allegrezza, A.E., Seymour, R.W., Ng, H.N., Cooper, S.L., *Polymer* **15**, 433-440 (1974).
3. Harrel, L.L., *Macromolecules* **2**, 607-612 (1969).
4. Ng, H.N., *Polymer* **14**, 255-261 (1973).
5. Versteegen, R.M., Sijbesma, R.P., Meijer, E.W., *Angew. Chem. Intern. Ed.* **38**, 2917-2919 (1999).
6. Bennekom van, A.C.M., Gaymans, R.J., *Polymer* **38**, 657-665 (1997).
7. Husken, D., Krijgsman, J., Gaymans, R.J., *Polymer* **45**, 4837-4843 (2004).
8. Hutten van, P.F., Mangnus, R.M., Gaymans, R.J., *Polymer* **34**, 4193-4202 (1993).
9. Krijgsman, J., Husken, D., Gaymans, R.J., *Polymer* **44**, 7573-7588 (2003).
10. Krijgsman, J., Gaymans, R.J., *Polymer* **45**, 437-446 (2004).
11. Niesten, M.C.E.J., Feijen, J., Gaymans, R.J., *Polymer* **41**, 8487-8500 (2000).
12. Schuur van der, J.M., *'Poly(propylene oxide) based segmented block copolymers'*, Ph.D. Thesis, University of Twente (2004).
13. Serrano, P.J.M., Thuss, E., Gaymans, R.J., *Polymer* **38**, 3893-3902 (1997).
14. Dreyfuss, P. *et al.*, *'Encyclopedia of Polymer Science and Engineering'*, New York (1989).
15. Niesten, M.C.E.J., Krijgsman, J., Gaymans, R.J., *Abstracts of Papers of the American Chemical Society* **218**, U521 (1999).
16. Niesten, M.C.E.J., ten Brinke, J.W., Gaymans, R.J., *Polymer* **42**, 1461-1469 (2001).
17. Krijgsman, J., Husken, D., Gaymans, R.J., *Polymer* **44**, 7043-7053 (2003).
18. Krijgsman, J., *'Segmented copolymers based on poly(2,6-dimethyl-1,4,phenylene ether)'*, Ph.D. Thesis, University of Twente (2002).
19. Costa, L., Luda, M.P., Cameron, G.G., Qureshi, M.Y., *Polym. Degrad. Stab.* **67**, 527-533 (2000).
20. Chapter 2 of this thesis

21. Dechant, J., *'Ultrarot-spektroskopische Untersuchungen an Polymeren'*, Maxim Gorki, Berlin (1972).

22. Gaymans, R.J., *J. of Polymer Science* **23**, (1985).

23. Zbinden, R., *'Infrared spectroscopy of high polymers'*, Academic Press, New York and London (1964).

24. Heijkants, R.G.J.C., *'Polyurethane scaffolds as meniscus reconstruction materials'*, Ph.D. Thesis, University of Groningen (2004).

25. Versteegen, R.M., *'Well-defined Thermoplastic Elastomers'*, Ph.D. Thesis, University of Eindhoven (2003).

26. Ryan, A.J., Stanford, J.L., Bras, W., Nye, T.M.W., *Polymer* **38**, 759-768 (1997).

27. Nielsen, L.E., *J. Macromol. Sci. Rev. Macromol. Chem.* 69-103 (1969).

28. Eisenbach, C.D., Stadler, E., Enkelmann, V., *Macromol. Chem. Phys.* **196**, 833-856 (1995).

29. Halpin, J.C., Kardos, J.L., *J. Appl. Phys.* **43**, 2235 (1972).

30. Hiemenz, P.C., *'Polymer chemistry'*, Marcel Dekker, 1st New York (1984).

31. Hull, D., *'An introduction to composite materials'*, Cambridge University, 1st Cambridge (1981).

32. Mc Crum, N.G., Buckley, C.P.,.Bucknall, C.B., *'Principles of polymer engineering'*, Oxford university press, 2nd New York (2001).

33. Flory, P.J., *Trans. Faraday Soc.* 848 (1955).

34. Hertzberg, R.W., *'Deformation and fracture mechanics of engineering materials'*, John Wiley, 3rd edition New York (1989).

35. Mark, J., Mandelkern, L. *'Physical properties of polymers'*. Cambridge University Press,(2004).

36. Niesten, M.C.E.J., Gaymans, R.J., *Polymer* **42**, 6199-6207 (2001).

CHAPTER 4

INFLUENCE OF TEMPERATURE ON THE TENSILE AND ELASTIC PROPERTIES OF PTMO-T6A6T COPOLYMERS

Abstract

Tensile and elastic properties of poly(ether-ester-amides) (PEEA) having uniform rigid segments were studied as a function of temperature and time. The uniform rigid segment (T6A6T) is based on adipic acid (A), terephthalic acid (T) and hexamethylene diamine (6). The tensile test, tensile set, cyclic tensile set and compression set were measured as a function of temperature and time. The stress relaxation process was studied as a function of strain and modulus.

Temperature has a strong influence on the tensile properties of these PEEA copolymers. The yield stress, yield strain, fracture stress and fracture strain decrease with increasing temperature. The E-modulus was temperature independent in the range of 20 - 110 °C, which implies that the morphology of the polymers does not change within this temperature range. The yield stress as a function of temperature could be fitted with the Eyring relationship. Consequently, the yield stress / modulus ratio decreases with temperature. At room temperature, strain hardening due to the crystallisation of PTMO takes place, thereby increasing the tensile properties.

Also the elastic properties, measured with tensile set and compression set, decrease with increasing temperature. The tensile set and compression set values decrease with relaxation time. The polymers behave almost completely viscoelastic in nature at strains below the yield strain. Stress relaxation measurements showed two processes, a fast initial decay in the first 10 seconds and a second slower relaxation process. The normalised stress relaxation values of this second process were independent of strain and modulus of the system.

Introduction

Thermoplastic elastomers have a two-phase structure, a continuous soft phase with a low glass transition (T_g) and a phase separated hard phase with a high melting temperature (T_m)[1]. The phase separated hard phase introduces physical crosslinks in the low T_g soft phase and it can also act as a filler for the soft phase[1-3]. Upon stretching of such a copolymer, both the soft and the hard phase are deformed and if the strain is high enough yielding of the hard phase occurs. The tensile and elastic properties of TPE's are sensitive to the type, concentration and morphology of the hard phase[1].

Morphology

As TPE's have more than one phase the mechanical properties are dependent on the morphology of the copolymer. Segmented copolymers have often a two-phase morphology and the hard phase consists of crystallised segments with a high melting temperature. Rigid segments of uniform length in the copolymers crystallise almost completely and as a result the soft phase contains little dispersed rigid segments[2,4-6]. The crystallites form ribbons with a high aspect ratio, which have a strong reinforcing effect (Figure 4.1a)[2,4]. These well-defined systems are very suitable to study the influence of the morphology on the elastic properties of polymers. Niesten[3] studied tensile and elastic properties of copolymers with uniform aramid rigid segments (PTMO$_x$-TΦT). Polymer samples were stretched and this led to a dramatic decrease of the initial E-modulus due to a lowering of the aspect ratio of the ribbon-like crystallites (Figure 4.1). With a 200% stretch, the E-modulus was lowered by a factor 10. However, during relaxation of the sample the E-modulus increased again. This effect was attributed to a very slow healing process of the crystallites[7,8]. The changing orientation of the crystalline ribbons as a function of strain was studied with infrared dichroïsm[3] and AFM microscopy[8]. The deformation was found to take place in steps. The crystalline ribbons are broken up into smaller ribbons and are oriented in the strain direction (Figure 4.1b). Upon further stretching of the polymer, the ribbons break up in very small crystallites with a low aspect ratio and the crystallites turn and are now oriented perpendicular to the strain direction (Figure 4.1c).
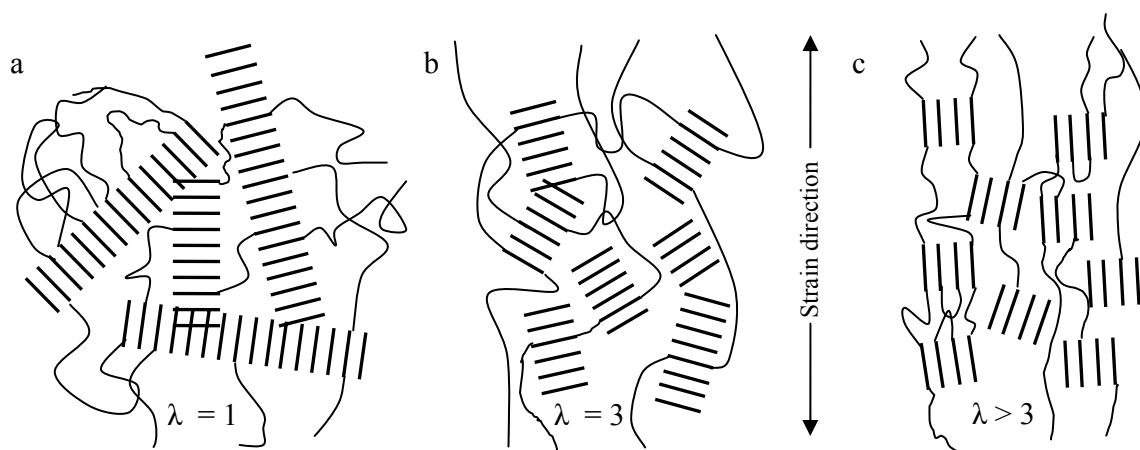
Figure 4.1: Schematic representation of the change in morphology in PTMO-TΦT copolymers during straining: a, long ribbons randomly oriented; b, broken up ribbons with ribbons oriented in the strain direction; c, very small ribbons oriented perpendicular to the strain[3,8].

Deformation behaviour of polymers

Deformation behaviour of polymers is often studied with tensile, tensile set or cyclic tensile set (TS), compression set (CS) and stress relaxation (SR) measurements. Tensile behaviour is studied by straining a dumbbell shaped polymer sample. Segmented block copolymers have relatively low yield stresses, high fracture strains and fracture stresses. In general, the stress levels in the tensile curve decrease with increasing temperature[1,9]. With increasing temperature the modulus decreases, the yield stress decreases, the fracture stress decreases and the fracture strain increases[1,10,11].

The elasticity of elastomers is the ability to recover after appreciable deformation[9]. Complete elastic behaviour is not observed for thermoplastic elastomers because irreversible changes in the morphology always occur. TPE's have physical crosslinks (crystallites) that are bonded by relatively weak secondary forces. The crystallites can be deformed upon stretching[1].

The elasticity of a polymer as measured with TS was found to decrease with increasing strain and increasing concentration of rigid segment[2,12,13]. In time, recovery of the deformation takes place and thus part of the deformation is viscoelastic in nature[2].

In stress relaxation experiments the stress decay is dependent on the type of copolymer, time, strain rate and temperature[14-16]. Le[15] studied stress relaxation as a function of the type of (co)polymer. Crosslinked NBR showed the lowest relaxation of stress followed by a poly(ether-block-amide) (Pebax) and the highest stress relaxation was observed for SEBS (tri-block copolymer). Often the relaxation stress is linear dependent on the logarithm of time, as was found for polyurethanes[17], poly(ether-block-amide) (Pebax)[18] and PP[19].

TPE's are used in a wide variety of applications and often at varying temperatures. However, the tensile and elastic properties of TPE's are temperature dependent[1]. Knowledge of the effect of temperature on tensile, elastic and stress relaxation processes of polymers is essential for developing a good understanding of their mechanical behaviour[14,20].

Segmented copolymers with uniform rigid segments have a simple two-phase morphology and are therefore interesting materials to study the effect of temperature and time on tensile and elastic properties. As system is chosen $PTMO_x$-T6A6T (Figure 4.2), with an emphasis on $PTMO_{2000}$-T6A6T[4].
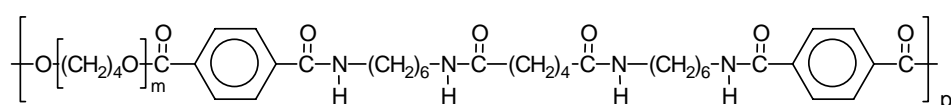
Figure 4.2: Polymer structure of $PTMO_x$-T6A6T.

$PTMO_x$-T6A6T segmented block copolymers are TPE materials that consist of alternating flexible (PTMO) and rigid segments (T6A6T) [1]. The rigid segments can crystallise in lamellae dispersed in the continuous low T_g phase (-65 to -70 °C). The morphology was studied with AFM and the tetra-amide segments form crystalline ribbons with a high aspect ratio[4]. The crystallinity of the tetra-amide segment in the copolymers was approximately 80 - 90%. The T_m of the polymers is about 185 °C and is slightly dependent on the content of rigid segment. The copolymer shows elastic behaviour between the glass transition temperature and the melting temperature. The rubber modulus in the plateau region of the copolymers is almost temperature independent. With increasing content of crystallisable segment in the copolymer (2 - 44 wt%), the rubber modulus at room temperature increases from 1 to 102 MPa. $PTMO_x$-T6A6T copolymers have a low compression set varying between 7 - 17%. Long PTMO segments (>1400 g·mol^{-1}) can crystallise and thereby negatively influencing the low temperature properties. PTMO segments can also strain crystallise resulting in higher ultimate properties. The yield strength increases linearly with increasing tetra-amide content.

The tensile and elastic properties as a function of temperature of copolymers with uniform rigid segments have, until now, hardly been studied. It is interesting to study the tensile and elastic properties as a function of temperature and time for $PTMO_x$-T6A6T copolymers.

Research aim

In this chapter the tensile and elastic properties of $PTMO_x$-T6A6T polymers (Figure 4.2) as a function of temperature and time are studied, with emphasis on $PTMO_{2000}$-T6A6T. These segmented copolymers have a well-defined two-phase morphology and are therefore interesting materials to study. The tensile properties, such as yield point, yield stress and ultimate properties are studied as a function of temperature (20 - 110 °C). The elasticity of $PTMO_x$-T6A6T polymers is measured with compression set, stress relaxation and tensile set.

Experimental

Materials: The copolymers $PTMO_x$-T6A6T were synthesised according to the solution/melt polymerisation route described before[4]. The inherent viscosity of these polymers was high, indicating a high molecular weight. Dumbbell shaped test bars were prepared by injection moulding the polymer using an Arburg Allrounder 221-55-250 injection moulding machine. $PTMO_{2000}$-T6A6T has a η_{inh} of 2.2 dl/g, T_g of -70 °C, a $G'_{25\,°C}$ of 20 MPa and a T_m of 185 °C.

Tensile test: Stress-strain curves were obtained using injection moulded dumbbell (ISO37 type 2), using a Zwick Z020 universal tensile machine equipped with a 500 N load cell. The strain was measured with extensometers. The tensile tests were carried out at a strain rate of 0.4 s^{-1} (test speed of 60 mm/min). For test temperatures other than room temperature a temperature controlled environment chamber was used. The E-moduli at each temperature were determined in 8-fold at a strain of 0.1 - 0.25%.

Tensile set: Cyclic stress-strain experiments were conducted with injection-moulded dumbbells (ISO 37 type 2). A Zwick Z020 universal tensile machine equipped with a temperature controlled environment chamber and 500 N load cell was used to measure the stress as a function of strain of each loading and unloading cycle at a strain rate of 0.4 s^{-1} (test speed of 60 mm/min).

Staircase loading: The strain of each loading-unloading cycle was increased (staircase loading) and the tensile set of the strain increment was determined as a function of the applied strain. The incremental tensile set (TS) was calculated from the following relation (Equation 4.1):

$$Tensile\ set = \frac{\Delta\varepsilon_{remaining}}{\Delta\varepsilon_{cycle}} = \frac{\varepsilon_{r,cycle(i)} - \varepsilon_{r,cycle(i-1)}}{\Delta\varepsilon_{cycle}} \times 100\% \qquad (Equation\ 4.1)$$

With: $\varepsilon_{r,cycle(i)}$ = remaining strain at the end of cycle i

$\varepsilon_{r,cycle(i-1)}$ = remaining strain at the end of the preceding cycle i-1.

Immediately after the stress was zero, a new cycle was started. The strain of the first cycle was 20% and for each following cycle the strain was increased with 40%.

Single/multiple cycle: The tensile set was determined by applying a 100% cyclic strain. The remaining strain immediately after unloading was used to calculated the tensile set (Equation 4.1, i = 1).

Compression set at room temperature: Samples for compression set were cut from injection moulded bars. The compression set was measured according to ASTM 395 B standard. After 24 h the compression was released at room temperature. After relaxation for half an hour, the thickness of the samples was measured. The compression set was taken as the average of four measurements. The compression set is defined as:

$$Compression \ set = \frac{d_0 - d_2}{d_0 - d_1} \times 100\% \qquad (\%)$$

(Equation 4.2)

With: d_0 = thickness before compression (mm)

d_1 = thickness during compression (mm)

d_2 = thickness after 0.5 h relaxation (mm)

Compression set at high temperatures: For a CS test at higher temperatures the compression is applied at room temperature and the holder is then placed in a vacuum oven at high temperatures. After 24 h the holder is opened and the samples are allowed to relax at room temperature.

Stress relaxation test: Injection moulded ISO 37 s2 dumbbells were used as samples for the stress relaxation experiments. The stress relaxation was measured on a Zwick Z020 universal tensile machine equipped with a 500 N load cell, the strain being measured as the clamp displacement with a starting clamp distance of 35 mm. The samples were strained at a rate of 0.33 s^{-1}. The decay of the stress was measured for 10,000 sec. The decay in the first 100 seconds, the initial stress decay, was calculated with Equation 4.3. The normalised stress relaxation is calculated with Equation 4.4.

$$initial \ stress \ decay = \frac{\sigma_{max} - \sigma_{100}}{\sigma_{max}} \quad (\%)$$

(Equation 4.3)

$$SR_n = \frac{\sigma_{100} - \sigma_{10,000}}{\sigma_{100} \times \Delta logt} \qquad (\text{-})$$

(Equation 4.4)

Results and discussion

The PTMO$_x$-T6A6T copolymers are TPE materials with a well-defined morphology[4]. The elastic and tensile behaviour of these polymers are studied as a function of temperature and time. First, tensile properties as a function of temperature are given. Second, tensile set and compression set measurements are discussed. Finally, stress relaxation is studied as a function of the applied strain and the rigid segment content.

Tensile properties

The tensile behaviour of segmented block copolymers at small strains is characterised by the initial modulus and the stress at 10% strain. The yield behaviour is characterised by the yield stress, the yield strain and the necking as a result of the localisation of the deformation. At higher strains the stress-strain behaviour is influenced by strain softening. Above 300% strain, strain hardening can take place. The degree of strain hardening depends on the crystallisation of the flexible segments taking place during straining and the amount of entanglements (molecular weight) in the polymer. In general, the stress levels in the tensile curve decrease with increasing temperature[1,9].

In chapter 3 of this thesis, the tensile properties at room temperature of $PTMO_x$-T6A6T and $(PTMO_{1000}$-T$)_x$-T6A6T with varying amorphous segment length (x) ranging from 650 - 20,000 g·mol^{-1} were discussed[4]. Here, the tensile properties of $PTMO_{2000}$-T6A6T as a function of temperature are studied in the temperature range 20 - 110 °C (Figure 4.3, Table 4.1).
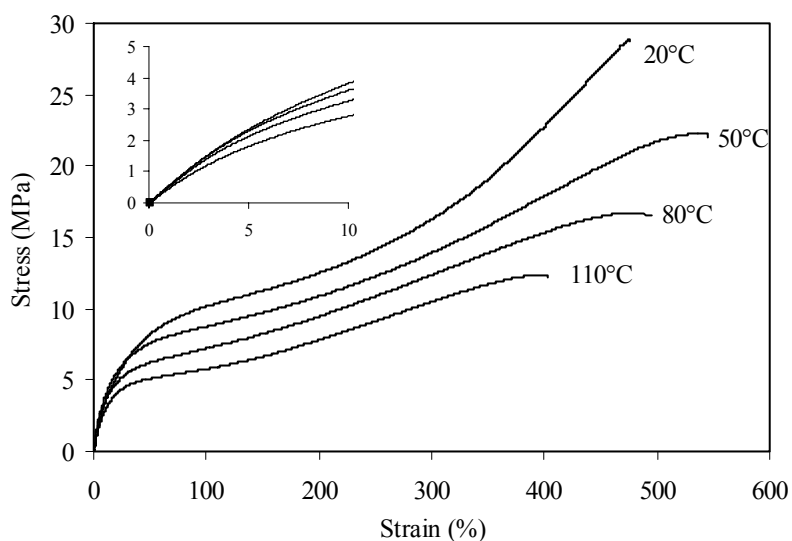
Figure 4.3: Tensile graph for PTMO$_{2000}$-T6A6T at different temperatures, η$_{inh}$ = 2.2 dl/g.

Initially, the stress increases in an approximately linear manner as the applied strain increases. Secondly, at the yield point the stress increases less steeply. Finally, at large strains the stress increases due to strain hardening.

At 20 °C, an extra upswing of the stress is observed at 300% strain. This upswing at high strains is due to strain induced crystallisation[7]. Upon straining of the polymer, PTMO chains

are aligned and can crystallise, thereby increasing the fracture stress. At higher temperatures this upswing is not observed, indicating that $PTMO_{2000}$ can not strain crystallise at temperatures above 50 °C.

Table 4.1: Tensile results of $PTMO_{2000}$-T6A6T at different temperatures, η_{inh} = 2.2 dl/g.

Temperature	G'	E-Modulus ± sd[a]	E/G'	$\sigma_{10\%}$	σ_{yield}	ε_{yield}	σ_{break}	ε_{break}	σ_{true}[b]
	(MPa)	(MPa)	(-)	(MPa)	(MPa)	(%)	(MPa)	(%)	(MPa)
20 °C	20	53 ± 3	2.7	4.5	8.7	49	29	480	165
50 °C	20	59 ± 7	3.0	3.8	7.2	42	22	550	143
80 °C	18	56 ± 3	3.1	3.4	5.8	37	17	490	98
110 °C	16	53 ± 2	3.3	2.9	4.7	33	12	400	61

[a] E-modulus was determined in 8-fold; [b] σ_{true} was obtained multiplying σ_{break} by the straining factor (= 1 + (ε_{break} / 100))

E-modulus

The Young's modulus (E) is fairly constant with increasing temperature as was also observed for the shear storage modulus (G')[4]. The modulus of the copolymer depends on the modulus of the soft phase and the reinforcement by the crystallites[1,2]. The reinforcement of the hard phase can be described by a composite model and is a function of the crystalline content and the aspect ratio of the crystallites[2,21]. Normally with semi-crystalline polymers and TPE's, the modulus decreases with increasing temperature[1,11]. However, for polymers with rigid segments of uniform length, the modulus is little temperature dependent[22]. The temperature independency of the E-modulus indicates that the crystallinity and the aspect ratio of the crystallites are unchanged. This is thought to be due to the fact that uniform segments crystallise over their full length and as a result no fringed layer on the crystallites is present that melts at lower temperatures.

The Young's (E) and storage modulus (G') are related according to[23]:

$$G' = \frac{E}{2(1+v)}$$

(Equation 4.5)

With v: poisson ratio.

For incompressible materials, like elastomers, there is no volume change on deformation and the poisson ratio is 0.5, giving E = 3*G. The relation between E/G' for these copolymers is

approximately 3. It should be noted that the E-modulus is determined at 0.1 - 0.25% strain and the Young's modulus is determined at 0.1% torsion (Table 4.1).

Stress at 10% strain

The stress at 10% strain decreased 36% with a temperature increase from 20 to 110 °C (Table 4.1). This decrease is less than was observed for other TPE's[24].

Yield behaviour

The yield point is generally seen as a point of onset of substantial plastic deformation[9]. For many applications one would not like to deform beyond the yield point. For semi-crystalline polymers the yield stress decreases about linearly with temperature (T < T_m)[11,25]. The yield stress and yield strain for PTMO$_{2000}$-T6A6T also decrease with increasing temperature (Figure 4.4). The yield strain values are high and this is interesting as it suggests that substantial plastic deformation starts at high strains. The yield stress values decrease with temperature as was expected. With increasing temperature the yield stress values decrease while the E-modulus remains about the same.
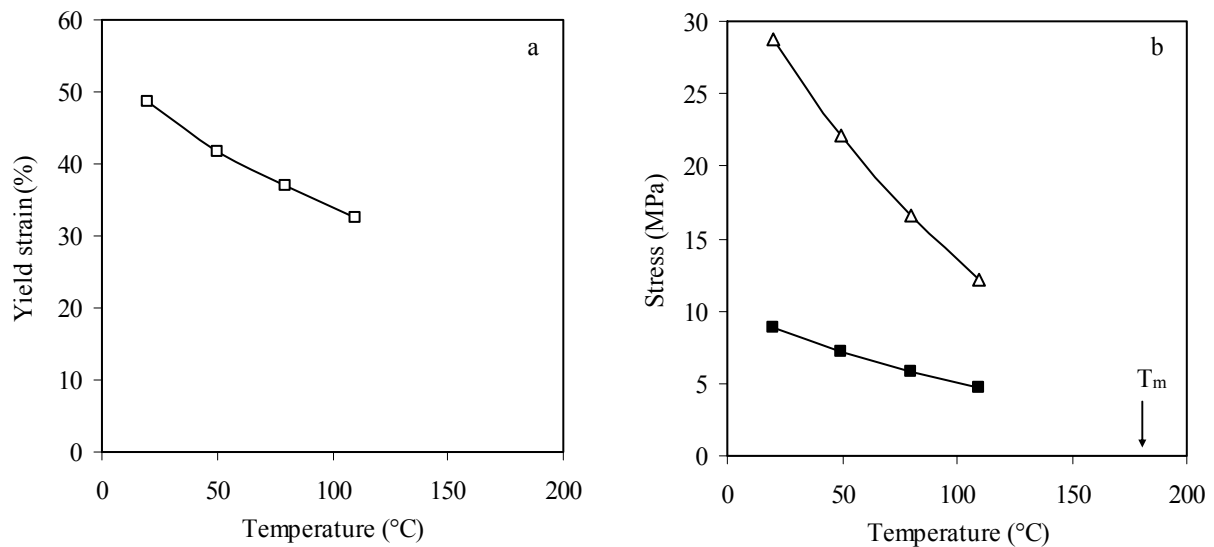

Figure 4.4: Tensile properties of PTMO$_{2000}$-T6A6T as a function of temperature a) □, yield strain b) ■, yield stress: △, fracture stress

The yield stress as a function of strain rate and temperature can be described by the Eyring relationship[25,26].

$$\frac{\sigma_y}{T} = \frac{R}{v}\left(\frac{\Delta H}{RT} + \ln\frac{2\dot{e}}{\dot{e}_0}\right)$$

(Equation 4.6)

Where σ_y is the yield stress, v the activation volume, ΔH is the activation enthalpy, R the gas constant, T the temperature, $\dot{e}$ the strain rate and $\dot{e}_0$ is a constant. A linear relationship is obtained if σ_y/T is plotted as a function of the reciprocal temperature (σ_y/T vs $1/T$). The yield stress as function of temperature for several amorphous and semi-crystalline polymers like PMMA, PK, PC, PP and PET could be described by this relationship[25,27,28]. Linearity is to be expected when one unique flow mechanism controls the yield stress. An Eyring plot was made for the yield stress as a function of temperature for PTMO$_{2000}$-T6A6T (σ_y/T vs $1/T$) and a linear relationship is obtained (Figure 4.5). This indicates that the yield behaviour can be described by this relationship.
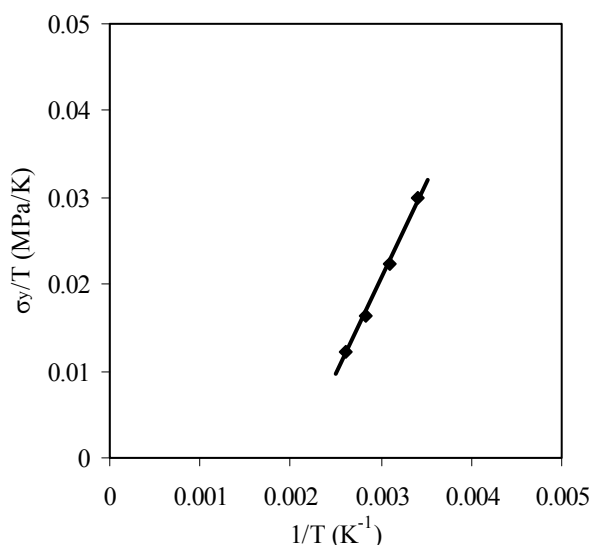
Figure 4.5: Eyring plot σ_y/T vs $1/T$ for PTMO$_{2000}$-T6A6T at 20, 50, 80 and 110 °C.

After the yield point

At strains higher than the yield strain the engineering stresses increased steadily. Also, no necking was observed during the tensile measurement and thus no localisation of stress takes place. Above 300% strain at room temperature a strong strain hardening effect is observed. This is due to strain induced crystallisation of the PTMO$_{2000}$ segments[7]. At higher

temperatures this strain crystallisation of $PTMO_{2000}$ cannot take place as the melting temperature of the strained crystallised segments (43 °C)[7] is below the test temperature.

Fracture behaviour

The fracture properties are very sensitive to the molecular weight and strain hardening of the polymer. Normally, the fracture stress decreases with increasing temperature and the fracture strain increases[23]. The fracture stress is often less dependent on temperature than the yield stress[9,11,23]. The fracture strains normally increase with temperature, however, if the fracture strains are very high (600 - 700%) they approach the natural draw ratio of coiled chains and then the fracture strain does not increase anymore[25]. At room temperature the fracture stress is high (Figure 4.3) and this is due to strain induced crystallisation of the PTMO segments. With increasing temperature from 50 to 110 °C a decrease of the stress and strain at break is observed (Figure 4.4b). Also the true fracture stress decreases strongly with temperature (Table 4.1).

Tensile set

The elastic properties of TPE's can be measured by tensile set measurements (TS). In the tensile set several parameters can be varied like the tensile strain, step size, the number of cycles, the loading and unloading rate and the relaxation time. We studied the tensile set with a loading/unloading strain rate of 0.4 s^{-1} and no relaxation time between the loading and unloading cycles. The strain in the unloading cycle at zero stress is used for the calculation of the TS. Three types of tensile set tests were carried out: single cycle tensile set, cyclic tensile set at increasing strain (staircase loading) and cyclic tensile set at one strain.

Single cycle tensile set

The effect of temperature (20 - 110 °C) on the elastic behaviour of $PTMO_{2000}$-T6A6T was studied with tensile set ($TS_{100\%}$) at a single loading cycle to a strain of 100% (Figure 4.6a). At 20 °C the polymer sample unloaded to 17% ($TS_{100\%}$ = 17%) of the applied strain and so 83% is recovered upon unloading. At higher temperatures the stress at 100% strain is clearly lower, as was also observed with the tensile test. Nevertheless, the TS values are higher at higher temperatures (Figure 4.6b). This means that the elasticity of the polymer decreases with increasing temperature.
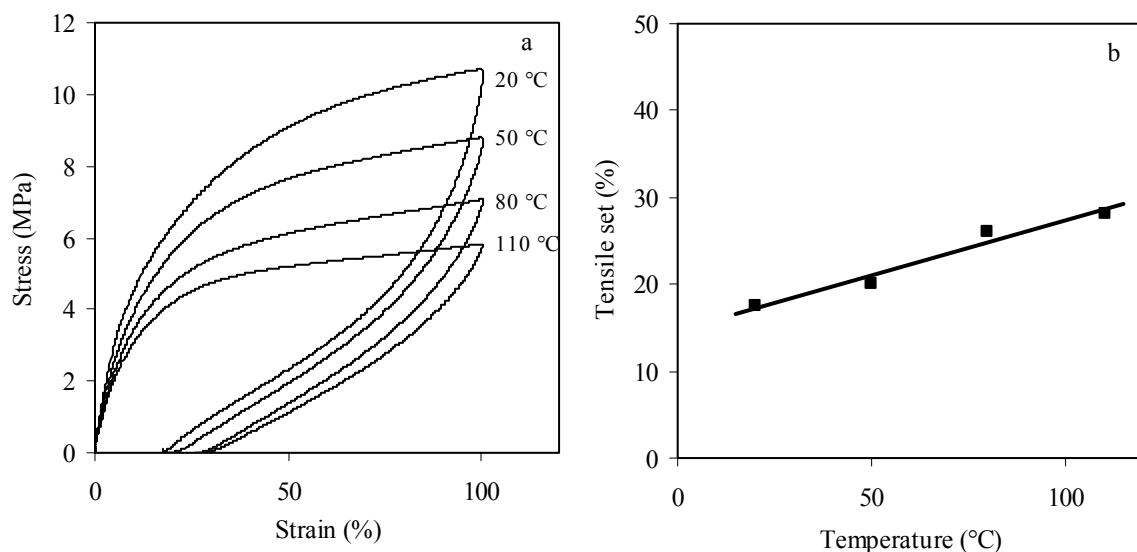
Figure 4.6: a) Single cycle TS$_{100\%}$ for PTMO$_{2000}$-T6A6T at different temperatures b) tensile set at 100% strain of the first cycle as a function of temperature for PTMO$_{2000}$-T6A6T.

Cyclic tensile set (staircase loading)

The tensile set measurement is a one-point test and only gives information at one strain. A staircase cyclic tensile set with increasing strain of each cycle gives insight in the elastic behaviour of the copolymer as a function of strain. The strain of the first cycle was 20% and for each following cycle the strain was increased with 40%. The tensile set (TS) of the strain increment was determined as a function of the applied strain at different temperatures (Equation 4.1, Figure 4.7).
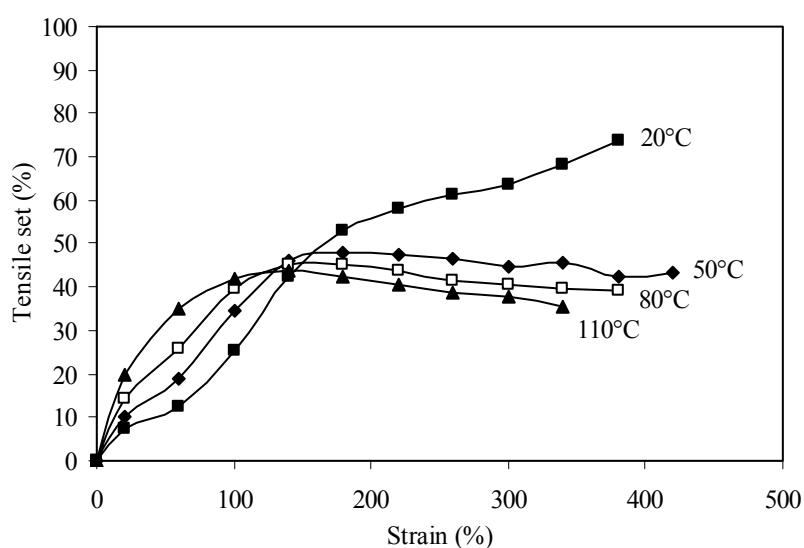
Figure 4.7: Cyclic staircase tensile set for PTMO$_{2000}$-T6A6T at different temperatures; ■, 20 °C; ♦, 50 °C; □, 80 °C; ▲, 110 °C

In the TS as a function of the strain two regions can be distinguished: up to 150% strain and above that strain. Up to 150% strain it is clear that at higher temperatures the TS are higher. An effect in this is that the yield strain is lowered with increasing temperatures. For elongations above 150% the inverse trend was observed and the TS are lower at higher temperatures. In the TS values at 20 °C a clear upsweep is observed at 300% strain, caused by strain induced crystallisation of $PTMO_{2000}$. The strain induced crystallisation negatively influences the elastic properties at high strains. At temperatures above 50 °C, crystallisation of $PTMO_{2000}$ cannot take place as the melting temperature of strained PTMO is 43 °C[7]. It even seems that at higher temperatures and higher strain the materials become more elastic but the difference in TS values between 50 and 110 °C is small.

Compression set

Compression set (CS) is often used in the study of elastic properties of TPE's. We studied the CS at 25% compression for 24 hours and with a relaxation time of 30 min[29]. The CS value is often taken as a measure of plastic deformation disregarding the viscoelastic effects[2]. The compression set values can also be determined at elevated temperatures according to ASTM D-395-89[29]. In this ASTM norm the compression is applied at elevated temperatures while the relaxation is carried out at room temperature. The CS values measured in this way were remarkable low at room temperature but strongly increased with increasing temperature (Figure 4.8).
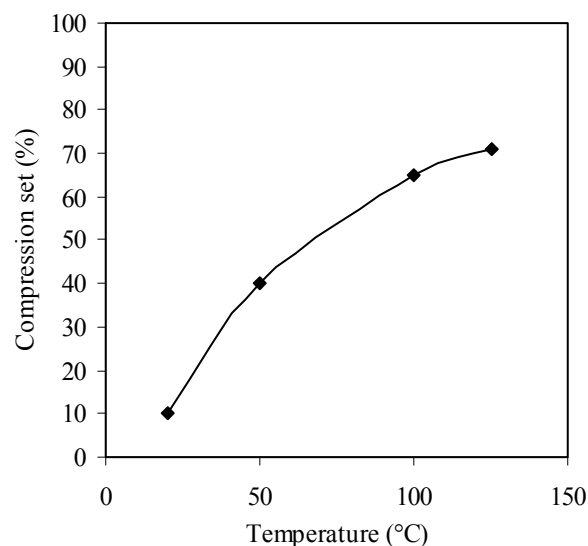
Figure 4.8: CS$_{25\%}$ for PTMO$_{2000}$-T6A6T as a function of temperature during compression. Relaxation temperature is 25 °C.

Often the compression set (CS) and tensile set (TS) values at similar strains are comparable, however the CS values as a function of temperature (Figure 4.8) increase much stronger than the TS values (Figure 4.6b). This difference can be due to viscoelastic effects as the deformation times at CS measurements are higher than for TS measurements.

Relaxation

In a standard compression set at the high temperatures, the unloading and relaxation is normally carried out at 25 °C. Here, the effect of the temperature during relaxation on the compression set values is studied. Polymer samples of $PTMO_{2000}$-T6A6T were 24 h compressed at 100 °C, unloaded and the relaxation was followed at different temperatures. The relaxation process of the samples was performed in vacuum ovens at 25, 75, 100 and 125 °C and the compression set of the samples was followed in time (Figure 4.9).
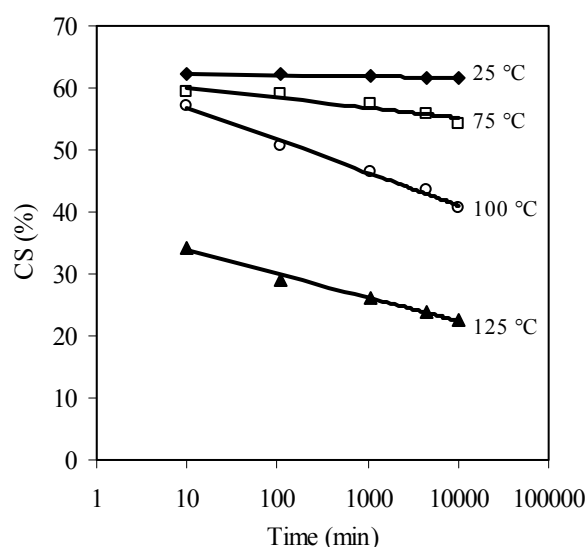
Figure 4.9: $CS_{25\%}$ of $PTMO_{2000}$-T6A6T performed at 100 °C as a function of relaxation temperature and time.

From Figure 4.9 it is clear that two processes must be involved in relaxation. One elastic process, as 40% of the applied compression is recovered within the first 10 min. The second process is a viscoelastic process giving a linear decrease of the CS value with log time. At the moment of unloading the "compression set" was 100%. Upon unloading, a fast elastic relaxation is taking place within our first measurement (10 min). The samples that were relaxed at 25, 75 and 100 °C all have a CS after 10 min of 60%. At room temperature the CS is almost independent of time and the test specimens relax at a minimum rate. At higher

temperatures the viscoelastic relaxation is faster. This can be explained by the higher mobility of the polymer at higher temperatures. However, the sample relaxed at 125 °C is different as the elastic relaxation appears to be stronger but the viscoelastic relaxation rate is not higher. The reason for this is as yet unclear. This relaxation experiment after the compression set test shows that viscoelastic relaxation is temperature dependent.

Relaxation in TS

Polymers are viscoelastic materials and their response to loading and unloading cycles is time dependent. In a cyclic tensile test the ability of these copolymers to recover after a deformation was tested. A polymer dumbbell of $PTMO_{2000}$-T6A6T was repeatedly loaded and unloaded to 100% (Figure 4.10).
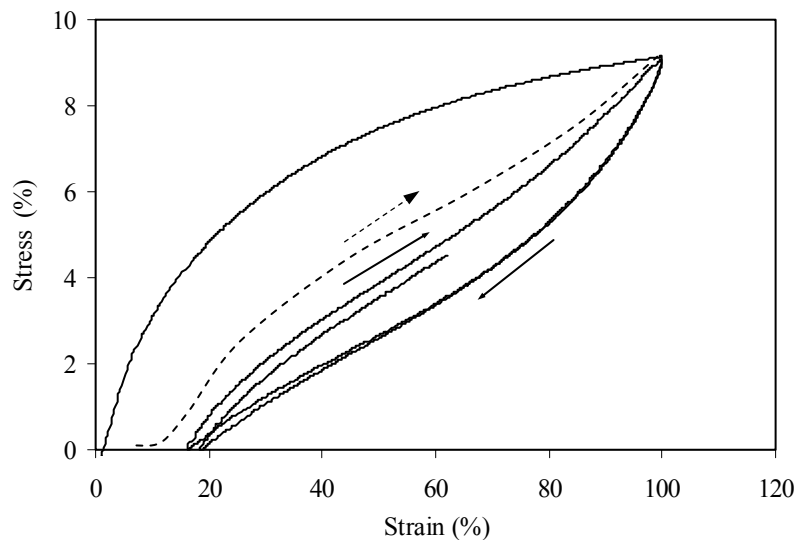
Figure 4.10: Cyclic tensile test to 100% strain for $PTMO_{2000}$-T6A6T: only the first two cycles are shown. --- cycle 5 after 16 hours of relaxation.

The cyclic tensile set was performed without relaxation time between unloading and loading and with a relaxation time of 16 hours. The first cycle shows a high tensile set value (Figure 4.11). In subsequent cycles the extra tensile set per cycle was only 1 - 2%. The E-modulus of the first cycle was 50 MPa but decreased to 20 MPa for the following cycles. The high TS and strong decrease of E-modulus in the first cycle indicate the break up of the crystallites in the first cycle. The maximum stress for a cycle is slightly lower than the stress in the previous cycle and this decay of the maximum stress is due to stress relaxation during unloading and loading. After 4 loading and unloading cycles to 100% strain the total TS in the sample was

21% (Figure 4.11). On subsequent relaxation for 16 h the total TS lowered to 8% but in the following cycle the TS was back at 20%. During the relaxation the TS decreased from 21% to 8% but the first cycle after relaxation shows a strong increase of the TS to almost the earlier level[3]. The E-modulus of the 4th cycle was not increased and therefore healing of the crystalline structure did not take place. The decrease in tensile set during relaxation can be attributed to the viscoelastic behaviour of the polymer.
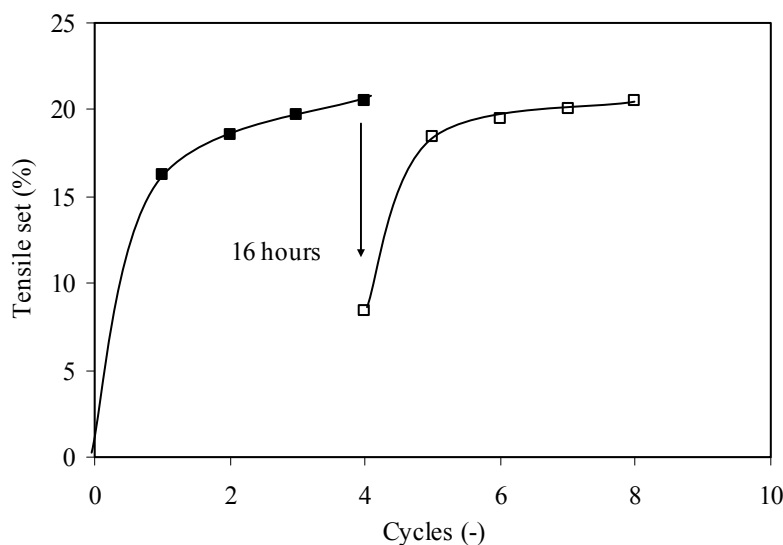
Figure 4.11: Tensile set$_{100\%}$ versus number of cycles. ■, cycles without relaxation; □, subsequent cycles after 16 h relaxation time.

The deformation and relaxation as a function of strain was studied into more detail with a tensile set measurement performed at different strains. Polymer samples were loaded to a certain strain directly followed by unloading of the stress. The remaining strain is used to calculate the tensile set (Equation 4.1). A new polymer sample was used for every strain. In Figure 4.12 the tensile set is plotted as a function of the applied strain. The tensile set slightly increases with increasing stain but the sample stretched to 80% has a TS below 10%. At higher strains, just above 80%, a strong upswing in the tensile set was observed so plastic deformation strongly increases. This increase in tensile set is somewhat above the yield point (50%) and was also observed in the staircase loading TS (Figure 4.7). It is commonly assumed that below the yield stress no plastic deformation occurs and above the yield stress, plastic deformation of polymers increases significantly. These TS values are lower than the staircase loading TS test values at 20 °C where the increment of the strain was measured (Figure 4.7).

After this loading and unloading cycle, the samples were relaxed for two weeks and the strain was remeasured. The tensile set values with two weeks relaxation are systematically lower (~7%) than the TS values without a relaxation time. With two weeks relaxation the TS in the region before the yield stress is almost completely decreased to zero. The viscoelastic relaxation is thus independent of strain and is the TS at the yield point. The TS in these materials is thus up to the yield point a viscoelastic strain and after the yield point plastic deformation is present.
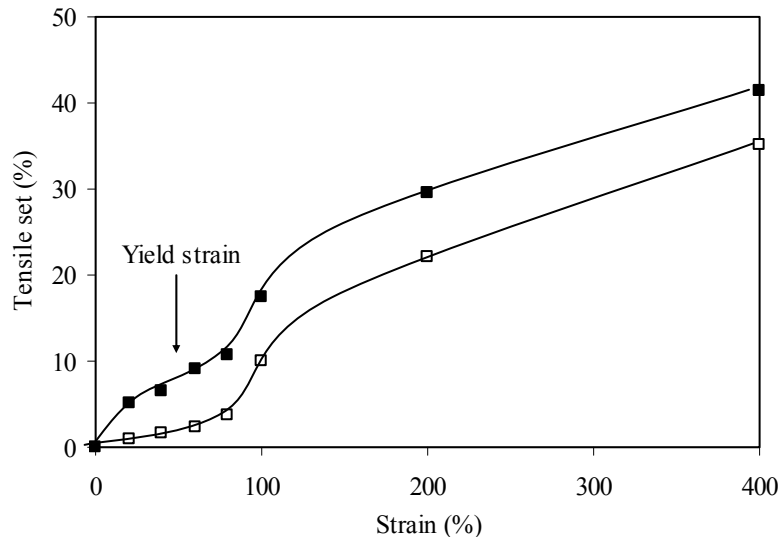
Figure 4.12: Tensile set of the first cycle for PTMO$_{2000}$-T6A6T at different strains; ■, Tensile set after unloading; □, tensile set after two weeks relaxation.

Stress relaxation

Stress relaxation measurements were performed to study the time dependent behaviour of these segmented block copolymers. In a stress relaxation test a polymer sample is strained to a certain value and the stress decay is measured in time. For ideal elastomers no stress relaxation occurs. The stress in segmented block copolymers at low strains depends on the reinforcing effect of crystallites. Thus, the stress relaxation depends on the deformation in time of untangling of amorphous chains and on changing reinforcement of the crystallites. The stress relaxation SR is quantified by the normalised slope of the stress with log time (Equation 4.4). This is the slope divided by the stress at 100 sec.

Dependence of strain

Stress relaxation in segmented block copolymers consists of two processes, one fast initial decay of the stress in the first seconds and a slower process[6]. The relaxation for PTMO$_{2000}$-

T6A6T was studied as a function of the applied strain (Figure 4.13). After the applied strain was reached the stress decay in the first 10 seconds was sharp and thereafter the stress decay was linear on log time scale. This implies that stress relaxation in these copolymers consist of two processes. An initial stress decay in the first seconds and after 10 seconds a viscoelastic process takes place. The initial stress decay was calculated over the first 100 seconds as a percentage of the maximum stress (Table 4.2). The second relaxation process is determined as the decay between 100 and 10,000 seconds normalised by the stress at 100 seconds (Equation 4.4).
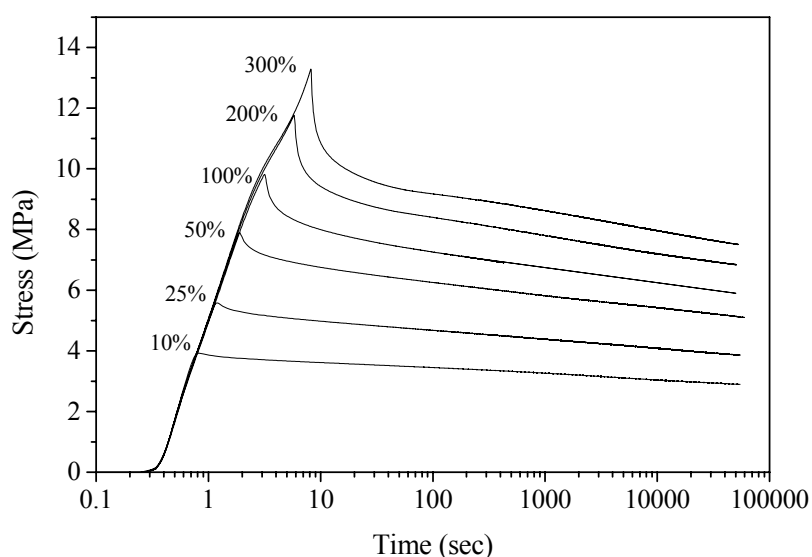
Figure 4.13: Stress relaxation of PTMO$_{2000}$-T6A6T at different strains.

Table 4.2: Relaxation properties of PTMO$_{2000}$-T6A6T

Strain	Stress decay	SR$_n$
	$(\sigma_{max}-\sigma_{100})/\sigma_{max}$	$(\sigma_{100}-\sigma_{10,000})/(\sigma_{100}\cdot\Delta log(t))$
(%)	(%)	(%/decade)
10	12	6
25	16	6
50	21	7
100	25	7
200	28	7
300	31	7

Applying higher strains increases the initial stress decay from 12 to 31%. Also the remaining stress after 100 seconds is always higher than 60% and this is good compared to other

polymer systems[15]. The normalised slope (SR_n) of the second relaxation process is fairly constant and thus the second relaxation process is independent of the applied strain.

Rigid segment content

Stress relaxation experiments at 25% strain were performed for copolymers with varying PTMO length (Figure 4.14) (series 1 of chapter 3). If in these $PTMO_x$-T6A6T copolymers the PTMO length is increased, then the T6A6T content is decreased and the modulus is lowered (Table 4.3)[4].
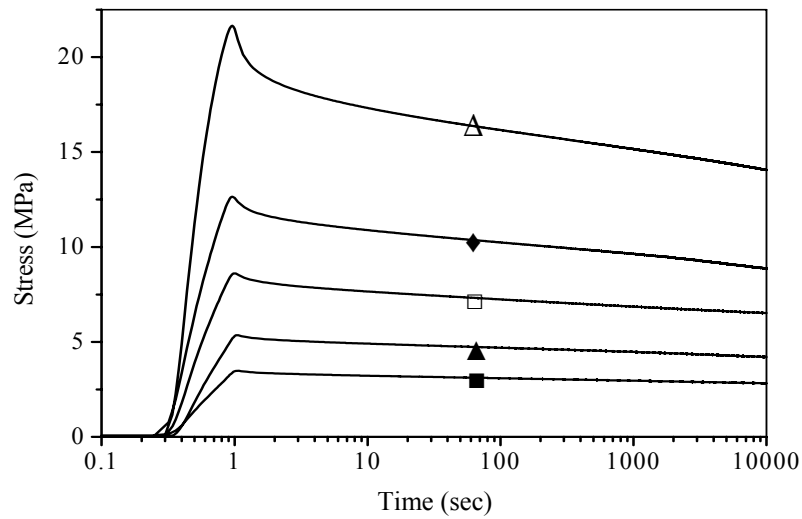
Figure 4.14: Relaxation measured at 25% strain for $PTMO_x$-T6A6T with different length of PTMO: Δ, $PTMO_{650}$-T6A6T (44 wt%); $\blacklozenge$, $PTMO_{1000}$-T6A6T (34 wt%); $\square$, $PTMO_{1400}$-T6A6T (27 wt%); $\blacktriangle$, $PTMO_{2000}$-T6A6T (21 wt%); $\blacksquare$, $PTMO_{2900}$-T6A6T (16 wt%).

Table 4.3: Relaxation properties of $PTMO_x$-T6A6T.

	T6A6T	G' (25 °C)	Stress decay	SR_n
			$(\sigma_{max}-\sigma_{100})/\sigma_{max}$	$(\sigma_{100}-\sigma_{10,000})/(\sigma_{100}\cdot\Delta\log(t))$
	(wt%)	(MPa)	(%)	(% decrease per decade)
Series 1				
$PTMO_{650}$-T6A6T	44	102	25	6.5
$PTMO_{1000}$-T6A6T	34	51	19	6.7
$PTMO_{1400}$-T6A6T	27	30	16	5.0
$PTMO_{2000}$-T6A6T	21	20	12	6.5
$PTMO_{2900}$-T6A6T	16	9	11	4.3
Series 2				
$(PTMO_{1000}$-T$)_{6000}$-T6A6T	8	6	16	4.0
$(PTMO_{1000}$-T$)_{10,000}$-T6A6T	5	3	22	4.6
$(PTMO_{1000}$-T$)_{20,000}$-T6A6T	3	1.6	35	6.1

The initial stress decay decreases with decreasing T6A6T content and rubber modulus up to 10 wt% (shear storage modulus of 10 MPa). However, polymers with very low T6A6T contents (low moduli) (series 2 of chapter 3) show an increase for the initial decay of the stress. These results suggest that for polymers with very low crystallisable segment contents (less than 10 wt%) the relaxation with time (0 - 10 seconds range) is stronger. Also the CS-values of these polymers increased again at very low T6A6T contents[3,4]. Apparently, if the concentration of tetra-amide is very low, the relaxation of the amorphous phase is stronger and/or the crystallites are more easily deformed.
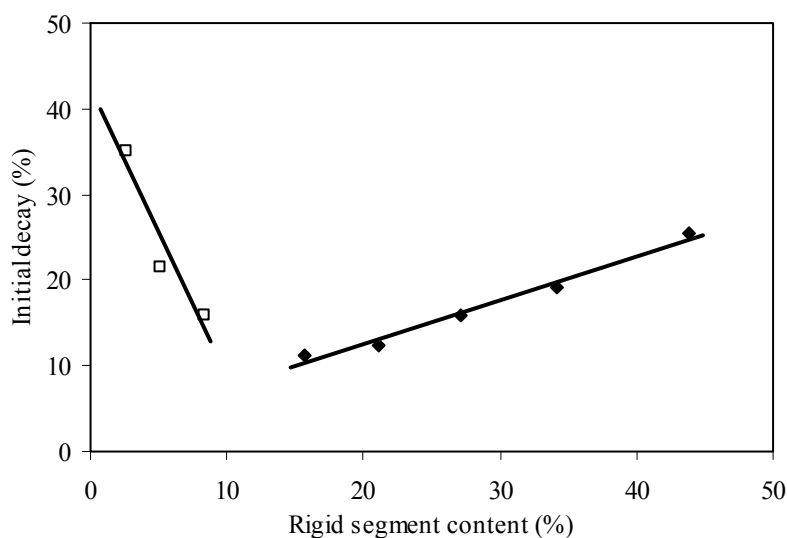
Figure 4.15: Initial stress decay of stress relaxation measured at 25% strain for polymers with varying content of T6A6T segment: ♦, series 1, PTMO$_x$-T6A6T; □, series 2, (PTMO$_{1000}$-T)$_x$-T6A6T.

The stress decay in the second part of the relaxation is a function of the T6A6T content (rubber modulus) of the polymer. An increase in stress relaxation with increasing rubber moduli of the polymer was also found in segmented poly(ether-block-amide) (PEBAX) thermoplastic elastomers[18] and for PTMO with uniform rigid aramid segments[3]. If the normalised SR is taken, then the SR$_n$ values are nearly independent of the rigid segment content (or modulus). The normalised SR value of these PTMO$_x$-T6A6T system is 5% per decade of time. As the normalised SR values are independent of applied strain and T6A6T content (modulus) they can be compared to other systems. The normalised SR value compares favourably with results from the literature on other TPE's[15,22].
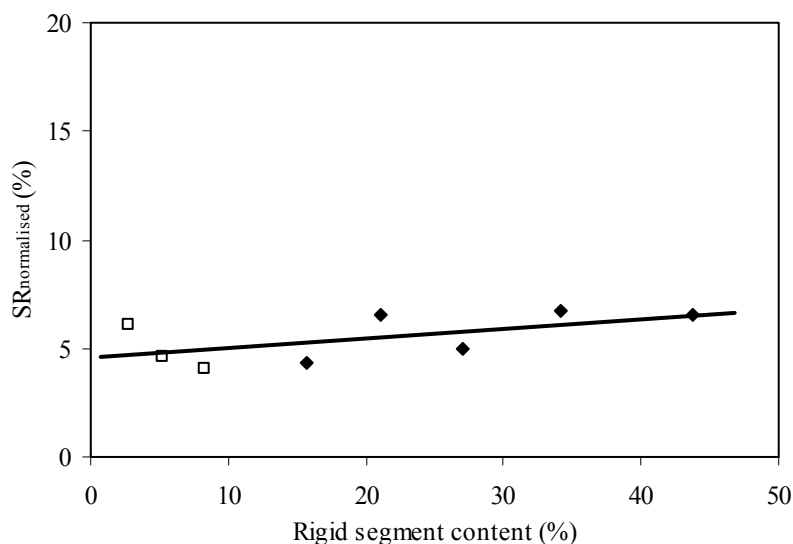
Figure 4.16: Stress relaxation at 25% strain as a function of rigid segment content: ♦, series 1, PTMO$_x$-T6A6T; □, series 2, (PTMO$_{1000}$-T)$_x$-T6A6T .

Conclusions

The tensile and elastic properties of segmented copolymers with PTMO flexible segments and uniform rigid segments were studied as a function of temperature and time. A complicating factor in the copolymers is that PTMO can strain crystallise. This strain crystallisation improves the ultimate properties but lowers the elastic properties at high strains. At temperatures above 50 °C the PTMO crystals are molten and strain crystallisation does not take place.

The tensile curve decreased with increasing temperature. The yield strain, yield stress, fracture stress and fracture strain all decreased with increasing temperatures. The yield stress as a function of temperature fitted well to the Eyring model. The E-modulus was found to be temperature independent between 20 - 110 °C due to the stable and unchanged morphology. The E-modulus and G'-modulus are related by a factor 3 indicating that the Poisson ratio is close to 0.5.

The elastic properties of these segmented copolymers as measured by tensile set and compression set decreased with increasing temperature. This temperature effect is stronger for the compression set, probably due to the longer deformation times. The tensile set

measurements showed a clear transition in the TS values at the yield point. Before the yield point the tensile set was low but when the yield stress was reached the tensile set strongly increased. At strains higher than 150% the TS between 50 - 110 °C did not increase further. For the polymer tested at 20 °C a strong increase of the tensile set was observed due to strain induced crystallisation of PTMO at strains above 150%.

The TS and CS values are a function of relaxation time. This suggests that part of the measured set values are viscoelastic in nature. The relaxation of the viscoelastic process is faster at higher temperatures. The TS seem to be fully viscoelastic in nature at strains below the yield strain.

Stress relaxation appears to consist of two processes, a fast initial decay of the stress in the first 10 seconds and a second slower relaxation process. Higher relaxation strains increased the first process while the second process was not dependent on the applied strain (or stress). With increasing modulus the initial decay processes increased, while the normalised SR remained constant. The normalised SR is thus independent of applied strain and the modulus of the sample with a value of approximately 5 - 7% per decade of time. The stress relaxation is thought to be due to the relaxation of amorphous chains in the copolymer and/or the time dependent deformation of the reinforcing crystallites.

References

1. Holden, G., Legge, N.R., Quirk, R.,.Schroeder, H.E., *'Thermoplastic elastomers'*, Hanser Publisher, Second Ed. Munich (1996).

2. Schuur van der, J.M., *'Poly(propylene oxide) based segmented blockcopolymers'*, Ph.D. Thesis, University of Twente (2004).

3. Niesten, M.C.E.J., Gaymans, R.J., *Polymer* **42**, 6199-6207 (2001).

4. Chapter 3 of this thesis

5. Krijgsman, J., *'Segmented copolymers based on poly(2,6-dimethyl-1,4,phenylene ether)'*, Ph.D. Thesis, University of Twente (2002).

6. Niesten, M.C.E.J., *'Polyether based segmented copolymers with uniform aramid units'*, Ph.D. Thesis, University of Twente (2000).

7. Niesten, M.C.E.J., Harkema, S., van der Heide, E., Gaymans, R.J., *Polymer* **42**, 1131-1142 (2001).

8. Sauer, B.B., McLean, S., Gaymans, R.J., Niesten, M.C.E.J., *J. Polym. Sci. part B Poly. Phys.* **42**, 1783-1792 (2004).

9. Hertzberg, R.W., *'Deformation and fracture mechanics of engineering materials'*, John Wiley, 3rd edition New York (1989).

10. Browstow, W., Cornelissen, R.D., *'Failure of plastics'*, Munich (1986).

11. Rodriguez, F., Cohen, C., Ober, C., Archer, L.A. *'Principles of polymer systems'.* Taylor & Francis, New York,(2005).

12. Beck, R.A., Truss, R.W., *Journal of Applied Polymer Science* **71**, 959-966 (1999).

13. Kim, H.D., Lee, T.J., Huh, J.H., Lee, D.J., *Journal of Applied Polymer Science* **73**, 345-352 (1999).

14. Khan, A.S., Lopez-Pamies, O., *Int. J. Plasticity* **18**, 1359-1372 (2002).

15. Le, H.H., Lupke, T., Pham, T., Radusch, H.-J., *Polymer* **44**, 4589-4597 (2003).

16. Patel, M., Soames, M., Skinner, A.R., Stephens, T.S., *Polym. Degrad. Stabil.* **83**, 111-116 (2004).

17. Prisacariu, C., Buckley, C.P., Caraculacu, A.A., *Polymer* **46**, 3884-3894 (2005).

18. Sheth, J.P., Xu, J., Wilkes, G.L., *Polymer* **44**, 743-756 (2003).

19. Akinay, A.E., Brostow, W., Castano, V.M., Maksimov, R., Olszynski, P., *Polymer* **43**, 3593-3600 (2002).

20. Kalkar, A.K., Siesler, H.W., Pfeifer, F., Wadekar, S.A., *Polymer* **44**, 7251-7264 (2003).

21. Halpin, J.C., Kardos, J.L., *J. Appl. Phys.* **43**, 2235 (1972).

22. Fakirov, S., Yamakawa, H., *'Handbook of condensation thermoplastic elastomers'*, Wiley-VCH, New York (2005).

23. Cowie, J.M.G., *'Polymers: chemistry & physics of modern materials'*, Blackie Academic & Professional, 2nd London (1991).

24. Arnitel data sheet, www.dsm.com

25. Ward, I.M., *'Mechanical properties of solid polymers'*, Wiley, 2nd New York (1979).

26. Mc Crum, N.G., Buckley, C.P.,.Bucknall, C.B., *'Principles of polymer engineering'*, Oxford university press, 2nd New York (2001).

27. Zuiderduin, W.C.J., Gaymans, R.J., and Huetink, J., *'Deformation and fracture of aliphatic polyketones'*, Ph.D. Thesis, University of Twente (2002).

28. Klompen, E.T.J., *'Mechanical properties of solid polymers'*, Ph.D. Thesis, Technical University Eindhoven (2005).

29. ASTM designation: D395-89Standard test methods for rubber property-Compression set.

CHAPTER 5

SEGMENTED COPOLYMERS HAVING UNIFORM TETRA-AMIDE UNITS

Abstract

Segmented copolymers with poly(tetramethylene oxide) (PTMO) and tetra-amide crystallisable segments (TxTxT and TxAxT) were studied. The tetra-amide segment consists of two terephthalic groups at the outside (T), two amide segments (x) and in the centre a terephthalic acid (T) or adipic acid (A) group. The composition of the tetra-amide segment was varied by changing the length of the diamine (x) and changing the centre group. The bisester tetra-amide units were synthesised prior to the polycondensation. The PTMO segments had a segment length varying from 650 - 2900 g·mol^{-1}. The polymerisation can be done either by a solution/melt route or a melt polymerisation route. The solution/melt route resulted in polymers with higher molecular weight and was therefore used for the synthesis of all the polymers.

The degree of crystallinity of the copolymers was high (70 - 90%) as was studied by DSC and FT-IR. The thermal mechanical properties were studied by DMTA. The type of tetra-amide segment had little effect on the glass transition temperature of the PTMO phase and the storage modulus at room temperature, but a clear effect on the melting temperature. A direct result of decreasing the PTMO segment length from 2900 to 650 g·mol^{-1} is an increase in tetra-amide segment content of 16 to 45 wt%. This results in an increase of the storage modulus at 25 °C (9 - 150 MPa) as well as an increase of the melting temperature (175 - 250 °C). Also the polyether glass transition temperature increased with decreasing soft segment length due to the increasing network density. The rubber modulus in the plateau region of these copolymers is almost temperature independent.

Introduction

Thermoplastic elastomers (TPE's) are polymers that show elastomeric behaviour at room temperature and are melt-processable. Special kinds of TPE's are segmented block copolymers or multi-block copolymers that consist of alternating crystallisable rigid segments and amorphous flexible segments. The flexible segments form the continuous amorphous phase with a low T_g and give the material low temperature flexibility. The rigid segments can crystallise and form lamellae in the low T_g phase, acting as physical crosslinks and giving the material dimensional stability and solvent resistance.

It has been found that the properties of segmented copolymers depend on the uniformity of the crystallisable segment. The effect of polydispersity of crystallisable segments has been studied with polyurethanes[1-3] and polyamides[4-12]. These studies showed that crystallisable segments of uniform length incorporated in polymers crystallise fast, have a relatively high rubber modulus, a temperature independent rubbery plateau, high elasticity and high fracture strains. The uniform segments in the polymers not only have a higher degree of crystallinity than polymers with non uniform segments, they also have a higher aspect ratio of the crystallites and are expected to reinforce the polymer matrix even better, resulting in a higher modulus[11,13,14].

In order to maintain the uniformity of the crystallisable segments during melt synthesis and melt processing, their thermal stability should be high[15]. Amide units are thermally more stable and less sensitive to randomisation of the uniform segment compared with urethane or ester units and therefore are more interesting to use[11].

Earlier research of segmented copolymers with uniform amide segments was focused on the use of bisester diamides[4-7,16], bisester tetra-amides[8,9,11,17] and bisester hexa-amides[11] units. Several bisester di-amide units with aliphatic diamides were studied; T6T[16], T4T[6] and T2T[5] based on 1,6-hexandiamine (6), 1,4-butanediamine (4), 1,2-ethanediamine (2) and terephthalic units (T) (Figure 5.1). In these copolymers, poly(tetramethylene oxide) (PTMO) was used as the polyether segment. The melting temperatures for $PTMO_{1000}$-T2T (132 °C), $PTMO_{1000}$-T4T (153 °C) and $PTMO_{1000}$-T6T (111 °C) were low.
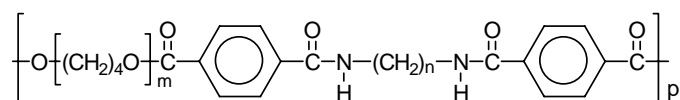
Figure 5.1: Structure of PTMO-TxT, x = (CH₂)ₙ with n = 2, 4 or 6.

Also a fully aromatic bisester diamide unit based on paraphenylene terephthalamide (TΦT-dimethyl) has been studied[10]. This bisester diamide unit had a very high melting temperature (375 °C) and was difficult to dissolve[10]. Niesten[10,18,19] studied the synthesis, structure and properties of segmented copolyetheresteramides based on TΦT-dimethyl and PTMO. The copolymers with $PTMO_{1000}$ had a melting temperature of 216 °C[10].

The relatively low melting temperatures of polymers with di-amide segments can be increased by increasing the amide segment length[9]. Polymer with tetra-amide segments have thicker crystalline ribbons than polymers with di-amide segments and therefore have higher melting temperatures[8,9,11] (Figure 5.2).
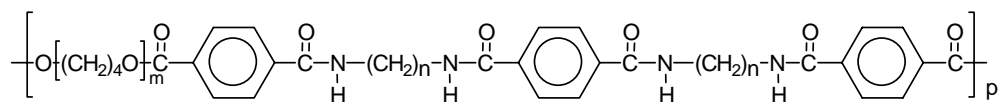
Figure 5.2: Structure of PTMO-TxTxT with x = (CH₂)ₙ.

Copolymers based on diamide or tetra-amide segments have low undercooling values (T_m - T_c), in the range of 10 - 15 °C, which suggests rapid crystallisation[5,6]. The fast crystallisation is possible due to the fact that the amide units have a pre-order in the melt[4,6,7,20-22]. Crystallisation of the uniform amide segments is almost complete, resulting in a low glass transition temperature and a low temperature flexibility of the copolymers. The amide units of uniform length crystallise rapidly in ribbons with a high aspect ratio[8,11,14] (Figure 5.3).

2 μm
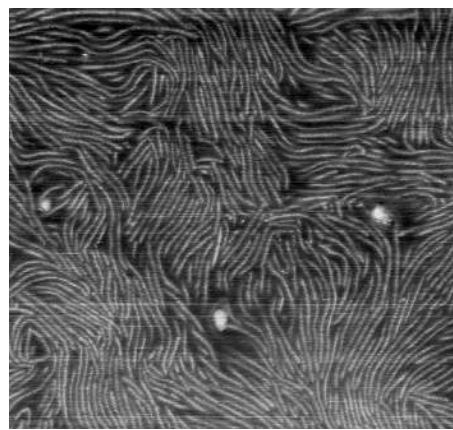
Figure 5.3: AFM image of (PTMO$_{1000}$-T)$_{20,000}$-T6A6T$^{[14]}$.

The moduli of the copolymers increase strongly with increasing amide content[8] and can be approximated with a model for fibre reinforced polymers[11,13,14,23,24]. The crystalline ribbons can be regarded as nano fibre reinforcement. With crystallisable segments of uniform length, the rubbery plateau is almost temperature independent[3,25,26]. The copolymers have high elongations at break, and fibres spun from these copolymers have fracture strains well above 1000%[5]. With increasing polyether length, the crystalline content decreases, resulting in a lower modulus, lower melting temperature and improved elasticity. The compression set and tensile set values improved with decreasing modulus and are low compared with industrial materials[8,11,19].

In earlier research, segmented copolymers with T6T6T segments were thoroughly investigated[8,11]. Due to the high melting temperature of the starting T6T6T-dimethyl (303 °C[9]), the polymerisation was carried out with a solvent[9]. A melt polymerisation with T6T6T units is difficult as degradation of PTMO occurs above 250 °C[27]. Furthermore, the melting temperatures of copolymers based on high concentrations of T6T6T will be high resulting in too high processing temperatures. It would be interesting to study copolymers with tetra-amides that have a melting temperature below 250 °C, so melt polymerisation is possible and polymerisation and processing is without degradation.

Research aim

In this chapter, segmented copolymers based on PTMO and different uniform crystallisable tetra-amide segments are synthesised. Two synthesis routes for the copolymers, a melt

polymerisation and solution/melt polymerisation, are compared. The composition of the tetra-amide segment and the length of the PTMO are varied. Segmented copolymers based upon two types of tetra-amide are synthesised; PTMO-TxTxT (Figure 5.2) and PTMO-TxAxT (Figure 5.4). The number of methylene groups (n) of the amide is 4, 6, 8 or 10 and the centre group of the tetra-amide can be a tetrephthalic or an adipate group. In these copolymers, the length of PTMO is varied between 650 and 2900 g·mol^{-1}.
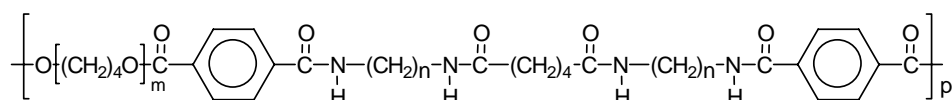
Figure 5.4: Structure of PTMO-TxAxT with x = (CH$_2$)$_n$ with n = 4, 6.

The synthesis and characterisation of the bisester tetra-amides were already discussed before[28]. The crystallisation of the segmented copolymers was studied with DSC and FT-IR. The thermal mechanical behaviour was studied with DMTA and the elastic behaviour with compression set measurements.

Experimental

Materials: N-methyl-2-pyrrolidone (NMP) was purchased from Aldrich and used as received. Tetra-isopropyl orthotitanate (Ti(i-OC$_3$H$_7$)$_4$) was purchased from Aldrich and was diluted in m-xylene (to 0.05 M). m-Xylene was purchased from Merck. Poly(tetramethylene oxide) (PTMO) 632 was a gift from Bayer. PTMO's with a length of 1000, 1400, 2000 and 2900 g·mol^{-1} were a gift from Dupont. Irganox 1330 was obtained from CIBA. The synthesis of TxTxT-dimethyl and TxAxT-dimethyl units was described before[28].

Solution/melt polymerisation of PTMO$_{1000}$ with tetra-amide: The polymerisation was carried out in a 250 ml stainless steel reactor with a nitrogen inlet and magnetic coupling stirrer. The polymerisation of PTMO$_{1000}$ with T6T6T-dimethyl is given as an example. The reactor was charged with PTMO$_{1000}$ (50 g, 0.05 mol), T6T6T-dimethyl (34.3 g, 0.05 mol), 100 ml NMP, 1 wt% Irganox 1330 (based on PTMO) and catalyst solution (5 ml of 0.05 M Ti(i-OC$_3$H$_7$)$_4$ in m-xylene) under nitrogen flow. The stirred reaction mixture was heated to 180 °C in 0.5 h and subsequently in 2 h to 250 °C. This temperature was maintained for 2 h. Subsequently, the pressure was carefully reduced (P<20 mbar) to distil off the NMP and then further reduced (P<0.3 mbar) over 1 h. The reactor was cooled slowly, maintaining the low pressure. The copolymers were transparent and tough.

Melt polymerisation of PTMO$_{1000}$ with tetra-amide: The same setup was used as described above. The reactor was charged with PTMO$_{1000}$ (50 g, 0.05 mol), T6A6T-dimethyl (33.3 g, 0.05 mol), 1 wt% Irganox 1330 (based on PTMO) and catalyst solution (5 ml of 0.05 M Ti(i-OC$_3$H$_7$)$_4$ in m-xylene) under nitrogen flow. The

initial reaction temperature was 10 °C higher than the melting temperature of the bisester tetra-amide unit. After 0.5 h the tetra-amide unit was molten and the reaction temperature was lowered to 250 °C. This temperature was maintained for 4 h. The pressure was then carefully reduced to (P<20 mbar) and then further reduced to (P<0.3 mbar) for 1 h. Subsequently, the reactor was cooled slowly maintaining the low pressure. The copolymers were transparent and tough.

Viscometry: The inherent viscosity was measured at a concentration of 0.1 g/dl in a mixture of phenol/1,1,2,2-tetrachloroethane (1:1 molar ratio) at 25 ºC using a capillary Ubbelohde type 1B.

DSC: DSC spectra were recorded on a Perkin Elmer DSC apparatus, equipped with a PE7700 computer and TAS-7 software. Dried samples of 5 - 10 mg were heated to approximately 30 °C above the melting temperature and subsequently cooled, both at a rate of 20 °C/min. The maximum of the peak in de heating scan was taken as the melting temperature. The second heating scan was used to determine the melting peak and enthalpy of the sample. The first cooling curve was used to determine the crystallisation temperature, which was taken as the onset of crystallisation. The crystallinity was calculated from the melting enthalpy of the polymer and the melting enthalpy of the bisester tetra-amide.

FT-IR: Infrared transmission spectra were recorded using a Nicolet 20SXB FTIR spectrometer with a resolution of 4 cm^{-1}. Solution cast polymer films (0.05 g/ml in HFIP) of <10 μm thick were used for temperature dependent FT-IR recorded at temperatures between room temperature and up to 20 °C above the melting temperature. The film was placed in-between two pressed KBr pellets under a helium flow. The degree of crystallinity of the rigid segments in the polymers was estimated with the following equations.

$$X_c \ FT\text{-}IR = \frac{Crystalline \ amide \ peak}{Amorphous + Crystalline \ amide \ peak} = \frac{\lambda_{25°C(1630\,cm^{-1})}}{a \times \lambda_{25°C(1670\,cm^{-1})} + \lambda_{25°C(1630\,cm^{-1})}} \quad (Equation \ 5.1)$$

With λ_T = height of absorption band at temperature T (°C)
The height of the amorphous and crystalline amide peak are related by factor a, which can be calculated according to;

$$a = \frac{decrease \ of \ crystalline \ peak \ {(25°C - melt)}}{increase \ of \ amorphous \ peak \ {(25°C - melt)}} = \frac{\lambda_{25°C(1630\,cm^{-1})} - \lambda_{melt(1630\,cm^{-1})}}{\lambda_{melt(1670\,cm^{-1})} - \lambda_{25°C(1670\,cm^{-1})}}$$

DMTA: Samples (70x9x2 mm) for the DMTA were prepared on an Arburg H manual injection moulding machine. The test samples were dried in vacuum at 50 °C for 24 h before use. DMTA spectra were recorded with a Myrenne ATM3 torsion pendulum at a frequency of 1 Hz and 0.1% strain. The storage modulus G' and the loss modulus G" were measured as a function of temperature. The samples were cooled to -100 °C and subsequently heated at a rate of 1 °C/min. The glass transition was determined as the peak in the loss modulus. The flow temperature (T_{flow}) is defined as the temperature where the storage modulus reaches 1 MPa. The start of the rubbery plateau, the intercept of the tangents, is called the flex temperature (T_{flex}). The decrease in storage modulus of the rubbery plateau with increasing temperature is quantified by ΔG', which is calculated from:

$$\Delta G' = \frac{G'_{(Tflex)} - G'_{(Tflow-50°C)}}{G'_{25°C}} \times \frac{1}{\Delta T} \qquad (°C^{-1}) \qquad\qquad (Equation\ 5.2)$$

ΔT is described as the temperature range: $(T_{flow}-50\ °C) - T_{flex}$.

Compression set: Samples for compression set were cut from injection moulded bars. The compression set was measured at room temperature according to ASTM 395 B standard. After 24 h the compression was released at room temperature. After relaxation for half an hour, the thickness of the samples was measured. The compression set was taken as the average of four measurements. The compression set is defined as:

$$Compression\ set = \frac{d_0 - d_2}{d_0 - d_1} \times 100\% \qquad (\%) \qquad\qquad (Equation\ 5.3)$$

Where: d_0 = thickness before compression (mm)

d_1 = thickness during compression (mm)

d_2 = thickness after 0.5 h relaxation (mm)

Results and discussion

In this chapter segmented copolymers based on uniform crystallisable tetra-amide segments and PTMO are studied (Figure 5.2, Figure 5.4). In a first series, the effect of the type of tetra-amide (T6T6T, T8T8T, T10T10T, T4A4T or T6A6T) in $PTMO_{1000}$-tetra-amide segmented block copolymers on the degree of crystallinity and thermal mechanical properties is evaluated. The flexibility of the tetra-amide segment is varied by changing the length of the diamine in the tetra-amides (x = 4 - 10) and by replacing the central terephthalic group (T) by an adipic group (A). In a second series the molecular weight of the PTMO segment is varied from 650 to 2900 g·mol^{-1}, thereby changing the amide concentration from 49 to 14%.

Polymers based on PTMO$_{1000}$

The copolymers were prepared by reacting the methyl ester groups of the bisester tetra-amide unit with the hydroxyl functionalised PTMO. Two polymerisation methods were studied, a melt polymerisation and a solution/melt polymerisation.

Melt polymerisation

A simple method for the synthesis of these copolymers is a melt polymerisation. In the melt polymerisation the bisester tetra-amide unit has to melt and mix with the PTMO units. The initial temperature during polymerisation needs to be 5 - 10 °C higher than the melting temperature of the bisester tetra-amide unit. The problem of a high polymerisation

temperature is the degradation of the polyether segment[27]. A maximum polymerisation temperature of 300 °C was taken. The T8T8T-dimethyl, T10T10T-dimethyl, T4A4T-dimethyl and T6A6T-dimethyl had sufficiently low melting temperatures to be used in a melt synthesis (Table 5.1). For T6T6T-dimethyl the melting temperature is above the maximum melting temperature of 300 °C. With the low melting T6A6T-dimethyl the maximum reaction temperature could be limited to 260 °C. Melt polymerisation results in copolymers with high inherent viscosities, particular for $PTMO_{1000}$-T6A6T. The high inherent viscosity of the $PTMO_{1000}$-T6A6T might have been due to the low maximum polymerisation temperature and less degradation of the polyether. This polymer was only slightly coloured, probably due to the low polymerisation temperature used.

Solution/melt polymerisation route

A different method to make these polymers is a solution/melt polymerisation. By using NMP as a solvent for the tetra-amide units the polymerisation starts with a solution and the initial polymerisation temperature can be low. When the rigid segment is incorporated in the copolymer, its melting temperature will decrease and the reaction can be continued in the melt at 250 °C. The NMP kept the reaction mixture homogeneous up to 250 °C but the use of NMP is less practical as it initiates discolouring of the segmented copolymer. The solution/melt polymerisation resulted in polymers with high inherent viscosities (Table 5.1).

Table 5.1: Polymerisation method.

	Melting temperature Bisester tetra-amide (°C)	Initial Polym. temperature (°C)	η_{inh} solution/melt (dl/g)	η_{inh} melt (dl/g)
$PTMO_{1000}$-T6T6T	303	-	2.2	-
$PTMO_{1000}$-T8T8T	275	280	1.6	1.2
$PTMO_{1000}$-T10T10T	244	255	2.4	2.0
$PTMO_{1000}$-T4A4T	287	290	2.2	1.6
$PTMO_{1000}$-T6A6T	255	260	2.5	2.2

The inherent viscosities of melt synthesised copolymers are however somewhat lower compared with the copolymers made from solution and therefore copolymers in the next sections were prepared with the solution/melt route. It is possible to synthesise these materials without a solvent but reaction conditions are more critical.

PTMO$_{1000}$-tetra-amide copolymers

Segmented polyether(ester-amide)s (PEEA) based on poly(tetramethylene oxide)$_{1000}$ and bisester tetra-amide segments of uniform length were synthesised starting with a solution in NMP and ending in the melt (Table 5.3). The inherent viscosities are in the range of 1.6 - 2.5 dl/g. The copolymers had transparent melts and the molecular weights are high so melt phasing had not taken place[11]. Melt phasing is likely to occur if the amide or PTMO segments are long[29]. Thus with PTMO$_{1000}$ segments and tetra-amide units melt phasing did not take place. This is in line with what has been observed previously[8,11].

The polymers are transparent solid materials, although the bisester tetra-amide segments had crystallised. This can be due to the fact that the crystallites formed are smaller than the wavelength of light and therefore do not scatter the light[11,17].

DSC

The melting and crystallisation behaviour of the copolymers were studied with DSC (Figure 5.5, Table 5.2). Melting data from the second heating run was used to exclude the influence of thermal history of the samples. The melting temperatures of the copolymers decrease with higher number of methylene groups in the diamines (*x*) and with the change of the centre terephthalic (T) to an adipic group (A). The melting temperatures of the tetra-amide segments in the copolymer are about 60 °C lower than the melting temperatures of the dimethyl tetra-amide units (Table 5.2).
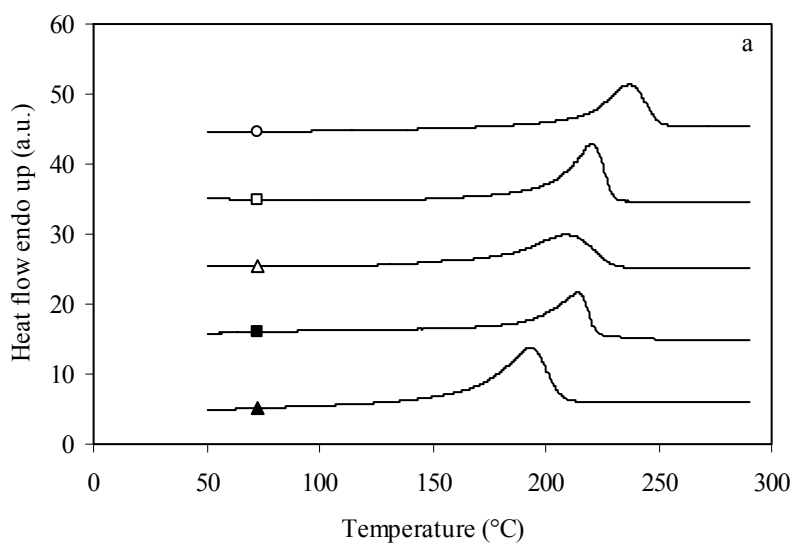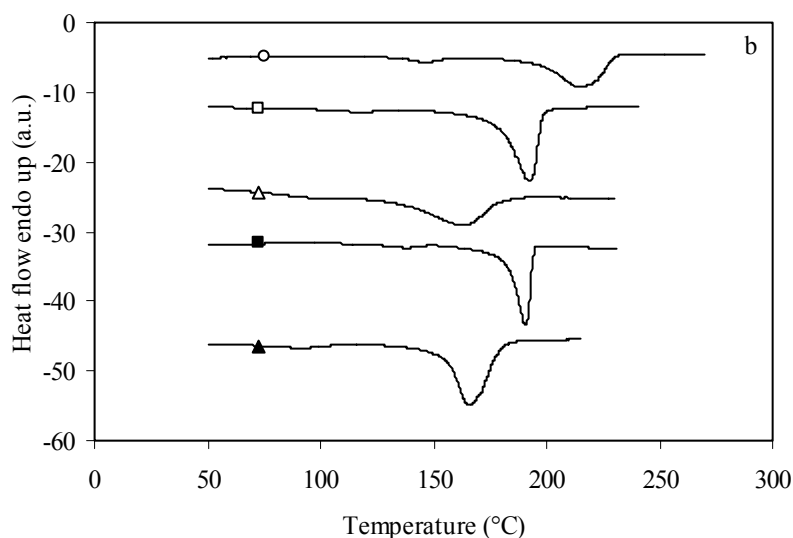
Figure 5.5: a) DSC second heating curve and b) cooling curve of PTMO based segmented copolymers with bisester tetra-amides: ○, PTMO$_{1000}$-T6T6T; □, PTMO$_{1000}$-T8T8T; △, PTMO$_{1000}$-T10T10T; ■, PTMO$_{1000}$-T4A4T; ▲, PTMO$_{1000}$-T6A6T.

Upon cooling, the amide segments crystallise and the crystallisation temperature of these copolymers is only a bit lower than their melting transition. A second, small crystallisation peak is visible and is clearly present for the polymers with the T6T6T, T4A4T and T6A6T segments. A double crystallisation peak was also observed for the dimethyl bisester tetra-amide units[28]. The second crystallisation exotherm is thought to be due to a change in crystalline structure[8,30,31].

Table 5.2: DSC properties of copolymers based on PTMO$_{1000}$.

	ΔH_m tetra-amide (J/g)	Amide content (%)	η_{inh} (dl/g)	T_m (°C)	T_c (°C)	T_m-T_c (°C)	ΔH_m Amide (J/g)	ΔH_c Amide (J/g)	X_c DSC (%)	X_c FT-IR (%)
PTMO$_{1000}$-T6T6T	150	35.0	2.2	241	229	12	43	36	82	92
PTMO$_{1000}$-T8T8T	184	37.2	1.6	211	198	13	50	45	73	89
PTMO$_{1000}$-T10T10T	114	39.2	2.4	203	186	17	39	27	87	78
PTMO$_{1000}$-T4A4T	138	31.9	2.2	216	197	19	42	35	82	88
PTMO$_{1000}$-T6A6T	161	34.2	2.5	196	180	16	44	38	80	86

The undercooling (T_m - T_c) in these copolymers is less than 20 °C, which indicates fast crystallisation of the tetra-amide segments in the copolymer. The melting enthalpies are high

for all copolymers, between 39 - 50 J/g. Based on the melting enthalpy of the bisester tetra-amide, an estimation of the degree of crystallinity can be made, which is in the order of 70 - 90%.

FT-IR

Infrared spectroscopy can be used to determine the degree of crystallinity of the tetra-amide segments in the copolymer[14]. In chapter 3 of this thesis, the ratio of crystalline amide C=O (v = 1630 cm^{-1}) and amorphous amide C=O (v = 1670 cm^{-1}) bands of PTMO$_{1000}$-T6A6T were studied with FT-IR using a heating-cooling cycle. The peak of crystalline C=O at room temperature was compared with the peak of the amorphous C=O in the melt and is 1:1.9[14]. This ratio (a) of the peak height was used to calculate the degree of crystallinity of PTMO$_{1000}$-T4A4T at room temperature (Equation 5.1).

For segmented copolymers with TxAxT segments a double peak at 1630 cm^{-1} (terephthalamide) and 1640 cm^{-1} (adipamide) was observed but with TxTxT segments only a single peak at 1630 cm^{-1} of the terephthalamide was observed (Figure 5.6)[32,33]. The peak ratio of C=O 'crystalline' and 'amorphous' is therefore different than for the PTMO-TxAxT.

In a heating cycle the ratio of crystalline over amorphous C=O was determined for PTMO$_{1000}$-T6T6T to be 1:2.4. This ratio was also used to calculate the degree of crystallinity at room temperature for PTMO$_{1000}$-T8T8T and PTMO$_{1000}$-T10T10T.

The degree of crystallinity of the copolymers, estimated with FT-IR were high, irrespective of the tetra-amide segment used (Table 5.2). The degree of crystallinity obtained with FT-IR is somewhat higher than obtained by DSC (Table 5.2).
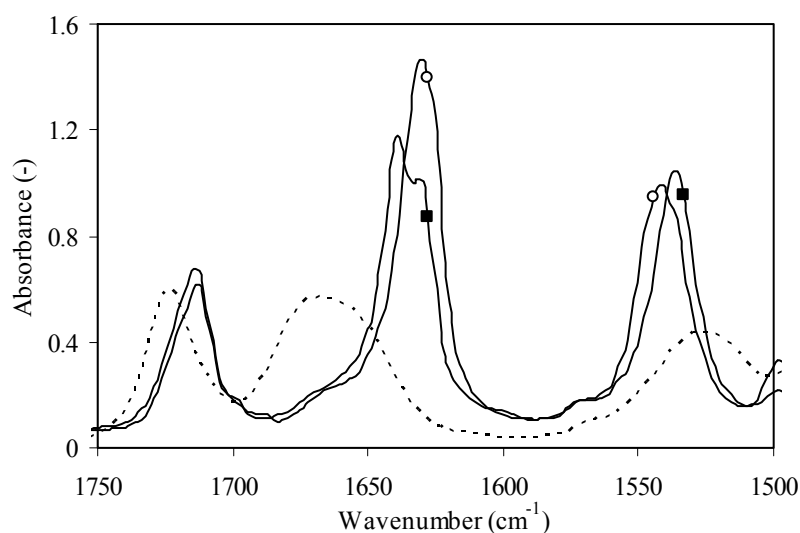
Figure 5.6: FT-IR at 25 °C for PTMO$_{1000}$ with different tetra-amides: ○, PTMO$_{1000}$-T6T6T; ■, PTMO$_{1000}$-T6A6T; --- PTMO$_{1000}$-T6A6T in the melt.

DMTA

Thermal mechanical properties of the polymers were studied by dynamic mechanical thermal analysis (DMTA) in torsion. The storage and loss modulus were measured as a function of temperature (Figure 5.7, Table 5.3).
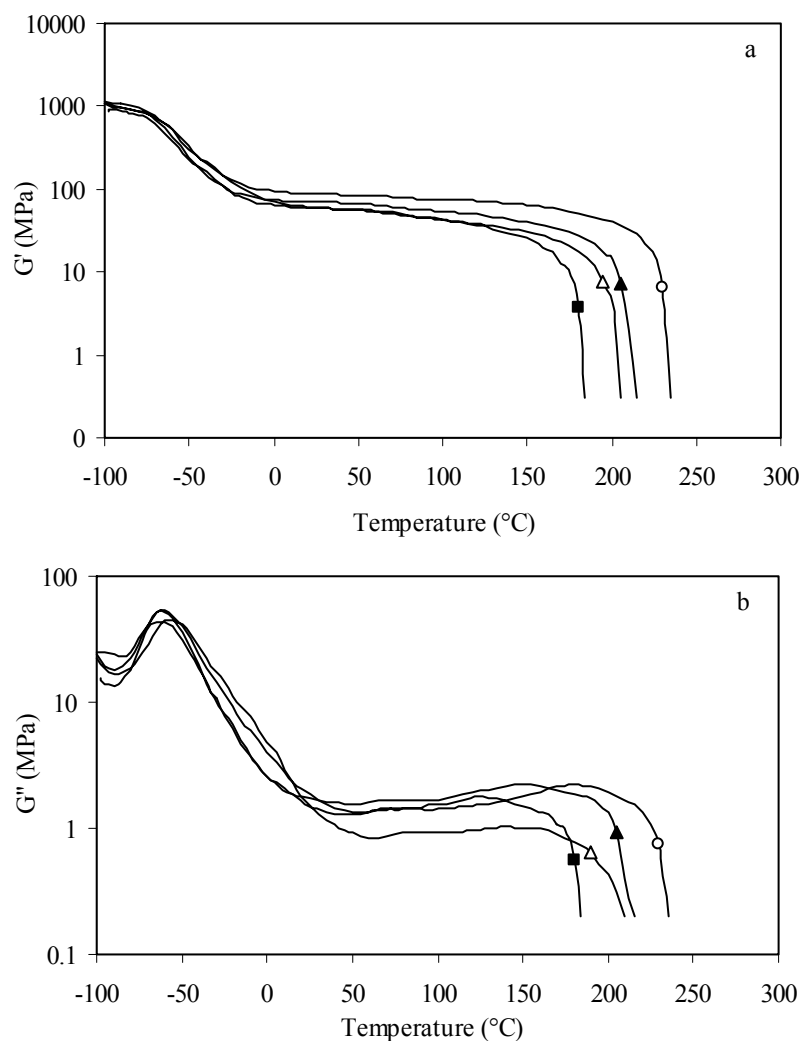
Figure 5.7: a) Storage modulus and b) loss modulus of PTMO$_{1000}$ with different blocks: ○, PTMO$_{1000}$-T6T6T; ▲, PTMO$_{1000}$- T4A4T; Δ, PTMO$_{1000}$ -T10T10T; ■, PTMO$_{1000}$-T6A6T; the curve for PTMO$_{1000}$-T8T8T is similar to that of PTMO$_{1000}$-T4A4T and is for that reason not shown.

Two transitions are observed: a glass transition of the polyether phase and a melting temperature of the amide segments. In the G" a vague shoulder is present at -20 °C, suggesting a minimal amount of crystalline PTMO. The glass transition temperatures (T$_g$) are low (~ -60°C) and this suggests a low amount of tetra-amide dissolved in the polyether phase[11,29]. The polyether T$_g$ is not influenced by the type of tetra-amide. The flex

temperature (T_{flex}) is the start of the rubbery plateau and is -15 °C due to the low T_g and the minimal amount of $PTMO_{1000}$ crystallisation. The rubbery plateau is fairly constant as is generally observed for polymers with segments of uniform length[2,3,5,6,8,10,11,34]. The stability of the rubber modulus is expressed as ΔG'. A low ΔG' represents a less temperature-dependent rubbery plateau (Table 5.3).

The moduli at 25 °C are high considering the low amide contents. For T6T6T, the modulus is higher than the modulus of a polymer made with T8T8T or T10T10T. Also, the modulus decreases when in the rigid segment a terephthalic group is replaced by an adipic group. The modulus in these types of materials is dependent on the degree of crystallinity and the aspect ratio of the crystallites[11,13]. As the degree of crystallinity is not different (Table 5.2) it must be an effect of the aspect ratio of the crystallites. The flow transitions are sharp as with other segments of uniform length[8,10,11,35]. The flow temperatures decrease with increasing number of methylene groups in the diamines and the change of the centre terephthalic to an adipic group. These flow temperatures correspond well with the melting temperatures as measured by DSC (Table 5.2). The peak in the loss modulus (G") represents the glass transition temperature (T_g) of the segmented copolymer. For all segmented copolymers based on $PTMO_{1000}$ a T_g of around -61 °C was obtained with DMTA. The low T_g indicates that little tetra-amide segments are dissolved in the amorphous phase and thus crystallinity is high for all the tetra-amide segments used (Table 5.3).

Table 5.3: Properties of segmented copolymers based on PTMO$_{1000}$.

	Amide content	η_{inh}	G' (25°C)	T_g	T_{flex}	ΔG'*10^{-3}	T_{flow}	CS (25°C)
	(%)	(dl/g)	(MPa)	(°C)	(°C)	(°C^{-1})	(°C)	(%)
PTMO$_{1000}$-T6T6T	35.0	2.2	87	-61	-15	3.7	235	18
PTMO$_{1000}$-T8T8T	37.2	1.6	72	-62	-15	4.7	215	20
PTMO$_{1000}$-T10T10T	39.2	2.4	60	-59	-5	5.0	210	15
PTMO$_{1000}$-T4A4T	31.9	2.0	70	-62	-15	3.8	215	19
PTMO$_{1000}$-T6A6T	34.2	2.5	51	-60	-15	4.9	185	14

Compression set

A compression set was performed as a measure of the elasticity of the polymers. A lower compression set refers to more elastic behaviour. These polymers have a compression set below 20%. Some polymers have lower compression sets but these also have a lower

modulus. Normally the compression set of a polymer decreases with decreasing rubber modulus[14].

PTMO segment length

In segmented copolymers with crystallisable tetra-amide segments, a change in PTMO molecular weight has a direct effect on the amide content[8,11,14,18]. Segmented copolymers were synthesised using tetra-amide segments and PTMO segments with a molecular weight ranging from 650 to 2900 g·mol^{-1} (Table 5.4). The segmented copolymers all had a high inherent viscosity, indicating high molecular weight. The inherent viscosities increased with PTMO length. This seems logical as, at a particular degree of polymerisation, the molecular weight increases with repeat length. The thermal mechanical behaviour of these copolymers was studied by DMTA (Table 5.4).

Table 5.4: Properties of segmented copolymers based on PTMO and bisester tetra-amide.

PTMO-tetra-amide	Amide content	η_{inh}	$G'_{25\,°C}$	T_g	T_{flex}	$\Delta G' *10^{-3}$	T_{flow}	$CS_{25°C}$
	(%)	(dl/g)	(MPa)	(°C)	(°C)	(°C^{-1})	(°C)	(%)
PTMO$_{650}$-T6T6T	44.6	1.9	125	-50	30	4.4	250	19
PTMO$_{1000}$-T6T6T	35.0	2.2	87	-61	-15	3.7	235	18
PTMO$_{2000}$-T6T6T	21.6	2.2	39	-68	5	1.7	225	13
PTMO$_{2900}$-T6T6T	16.1	1.9	22	-69	10	0.9	215	10
PTMO$_{650}$-T8T8T	47	1.4	150	-40	30	7.4	230	22
PTMO$_{1000}$-T8T8T	37.2	1.6	72	-62	-15	4.7	215	20
PTMO$_{2000}$-T8T8T	23.3	2.7	20	-67	5	2.1	210	16
PTMO$_{2900}$-T8T8T	17.4	2.7	13	-72	15	1.1	200	9
PTMO$_{650}$-T10T10T	49.1	1.4	149	-38	20	4.3	220	18
PTMO$_{1000}$-T10T10T	39.2	2.4	60	-59	-5	5.0	210	15
PTMO$_{2000}$-T10T10T	24.9	2.9	20.5	-68	5	2.9	200	14
PTMO$_{2900}$-T10T10T	18.7	2.8	14.5	-71	15	2.6	190	9
PTMO$_{650}$-T4A4T	41.1	2.1	79	-56	30	4.3	225	20
PTMO$_{1000}$-T4A4T	31.9	2.2	70	-62	-15	3.8	215	19
PTMO$_{2000}$-T4A4T	19.3	2.3	19	-68	5	1.8	205	12
PTMO$_{2900}$-T4A4T	14.3	2.5	8.3	-69	15	0.6	195	10
PTMO$_{650}$-T6A6T	43.8	1.8	102	-45	35	5.0	200	17
PTMO$_{1000}$-T6A6T	34.2	2.5	51	-60	-15	4.9	185	14
PTMO$_{2000}$-T6A6T	21.1	2.9	18	-70	10	2.9	180	9
PTMO$_{2900}$-T6A6T	15.7	3.5	9	-70	20	1.8	175	7

The T_g's of the polymers were low but increased with decreasing PTMO length, probably due to increasing of the physical network density. The mechanical properties of the PTMO$_{650}$ polymers seem to be dependent on the type of tetra-amide used. With increasing number of methylene groups in the tetra-amide the T_g of the PTMO$_{650}$ copolymer increases and exchanging the central terephthalic group for an adipic group increases the T_g as well.

This difference must be due to the amount of dissolved tetra-amide in PTMO$_{650}$ and probably a higher aliphatic content of the tetra-amide makes it easier to dissolve the tetra-amide segment in PTMO. This trend was only observed for PTMO$_{650}$. The relation of T_{flex} as a function of PTMO length is remarkably similar for the different tetra-amide units, although for T6A6T it is possibly slightly higher than for the other amide units. The copolymers with PTMO$_{1000}$ have the lowest T_{flex}. Longer blocks than PTMO$_{1000}$ can crystallise and thereby increases the T_{flex}, while PTMO$_{650}$ copolymers have a small extra phase at 0 °C.

The rubber modulus at room temperature increases strongly from 9 to 149 MPa with increasing amide content (16 to 50 wt%). The moduli are lower for T4A4T and T6A6T than for the TxTxT series particularly at higher amide contents. The temperature-dependence of the modulus (ΔG') increases with decreasing PTMO length or increasing amide content. This effect was also observed in PPO-T6T6T polymers[11] and suggests a less than perfect packing of the segments of uniform length at higher contents. The flow temperature decreases with increasing PTMO length (PTMO content). This effect is described earlier as the solvent effect of the PTMO segments on the amide crystallites[14]. The T_{flow} decreases with diamine length and by exchanging the central terephthalic acid unit for an adipate unit. This effect is similar to that in the bisester tetra-amide starting units[28].

The compression set (CS) for polymers decreases with decreasing modulus. The same trend was observed for all tetra-amides units used. The CS values are below 20%. A clear difference between the polymers with different tetra-amides units was not observed and the elastic behaviour is expected to be the same. Some polymers seem to have a lower compression set but these polymers also have a lower modulus as is the case for the PTMO-T6A6T series.

Increasing the amide concentration in the segmented copolymer increases both the rubber modulus and the flow temperature. The increase of the modulus can be described with the Halpin-Tsai model as was discussed in chapter 3 (Figure 3.15). The increase of the flow

temperature can be described with the solvent effect theory, proposed by Flory, and this was shown in Figure 3.16. However, the flow temperature is not only dependent on the crystalline content but is also dependent on the chemical structure of the tetra-amide (Table 5.4). For engineering polymer properties, it is interesting to see the effect of the tetra-amide used on the correlation between the modulus (at 25 °C) and the flow temperature (Figure 5.8).
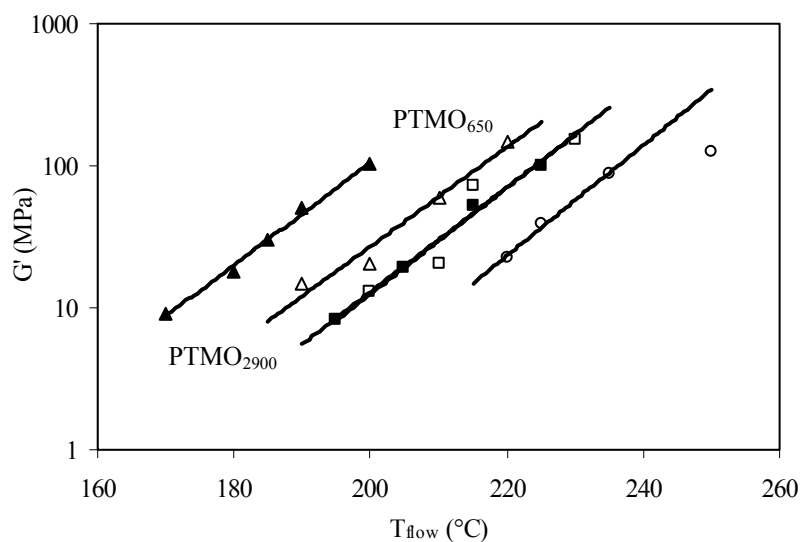
Figure 5.8: Correlation of storage modulus at 25 °C and flow temperature: ○, PTMO-T6T6T; □, PTMO-T8T8T; Δ, PTMO-T10T10T; ■, PTMO-T4A4T; ▲, PTMO-T6A6T; with PTMO lengths of 650 - 1000 - 2000 - 2900 g·mol^{-1}.

The polymers with different tetra-amides all have a similar relationship between the rubber modulus and the flow temperature. This graph simplifies the choice of a copolymer that has a particular rubber modulus and flow temperature.

Conclusions

Segmented block copolymers based on PTMO and tetra-amide units can be synthesised by a solution/melt route and by melt polymerisation. Solution/melt polymerisation resulted in higher molecular weights but the melt synthesised copolymers were less coloured. Melt polymerisation is well possible if the melting temperature of the used bisester tetra-amide was less than 260 °C.

The tetra-amide segments in the copolymers were T6T6T, T8T8T, T10T10T, T4A4T or T6A6T. The molecular weight of the PTMO segment was varied from 650 - 2900 g·mol^{-1}. These segmented copolymers generally have a two-phase structure: a continuous polyether phase with a low T_g and a dispersed crystalline amide phase. The crystalline tetra-amide segments are present as nano ribbons. The degree of crystallinity of these tetra-amide units in the copolymers with PTMO$_{1000}$ was studied both by DSC and FT-IR. The degree of crystallinity as determined by these techniques was very high, on average 80 - 90 %.

The glass transition temperatures were low and increased with decreasing PTMO length. The type of tetra-amide had only an effect on the copolymers with PTMO$_{650}$. Higher number of methylene groups and an aliphatic diacid in the tetra-amide segment gave higher T_g's of the copolymers. With PTMO$_{650}$ the solubility of the tetra-amide seems to play a role. The flex temperatures were low for PTMO$_{1000}$ (about -15 °C). The PTMO$_{650}$ showed an extra transition and the PTMO$_{2000}$ and PTMO$_{2900}$ had a crystalline ether fraction.

The moduli are higher for TxTxT copolymers than for TxAxT copolymers. As the crystallinities of the copolymers with T4A4T and T6A6T are not lower, the lower modulus must be due to a lower aspect ratio of crystallites of T4A4T and T6A6T. All the copolymers had a rubber modulus that was little dependent on temperature.

By decreasing the PTMO length from 2900 to 650 g·mol^{-1}, the amide content in the copolymer increased from 16 to 50 wt% and as a result of this the storage modulus increased from 9 to 150 MPA. This increase in modulus is very strong and is due to the high degree of crystallinity and the high aspect ratio of the crystallites of the uniform amide segments.

References

1. Eisenbach, C.D., Stadler, E., Enkelmann, V., *Macromol. Chem. Phys.* **196**, 833-856 (1995).

2. Ng, H.N., *Polymer* **14**, 255-261 (1973).

3. Harrel, L.L., *Macromolecules* **2**, 607-612 (1969).

4. Bennekom van, A.C.M., Gaymans, R.J., *Polymer* **38**, 657-665 (1997).

5. Bouma, K., Wester, G.A., Gaymans, R.J., *J. Appl. Polym. Sci.* **80**, 1173-1180 (2001).

6. Gaymans, R.J., Dehaan, J.L., *Polymer* **34**, 4360-4364 (1993).

7. Hutten van, P.F., Mangnus, R.M., Gaymans, R.J., *Polymer* **34**, 4193-4202 (1993).

8. Krijgsman, J., Husken, D., Gaymans, R.J., *Polymer* **44**, 7573-7588 (2003).

9. Krijgsman, J., Husken, D., Gaymans, R.J., *Polymer* **44**, 7043-7053 (2003).

10. Niesten, M.C.E.J., Feijen, J., Gaymans, R.J., *Polymer* **41**, 8487-8500 (2000).

11. Schuur van der, J.M., *'Poly(propylene oxide) based segmented blockcopolymers'*, Ph.D. Thesis, University of Twente (2004).

12. Serrano, P.J.M., Thuss, E., Gaymans, R.J., *Polymer* **38**, 3893-3902 (1997).

13. Halpin, J.C., Kardos, J.L., *J. Appl. Phys.* **43**, 2235 (1972).

14. Chapter 3 of this thesis

15. Szycher, M., *'Szycher's handbook of polyurethanes'*, Boca Raton: CRC Press LLC, (1999).

16. Sorta, E., Della Fortuna, G., *Polymer* **21**, 728 (1980).

17. Krijgsman, J., *'Segmented copolymers based on poly(2,6-dimethyl-1,4,phenylene ether)'*, Ph.D. Thesis, University of Twente (2002).

18. Niesten, M.C.E.J., *'Polyether based segmented copolymers with uniform aramid units'*, Ph.D. Thesis, University of Twente (2000).

19. Niesten, M.C.E.J., Gaymans, R.J., *J. Appl. Polym. Sci.* **81**, 1372-1381 (2001).

20. Garcia, D., Starkweather, H., *J. polym. sci. phys. ed.* **32**, 537 (1985).

21. Niesten, M.C.E.J., Harkema, S., van der Heide, E., Gaymans, R.J., *Polymer* **42**, 1131-1142 (2001).

22. Ramesh, C., Keller, A., Eltink, S.J.E.A., *Polymer* **35**, 5293-5299 (1994).

23. Cella, R.J.J., *J. Polym. Sci. : Symp. no. 47* (1973).

24. Versteegen, R.M., *'Well-defined Thermoplastic Elastomers'*, Ph.D. Thesis, University of Eindhoven (2003).

25. Allegrezza, A.E., Seymour, R.W., Ng, H.N., Cooper, S.L., *Polymer* **15**, 433-440 (1974).

26. Eisenbach, C.D., Heinemann, T., Ribbe, A., Stadler, E., *Angew. Makromol. Chem.* **202**, 221-241 (1992).

27. Costa, L., Luda, M.P., Cameron, G.G., Qureshi, M.Y., *Polym. Degrad. Stab.* **67**, 527-533 (2000).

28. Chapter 2 of this thesis

29. Holden, G., Legge, N.R., Quirk, R., Schroeder, H.E. *'Thermoplastic elastomers'*. Hanser Publisher, Munich,(2005).

30. Lips, P.A.M., *'Aliphatic segmented poly(ester amide)s based on symmetrical bisamide-diols'*, Ph.D. Thesis, University of Twente (2005).

31. Stapert, H.R., *'Environmentally degradable polyesters, poly(ester-amide)s and poly(ester-urethane)s'*, Ph.D. Thesis, University of Twente (1998).

32. Dechant, J., *'Ultrarot-spektroskopische Untersuchungen an Polymeren'*, Maxim Gorki, Berlin (1972).

33. Gaymans, R.J., *J. Polym. Sci.* **23**, 1599-1605 (1985).

34. Shirasaka, H., Inoue, S., Asai, K., Okamoto, H., *Macromolecules* **33**, 2776-2778 (2000).

35. Krijgsman, J., Gaymans, R.J., *Polymer* **45**, 437-446 (2004).

CHAPTER 6

INFLUENCE OF POLYDISPERSITY OF CRYSTALLISABLE SEGMENTS ON THE PROPERTIES OF SEGMENTED BLOCK COPOLYMERS

Abstract

Poly(ether-ester-amide)s (PEEA's) based on PTMO$_{2000}$ and uniform T6A6T were synthesised by a solution/melt polymerisation. The T6A6T unit is based on adipic acid (A), terephthalic acid (T) and hexamethylene diamine (6) and was synthesised prior to the polymerisation. The thermal and mechanical properties of these copolymers were measured by DSC, FT-IR, DMTA, CS and TS. The polymer with uniform crystallisable segments crystallises fast, has an almost temperature independent rubbery plateau, a low compression set and a low tensile set.

The properties of the polymer with uniform amide segments are compared with polymers having polydisperse amide segments. Polymers with polydisperse amide segments have a mixture of uniform amide segments of diamide (T6T), tetra-amide (T6A6T) and hexa-amide (T6A6A6T). The mol% of T6A6T in the copolymers was varied while the mol ratio of T6T and T6A6A6T was kept constant. Block copolymers with a mixture of different uniform crystallisable amide segments crystallise slower, have a lower rubber modulus and a higher T$_{flex}$ compared to the polymer with uniform amide segments. Also the elastic properties, measured by CS and TS, are lower for the polymer with polydisperse amide segments.

One copolymer was made via a one pot polymerisation and this copolymer had a "random" distribution of amide sequence length. In general, the copolymers with random amide segments were inferior compared with the properties of copolymers with mixtures of uniform amide segments. A uniformity of 80% (PDI 1.03) of the rigid segments gives a polymer with still good properties.

Introduction

Segmented copolymers consist of alternating flexible and rigid segments. A method to influence the properties of the copolymers is to use uniform rigid or uniform flexible segments. The structure of the rigid segments in segmented block copolymers have generally an effect on the rubber modulus, yield stress, elastic properties, melting temperatures and the T_g of the soft phase[1,2]. Several studies were done at block copolymers with uniform rigid segments. Van der Schuur[2] compared uniform and random crystallisable amide segments in poly(propylene oxide) (PPO) based segmented block copolymers with amide rigid segments. He found that copolymers with uniform amide segments had a higher modulus, a higher melting temperature and a lower compression set compared to copolymers with random amide segments. The uniform segments crystallised in nano-ribbons with a high aspect ratio. The random amide segments had a lower crystallinity and the aspect ratio of the nano-ribbons was lower.

Harrel and Ng et al.[3,4] studied polyurethanes with uniform rigid segments and found that a narrow distribution of the rigid segments compared with a broad distribution increases modulus, tensile strength and elongation dramatically. As was discussed in Chapter 3 and 5 of this thesis, uniform crystallisable segments crystallise fast and the copolymers have a high modulus, good phase separation, a temperature independent rubber modulus, high elasticity and high fracture strains.

Flexible segments in segmented block copolymers largely control the low temperature properties of the copolymers[1] and have an effect on the fracture properties if strain hardening takes place[5]. Several studies were done at segmented block copolymers with uniform flexible segments[3,4,6-10]. These studies report a minor increase in modulus, tensile strength and strain at break while the T_g and T_{flex} were slightly lower. Polymers with uniform flexible segments show only small improvements in properties compared to polymers with a broad distribution of flexible segments.

All studies on the polydispersity of the rigid segment showed an improvement in polymer properties when a uniform rigid segment was used. Uniform crystallisable segments result in a much greater improvement of polymer properties than uniform flexible segments and therefore the study was focused on the polydispersity of the rigid segments. Until now, only

the difference between uniform (narrow) and polydisperse (broad) rigid segments was pointed out but it was not yet studied how the properties of the polymers change with the polydispersity of the rigid segment. As segmented block copolymers with uniform rigid segments are more difficult to synthesise it would be interesting to study how critical the influence of the polydispersity of the rigid segments is on polymer properties.

Research aim

The influence of the polydispersity of the rigid segments on the properties of segmented block copolymers is studied. The properties of polymers with uniform rigid segments are compared to polymers having polydisperse rigid segments. Polymers with polydisperse amide segments have a mixture of uniform amide segments of diamide (T6T), tetra-amide (T6A6T) and hexa-amide (T6A6A6T). The mol% of T6A6T in the copolymers was varied while the mol ratio of T6T and T6A6A6T was kept constant. The wt% of crystallisable segment was kept constant as well as the degree of possible hydrogen bonding, so the polydispersity of the crystallisable segments is the only parameter that is changed. Also, a copolymer in a one pot reaction was synthesised giving an amide segment with a "random" length distribution. The crystallisation of the polymers was studied with DSC and FT-IR. The thermal and mechanical behaviour was studied with DMTA and tensile test. The elastic behaviour of the polymers was measured with compression set and tensile set.

Experimental

Materials: 1,6-hexamethylenediamine (HMDA), dimethyl terephthalate (DMT), dimethyl adipate, N-methyl-2-pyrrolidone (NMP) and a 0.5 M sodium methoxide solution in methanol were purchased from Aldrich and used as received. Tetra-isopropyl orthotitanate (Ti(i-OC$_3$H$_7$)$_4$) was purchased from Aldrich and was diluted with m-xylene (0.05 M). m-Xylene was purchased from Merck. PTMO with a length of 1000 (PTMO$_{1000}$) and 2000 g·mol^{-1} (PTMO$_{2000}$) were a gift from Dupont. Irganox 1330 was obtained from CIBA. The synthesis of diphenyl terephthalate (DPT) and methylphenyl terephthalate (MPT) was performed as described before[11,12]. The synthesis of T6A6T was performed as described before[11]

Synthesis of T6T-dimethyl[2,13]: T6T-dimethyl was synthesised from 1,6-hexamethylenediamine (HMDA) and dimethyl terephthalate (DMT). An excess amount of DMT (97 g, 0.5 mol) was dissolved in 350 ml toluene and 30 ml methanol at 70 °C in a round bottomed flask. A solution of 50 ml toluene and HMDA (12 g, 0.1 mol) was added to the flask. Sodium methoxide (50 ml of a 0.5 M solution in methanol) was added as a catalyst. The reaction was carried out at 70 °C for three h and subsequently four h at 95 °C, distilling off the methanol. The

precipitated product was filtered over a hot filter no. 3 and washed three times with hot toluene 65 °C each time filtering over a hot filter. The product was washed once with diethyl ether to dry the product.

To increase the purity, the T6T-dimethyl was recrystallised from hot NMP (160 °C, 30 g/l). The recrystallised product was washed twice with acetone and dried in a vacuum oven. The T_m using DSC was 232 °C with a ΔH_m of 64 J/g. The purity calculated from the ratio of terephthalic protons from the NMR spectra was found to be >99%. ^{1}H-NMR (TFA-*d*): δ 8.28 (d, 4H, terephthalic H methyl ester side), δ 7.95 (d, 4H, terephthalic H amide side), δ 4.10 (s, 6H, methyl ester endgroup), δ 3.72 (t, 4H, 1st and 6th CH_2 HMDA), δ 1.87 (t, 4H, 2nd and 5th CH_2 HMDA), δ 1.60 (t, 4H, 3rd and 4th CH_2 HMDA).

Synthesis of T6A6A6T-dimethyl: The synthesis of T6A6A6T-dimethyl was performed in 3 steps.

First, A6A-dimethyl ester was synthesised in a bulk reaction. To a 1 l round bottomed flask fitted with nitrogen inlet, a reflux condenser and a mechanical stirrer was added HMDA (26 g, 0.23 mol), an excess of dimethyl adipate (627 g, 3.6 mol) and the catalyst sodium methoxide (10 ml of a 0.5 M solution in methanol). The reaction was carried out for 16 h at 120 °C. After cooling the product was precipitated in diethyl ether and collected on a glass filter (no. 4) and subsequently washed three times with diethyl ether. The purity of the product estimated with ^{1}H-NMR was 97%. With DSC the T_m was determined at 129 °C with a ΔH_m of 79 J/g. A crystallisation peak was determined at 111°C with a ΔH_c of 76 J/g.

Second, 6A6A6 was synthesised by reacting A6A-dimethyl diester (50 g, 0.13 mol), HMDA (464 g, 4.0 mol) in the presence of sodium methoxide catalyst solution (10 ml of a 0.5 M in methanol). The reaction was carried out for 16 h at 120 °C. Upon cooling the product precipitated, was collected by filtration and washed three times with diethyl ether and once with chloroform. The purity of the product estimated from ^{1}H-NMR was 97%. The T_m was 180 °C with a ΔH_m of 133 J/g using DSC. A crystallisation peak was observed at 165 °C with a ΔH_c of 105 J/g.

Last, T6A6A6T-dimethyl ester was synthesised from 6A6A6-diamine and MPT. A mixture of 6A6A6-diamine (50 g, 0.09 mol) and MPT (55 g, 0.21 mol) was dissolved in 1.5 l NMP in a 2 l round bottomed flask fitted with nitrogen inlet, a reflux condenser and a mechanical stirrer. The mixture was heated to 135°C and the reaction was carried out for 16 h at 135 °C. After cooling, the precipitated product was collected by filtration and washed with NMP, toluene and acetone respectively. The purity estimated with ^{1}H-NMR was 95% and had a T_m of 251 °C with a ΔH_m of 73 J/g and a T_c of 224 °C with a ΔH_c of 85 J/g. ^{1}H-NMR (TFA-*d*): δ 8.24 (d, 4H, terephthalic H methyl ester side), δ 7.90 (d, 4H, terephthalic H amide side), δ 4.10 (s, 6H, methyl ester endgroup), δ 3.68 (t, 4H, CH_2 HMDA terephthalic amide side), δ 3.54 (s, 8H, CH_2 HMDA aliphatic amide side), δ 2.76 (s, 8H, 1st and 4th CH_2 adipate), δ 1.91 (t, 8H, 2nd and 3rd CH_2 adipate), δ 1.78 (t, 12H, 2nd and 5th CH_2 HMDA), δ 1.48 (s, 12H, 3rd and 4th CH_2 HMDA).

Synthesis of PTMO$_{2000}$-T6A6T with different rigid segment polydispersity: The polymerisation was carried out in a 250 ml stainless steel reactor with a nitrogen inlet and magnetic coupling stirrer. The polymerisation of PTMO$_{2000}$ with 70 mol% of T6A6T, 15 mol% T6T and 15 mol% T6A6A6T is given as an example. The reactor was charged with PTMO$_{2000}$ (50 g, 0.025 mol), T6T-dimethyl (1.65 g, 0.004 mol), T6A6T-dimethyl (11.7 g, 0.017 mol), T6A6A6T-dimethyl (3.35 g, 0.004 mol), 100 ml NMP, 1 wt% Irganox 1330 (based on PTMO) and a catalyst solution (2.5 ml of 0.05 M Ti(i-OC$_3$H$_7$)$_4$ in m-xylene) under nitrogen flow. The stirred reaction

mixture was heated to 180 °C in 30 min and subsequently in 2 h to 250 °C. The reaction was continued for 2 h at 250 °C, after which the pressure was carefully reduced (P<20 mbar) to distil off the NMP and then further reduced (P<0.3 mbar) and the reaction mixture was kept at this pressure for 1 h. The reactor was cooled slowly maintaining the low pressure. The copolymers are tough. Copolymers with up to 10 mol% of other blocks were transparent and at higher contents of other blocks the copolymers were opaque.

One pot synthesis of (PTMO$_{1000}$-T)$_{2000}$-T6A6T with random rigid segment: The polymerisation was carried out in a 50 ml glass reactor. First, HMDA (3.7 g, 0.0315 mol), dimethyl adipate (2.61 g, 0.015 mol) and Irganox 1330 (0.3 g) were added to the reactor in an argon atmosphere. Sodium methoxide (1 ml of a 0.5 M solution in methanol) was added as a catalyst. The reaction was carried out for two h at 100 °C. Subsequently, a solution of PTMO$_{1000}$ (30 g, 0.03 mol) in 25 ml NMP and a solution of DPT (14.3 g, 0.045 mol) in 25 ml NMP and a catalyst solution of (3 ml of 0.05 M Ti(i-OC$_3$H$_7$)$_4$ in m-xylene) were added. The reaction was continued for two h at 180 °C and two h at 250 °C. Subsequently, the pressure was carefully reduced (P<20 mbar) to distil off the NMP and then further reduced (P<0.3 mbar) for 60 min under these conditions. The reactor was cooled slowly maintaining the low pressure. The obtained polymer was opaque.

One pot synthesis of the T6A6T unit: In a 50 ml glass reactor HMDA (1 g, 8.6 mmol) and dimethyl adipate (0.75 g, 4.3 mmol) were reacted for two hours at 100 °C in the presence of sodium methoxide (0.15 ml of a 0.5 M solution in methanol) catalyst. A solution of DPT (2.74 g, 8.6 mmol) in 40 ml NMP was added to the reaction. The temperature was increased to 120 °C and the reaction was continued for 4 h. Initially the solution is transparent but after some time the product precipitates and the solution becomes white. The reaction product was precipitated in ether and filtered over a glass filter (no.4). The product was dried in a vacuum oven at 50 °C.

Viscometry: The inherent viscosity was measured at a concentration of 0.1 g/dl in a mixture of phenol/1,1,2,2-tetrachloroethane (1:1 molar ratio) at 25 ºC using a capillary Ubbelohde type 1B.

^{1}H-NMR: NMR spectra were recorded using a Bruker AC 300 spectrometer at 300 MHz. Deuterated trifluoro acid (TFA-*d*) was used as a solvent.

MALDI-TOF (matrix assisted laser desorption ionization time-of-flight): Mass spectroscopy was performed using a voyager-DE-RP MALDI-TOF mass spectrometer (applied biosystem / perseptive biosystems, INC., Framingham, MA, USA) equipped with delayed extraction. Mass spectra were obtained in reflection mode with a 337 nm UV nitrogen laser producing 3 ns pulses. Samples were dissolved in 10 μl of trifluoracetic acid and 30 μl water / acetonitrile solution (50/50 molar). 1 mg dihydroxybenzoic acid (DHB) was added to the solution as the matrix. One μl of the solution was placed on a gold 100-well plate. The solvent was evaporated and the plate was transferred to the mass spectrometer.

DSC: DSC spectra were recorded on a Perkin Elmer DSC apparatus, equipped with a PE7700 computer and TAS-7 software. Dried samples of 5 - 10 mg were heated to approximately 30 °C above the melting temperature and subsequently cooled, both at a rate of 20 °C/min. The maximum of the peak in de heating scan was taken as

the melting temperature. The second heating scan was used to determine the melting peak and enthalpy of the sample. The first cooling curve was used to determine the crystallisation temperature, which was taken as the onset of crystallisation. The degree of crystallinity was calculated from the melting enthalpy of the polymer and the melting enthalpy of the bisester tetra-amide (138 J/g).

FT-IR: Infrared transmission spectra were recorded using a Nicolet 20SXB FTIR spectrometer with a resolution of 4 cm^{-1}. Solution cast polymer films (0.05 g/ml in HFIP) of <10 μm thick were used for temperature dependent FT-IR recorded at temperatures between room temperature and 260 °C. The film was placed in-between two pressed KBr pellets under a helium flow. The degree of crystallinity of the rigid segments in the polymers was estimated with the following equations.

$$X_c \, FT\text{-}IR = \frac{Crystalline \; amide \; peak}{Amorphous + Crystalline \; amide \; peak} = \frac{\lambda_{25°C(1630\,cm^{-1})}}{a \times \lambda_{25°C(1670\,cm^{-1})} + \lambda_{25°C(1630\,cm^{-1})}} \qquad (Equation \; 6.1)$$

With λ_T = height of absorption band at temperature T (°C)

The height of the amorphous and crystalline amide peak are related by factor a, which can be calculated according to;

$$a = \frac{decrease \; of \; crystalline \; peak \; _{(25°C - melt)}}{increase \; of \; amorphous \; peak \; _{(25°C - melt)}} = \frac{\lambda_{25°C(1630\,cm^{-1})} - \lambda_{melt(1630\,cm^{-1})}}{\lambda_{melt(1670\,cm^{-1})} - \lambda_{25°C(1670\,cm^{-1})}}$$

DMTA: Samples (70x9x2 mm) for the DMTA were prepared on an Arburg H manual injection moulding machine. The test samples were dried in vacuum at 50 °C for 24 h before use. DMTA spectra were recorded with a Myrenne ATM3 torsion pendulum at a frequency of 1 Hz and 0.1% strain. The storage modulus G' and the loss modulus G" were measured as a function of temperature. The samples were cooled to -100 °C and subsequently heated at a rate of 1 °C/min. The glass transition was determined as the peak in the loss modulus. The flow temperature (T_{flow}) is defined as the temperature where the storage modulus reaches 1 MPa. The start of the rubbery plateau, the intercept of the tangents, is called the flex temperature (T_{flex}). The decrease in storage modulus of the rubbery plateau with increasing temperature is quantified by ΔG', which is calculated from:

$$\Delta G' = \frac{G'_{(Tflex)} - G'_{(Tflow-50°C)}}{G'_{25°C}} \times \frac{1}{\Delta T} \qquad (°C^{-1}) \qquad\qquad (Equation \; 6.2)$$

ΔT is described as the temperature range: (T_{flow}-50 °C) - T_{flex}.

Compression set: Samples for compression set were cut from injection moulded bars. The compression set was measured at room temperature according to ASTM 395 B standard. After 24 h the compression was released at room temperature. After relaxation for half an hour, the thickness of the samples was measured. The compression set was taken as the average of four measurements. The compression set is defined as:

$$Compression \; set = \frac{d_0 - d_2}{d_0 - d_1} \times 100\% \qquad (\%) \qquad\qquad (Equation \; 6.3)$$

With: d_0 = thickness before compression (mm)

d_1 = thickness during compression (mm)

d_2 = thickness after 0.5 h relaxation (mm)

Tensile set: Stress-strain experiments were conducted on injection-moulded bars cut to dumbbells (ISO 37 type 2). A Zwick Z020 universal tensile machine equipped with 500 N load cell was used to measure the stress as function of strain of a loading and unloading cycle to 100% strain at a strain rate of 0.4 s^{-1} (test speed of 60 mm/min). The tensile set at 100% ($TS_{100\%}$) was determined as the remaining strain when the stress was zero at the unloading cycle.

Tensile test: Stress-strain curves were obtained using injection moulded bars with a thickness of 2.2 mm, cut to dumbbell (ISO 37 type 2), using a Zwick Z020 universal tensile machine equipped with a 500 N load cell. The strain was measured with extensometers. Standard tensile test were performed in three-fold according to ISO 37 at a strain rate of 0.4 s^{-1} (test speed of 60 mm/min).

Results and discussion

Segmented block copolymers were synthesised based on $PTMO_{2000}$ and amide containing rigid segments. The polydispersity of the rigid segment in the copolymers was varied. Three polymer series were synthesised, namely; polymers with uniform rigid segments (a), polymers with mixtures of uniform rigid segments (b) and polymers with random rigid segments (c).
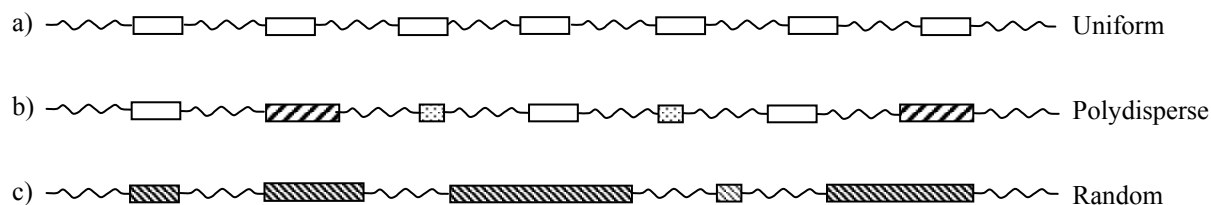
Figure 6.1: Segmented block copolymer based on $PTMO_{2000}$ with: (a), uniform crystallisable segments; (b) polydisperse crystallisable segments; (c) random crystallisable segments.

(a) Segmented copolymers with uniform rigid segments

The segmented block copolymer was synthesised from $PTMO_{2000}$ and uniform T6A6T units (Figure 6.2) by a polycondensation reaction. The T6A6T was synthesised prior to the polycondensation to ensure the uniformity of the unit. As the melting temperatures of the T6A6T unit is high (Table 6.1) a solvent (NMP) was used in the initial part of the polymerisation. At 250 °C the reaction mixture was homogeneous, indicating that melt phasing did not occur. When the rigid segment is incorporated in the copolymer, its melting temperature decreases and the reaction could be continued in the melt at 250 °C. The polymer

had a high inherent viscosity, indicating high molecular weight. The resulting polymer was transparent and slightly yellow coloured.

(b) Segmented copolymers with mixtures of T6T/T6A6T/T6A6A6T

The segmented block copolymers were synthesised from $PTMO_{2000}$ and bisester amide units by a polycondensation reaction. The polydispersity of the rigid segments in the copolymer was varied by using a mixture of uniform crystallisable amide units of varying length in the polymerisation reaction. The amide segments were synthesised and characterised before the polymerisation reaction.

Amide units

Three uniform rigid units were used in the polymerisation namely; di-amide (T6T), tetra-amide (T6A6T) and hexa-amide (T6A6A6T) crystallisable units (Figure 6.2).
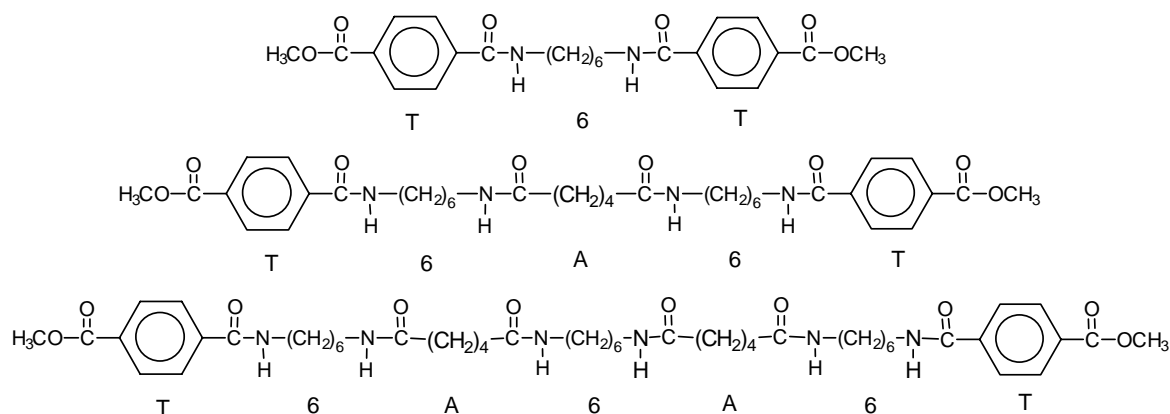
Figure 6.2: Structures of T6T-dimethyl ester, T6A6T-dimethyl ester and T6A6A6T-dimethyl ester.

The purity was checked with ^{1}H-NMR and the three amide units had a high purity (> 95%) (Table 6.1). MALDI-TOF measurements confirmed the expected M_w of these bisester amide units (Table 6.1). No impurities were observed. The melting and crystallisation temperatures determined with DSC were high because of hydrogen bonding and terephthalic rings in the crystallisable units (Table 6.1). The melting temperatures are expected to increase with segment length but at the same time the adipic acid content is increased. As a result of these two effects the melting temperature and melting enthalpy of the T6A6A6T unit even lower than of the T6A6T unit.

Table 6.1: Properties of uniform bisester amide units.

	M_w (g/mol)	Purity (%)	MALDI-TOF (m/z)	T_m (°C)	T_c (°C)	ΔH_m (J/g)	ΔH_c (J/g)
T6T-dimethyl	440	99	441	232	201	87	83
T6A6T-dimethyl	666	98	667	255	235	138	111
T6A6A6T-dimethyl	892	95	893	251	224	87	82

Polymers

By decreasing the mol% of T6A6T and increase the mol% of T6T and T6A6A6T the polydispersity of the rigid segment in the copolymer increases (Table 6.2). The mol ratio of T6T to T6A6A6T is always 1. In this way the mol% of amide groups to PTMO is constant and the rigid segment content is the same. The polymers had high inherent viscosities but the values decrease with increasing polydispersity of the rigid segments (Table 6.2). The decrease in inherent viscosity could have been caused by a low miscibility of the hexa-amide segments.

(c) Segmented copolymers with random rigid segments

A $(PTMO_{1000}-T)_{2000}$-T6A6T "random copolymer" was studied in which the amide segments were formed during the polymerisation reaction in a one pot synthesis. The reactor was charged with HMDA and dimethyl adipate in a mol ratio of 2:1 and a sodium methoxide catalyst solution was added. After 2 h at 100 °C all the methyl adipate is expected to have reacted and a mixture of compounds is formed (6, 6A6, 6A6A6, etc). Subsequently, a solution of $PTMO_{1000}$ in NMP and a second solution of DPT in NMP were added. The rigid segments are formed during the polymerisation (T6T, T6A6T, T6A6A6T). The polymerisation was continued at 250 °C. After two hours the solvent was stripped and the reaction was continued in the melt. The resulting polymer was opaque with a brown colour.

Calculation of polydispersity

Calculation of polydispersity of polymers with mixtures of T6T/T6A6T/T6A6A6T (b)

Calculation of the polydispersity of the rigid segments in the copolymer based on mixtures of uniform amide units is relatively easy since the composition of the mixture of the three amide segments is known. The molecular weight distribution or polydispersity of the rigid segments in the segmented copolymer can be calculated by using Equation 6.4.

$$polydispersity = \frac{M_w}{M_n} \qquad \text{(Equation 6.4)}$$

The number average (M_n) and weight average (M_w) of the rigid segments can be calculated according to the following formula (Equation 6.5 and 6.6).

$$< M_w >= \frac{\sum N_i M_i^2}{\sum N_i M_i} \qquad \text{(Equation 6.5)}$$

$$< M_n >= \frac{\sum N_i M_i}{\sum N_i} \qquad \text{(Equation 6.6)}$$

These equations are normally used to calculate the polydispersity of a polymer but in this case they were used to calculate the polydispersity of the crystallisable rigid segments, present in the segmented copolymer. The composition of the copolymers with mixtures of uniform rigid units and their calculated polydispersity are listed in Table 6.2.

Table 6.2: Polymer compositions.

	Amide segment (wt%)	T (mol%)	T6T (mol%)	T6A6T (mol%)	T6A6A6T (mol%)	T(6A)$_n$6T (mol%)	Polydispersity (-)	η_{inh} (dl/g)
a	21.1	-	0	**100**	0	-	1.00	2.2
b	21.1	-	2.5	**95**	2.5	-	1.01	2.2
	21.1	-	10	**80**	10	-	1.03	2.2
	21.1	-	15	**70**	15	-	1.04	1.9
	21.1	-	25	**50**	25	-	1.07	1.7
	21.1	-	33	**33**	33	-	1.09	1.2
c	21.1		-	**-**	-		1.2^d	1.2
	-	33	22	**15**	10	20	1.89^e	-

^{d} synthesised random polymer; ^{e} polydispersity calculated with most probable function of Flory

Calculation polydispersity rigid segments one-pot synthesis (c)

For the one pot synthesis the polydispersity of the crystallisable segments can be calculated with the most probable function of Flory[14]. In this calculation it is assumed that the endgroups have equal reactivity during the reaction. As there is an excess of one of the

components the stoichiometric balance is not one (r $\neq$ 1). The distribution of random segments can then be calculated with Equation 6.7 and 6.8.

$$w_n = nr^{\frac{(n-1)}{2}} \frac{(1-r)^2}{(1+r)}$$ *(Equation 6.7)*

$$N_r = \frac{w_n}{n}$$ *(Equation 6.8)*

$w_{n=}$ % weight fraction of n-mer with n = odd numbers (1,3,5..etc)

n = n-mer (n is odd numbered, referring to the odd specimen)

r = stoichiometric balance (<1)

N_r = number fraction (%)

The weight fraction and number fraction depend on the stoichiometric balance (r) of amine and ester groups of the components. A higher excess of one of the components gives a high percentage of segments with a low molecular weight (n-mer). In this case the specimens that can be present are the following units; terephthalic (n = 1), diamide (n = 3), tetra-amide (n = 5), hexa-amide (n = 7), octa-amide (n = 9), etc.
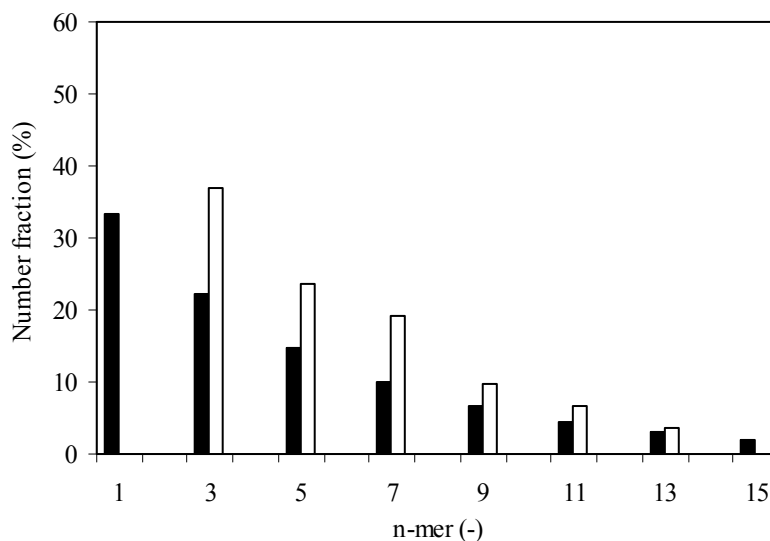
Figure 6.3: Number distribution of random segment; closed bars, calculated Flory distribution with r = 0.67; open bars, MALDI-TOF distribution of one pot synthesis of the rigid segment; (n is only odd numbered).

For the random polymer the stoichiometric ratio r (amine:ester) is 2:3, equal to the composition of a tetra-amide unit. The number fraction of n-mer = 1 is calculated at 33% and decreases with increasing n-mer (Figure 6.3, closed bars). The polydispersity of the rigid

segment can be calculated from the number fraction distribution and is 1.89. In Table 6.2 the calculated number fraction of n-mer is given for the polymer with random rigid segments.

MALDI-TOF "random" segment

A one pot synthesis of the T6A6T unit with amine to ester ratio of 2:3 was carried out to investigate the distribution of the amide unit sequence length. The resulting product was studied by MALDI-TOF (Figure 6.4). Although MALDI-TOF is not an absolute method, a rough estimation of the composition can be made. The number fraction distribution is given in Figure 6.3 (open bars). The polydispersity of this one pot synthesis of the amide unit is 1.18. The n-mer of 1, DPT, was not present due to the higher reactivity of the first ester group compared to the second. The diamide (n = 3) peak is very strong and it is clear that for increasing 'n' the number fraction decreases. Longer segments than dodeca-amide are not present due to demixing of long amide segments and thereby limiting further reactions.

The number fraction distribution of the synthesised "random segment" has the same trend as was calculated with the most probable distribution of Flory. However, the measured distribution of 1.18 is much smaller than was calculated with the most probable function of Flory of 1.89 (Equations 6.7 and 6.8). This can be explained by the difference in reactivity of the two ester groups of the starting compounds and by the precipitation of long units. If in the calculation of the polydispersity of Flory is taken into account that isolated terephthalate (T) groups and groups with a length longer than dodeca-amide (n = 13) are not present then the polydispersity decreases from 1.89 to 1.20. Both the isolated terephthalic groups as well as the very long amide segments have a very strong effect on the calculated polydispersity. If these two effects are taking into account then a polydispersity of the rigid segments of 1.20 can be expected. A narrow distribution (1.15) for solution synthesis of random amide units with r = 2/3 was reported before[2].

Randomisation of T6A6T segments during polymerisation

The starting bisester amide units were uniform, as was confirmed with NMR and MALDI-TOF (Table 6.1). The question is whether during polymerisation for three hours at 250 °C randomisation of the segments might have occurred. To study the uniformity by MALDI-TOF the amide segments had to be isolated. For this, the ester bonds linking the amide and the ether in the copolymer were hydrolysed by refluxing the copolymer in a solution of 1 M NaOH for 8 h. By the hydrolysis the ester groups in the amide segments were converted to acids. The now free polyether prepolymers were washed out with acetone. The insoluble

amide segments were collected by filtration. The amide product was dissolved in TFA and a MALDI-TOF spectrum was recorded using dihydroxybenzoate (DHB) as a matrix (Figure 6.4).
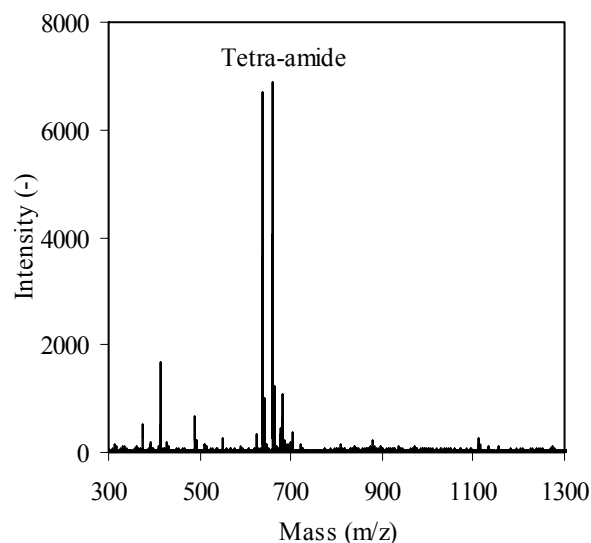

Figure 6.4: MALDI-TOF spectrum of amide segments after decomposition of PTMO$_{2000}$-T6A6T.

In the MALDI-TOF spectrum of the amide segments two peaks are visible and these both correspond with the T6A6T-diacid (M+H, M+Na). It can be concluded that after polymerisation the T6A6T segment is still intact and no transreactions had occurred. Therefore no randomisation of the rigid segment takes place during polymerisation. The starting distribution of the rigid segments is the distribution of the rigid segments in the copolymer.

Thermal properties

The melting and crystallisation behaviour of the copolymers were studied using DSC (Figure 6.5). In the heating cycle two peaks are present, the first is from the melting of crystalline PTMO, the second peak at about 180 °C is from the melting of the amide segment. Upon cooling, the amide segments crystallise at about 165 °C and upon further cooling the PTMO crystallises at -10 °C. The DSC spectrum of the segmented copolymer with random amide segments did not show a crystallisation and melting peak of the amide segment.
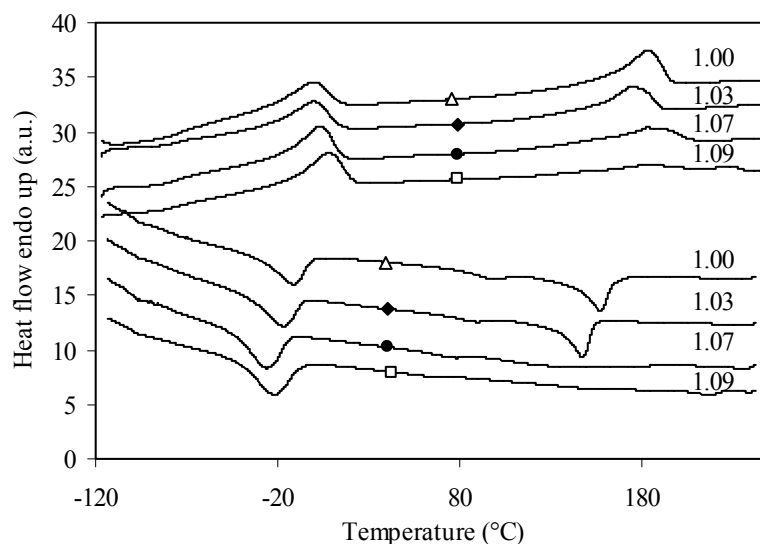
Figure 6.5: DSC spectrum of segmented copolymers based on PTMO$_{2000}$ and amide segments with different polydispersity: Δ, 1.00; ♦, 1.03; ●, 1.07; □, 1.09.

Table 6.3: Thermal transition properties of copolymers with different polydispersity.

Polydispersity	PTMO segment				Amide segment					
	T_{m1}	T_{c1}	$T_{m1}-T_{c1}$	ΔH_{m1}	T_{m2}	T_{c2}	$T_{m2}-T_{c2}$	ΔH_{m2}	X_c DSC	X_c FT-IR
(-)	(°C)	(°C)	(°C)	(J/g)	(°C)	(°C)	(°C)	(J/g)	(%)	(%)
1.0	-1	-1	0	16	183	164	19	27	93	92
1.01	-2	-13	11	16	180	163	17	26	89	84
1.03	0	-6	6	23	174	154	20	24	83	85
1.04	-1	-17	16	17	182	159	23	22	75	74
1.07	3	-13	16	25	190	165	25	19	65	80
1.09	8	-7	15	28	184	154	30	7[a]	24[a]	80
1.2	*6*	*-33*	*39*	*12*	-	-	-	-	-	71

[a] *low due to limitation in sensitivity of the DSC apparatus*

In Table 6.3 the thermal properties of the copolymers are given. The melting and crystallisation of PTMO is influenced by the polydispersity of the rigid segments. For polymers with a higher polydispersity of the crystallisable amide segment, the melting temperature of the crystalline PTMO phase increases and the crystallisation temperature decreases, resulting in a higher undercooling of the crystalline PTMO segments. The higher melting temperature of the PTMO segments is expected to reduce the low temperature flexibility of the copolymers. Also, the ΔH_m of the crystalline PTMO phase is increased

suggesting an increased degree of crystallinity of the PTMO. A higher polydispersity of the rigid segments decreases the crystallisation rate of the PTMO phase.

The thermal behaviour of the amide segments also changed for polymers with a higher polydispersity of the amide segments. The melting temperature seems to be little affected but the crystallisation temperature decreased as well as the melting enthalpy. The undercooling (T_m - T_c) is higher for polymers with a higher polydispersity (Figure 6.6). These results suggest that polymers with a higher polydispersity of the rigid segments crystallise slower and that the degree of crystallinity is lower. For the copolymers with "random" amide segments no melting transition of the amide phase could be measured probably due to the broad melting transition due to the variation in rigid segment length. It can be concluded that uniform segments crystallise faster and more easily compared with polymers having polydisperse segments.
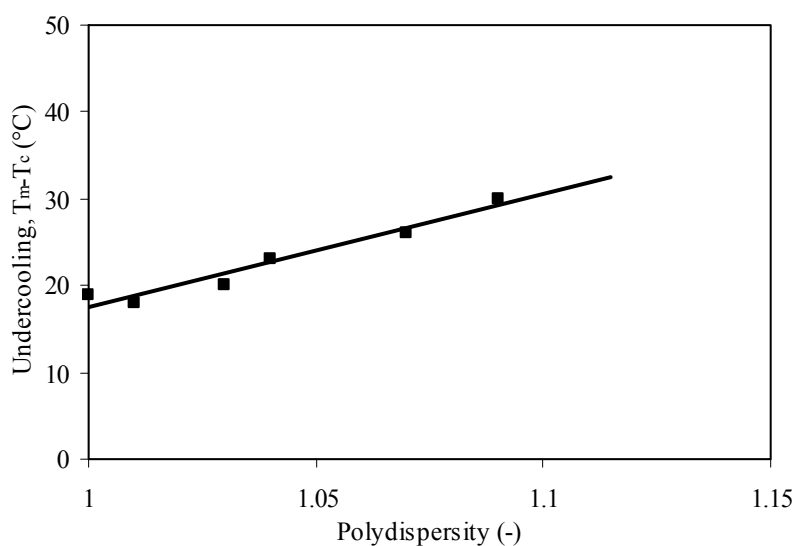
Figure 6.6: Difference between the melting temperature and the onset of crystallisation of the amide segments as a function of the polydispersity.

FT-IR

As with DSC the melting and crystallisation peaks are often broad, the degree of crystallinity is not always accurate to determine, particularly not in copolymers with a low content of crystallisable segments. FT-IR might be a more suitable method for determining the degree of crystallinity for the polymers. Infrared spectra were recorded with ~10 μm thick films solvent casted on a KBr pellet from a solution in HFIP. The degree of crystallinity of amide segments

in the copolymers was calculated comparing the ratio of crystalline amide peak (1630 cm^{-1}) and amorphous amide peak (1670 cm^{-1}) by using Equation 6.1. A detailed example was already discussed in chapter 5 and 3 of this thesis.

The degree of crystallinity of the amide segments decreases with increasing polydispersity of the rigid segments in the polymer. However, for the random polymer the degree of crystallinity was still 71%. Apparently, the decrease of properties of the polymers with increasing polydispersity is not only due to a lower degree of crystallinity of the rigid segments but also due to a decrease in aspect ratio. The degrees of crystallinity obtained by FT-IR and DSC are comparable for most copolymers but for copolymers with PDI 1.07, 1.09 and 1.2 the values estimated with DSC are lower, probably due to limitation in sensitivity of the DSC apparatus (Table 6.3).

For the PTMO$_{2000}$-T6A6T copolymer with uniform (PDI = 1.0) and random (PDI = 1.2) rigid segments, temperature dependent infrared spectra were recorded in a heating and cooling cycle. The degree of crystallinity can then be estimated as a function of temperature. The degree of crystallinity of the uniform T6A6T segment in the copolymer was high (92 %) at room temperature and remained high up to 150 °C. At 170 °C, just before the melting temperature, a sharp decrease in crystallinity was observed. The cooling cycle shows a similar path as the heating curve and the degree of crystallinity recovered completely. For the copolymer with random T6A6T segments the degree of crystallinity at room temperature is 71% and gradually decreases during heating. At temperatures above the melting temperature still some crystallinity of the T6A6T segments was observed probably due to longer amide segments, which have a higher melting temperature.
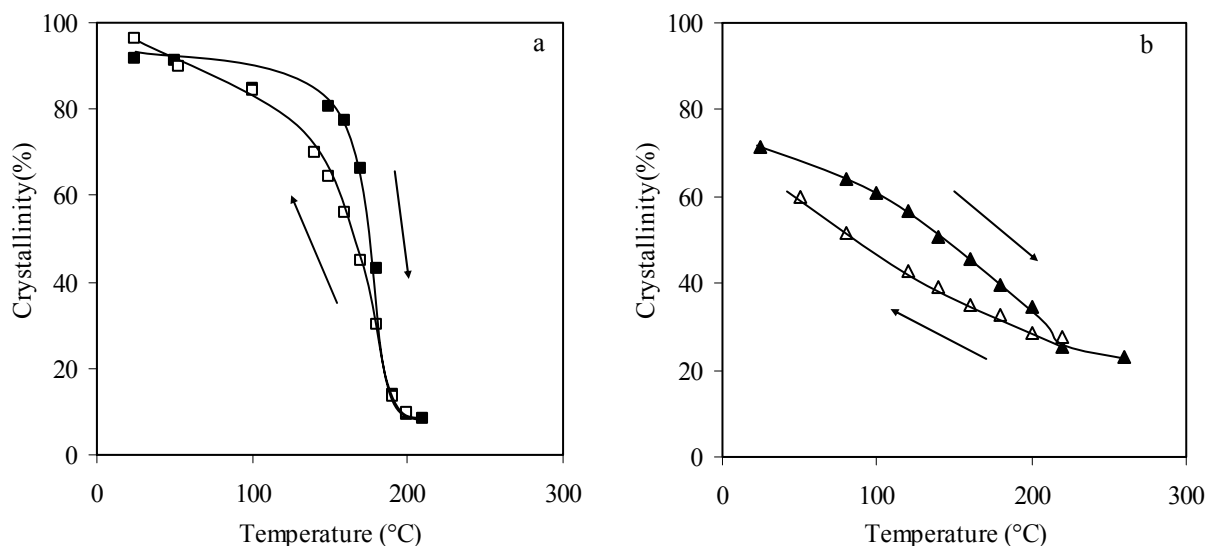
Figure 6.7: Degree of crystallinity of the amide segments as a function of temperature: a) ■, □, PTMO$_{2000}$-T6A6T with uniform rigid segments; b) ▲, Δ, PTMO$_{2000}$-T6A6T with random rigid segments; closed symbols, heating run; open symbols, cooling run.

DMTA

Thermal mechanical properties of the polymers were determined by means of DMTA (Figure 6.8, Table 6.4). The glass transition of the PTMO phase was low and not affected by the increasing polydispersity. The low T$_g$ (~ -70 °C) suggest that the amount of dissolved amide in the PTMO is low. However, the PTMO$_{2000}$ melting temperature and thereby the flex temperature (T$_{flex}$) increased with increasing polydispersity of the rigid segments. In the storage and loss modulus a crystallisation peak of PTMO at -10 °C is visible as a shoulder of the T$_g$ for polymers with a higher polydispersity of crystallisable segments. A higher melting temperature and a higher PTMO crystallinity were also observed with DSC (Table 6.3). It is not clear what the actual reason for this higher PTMO melting temperature and higher degree of crystallinity is. Possibly the non crystallised amide segments play a role in this. The copolymer with uniform segments has a high rubber modulus (at room temperature) and the rubber modulus decreases with polydispersity. This decrease in modulus might be due to a change of crystallinity and/or a change in the aspect ratio of the crystallites [2,15].
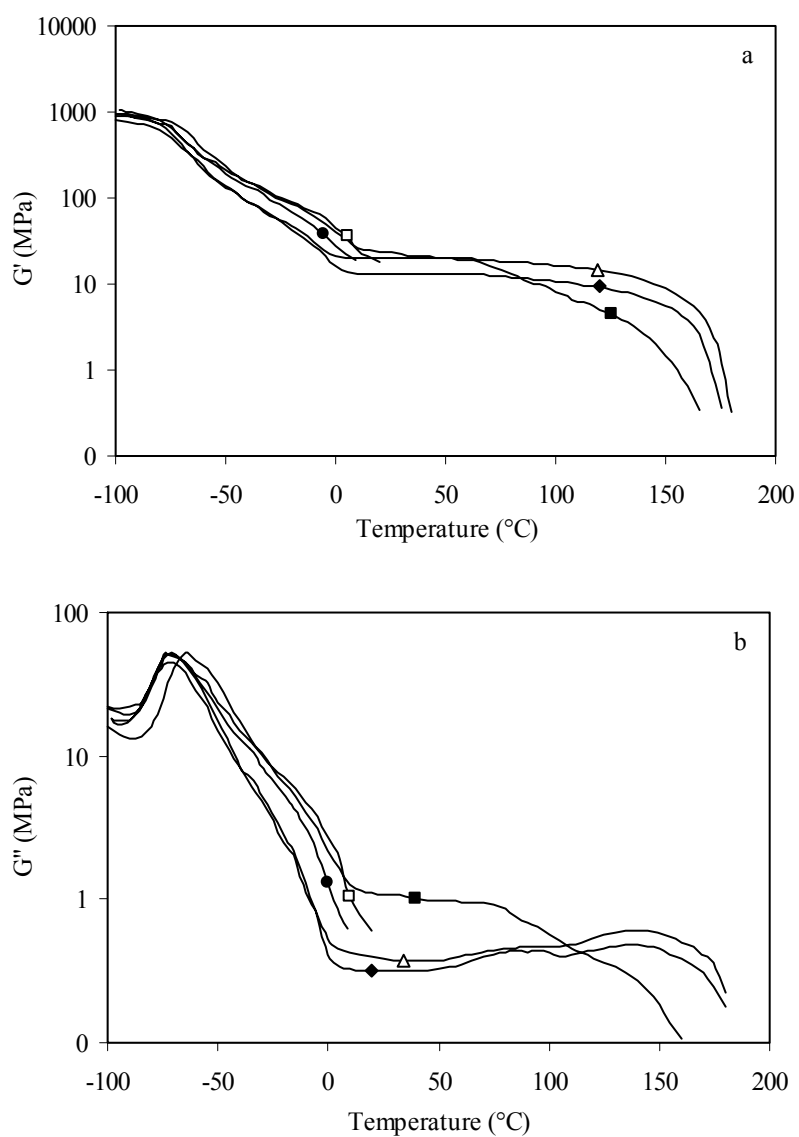
Figure 6.8: a) Storage and b) loss modulus versus temperature of PTMO$_{2000}$-T6A6T with different polydispersity: Δ, uniform; ♦, 1.03; ●, 1.07; □, 1.09; ■, 1.20.

The tan δ in the rubbery region is low but the values increase with increasing polydispersity of the rigid segments (Table 6.4). This suggests that the dynamic behaviour at low strains is excellent but decreases with increasing polydispersity.

Table 6.4: Influence of amide segment distribution on DMTA properties.

PDI RS[a]	Amide segment	η_{inh}	T_g	T_{flex}	$G'_{25°C}$	tan δ 25 °C	T_{flow}	$\Delta G'$ *10^{-3}	$CS_{25\%}$	$TS_{100\%}$
(-)	(%)	(dl/g)	(°C)	(°C)	(MPa)	(-)	(°C)	(°C^{-1})	(%)	(%)
1.0	21.1	2.2	-72	0	20.2	0.019	180	2.9	14	12
1.01	21.1	2.2	-69	0	14.4	0.022	180	3.2	14	11
1.03	21.1	2.2	-68	5	12.8	0.023	175	3.3	14	12
1.04	21.1	1.9	-71	0	14.3	0.022	180	3.7	15	13
1.07	21.1	1.7	-71	10	18.5	0.029	185	4.4	17	15
1.09	21.1	1.1	-72	20	17.4	0.038	185	5.5	18	18
1.2	20.5	0.9	-63	20	23.0	0.047	165	11.0	31	24

[a] *polydispersity of the rigid segment in the copolymer*

The amide flow temperature (T_{flow}) changed little up to a polydispersity of 1.09, but the random copolymer had a much lower T_{flow}. The T_{flow} corresponds well with the T_m measured with DSC (Table 6.3). The temperature dependence of the rubber modulus in the rubbery plateau ($\Delta G'$) is low for copolymers with uniform rigid segments, and increases with polydispersity of the rigid segments. Thus, increasing the polydispersity of the amide segments from 1.00 to 1.09 had already deteriorating effects on the thermal mechanical properties and particular the copolymer with the highest polydispersity of 1.2 (one pot synthesis) had the poorest DMTA properties.

Compression set

The elasticity of segmented block copolymers is commonly quantified by means of a compression set at 25% compression at room temperature ($CS_{25\%}$). A low compression set value refers to elastic behaviour of the polymer sample. In chapter 3 and chapter 5 it was shown that the CS values for copolymers with monodisperse amide segments are low. In Figure 6.9 it is shown that the CS of copolymers increases with increasing polydispersity of the rigid segments (Table 6.4).
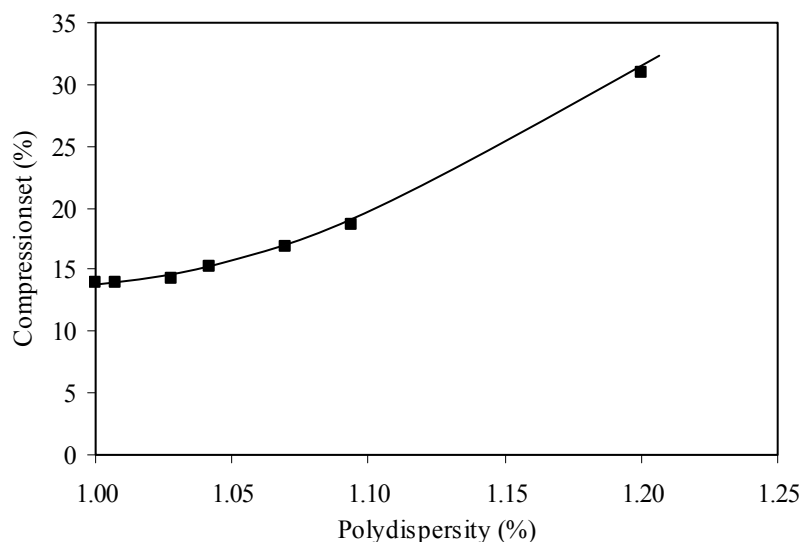
Figure 6.9: Compression set measured at 25% compression at 25 °C as a function of polydispersity.

The compression set is mainly due to viscoelastic and plastic deformation of the amide phase. Increasing the thickness of the crystallites in the copolymer lowers the CS values[2]. With increasing polydispersity of the rigid segments it is expected that the amide crystallites have an increased variation in thickness. As a result of this the amount of thin (weak) places in the crystallites increases. A thin place in a crystallite is expected to deform more easily on deformation and therefore the CS is higher. The 'random' polymer, with a polydispersity of the amide segments of 1.2, has a significantly higher CS value.

Tensile set

The elastic properties of the copolymers were also studied with a tensile set test performed to 100% strain ($TS_{100\%}$) (Figure 6.10, Table 6.4). The tensile set of the polymers with uniform segments was low and increased with increasing polydispersity of the amide segments. This trend is in accordance with the compression set measurement and can also be explained by the variation in crystal thickness with increasing polydispersity.
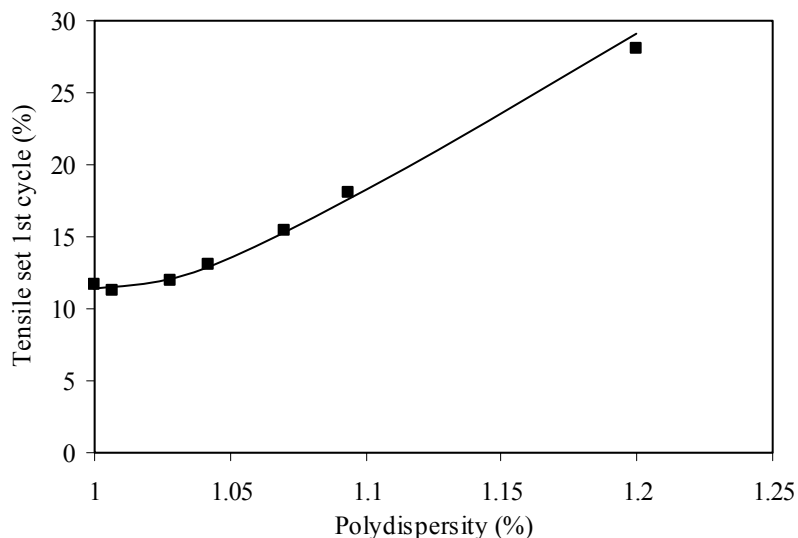
Figure 6.10: Tensile set at 100% strain as a function of polydispersity.

Tensile test

Tensile properties of the segmented block copolymers were studied on injection moulded in bars cut to dumbbells (ISO37 s2) (Table 6.5, Figure 6.11). At small deformations the stress increases linearly with the strain (Hooke's Law)[16]. Above the yield strain the stress gradually increases and above 300% strain, strain hardening can take place.

Figure 6.11: Tensile graph for polymers with rigid segments having different degrees of polydispersity.

Already for a small increase in polydispersity of the amide segments in the copolymer, a decrease of E-modulus, yield stress and stress at a certain strain was observed (Figure 6.11, Table 6.5). The (log) modulus and the yield stress are directly related to the degree of crystallinity and the aspect ratio of the crystallites[12]. Above we have seen that increasing the polydispersity of the amide segments in the copolymers slightly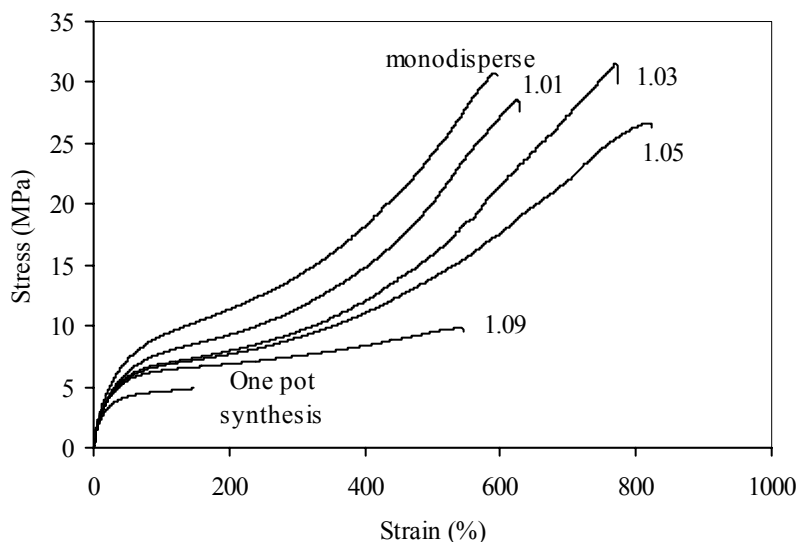 decreases the degree of crystallinity, however the change in modulus on a log scale is also small. The trend for the E-modulus is similar to that of the G'-modulus (Table 6.4 and 6.5). The observed decrease of the E-modulus as a function of polydispersity is due to the lower degree of crystallinity and/or the lower aspect ratio of the ribbons. The yield stress is normally linearly related to the change in E-modulus and therefore the yield stress also decreases with increasing polydispersity[12]. The ultimate properties in segmented block copolymers depend strongly on the molecular weight of the copolymer[5,17]. The polymer with "random" amide segments and with a polydispersity of 1.09 both had low fracture stress and strain. The reason for this is probably the low inherent viscosity of these polymers. The ultimate properties of the other copolymers are high.

Table 6.5: Tensile properties as function of polydispersity.

Polydispersity (-)	Amide segment (%)	η_{inh} (dl/g)	E-modulus (MPa)	σ_y (MPa)	ε_y (%)	σ_b (MPa)	ε_b (%)
1.0	21.1	2.2	46	8.8	49	31	583
1.01	21.1	2.2	39	6.7	61	29	627
1.03	21.1	2.2	33	7.2	65	32	595
1.04	21.1	1.9	38	6.5	52	31	770
1.07	21.1	1.7	37	5.8	49	27	657
1.09	21.1	1.1	34	5.4	47	10	552
1.2	20.5	0.9	42	3.7	29	5	148

The polydispersity of rigid segments in the polymer has an effect on the modulus and the yield stress, but as far as we can see not on the ultimate properties.

Conclusions

In this chapter the influence of the polydispersity of the crystallisable segment in segmented block copolymers on the polymer properties was studied. Three polymer series were synthesised having either uniform, polydisperse or random length rigid segments.

The polymer with uniform rigid segments crystallises fast, has an almost temperature independent rubbery plateau with a high modulus, a low CS and a low TS.

The polymer with mixtures of uniform blocks with different length were synthesised via solution/melt polymerisation. The polydispersity of the rigid segments in the polymers varied from 1.01 to 1.09. It can be expected that the polydispersity of the rigid segment has a direct effect on the thickness variations in the crystallites. The degree of crystallinity decreased with increasing polydispersity of the rigid segments due to the variation in crystallite thickness. As a result of the decreasing degree of crystallinity, the rubber modulus and the yield stress were lowered. The increasing variations in thickness of the crystallites lowered the elastic properties like compression set and tensile set but also increased the temperature dependence of the rubber modulus in the plateau region. The thin regions in the crystallites due to the thickness variations are thought to be responsible for the lower elastic properties. The ultimate tensile properties seem to depend little on the polydispersity and more on the molecular weight of the copolymers.

Another copolymer was made via a one pot polymerisation and this copolymer had a "random" distribution of amide sequence length. The copolymer with "random" amide segments had a polydispersity of 1.2 and this was lower than was anticipated, probably due to phase separation of longer blocks and an uneven reactivity of the difunctional monomers (terephthalate). The polydispersity was higher than for the polymers with a mixture of rigid segments. Also the properties of the random copolymer were inferior to the properties of the polymers with a mixture of rigid segments.

Thus, segmented polymers having uniform segments show superior properties compared with polymers having polydisperse segments. The low temperature properties were better. It was shown that even small changes in the polydispersity of the rigid segment have an effect on the properties of the segmented block copolymers.

References

1. Holden, G., Legge, N.R., Quirk, R.,.Schroeder, H.E., *'Thermoplastic elastomers'*, Hanser Publisher, Second Ed. Munich (1996).

2. Schuur van der, J.M., *'Poly(propylene oxide) based segmented block copolymers'*, Ph.D. Thesis, University of Twente (2004).

3. Harrel, L.L., *Macromolecules* **2**, 607-612 (1969).

4. Ng, H.N., *Polymer* **14**, 255-261 (1973).

5. Niesten, M.C.E.J., Gaymans, R.J., *Polymer* **42**, 6199-6207 (2001).

6. Shirasaka, H., Inoue, S., Asai, K., Okamoto, H., *Macromolecules* **33**, 2776-2778 (2000).

7. Versteegen, R.M., *'Well-defined Thermoplastic Elastomers'*, Ph.D. Thesis, University of Eindhoven (2003).

8. Heijkants, R.G.J.C., *'Polyurethane scaffolds as meniscus reconstruction materials'*, Ph.D. Thesis, University of Groningen (2004).

9. Lunardon, G., Sumadia, Y., Vogl, O., *Angew. Makromol. Chem.* **87**, 1-33 (1980).

10. Pechold, E., Pruckmayr, G., *Rubber Chem. Techn.* **55**, 76-87 (1982).

11. Chapter 2 of this thesis

12. Chapter 3 of this thesis

13. Sorta, E., Della Fortuna, G., *Polymer* **21**, 728 (1980).

14. Flory, P.J., *'Priciples of Polymer Chemistry'*, Cornell University Press, Menasha, 4th ed. Wisconsin (U.S.) (1964).

15. Halpin, J.C., Kardos, J.L., *J. Appl. Phys.* **43**, 2235 (1972).

16. Hertzberg, R.W., *'Deformation and fracture mechanics of engineering materials'*, John Wiley, 3rd edition New York (1989).

17. Krijgsman, J., Gaymans, R.J., *Polymer* **45**, 437-446 (2004).

CHAPTER 7

SYNTHESIS AND PROPERTIES OF SEGMENTED BLOCK COPOLYMERS CONTAINING NON HYDROGEN BONDING SEGMENTS OF UNIFORM LENGTH

Abstract

Segmented copolymers based on non hydrogen bonding crystallisable amide based segments of uniform length and poly(tetramethylene oxide) segments were synthesised. The non hydrogen bonding segments are based on alternating terephthalic acid and piperazine units connected through amide bonds which are not able to form hydrogen bonds (TPTPT). Poly(tetramethylene oxide) with a segment length of 1000 and 2000 $g \cdot mol^{-1}$ were reacted with pre-synthesised TPTPT. The resulting polymers were characterised by DSC and temperature dependent FT-IR, SAXS and DMTA. The elastic properties of the polymers were evaluated by compression set and tensile set measurements.

The segmented copolymers had a low glass transition temperature (T_g, -70 °C), moderate modulus (G', 10 - 33 MPa) and high melting temperatures (185 - 220 °C). The rubber modulus of the plateau region of the segmented copolymers is almost temperature independent due to the presence of uniform crystallisable segments. The rubber moduli, yield stress and elasticity of these copolymers are lower compared to those of segmented copolymers which are able to form hydrogen bonds.

Introduction

The physical and chemical properties such as melting temperature, solubility and adhesion of polymers are strongly influenced by the type and number of hydrogen bonds[1]. Hydrogen bonds are strong secondary forces that increase the chain interaction both in the crystalline and amorphous state. However, hydrogen bonds are not required for crystallisation or a high degree of crystallinity.

The effect of hydrogen bonding on polymer properties was studied using polyurethanes[2-4]. Harrel[4] and Ng et al.[2,5] studied polyurethanes based on $PTMO_{1000}$ and monodisperse piperazine-butanediol urethane rigid segment with a segment size of y = 2-4 (Figure 7.1). The glass transition of these segmented copolymers was -50 °C and the rubber modulus in the plateau region only slightly decreased with temperature. The melting temperature increased with increasing rigid segment length n from 100 °C (y = 2) to 160 °C (y = 4)[6]. Piperazine containing polyurethanes exhibit an increased thermal stability because they do not show transurethanisation as is normally observed for polyurethanes. The piperazine based polyurethanes had poorer elastic properties compared with hydrogen bonded polyurethanes. This was explained by the less stable rigid segment domains.
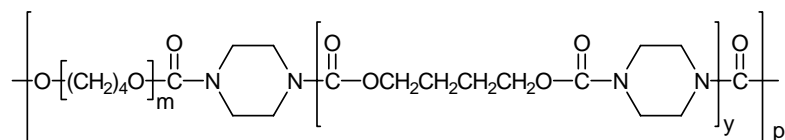
Figure 7.1: Structure of polyurethane based on PTMO flexible segments and a piperazine based rigid segment.

Polyurethanes are thermally instable and can have a complex morphology, which complicates the study on the effect of hydrogen bonding on polymer properties. Segmented polyamides are thermally stable, have a two-phase morphology and can therefore be studied in a simplified manner. In earlier research, segmented copolymers with uniform amide segments that can form hydrogen bonds were investigated[7,8]. Segmented copolymers based on PTMO and uniform tetra-amides crystallise fast and almost completely[7-9]. The amide segments form crystalline ribbons with a high aspect ratio[7,8]. The moduli of these copolymers increase strongly with increasing amide content and can be approximated using a model for fibre

reinforced polymers[8,10-12]. The rubber modulus in the plateau region is almost temperature independent and the melting transition is sharp[2,4,8,11-13].

To what extend these properties are due to the hydrogen bonding in the crystallisable segments is as yet unclear. Therefore it would be interesting to synthesise a series of segmented copolymers without hydrogen bonding segments.

Research aim

In this chapter the synthesis and properties of segmented copolymers based on PTMO and TPTPT units of uniform length are discussed (Figure 7.2). The TPTPT segment has tertiary amide groups and is therefore unable to form hydrogen bonds. The properties of the $PTMO_x$-TPTPT copolymer are compared to the properties of segmented copolymers with hydrogen bonding $PTMO_x$-T6T6T from Chapter 5. A direct comparison between hydrogen bonding and non hydrogen bonding amide systems gives insight in the effect of hydrogen bonding on the properties of segmented block copolymers.
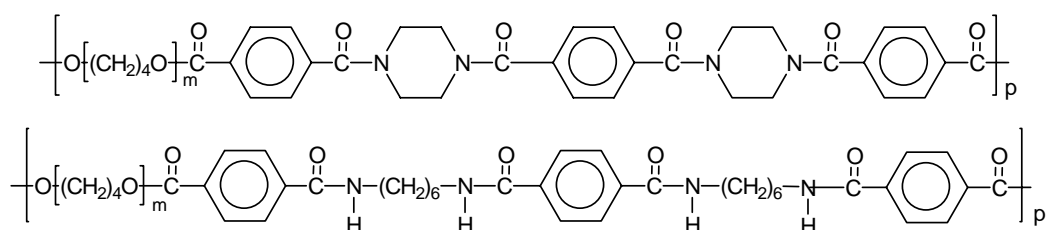

Figure 7.2: Segmented block copolymers based on PTMO and crystallisable segments, which either do not contain hydrogen bonds (above, PTMO-TPTPT) or which form hydrogen bonds (below, PTMO-T6T6T).

Experimental

Materials: Dimethyl terephthalate (DMT), N-methyl-2-pyrrolidone (NMP), phenol, 1,2,4-trichlorobenzene and toluene were purchased from Aldrich and used as received. Tetra-isopropyl orthotitanate ($Ti(i-OC_3H_7)_4$) was purchased from Aldrich and was diluted with m-xylene (0.05 M). m-Xylene was purchased from Merck. PTMO's with a length of 1000 and 2000 $g \cdot mol^{-1}$ were a gift from Dupont. Irganox 1330 was obtained from CIBA. Methyl phenyl terephthalate (MPT) and diphenyl terephthalate (DPT) were synthesised as described before[14,15]. $PTMO_x$-T6T6T copolymers were synthesised as described before[9].

Synthesis of TPTPT-dimethyl: TPTPT-dimethyl was synthesised from piperazine, DPT and MPT. First PTP (1-[4-(piperazine-1-ylcarbonyl)benzoyl]piperazine) was synthesised from piperazine and DPT in a round

bottomed flask with a nitrogen inlet, mechanical stirrer and a reflux condenser. Piperazine (120 g, 1.4 mol) was melted at 140 °C and reacted with DPT (39 g, 0.12 mol) for 16 h at 140 °C. The product was a transparent liquid that partly solidified during the reaction. The reaction mixture was added to 2 l of methanol to dissolve the product and subsequently part of the methanol was distilled off until 0.5 l of the solution was left. On adding ether to the solution, a white product precipitated. The product PTP was collected by filtration over a no.4 glass filter. The yield of the reaction was 67%. The T_m was determined with DSC to be 198 °C with a ΔH_m of 70 J/g. The purity of the product estimated with NMR was found to be >95%. ^{1}H-NMR (TFA-*d*): δ 7.68 (s, 4H, terephthalic H), δ 4.34 (s, 4H, CH_2 piperazine), δ 3.97 (s, 4H, CH_2 piperazine), δ 3.71 (s, 4H, CH_2 piperazine), δ 3.55 (s, 4H, CH_2 piperazine).

Second, PTP was reacted with MPT to give TPTPT-dimethyl. PTP (85 g, 0.28 mol) was dissolved in trichlorobenzene at 120 °C. MPT (200 g, 0.8 mol) was added to the solution and the reaction was carried out at 140 °C for 16 h. After one hour, a white product started to precipitate. The product was collected by filtration of the hot solution over a hot no.4 glass filter and washed three times with acetone. The yield of the reaction was 74%. TPTPT-dimethyl had a melting temperature of 250 °C and a melting enthalpy of 40 J/g. The purity estimated from NMR was found to be >95%. ^{1}H-NMR (TFA-*d*): δ 8.28 (t, 4H, terephthalic H ester side), δ 7.69 (s, 4H, terephthalic H, centre terephthalic), δ 7.6-7.75 (t, 4H, terephthalic H, piperazine side), δ 4.2 (d, 4H, CH_2 piperazine), δ 4.12 (d, 6H, methyl endgroup), δ 4.05 (s, 4H, CH_2 piperazine), δ 3.82 (s, 4H, CH_2 piperazine), δ 3.66 (d, 4H, CH_2 piperazine).

Segmented copolymers: The polymerisation was carried out in a 250 ml stainless steel reactor with a nitrogen inlet and magnetic coupling stirrer. The polymerisation of $PTMO_{1000}$ with TPTPT-dimethyl is given as an example. The reactor was charged with $PTMO_{1000}$ (50 g, 0.05 mol), TPTPT-dimethyl (34.3 g, 0.05 mol), 100 ml NMP, 1 wt% Irganox 1330 (based on PTMO) and a catalyst solution (5 ml of 0.05 M $Ti(i-OC_3H_7)_4$ in m-xylene) under nitrogen flow. The stirred reaction mixture was heated to 180 °C in 30 min. The temperature was increased over 2 h to 250 °C and this temperature was maintained for 2 h. Subsequently, the pressure was carefully reduced (P<20 mbar) to distil off the NMP and then further reduced (P<0.3 mbar) over 60 min. At the end the reactor was cooled slowly, maintaining the low pressure. The copolymers were transparent and tough. The segmented copolymers were characterised by DMTA, viscometry, DSC, FT-IR, NMR and SAXS. ^{1}H-NMR (TFA-*d*): δ 8.36 (t, 4H, terephthalic H, ester side), δ 7.69 (s, 4H, terephthalic H, centre terephthalic), δ 7.6-7.85 (t, 4H, terephthalic H, piperazine side), δ 4.6 (s, 4H, CH_2 PTMO, ester side), δ 4.28 (s, 4H, CH_2 piperazine), δ 4.13 (s, 4H, CH_2 piperazine), δ 3.88 (m, 52H, CH_2 PTMO), δ 3.82 (s, 4H, CH_2 piperazine), δ 3.74 (s, 4H, CH_2 piperazine), δ 2.07 (t, 8H, CH_2 PTMO, ester side), δ 1.91 (s, 48H, CH_2 PTMO, ether side).

^{1}H-NMR: ^{1}H-NMR spectra were recorded on a Bruker AC 300 spectrometer at 300 MHz. Deuterated trifluoro acid (TFA-*d*) was used as a solvent.

Viscometry: The inherent viscosity was measured at a concentration of 0.1 g/dl in a mixture of phenol/1,1,2,2-tetrachloroethane (1:1 molar ratio) at 25 ºC using a capillary Ubbelohde type 1B.

DSC: DSC spectra were recorded on a Perkin Elmer DSC apparatus, equipped with a PE7700 computer and TAS-7 software. Dried samples of 5 - 10 mg were heated to approximately 30 °C above the melting temperature and subsequently cooled, both at a rate of 20 °C/min. The maximum of the peak in de heating scan was taken as the melting temperature. The second heating scan was used to determine the melting peak and enthalpy of the sample. The first cooling curve was used to determine the crystallisation temperature, which was taken as the onset of crystallisation. The degree of crystallinity was calculated from the melting enthalpy of the polymer and the melting enthalpy of the bisester tetra-amide.

FT-IR: Infrared transmission spectra were recorded using a Nicolet 20SXB FTIR spectrometer with a resolution of 4 cm^{-1}. Samples were prepared by adding a droplet of a polymer solution in HFIP (1 g/l) on a pressed KBr pellet. Temperature dependent FT-IR spectra were recorded at temperatures between 25 and 210 °C under helium flow.

AFM: AFM measurements were carried out with a Nanoscope IV controller (Veeco) operating in tapping mode. The AFM was equipped with a J-scanner with a maximum size of 200 μm^2. Si-cantilevers (Veeco) were used to obtain height and phase images. The amplitude in free oscillation was 5.0 V. The operating setpoint value (A/A_0) was set to relatively low values of 0.70. Scan sizes were 1-3 μm^2 to obtain the best contrast. Solvent cast samples of ~20 μm thick were prepared from a 3 wt% solution in TFA.

SAXS: Small angle X-ray scattering (SAXS) experiments were performed at the Dutch-Belgium (DUBBLE) beamline, BM26 at the European Synchotron Radiation Facility (ESRF) in Grenoble. The wavelength of the beam was 1.2 Å. A two dimensional SAXS detector was used and a q-range of 0-1.8 nm^{-1} was measured. Temperature dependent profiles were recorded using a remote controlled LINKAM DSC stage at a heating and cooling rate of 10 °C/min. The background was subtracted from the intensity. The two dimensional SAXS intensity was azimuthally integrated to obtain the scattering pattern as a function of $q = 2 \sin \theta/\lambda$.

DMTA: Samples (70x9x2 mm) for the DMTA were prepared on an Arburg H manual injection moulding machine. The test samples were dried in vacuum at 50 °C for 24 h before use. DMTA spectra were recorded with a Myrenne ATM3 torsion pendulum at a frequency of 1 Hz and 0.1% strain. The storage modulus G' and the loss modulus G" were measured as a function of temperature. The samples were cooled to -100 °C and subsequently heated at a rate of 1 °C/min. The glass transition was determined as the peak in the loss modulus. The flow temperature (T_{flow}) is defined as the temperature where the storage modulus reaches 1 MPa. The start of the rubbery plateau, the intercept of the tangents, is called the flex temperature (T_{flex}). The decrease in storage modulus of the rubbery plateau with increasing temperature is quantified by ΔG', which is calculated from:

$$\Delta G' = \frac{G'_{(Tflex)} - G'_{(Tflow-50°C)}}{G'_{25°C}} \times \frac{1}{\Delta T} \qquad (°C^{-1}) \qquad\qquad (Equation\ 7.1)$$

ΔT is described as the temperature range: (T_{flow}-50 °C) - T_{flex}.

Compression set: Samples for compression set measurements were cut from injection moulded bars. The compression set was measured at room temperature according to ASTM 395 B standard. After 24 h the compression was released. After relaxation for half an hour, the thickness of the samples was measured. The compression set was taken as the average of four measurements. The compression set is defined as:

$$Compression\ set = \frac{d_0 - d_2}{d_0 - d_1} \times 100\% \qquad (\%) \qquad\qquad (Equation\ 7.2)$$

With: d_0 = thickness before compression (mm)

d_1 = thickness during compression (mm)

d_2 = thickness after 0.5 h relaxation (mm)

Tensile set: Cyclic stress-strain experiments were conducted with injection-moulded bars with a thickness of 2.2 mm, cut to dumbbells (ISO 37 type 2). A Zwick Z020 universal tensile machine equipped with 500 N load cell was used to measure the stress as a function of strain of each loading and unloading cycle at a strain rate of 0.4 s^{-1} (test speed of 60 mm/min). The strain of each loading-unloading cycle was increased (stair-case loading) and the tensile set of the strain increment was determined as a function of the applied strain. The incremental tensile set (TS) was calculated from the following relation (Equation 7.3):

$$Tensile\ set = \frac{\Delta\varepsilon_{remaining}}{\Delta\varepsilon_{cycle}} = \frac{\varepsilon_{r,cycle(i)} - \varepsilon_{r,cycle(i-1)}}{\Delta\varepsilon_{cycle}} \times 100\% \qquad\qquad (Equation\ 7.3)$$

With: $\varepsilon_{r,cycle(i)}$ = remaining strain at the end of cycle i

$\varepsilon_{r,cycle(i-1)}$ = remaining strain at the end of the preceding cycle i-1.

Immediately after the stress was zero, a new cycle was started. The strain of the first cycle was 20% and for each following cycle the strain was increased with 40%.

Tensile test: Stress-strain curves were obtained using injection moulded bars with a thickness of 2.2 mm, cut to dumbbell (ISO 37 type 2), using a Zwick Z020 universal tensile machine equipped with a 500 N load cell. The strain was measured with extensometers. Standard tensile test were performed in three-fold according to ISO 37 at a strain rate of 0.4 s^{-1} (test speed of 60 mm/min).

Results and discussion

Segmented polyether(ester)s based on PTMO and uniform TPTPT segments were synthesised (Figure 7.2). The TPTPT (Figure 7.3) has a regular structure with amide groups which are not able to form hydrogen bonds. TPTPT-dimethyl was synthesised first in a step wise manner from dimethyl terephthalate and methyl phenyl terephthalate (T) and piperazine (P). This uniform unit is expected to crystallise. The properties of the copolymers with non hydrogen bonding segments were compared with analogous copolymers with hydrogen bonding; the PTMO$_x$-T6T6T copolymers from chapter 5.

Synthesis of TPTPT-dimethyl

TPTPT-dimethyl was synthesised in two steps (Figure 7.3). The first step was the synthesis of PTP. An excess of piperazine was used to limit the formation of longer blocks. PTP was precipitated using a solvent non-solvent system to obtain monodisperse units. In the second step, TPTPT-dimethyl was synthesised from PTP and MPT. The phenyl group of MPT is a better leaving group and reacts faster than the methyl group, so further reaction was limited.
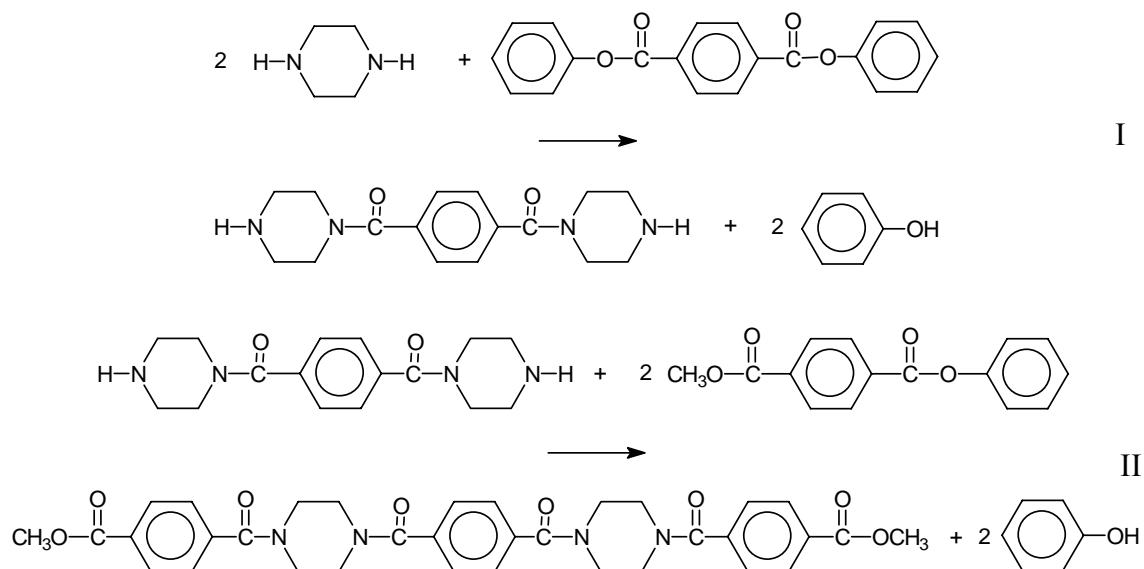

Figure 7.3: Synthesis of PTP (I) and TPTPT-dimethyl (II).

^{1}H-NMR

The molecular structures of PTP and TPTPT-dimethyl were analysed with ^{1}H-NMR.

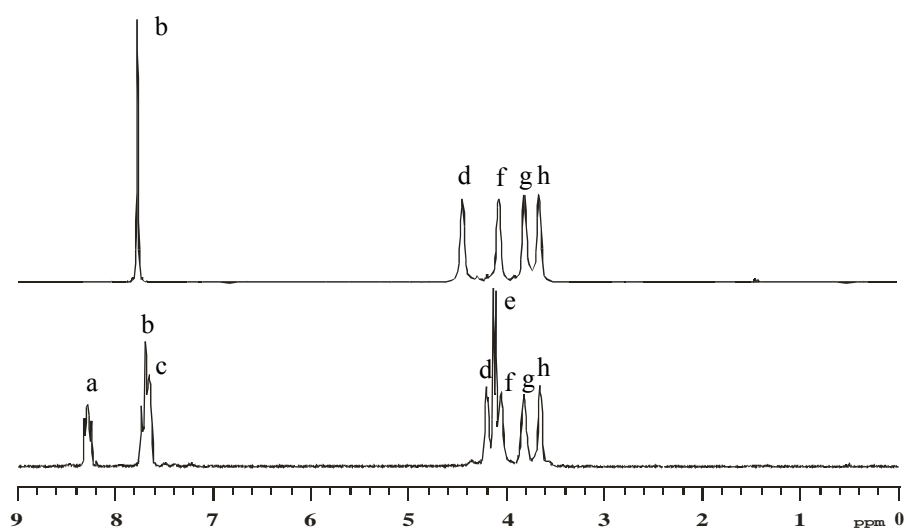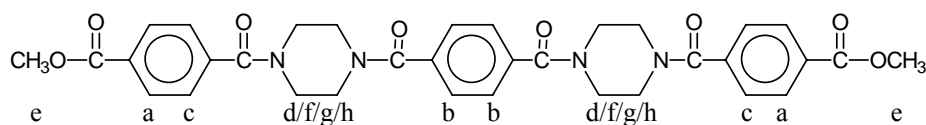*Figure 7.4: NMR spectrum of PTP (above) and TPTPT-dimethyl (below).*

Figure 7.5: ^{1}H-NMR peak assignments of protons of TPTPT-dimethyl.

The CH_2 peaks from piperazine are split into equatorial and axial proton peaks and give four broad singlets. Piperazine rings can either have a chair or boat conformation but six membered rings normally favour the chair conformation of the ring[16].

Table 7.1: Chemical shifts and assignment of protons of PTP and TPTPT-dimethyl.

	Chemical shift (ppm)	PTP integral	TPTPT integral	Type
a	8.28	-	4.0	Triplet
b	7.69	4.0		Singlet
c	7.6-7.75	-	8.3	Triplet
d	4.2	3.8	4.0	Doublet
e	4.12	-	6.3	Doublet
f	4.05	4.0	4.2	Singlet
g	3.82	4.0	4.6	Singlet
h	3.66	3.9	3.9	Doublet

For PTP, the integral of the CH_2 of the piperazine groups (16 H's) is in agreement with the integral of the terephthalic protons (4 H's). The purity was estimated as the ratio of terephthalic protons to piperazine protons and was 95% (Table 7.2). No split up of terephthalic protons was observed so longer units were not present.

The terephthalic peaks of TPTPT-dimethyl are split in terephthalic protons at the ester endgroup (a) and next to a piperazine group (b+c). The methyl ester endgroup gives a doublet at 4.1 ppm (e). The other four peaks correspond to the CH_2 of the piperazine groups (d, f, g, h). The purity was estimated as the ratio of terephthalic protons and was 97%[17].

DSC

The melting and crystallisation behaviour of the segments were studied by means of DSC. PTP has a melting temperature of 198 °C and a melting enthalpy of 70 J/g. The PTP unit crystallises at 153 °C with a crystallisation enthalpy of 73 J/g. The TPTPT-dimethyl unit has

a melting temperature of 250 °C with a low melting enthalpy of 40 J/g. The melting temperature of TPTPT-dimethyl is 50°C lower compared with T6T6T-dimethyl. Although chain flexibility is reduced, the melting temperature decreases by the diminished possibilities of hydrogen bonding. The low melting enthalpy is probably due to difficult packing of the non planar piperazine group and/or the absence of hydrogen bonds. No crystallisation peak of the TPTPT unit was observed with DSC, indicating difficult crystallisation.

Table 7.2: Properties of PTP, TPTPT-dimethyl and T6T6T-dimethyl.

| | M_w | Yield | Purity | T_m | T_c | ΔH_m |
	(g/mol)	(%)	(%)	(°C)	(°C)	(J/g)
PTP	302	67	95	198	153	70
TPTPT-dimethyl	627	81	97	250	-	40
T6T6T-dimethyl	686	80	97	303	284;259	150

PTMO$_x$-TPTPT segmented copolymers

Two segmented copolymers with PTMO and uniform TPTPT segments were synthesised by a polycondensation reaction; PTMO$_{1000}$-TPTPT and PTMO$_{2000}$-TPTPT. Both segmented copolymers were transparent in the melt, so melt phasing did not occur. Upon cooling, the polymers were tough, elastic and transparent materials with high inherent viscosities (Table 7.3).

DSC

The melting and crystallisation behaviour of the segmented PTMO$_x$-TPTPT copolymers were studied with DSC (Figure 7.6 , Table 7.3). Melting and crystallisation temperatures were only observed for the segmented copolymer with PTMO$_{1000}$ having a relatively high concentration of crystallisable segment. The undercooling (T_m - T_c) is 23 °C for PTMO$_{1000}$-TPTPT. The melting and crystallisation enthalpy is only 10 J/g. The degree of crystallinity was calculated from the melting enthalpy of the polymer and the melting enthalpy of the TPTPT-dimethyl unit and was approximately 77%.

The melting peak of PTMO$_{1000}$-TPTPT is 15 °C lower than for PTMO$_{1000}$-T6T6T, while the difference of the pure rigid units is 53 °C. Probably PTMO acts as a poorer solvent for TPTPT than for T6T6T. The melting enthalpy for PTMO$_{1000}$-TPTPT is four times lower compared to PTMO$_{1000}$-T6T6T. This can be explained by a poorer packing and weaker bonding between segments due to the absence of hydrogen bonds.

The crystallisation curve for PTMO$_{1000}$-T6T6T shows two peaks. The second peak can probably be attributed to a crystalline transition, which is commonly observed for polyamides[18,19]. The undercooling (T_m - T_c) is 23 °C for PTMO$_{1000}$-TPTPT and only 12 °C for PTMO$_{1000}$-T6T6T. For uniform polyamide segments, such as T6T6T, a pre-order in the melt was reported before[20-25]. Hydrogen bonds in the crystallisable segments increase the rate of crystallisation but do not have an effect on the degree of crystallinity, as for both polymers the degree of crystallinity is approximately 80%. Hydrogen bonds in the crystallisable segments increase the melting enthalpy and the rate of crystallisation.
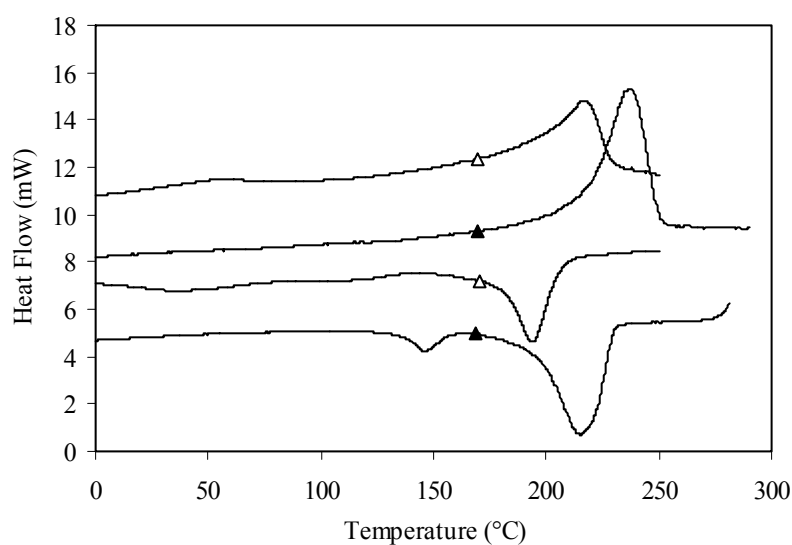
Figure 7.6: DSC heating and cooling traces of segmented copolymers without hydrogen bonding segments (TPTPT) and with hydrogen bonding segments (T6T6T): Δ, PTMO$_{1000}$-TPTPT; ▲, PTMO$_{1000}$-T6T6T.

Table 7.3: DSC properties of copolymers based on PTMO$_{1000}$ and PTMO$_{2000}$.

	Rigid segment (%)	η_{inh} (dl/g)	T_m (°C)	T_c (°C)	T_m-T_c (°C)	ΔH_m (J/g)	ΔH_c (J/g)	X_c (DSC) (%)
PTMO$_{1000}$-TPTPT	32.5	2.0	226	203	23	10	9	77
PTMO$_{2000}$-TPTPT	19.8	1.5	-	-	-	-	-	-
PTMO$_{1000}$-T6T6T	35.0	2.0	241	229	12	43	36	82
PTMO$_{2000}$-T6T6T	21.6	2.2	229	218	11	32	20	86

FT-IR

In Figure 7.7 the infrared spectra of TPTPT-dimethyl and PTMO$_{1000}$-TPTPT are given. Piperazine is a tertiary amide and therefore the amide bands (3000 - 3500 cm^{-1}) were not observed. Here the peak at 1630 cm^{-1} is from the carbonyl next to the di-substituted amine and the peak at 1730 cm^{-1} is from the ester group. Upon increasing the temperature of TPTPT-dimethyl and PTMO$_{1000}$-TPTPT, no change in the spectrum was observed and therefore a calculation of the degree of crystallinity of the polymer from the FT-IR spectrum was not possible. For PTMO$_{1000}$-T6T6T the change in the intensity and location of the of amide bands was used to calculate the degree of crystallinity[14].
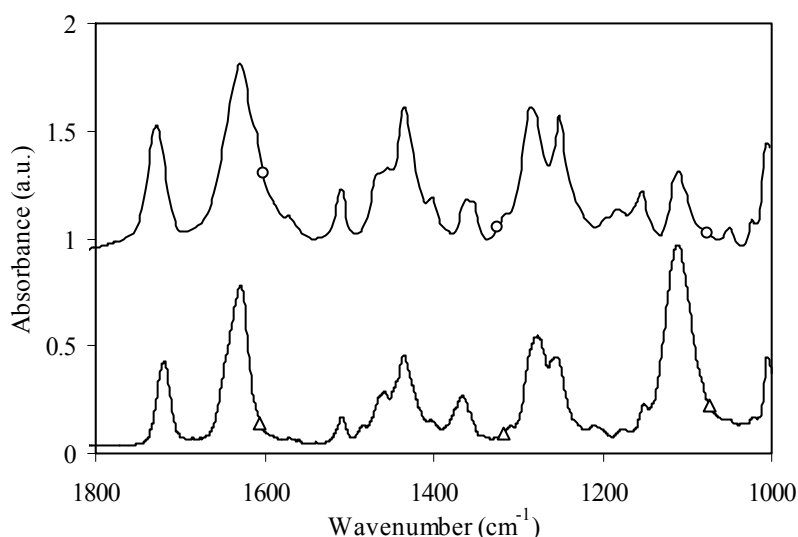

Figure 7.7: FT-IR spectrum of TPTPT-dimethyl (○) and PTMO$_{1000}$-TPTPT (Δ).

AFM

The morphology of PTMO$_{2000}$-TPTPT was studied by AFM (Figure 7.8). A polymer film was solvent cast from a TFA solution. In the AFM image the difference in phase hardness can be seen. The white ribbons are the hard phase that consists of TPTPT or T6T6T crystallites. It seems that PTMO$_{2000}$-TPTPT and PTMO$_{2000}$-T6T6T polymers both have ribbon crystallites (Figure 7.8). The TPTPT or T6T6T segments are aligned and so the length of a TPTPT or T6T6T crystallite (calculated at 2.8 nm and 3.6 nm) is the width of the ribbon. The width of the TPTPT ribbon is not expected to be different than the T6T6T ribbon. The length of the ribbons is difficult to determine from the AFM micrographs as the ribbons can bend out of the surface.
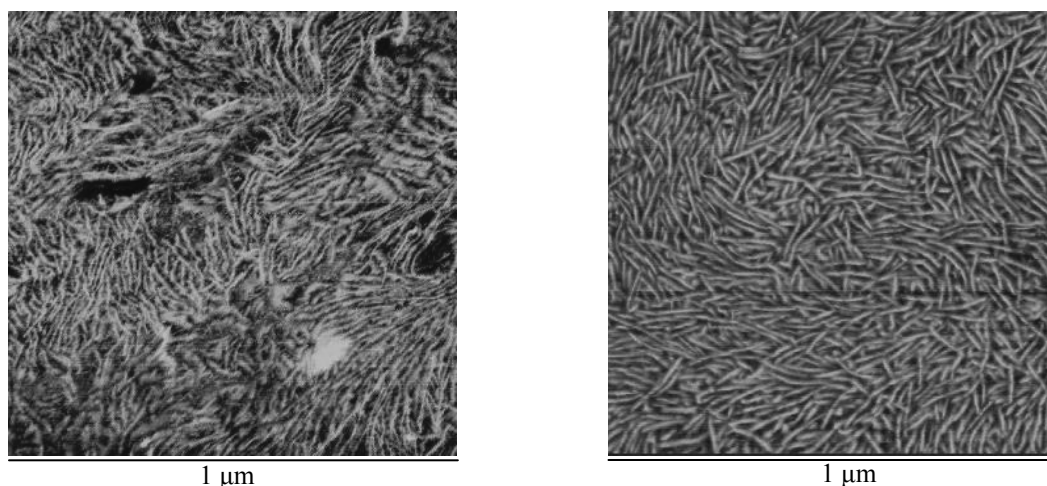
<table>
<tr><td>1 μm</td><td>1 μm</td></tr>
</table>

Figure 7.8: AFM picture of PTMO$_{2000}$-TPTPT (left) and PTMO$_{2000}$-T6T6T (right).

SAXS

From SAXS measurements the average repeat distance of crystalline segments, the so called long-spacing, can be obtained. PTMO$_{1000}$-TPTPT has at room temperature a long spacing of 12.0 nm and this is lower than the long spacing of PTMO$_{1000}$-T6T6T that is 15.3 nm. The reason for this is as yet not clear. However, the long spacing of PTMO$_{1000}$-TPTPT is similar to that of PTMO$_{1000}$-T6A6T (Figure 3.10, Table 3.3). The long spacing of PTMO$_{1000}$-TPTPT was studied with increasing and decreasing temperature (Figure 7.9) and is constant up to temperatures close to the melting temperature. This behaviour is similar to that of PTMO$_{1000}$-T6T6T. If partial melting of the crystallites would have taken place then the long spacing should have increased[26].
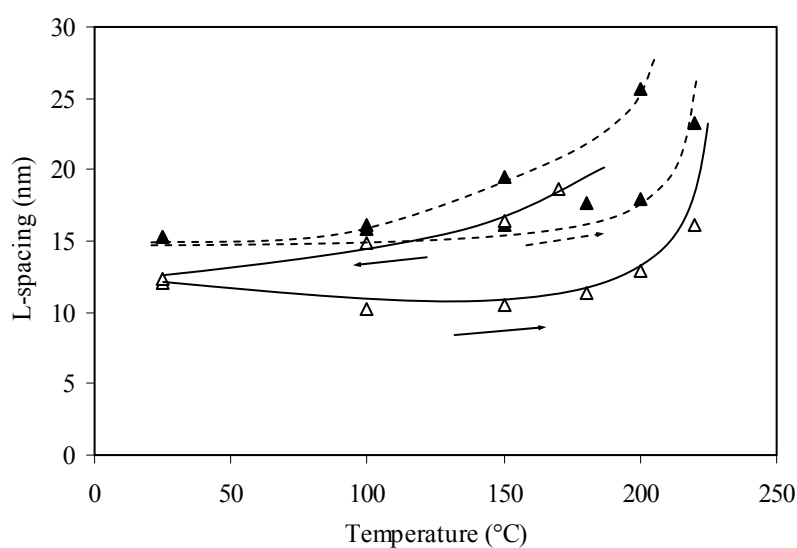

Figure 7.9: L-spacing as a function of temperature for non-hydrogen bonded and hydrogen bonded segmented copolymers: Δ, PTMO$_{1000}$-TPTPT; ▲, PTMO$_{1000}$-T6T6T.

Upon cooling, the long spacing decreases and this is more gradual than on heating. The fully crystalline state was obtained after some time. This hysteresis in long spacing is due to the rate of crystallisation and is clearer for the TPTPT segments than for the T6T6T segments, thus the T6T6T segments crystallise faster.

Dynamical mechanical thermal analysis (DMTA)

The storage and loss modulus of PTMO-TPTPT copolymers as a function of temperature are presented in Figure 7.10 and Table 7.4. Two transitions can be observed, a glass transition near -70 °C and a melting temperature around 200 °C. The glass transition temperature is very low, suggesting good phase separation of the two phases. For $PTMO_{2000}$ a shoulder in the glass transition at -10 °C is observed caused by the crystallisation of the $PTMO_{2000}$[27]. The start of the rubbery plateau (T_{flex}) is low for $PTMO_{1000}$, as it is not influenced by the crystallisation of PTMO. The rubber modulus in the plateau region decreases slightly with temperature and the melting transition is sharp. This behaviour is typical for copolymers with crystallisable segments of uniform length.
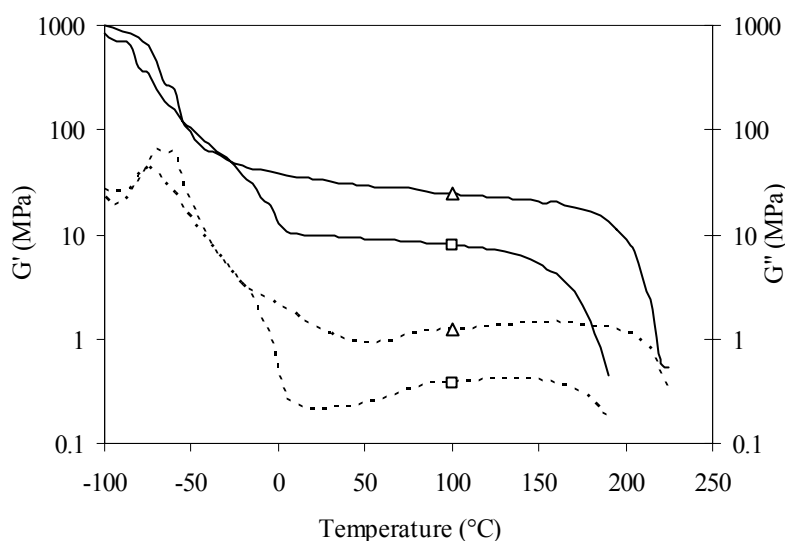
Figure 7.10: Storage (drawn line, left axis) and loss modulus (dotted line, right axis) for segmented block copolymers based on PTMO and uniform TPTPT segments: △, $PTMO_{1000}$-TPTPT; □, $PTMO_{2000}$-TPTPT.

In Table 7.4 the DMTA properties of PTMO-TPTPT are compared to PTMO-T6T6T. TPTPT based copolymers have a 6 °C lower glass transition temperature (T_g) compared with T6T6T based copolymers. This difference was also observed in piperazine based polyurethanes and was ascribed to the influence of hydrogen bonding interactions on the flexible segment

mobility[28]. Infrared measurements in that study established a significant amount of hydrogen bonding between flexible and rigid segments.

Table 7.4: Properties of PTMO-TPTPT and PTMO-T6T6T.

	rigid segment (%)	η_{inh} (dl/g)	T_g (°C)	T_{flex} (°C)	G' $_{25°C}$ (MPa)	$\Delta G'$ *10^{-3} (°C^{-1})	T_{flow} (°C)	CS (%)	TS$_{50\%}$ (%)
PTMO$_{1000}$-TPTPT	32.5	2.0	-67	-35	33	4.7	220	28	29
PTMO$_{2000}$-TPTPT	19.8	1.5	-75	5	9.8	3.5	185	22	13
PTMO$_{1000}$-T6T6T	35.0	2.0	-61	-15	87	3.7	240	18	33
PTMO$_{2000}$-T6T6T	21.6	2.2	-68	5	39	1.7	225	13	17

PTMO-TPTPT copolymers have a three times lower modulus at room temperature than PTMO-T6T6T. These lower rubber moduli of the TPTPT copolymers might be due to a lower crystallinity and/or lower aspect ratio of the crystallites. The crystallinity of PTMO$_{1000}$-TPTPT estimated from the DSC measurements is not lower than for PTMO$_{1000}$-T6T6T (Table 7.3) and the T_g and long spacing had not increased compared to PTMO-T6T6T copolymers, thus the crystallinity does not seem to be the cause. The lower aspect ratio of the TPTPT crystallites in the copolymer (Figure 7.8) could be the reason for the low rubber modulus. The flow temperature of the TPTPT segmented copolymers compared to the T6T6T copolymers is influenced by two opposing factors; the absence of hydrogen bonds and the increased stiffness of the piperazine units compared to the hexamethylene units.

Compression set

A standard way to study the elastic behaviour of segmented copolymers is to measure the compression set (CS). A general trend is that the compression set increases with increasing modulus[9,15]. The PTMO-TPTPT copolymers also show an increase in CS with increasing modulus (Figure 7.11). The CS of PTMO-TPTPT are higher than for PTMO-T6T6T, although the modulus is much lower (Table 7.4). The higher CS for the TPTPT copolymers is probably due to easily deformable crystalline ribbons as a result of the absence of hydrogen bonds and less good packing in the crystalline state.
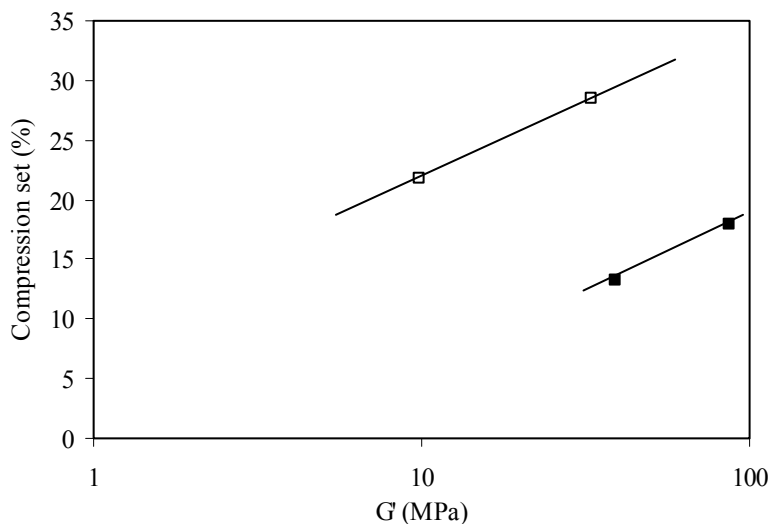
Figure 7.11: Compression set at 25% compression measured at room temperature as a function of rubber modulus: □, PTMO-TPTPT; ■, PTMO-T6T6T.

Tensile set

A test that gives more insight in the elastic behaviour is the tensile set as a function of the applied strain. The strain of each loading-unloading cycle was increased (stair-case loading) and the tensile set (TS) of the strain increment was determined as function of the applied strain (Equation 7.3). The TS was performed for PTMO-TPTPT and PTMO-T6T6T (Figure 7.12, Figure 7.6). The TS for PTMO-TPTPT are slightly lower than for PTMO-T6T6T. The TS-values of the copolymers based on $PTMO_{1000}$ increase with strain and then level off after approximately 100%. For the copolymers based on $PTMO_{2000}$ a less steep increase of the TS was observed that levels off at 350%. Due to strain crystallisation the TS of $PTMO_{2000}$ copolymers is finally increased to a higher level than for $PTMO_{1000}$ copolymers. The TPTPT copolymers show slightly lower TS-values but also have a much lower modulus (Table 7.4).
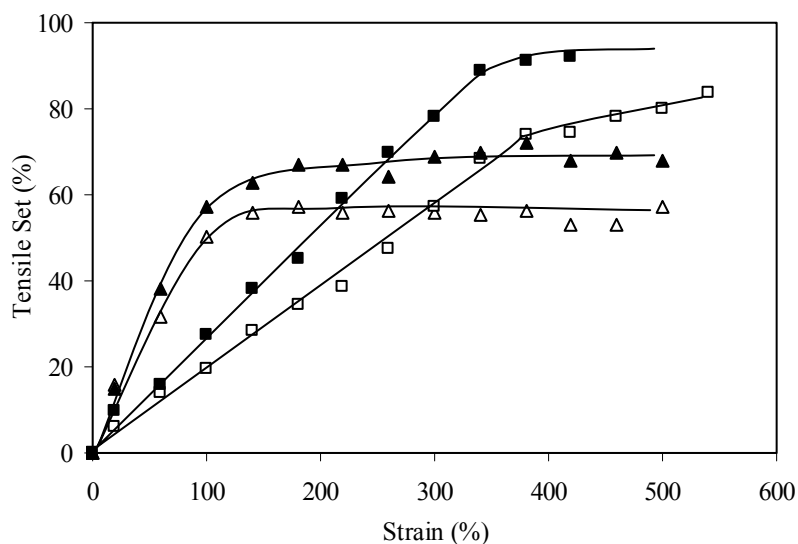
Figure 7.12: Tensile set as a function of strain: Δ, *PTMO$_{1000}$-TPTPT;* □, *PTMO$_{2000}$-TPTPT;* ▲, *PTMO$_{1000}$-T6T6T;* ■, *PTMO$_{2000}$-T6T6T.*

A typical value is the TS at 50% strain (TS$_{50\%}$). For PTMO$_x$-T6A6T series a TS$_{50\%}$ curve was plotted versus the modulus of the copolymers (Figure 7.13). Polymers with higher moduli have considerable higher TS$_{50\%}$ values[15]. For PTMO$_x$-T6T6T, the TS$_{50\%}$ is in accordance with the result of the PTMO-T6A6T series[15]. The TS$_{50\%}$ of PTMO-TPTPT shows higher values than PTMO-T6T6T and PTMO-T6A6T at corresponding moduli (Figure 7.13).

Figure 7.13: TS$_{50\%}$ as a function of rubber modulus at 25 °C: □, *PTMO-TPTPT;* ▲, *PTMO-T6T6T;* ------, *PTMO-T6A6T[15].*

Both the $TS_{50\%}$ and $CS_{25\%}$ measurements show a less elastic behaviour of the TPTPT copolymers compared with the T6T6T copolymers. This difference is stronger in the CS test and is probably due to the fact that in the CS test during 24 h more flow can take place. These tests show that TPTPT lamellae can be more easily deformed than the T6T6T lamellae as a result of the absence of hydrogen bonds.

Tensile properties

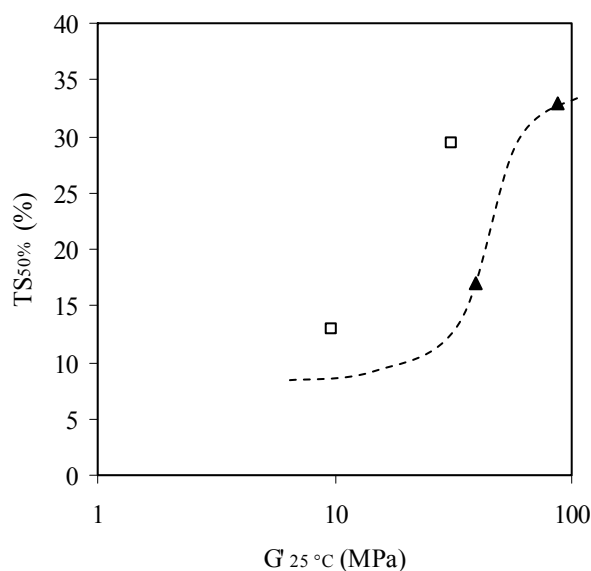The tensile curves of PTMO-TPTPT and PTMO-T6T6T are shown in Figure 7.14.
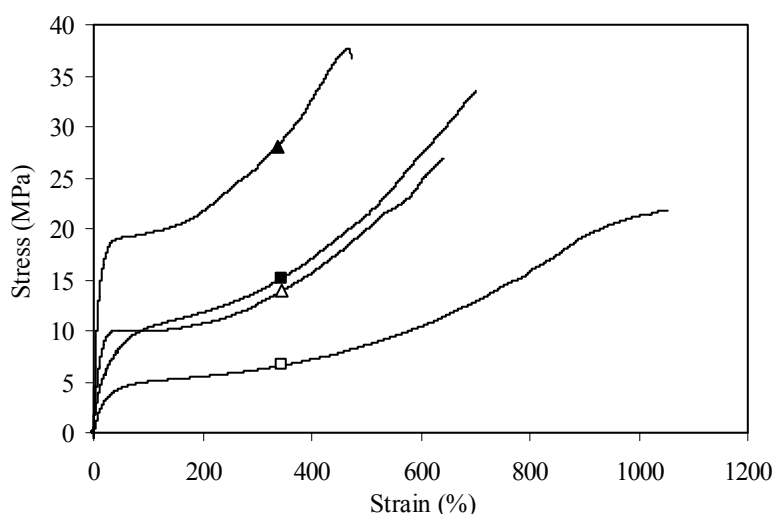
Figure 7.14: Stress-strain curves: Δ, PTMO$_{1000}$-TPTPT; □, PTMO$_{2000}$-TPTPT; ▲, PTMO$_{1000}$-T6T6T; ■, PTMO$_{2000}$-T6T6T.

Necking was not observed during the tensile measurements. The stress-strain curves are typical for thermoplastic elastomeric materials. The E-modulus for TPTPT copolymers is much lower than for the T6T6T copolymers (Table 7.5). The yield strain is for both polymers about the same. However, the yield stress for PTMO-TPTPT is a factor two lower than for PTMO-T6T6T. Apparently the stress necessary to deform TPTPT crystallites is lower than for T6T6T crystallites. This can be explained by the absence of hydrogen bonding, the poorer crystalline packing and the lower aspect ratio of the crystallites. Possibly all three aspects play a role.
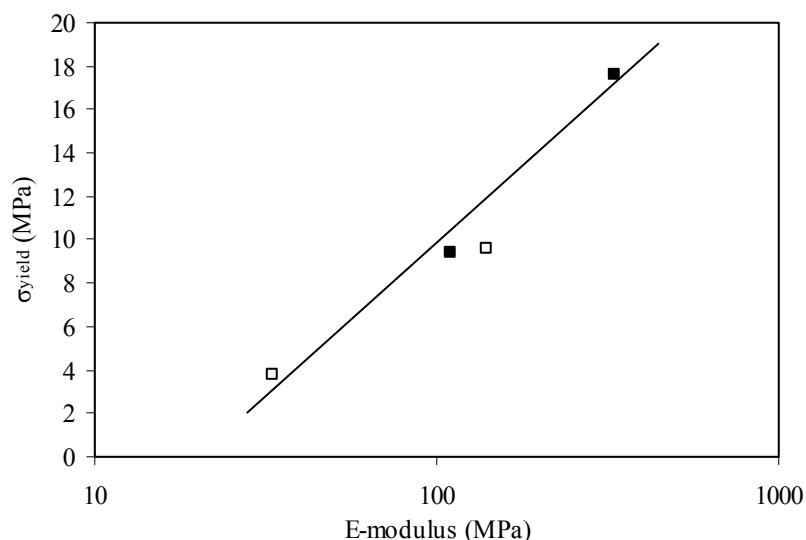
Figure 7.15: Yield stress as a function of E-modulus: □, PTMO-TPTPT; ■, PTMO-T6T6T.

The log E-modulus and yield stresses are both dependent on the reinforcing effect of the crystalline ribbons and when one decreases the other decreases as well (Figure 7.15). After the yield point, strain hardening of the PTMO phase occurred, increasing the strength of both polymers. The fracture stresses of the TPTPT based polymers are lower than for the T6T6T based polymer and this can be due to the lower aspect ratio of the TPTPT lamellae. The fracture strains are however higher. Piperazine segments are known to have a high orientability, while in hydrogen bonded polymers the orientation is restricted due to hydrogen bonding between flexible and rigid segments[5]. The true fracture strength of TPTPT or T6T6T based copolymers are comparable (Table 7.5).

Table 7.5: Tensile properties of PTMO-TPTPT and PTMO-T6T6T.

	rigid segment (%)	η_{inh} (dl/g)	E-modulus (MPa)	σ_y (MPa)	ε_y (%)	σ_b (MPa)	ε_b (%)	σ_{true}[a] (MPa)
PTMO$_{1000}$-TPTPT	32.5	2.0	140	10	27	28	642	208
PTMO$_{2000}$-TPTPT	19.8	1.9	33	4	48	22	1050	253
PTMO$_{1000}$-T6T6T	35.0	2.0	333	18	25	38	468	216
PTMO$_{2000}$-T6T6T	21.6	2.2	110	9	57	33	702	265

[a] σ_{true} was obtained by multiplying σ_b by the straining factor (= 1 + (ε_{break} / 100))

Conclusions

Segmented copolymers PTMO$_x$-TPTPT with non hydrogen bonding crystallisable TPTPT segments were synthesised. The polymers had a relatively high inherent viscosity and were transparent. The TPTPT units are based on alternating terephthalic acid and piperazine units connected through amide bonds, which are unable to form hydrogen bonds. The polymerisation was carried out with the TPTPT-dimethyl unit that was synthesised prior to the polycondensation reaction to ensure the uniformity of the segment. Two lengths of PTMO were used as amorphous segment, PTMO 1000 g·mol^{-1} and 2000 g·mol^{-1}.

The melting temperatures for PTMO$_{1000}$-TPTPT and PTMO$_{2000}$-TPTPT were 220 and 185 °C respectively and these polymers could easily be melt processed. The glass transition of the PTMO$_x$-TPTPT segmented copolymers was low (-70 °C), so phase separation was almost complete. The rubber modulus in the plateau region decreases slightly with temperature and the melting transition is sharp as often observed with polymers containing uniform crystallisable segments. The rubber moduli of the copolymers are relatively low. The degree of crystallinity of the TPTPT segments in the copolymer estimated with DSC was still high, despite the low melting enthalpy. The TPTPT segments in the copolymers form nano-ribbons but the aspect ratio of these ribbons does not seem to be very high.

The SAXS pattern of PTMO$_{1000}$-TPTPT is comparable to that of PTMO$_{1000}$-T6T6T, which has a well defined morphology. The CS and TS measurements of PTMO$_x$-TPTPT showed poorer elastic behaviour compared to PTMO$_x$-T6T6T. The TPTPT lamellae seem to be less resistant to deformation. The rubber modulus, E-modulus and yield stress were factors lower for the copolymers with TPTPT than for the copolymers with T6T6T. The change in the yield stress followed the change in the E-modulus. The low values for the modulus and yield stress for the PTMO$_x$-TPTPT copolymers are thought to be due to the lower reinforcing effect of the crystallites as a result of the absence of hydrogen bonding, the poorer crystalline packing and the lower aspect ratio of the crystallites.

References

1. Kaczmarczyk, B., Sek, D., *Polymer* **36**, 5019-5025 (1995).

2. Allegrezza, A.E., Seymour, R.W., Ng, H.N., Cooper, S.L., *Polymer* **15**, 433-440 (1974).

3. Eisenbach, C.D., Heinemann, T., *Macromolecules* **28**, 2133-2139 (1995).

4. Harrel, L.L., *Macromolecules* **2**, 607-612 (1969).

5. Ng, H.N., *Polymer* **14**, 255-261 (1973).

6. Reynolds, N., Spiess, H.W., Hayen, H., Nefzger, H., Eisenbach, C.D., *Macromol. Chem. Phys.* **195**, 2855-2873 (1994).

7. Krijgsman, J., Husken, D., Gaymans, R.J., *Polymer* **44**, 7573-7588 (2003).

8. Schuur van der, J.M., *'Poly(propylene oxide) based segmented block copolymers'*, Ph.D. Thesis, University of Twente (2004).

9. Chapter 5 of this thesis

10. Cella, R.J.J., *J. Polym. Sci. : Symposium no. 47* (1973).

11. Halpin, J.C., Kardos, J.L., *J. Appl. Phys.* **43**, 2235 (1972).

12. Versteegen, R.M., *'Well-defined Thermoplastic Elastomers'*, Ph.D. Thesis, University of Eindhoven (2003).

13. Eisenbach, C.D., Heinemann, T., Ribbe, A., Stadler, E., *Angew. Makromol. Chem.* **202**, 221-241 (1992).

14. Chapter 2 of this thesis

15. Chapter 3 of this thesis

16. Michinori, O., *'Applications of dynamic NMR spectroscopy to organic chemistry'*, VCH, Deerfield Beach (1985).

17. Krijgsman, J., Husken, D., Gaymans, R.J., *Polymer* **44**, 7043-7053 (2003).

18. Hirschinger, J., Miura, H., Gardner, K.H., English, A.D., *Macromolecules* **23**, 2153 (1990).

19. Todoki, M., Kawaguchi, T., *J. Polym. Sci. Phys. Ed.* **15**, 1067 (1977).

20. Bennekom van, A.C.M., Gaymans, R.J., *Polymer* **38**, 657-665 (1997).

21. Garcia, D., Starkweather, H., *Journal of polymer sciene phys. ed.* **32**, 537 (1985).

22. Gaymans, R.J., Dehaan, J.L., *Polymer* **34**, 4360-4364 (1993).

23. Hutten van, P.F., Mangnus, R.M., Gaymans, R.J., *Polymer* **34**, 4193-4202 (1993).

24. Niesten, M.C.E.J., Harkema, S., van der Heide, E., Gaymans, R.J., *Polymer* **42**, 1131-1142 (2001).

25. Ramesh, C., Keller, A., Eltink, S.J.E.A., *Polymer* **35**, 5293-5299 (1994).

26. Lips, P.A.M., *'Aliphatic segmented poly(ester amide)s based on symmetrical bisamide-diols'*, Ph.D. Thesis, University of Twente (2005).

27. Dreyfuss, P. *et al.*, *'Encyclopedia of Polymer Science and Engineering'*, New York (1989).

28. Seymour, R.W., Estes, G.M., Cooper, S.L., *Macromolecules* **3**, (1970).

CHAPTER 8

SEGMENTED POLYURETHANES WITH MONODISPERSE RIGID SEGMENTS BASED ON PTMO ENDCAPPED WITH DIFFERENT DIISOCYANATES, AND DIAMINE-DIAMIDE CHAIN EXTENDERS

Abstract

Poly(tetramethylene oxide) based polyether(bisurethane-bisurea-bisamide)s (PEUUA) were synthesised by chain extension of PTMO, endcapped with diisocyanates (DI), with a uniform amide extender. The starting prepolymers were PTMO with a molecular weight of 1270 and 2000 g·mol^{-1}, either endcapped with 4,4'-diphenylmethane diisocyanate (MDI), 2,4-toluene diisocyanate (2,4-TDI) or 1,6-hexane diisocyante (HDI) and having a low free diisocyanate content (<0.1 wt%). A diamine-diamide (6A6) based on hexamethylene diamine (6) and adipic acid (A) was used a chain extender. In this way segmented polyurethanes with monodisperse rigid segments (DI-6A6-DI) were obtained.

The PEUUA's were characterised by DSC and temperature dependent FT-IR and DMTA. The mechanical properties of the polymers were evaluated by compression set and tensile test measurements. The degrees of crystallinity of the amide groups in the rigid segment determined by FTIR were 70 - 80% before heating and 40 - 60% after cooling. The rate of crystallisation (T_m - T_c) was moderately fast (36 - 54 °C). Polyurethanes with monodisperse rigid segments have a low glass transition temperature, an almost temperature independent rubbery plateau and a sharp melting temperature. The polyurethanes based on HDI have a much higher rubber modulus compared to the MDI and 2,4-TDI based polymers due to a higher degree of crystallinity and/or higher aspect ratio of the crystallites. The HDI residues are flexible and not sterically hindered and can therefore be more easily packed than MDI or 2,4-TDI residues.

Introduction

Polyurethane elastomers consist of alternating flexible polyether segments and rigid urethane or urea segments and are classified as thermoplastic polyurethanes (TPU's)[1,2]. Due to incompatibility of the alternating segments, micro-phase separation easily occurs. The rigid segments phase separate into hard domains dispersed in a soft matrix. The hard phase acts as thermoreversible physical crosslinks which allows melt processing. Phase separation either occurs by liquid-liquid demixing and/or (partial) crystallisation of the rigid segments. Liquid-liquid demixing leads to aggregation of rigid segments, resulting in spherical hard domains that hardly contribute to reinforcement of the polymer matrix. Liquid-liquid demixing is favoured by the presence of long rigid segments and can be avoided by using short uniform rigid segments[3]. Most commercial TPU's have a random distribution of the rigid segments resulting in a complex morphology and a low degree of crystallinity, normally lower than 20%[4]. When rigid segments are dissolved in the polyether phase, the T_g of the soft phase is increased and broadened, resulting in a poor low temperature flexibility.

To induce phase separation by crystallisation, monodisperse crystallisable segments can be used[3,5-9]. Polyurethanes with monodisperse rigid segments have a low T_g of the polyether phase, a relatively high modulus at room temperature, an almost temperature independent rubber modulus and a sharp melting transition[3,7-9]. The rubber modulus at room temperature of these polymers depends on the content of rigid segment and the morphology of the phase separated rigid segments[3]. The mechanical properties of polyurethanes containing monodisperse rigid segments deteriorate when the dispersity of the rigid segments is increased, for instance by transurethanisation, or when degradation takes place. These phenomena can occur above 180 - 210 °C[2,10]. It is therefore difficult to synthesise polyurethanes with monodisperse rigid segments via melt polymerisation and to process these polymers without loosing the uniformity of the rigid segments.

The dispersity of the rigid segments depends on the polymerisation procedure. The polymerisation temperature should be low, the prepolymer should not contain free diisocyanates and the extender should be uniform in length. Free diisocyanates in the prepolymer can react with an extender and form longer blocks. Another reason to use prepolymers with low diisocyanate contents is the toxicity of the free diisocyanates.

In several studies polyurethanes with uniform extenders were reported[3,5,7-9]. Versteegen[9] prepared block copoly(ether urea)s with amine-terminated prepolymers as flexible segments. Via protective group strategy and novel isocyanate chemistry, segmented block copolymers with uniform rigid segments were synthesised. These polymers with monodisperse rigid segments had Young's moduli up to 96 MPa. In general, these polymers have higher moduli, higher yield stress, higher strength and toughness compared to analogous polymers with polydisperse rigid segments. Heijkants[11] studied polyurethanes based on poly(ε-caprolactone) endcapped with 1,4-butane diisocyanate and 1,4-butanediol as extender. These polyurethanes with 12 - 33 wt% aliphatic urethane rigid segment had Young's moduli varying from 30 to 90 MPa and melting temperatures below 125 °C. These studies show that polyurethanes with monodisperse rigid segments based on aliphatic isocyanate endcappers can have high moduli.

Van der Schuur made poly(ether-urethane-urea-amide)'s (PEUUA) from poly(propylene oxide) endcapped with 2,4-toluene diisocyanate (2,4-TDI) and uniform amide extenders (e.g. 6T6-diamine diamide)[3].
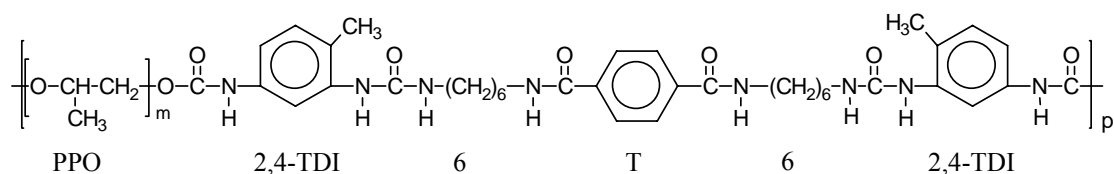
Figure 8.1: Structure of PPO based polyether(bisurethane-bisurea-bisamide) with uniform rigid segments (PPO-TDI-6T6-TDI).

These TPU's with monodisperse TDI-6T6-TDI segments had an almost temperature independent rubbery plateau and a well defined melting temperature (169 °C). The storage modulus at 25 °C of PPO_{2300}-TDI-6T6-TDI was only 13 MPa compared to a storage modulus of 28 MPa for an analogous poly(etherester amide) PPO_{2300}-T6T6T with the same rigid segment content[3]. This suggests that for PEUUA copolymers either the degree of crystallinity and/or aspect ratio of the crystallites are lower than for the PEEA copolymers.

Generally, rubber moduli of segmented polyurethanes with random rigid segment distributions are low and temperature dependent. It would be interesting to study

polyurethanes with monodisperse rigid segments in more detail, as these are expected to have a high degree of crystallinity.

Research aim

Polyether(bisurethane-bisurea-bisamide)s with monodisperse rigid segments are synthesised using diisocyanate endcapped PTMO (DI-PTMO-DI) and a uniform diamine-diamide chain extender. The 6A6-diamine-diamide chain extender is based on hexamethylene diamine (6) and adipic acid (A). DI-PTMO-DI's with a PTMO length of about 1270 or 2000 g·mol^{-1} and with a low free diisocyanate content (<0.1wt%) are used. Three diisocyanates are applied as endcapper for PTMO: MDI, 2,4-TDI and HDI. The crystallisation behaviour of the resulting polymers is studied using DSC and FT-IR. The thermal mechanical behaviour of these polymers is studied with DMTA, their elastic behaviour with compression set measurements and the stress-strain behaviour with tensile test measurements.

Experimental

Materials: 1,6-Diaminohexane, dimethyl adipate, N,N-dimethylacetamide (anhydrous), 1,1,1,3,3,3-hexafluoroisopropanol (HFIP) and a 0.5 M sodium methoxide solution in methanol were purchased from Aldrich and used as received. Poly(tetramethylene oxide) endcapped with diisocyanates were a gift from Crompton Corporation. Obtained were HDI-PTMO-HDI (M_w 2000 g·mol^{-1}, non commercial sample and M_w 1270 g·mol^{-1} LFH520), 2,4-TDI-PTMO-2,4-TDI (M_w 1890 g·mol^{-1}, LF900A) and MDI-PTMO-MDI (M_w 2210 g·mol^{-1}, LFM300). All prepolymers had a low free diisocyanate content (<0.1wt%). The prepolymers were dried in vacuo at 80 °C overnight before use. The synthesis of the chain extender 6A6 was performed as described before[12].

Copolymerisation: The polymerisation of (-PTMO$_{2000}$-HDI-6A6-HDI-) is given as an example. A dried 250 ml stainless steel reactor with a nitrogen inlet and magnetic coupling stirrer was charged with HDI-PTMO$_{2000}$-HDI (30 g, 0.0128 mol) and a solution of 6A6-diamine (4.39 g, 0.0128 mol) in 100 ml anhydrous N,N-dimethylacetamide (DMAc). The stirred reaction mixture was heated to 140 °C and reacted for 5 h under nitrogen flow. Subsequently, the pressure was carefully reduced (P<20 mbar) to distil off the DMAc and then further reduced (P<0.3 mbar) for 60 min. The reactor was then slowly cooled, maintaining the low pressure. The copolymer obtained was transparent, colourless and tough.

Compression moulding: Test samples for DMTA, CS and tensile testing were made by compression moulding with the use of a 40 ton Lauffer 40 press. The TPU (2.1 g) cut in small pieces and dried overnight was spread into a bar-shaped mould (80x9x2 mm) with press plates. The temperature of the press was set at 20 degrees

above the melting temperature with a maximum of 230 °C. First, air was removed from the polymer in the mould by quickly pressurising followed by depressurising of the sample. This procedure was repeated three times before pressing the samples at 10 MP ($\approx$ 8.5 MPa) for 2 min. After this, the press was cooled and the test bars were removed from the mould.

Viscometry: The inherent viscosity was measured at a concentration of 0.1 g/dl in a mixture of phenol/1,1,2,2-tetrachloroethane (1:1 molar ratio) at 25 ºC using a capillary Ubbelohde type 1B.

FT-IR: Infrared transmission spectra were recorded using a Nicolet 20SXB FTIR spectrometer with a resolution of 4 cm^{-1}. Solution cast polymer films (0.05 g/ml in HFIP) of <10 μm thick were used for temperature dependent FT-IR recorded at temperatures between room temperature and 210 °C. The film was placed in-between two pressed KBr pellets under a helium flow. The degree of crystallinity of the rigid segments in the polymers was estimated with the following equations.

$$X_c \, FT\text{-}IR = \frac{Crystalline \; amide \; peak}{Amorphous + Crystalline \; amide \; peak} = \frac{\lambda_{25°C(1630cm^{-1})}}{a \times \lambda_{25°C(1670cm^{-1})} + \lambda_{25°C(1630cm^{-1})}} \quad \text{(Equation 8.1)}$$

With λ_T = height of absorption band at temperature T (°C)

The height of the amorphous and crystalline amide peak are related by factor a, which can be calculated according to;

$$a = \frac{decrease \; of \; crystalline \; peak \;_{(25°C \, - \, melt)}}{increase \; of \; amorphous \; peak \;_{(25°C \, - \, melt)}} = \frac{\lambda_{25°C(1630cm^{-1})} - \lambda_{melt(1630cm^{-1})}}{\lambda_{melt(1670cm^{-1})} - \lambda_{25°C(1670cm^{-1})}}$$

DSC: DSC spectra were recorded on a Perkin Elmer DSC apparatus, equipped with a PE7700 computer and TAS-7 software. Dried samples of 5 - 10 mg were heated to approximately 30 °C above the melting temperature and subsequently cooled, both at a rate of 20 °C/min. The maximum of the peak in de heating scan was taken as the melting temperature. The second heating scan was used to determine the melting peak and enthalpy of the sample. The first cooling curve was used to determine the crystallisation temperature, which was taken as the onset of crystallisation.

DMTA: The compression moulded test samples (70x9x2 mm) were dried in vacuum at 50 °C for 24 h before use. DMTA spectra were recorded with a Myrenne ATM3 torsion pendulum at a frequency of 1 Hz and 0.1% strain. The storage modulus G' and the loss modulus G" were measured as a function of temperature. The samples were cooled to -100 °C and subsequently heated at a rate of 1 °C/min. The glass transition was determined as the peak in the loss modulus. The flow temperature (T_{flow}) is defined as the temperature where the storage modulus reaches 1 MPa. The start of the rubbery plateau, the intercept of the tangents, is called the flex temperature (T_{flex}). The decrease in storage modulus of the rubbery plateau with increasing temperature is quantified by ΔG', which is calculated from:

$$\Delta G' = \frac{G'_{(Tflex)} - G'_{(Tflow-50°C)}}{G'_{25°C}} \times \frac{1}{\Delta T} \qquad (°C^{-1}) \qquad\qquad \text{(Equation 8.2)}$$

ΔT is described as the temperature range: $(T_{flow}-50\ °C) - T_{flex}$.

Compression set: Samples for compression set were cut from compression moulded bars. The compression set was measured at room temperature according to ASTM 395 B standard. After 24 h the compression was released at room temperature. After relaxation for half an hour, the thickness of the samples was measured. The compression set was taken as the average of four measurements. The compression set is defined as:

$$Compression\ set = \frac{d_0 - d_2}{d_0 - d_1} \times 100\% \qquad (\%)$$

<div align="right">*(Equation 8.3)*</div>

With: d_0 = thickness before compression (mm)

   d_1 = thickness during compression (mm)

   d_2 = thickness after 0.5 h relaxation (mm)

Tensile test: Stress-strain curves were obtained using compression moulded bars with a thickness of 2.2 mm, cut to dumbbell (ISO 37 type 2), using a Zwick Z020 universal tensile machine equipped with a 500 N load cell. The strain was measured with extensometers. The tensile tests were performed in three-fold according to ISO 37 at a strain rate of 0.4 s^{-1} (test speed of 60 mm/min).

Results and discussion

Polyether(bisurethane-bisurea-bisamide)s with monodisperse rigid segments were synthesised from prepolymers based on poly(tetramethylene oxide) (PTMO) endcapped with different diisocyanates (DI) and a uniform diamine-diamide extender. The three diisocyanates used in this series are 2,4-toluene diisocyanate (2,4-TDI), diphenylmethane diisocyanate (MDI) and 1,6-hexane diisocyanate (HDI) (Figure 8.2).
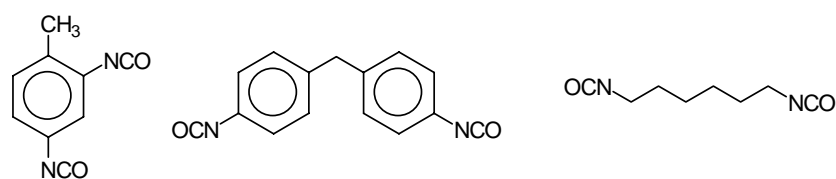
Figure 8.2: Different diisocyanates; 2,4-TDI, MDI, HDI.

A uniform aliphatic chain extender, 6A6-diamine-diamide, was made from hexamethylene diamine (6) and adipic acid (A)[12]. In synthesising TPU's with monodisperse rigid segments the uniformity of the extender is important as well as a low content of free diisocyanates in the endcapped prepolymer. Free diisocyanates can form double blocks (DI-6A6-DI-6A6-DI), resulting in a loss of the monodisperse character of the rigid segments in the copolymer. The prepolymers in this study have a very low content of free diisocyanates (<0.1%), and

therefore the formation of double blocks is limited and the rigid segments are monodisperse. The prepolymers have a molecular weight of the PTMO of 2000 g·mol^{-1} and 1270 g·mol^{-1} (Table 8.1). The PTMO prepolymers are not extended with diisocyanates (-PTMO-DI-PTMO-) to higher molecular weights as confirmed by the very low T_g of the polymers (-72 °C). The molecular weights of the polyether and prepolymers are given in Table 8.1.

Table 8.1: Prepolymer composition.

Prepolymer	M_n of polyether (g·mol^{-1})	M_n of the prepolymer[a] (g·mol^{-1})
2,4-TDI-PTMO$_{1886}$-2,4-TDI	1886	2234
MDI-PTMO$_{2209}$-MDI	2209	2710
HDI-PTMO$_{2000}$-HDI	2000	2336
HDI-PTMO$_{1270}$-HDI	1270	1606

[a] *molecular weights calculated from the NCO concentrations as determined by Crompton Corporation*

Synthesis of PEUUA copolymers

The prepolymer, extender and polymerisation set-up were dried overnight at 80 °C in vacuo to remove traces of water. The reaction of the isocyanate endcapped polyether (DI-PTMO-DI) and the diamine-diamide (6A6) is fast and the polymerisation is carried out at relatively low temperatures (140 - 160 °C). However, the polymerisation was carried out for four hours to ensure completion. The resulting polymers are non-sticky and transparent materials with inherent viscosities of 1.3 - 1.6 dl/g (Table 8.2) indicating that the copolymers have a molecular weight in the range commonly obtained by other investigators. The segmented polyurethanes with HDI are colourless while the copolymers with MDI and 2,4-TDI are slightly yellow. The structure of the HDI copolymer with monodisperse rigid segments (-PTMO-HDI-6A6-HDI-) is presented in Figure 8.3.
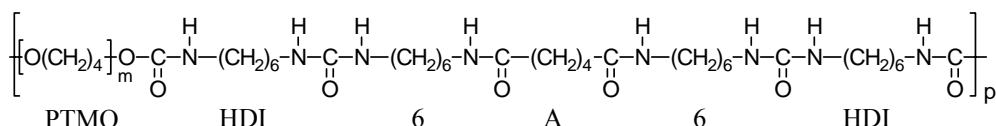

Figure 8.3: Structure of -PTMO$_x$-HDI-6A6-HDI-.

FT-IR

Infrared spectroscopy was used to study hydrogen bonding in the PEUUA systems. The absorption bands of carbonyl and N-H groups depend on hydrogen bond formation. Three

different groups that can form hydrogen bonds are present; urethane, urea and amide groups. In Figure 8.4 the absorption bands of polyurethanes in the crystalline and amorphous state, as reported in literature, are given[2,3,9,13-16]. Urea groups can form either bidentate or monodentate hydrogen bonds.
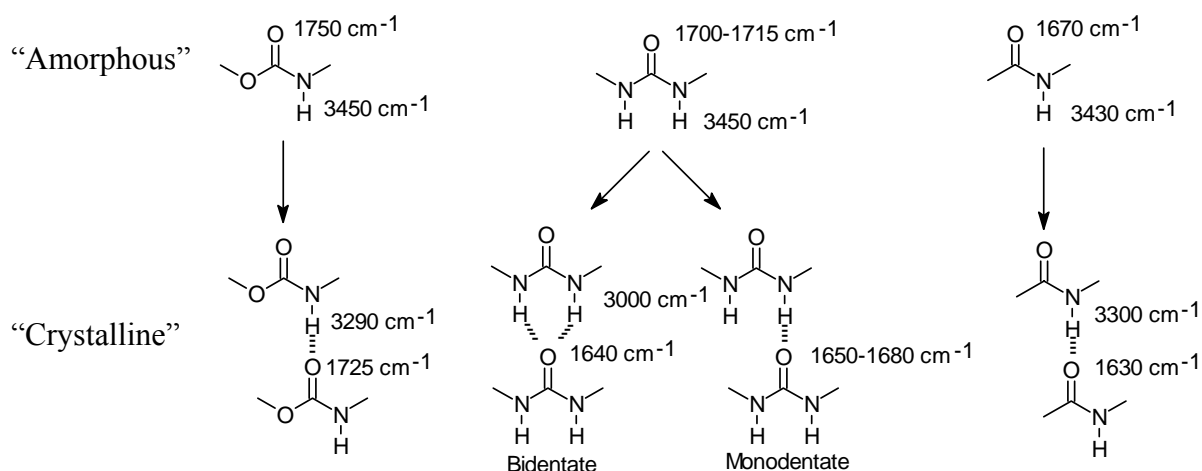
Figure 8.4: Infrared absorption bands for urethane, urea and amide groups in the amorphous or crystalline state.

The FT-IR spectra of the segmented polyurethanes are shown in Figure 8.5. In the infrared spectrum peaks are observed at 3290 cm^{-1} for the crystalline N-H groups, at 1730 cm^{-1} for the amorphous urethane carbonyl group, at 1707 cm^{-1} for the crystalline urethane carbonyl groups, at 1680 cm^{-1} for the monodentate crystalline urea groups and at 1633 cm^{-1} for crystalline amide carbonyl groups (Amide I). The peak at 1599 cm^{-1} is related to the benzene ring and was only observed for the polyurethanes based on MDI and 2,4-TDI. The peaks at 1573 cm^{-1}, 1538 cm^{-1} and 1512 cm^{-1} are for δ(N-H) + v(C-N) (Amide II).

Figure 8.5: Infrared spectra of PEUUA: ■, PTMO$_{2000}$-HDI-6A6-HDI; ▲, PTMO$_{2209}$-MDI-6A6-MDI; ●, PTMO$_{1886}$-TDI-6A6-TDI.

Although the three segmented polyurethanes almost have the same composition, the infrared spectra of the carbonyl groups show different absorption bands. The infrared spectra of the polyurethanes based on TDI and MDI show a strong peak at 1633 cm^{-1} for crystalline amide carbonyl groups. Next to the amide groups also some urethane groups are crystalline as a small peak at 1707/1696 cm^{-1} 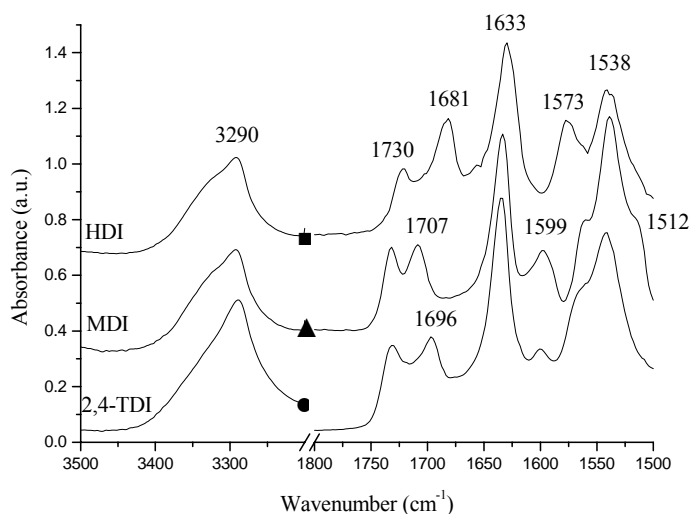is present. However, amorphous urethane groups are also present, indicated by the peak at 1730 cm^{-1}. No infrared peaks corresponding with urea groups were observed. The infrared spectrum of the polyurethane based on HDI shows a strong peak of crystalline amide groups at 1633 cm^{-1} and of monodentate bonded crystalline urea at 1680 cm^{-1}. The peak at 1730 cm^{-1} indicates that some amorphous urea or urethane groups are present. No peaks were observed for crystalline urethane groups.

Temperature dependent infrared spectroscopy was used to study the crystallinity of the amide segments as a function of temperature (Figure 8.6). The MDI and 2,4-TDI based polyurethanes show the same peak changes in the infrared spectra and therefore only the infrared spectrum of the MDI based polyurethanes is shown (Figure 8.6a). The amide I peaks for the crystalline phase (1630 cm^{-1}) are strong up to the melting temperature of the copolymer. Upon melting, the intensity of this peak decreases, while at the same time the intensity of the peak at 1670 cm^{-1} of amorphous C=O groups increases. The absorption bands of crystalline urethane carbonyl group at 1707 cm^{-1} also decrease in intensity with increasing temperature. Upon cooling of the molten samples, the peaks of crystalline carbonyl amide (1630 cm^{-1}) and crystalline carbonyl urethane (1707 cm^{-1}) only partially recovered.
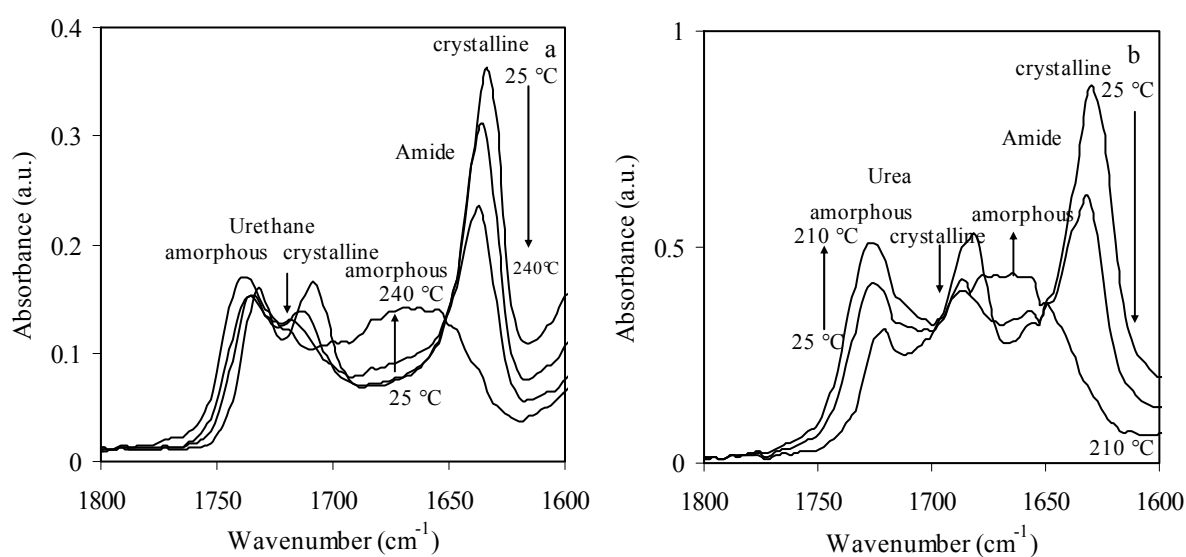

Figure 8.6: Temperature dependent infrared spectra at increasing temperatures of a) PTMO$_{2209}$-MDI-6A6-MDI (T$_m$ = 212 °C); 25, 180, 240 °C; b) PTMO$_{2000}$-HDI-6A6-HDI (T$_m$ = 231 °C); 25, 160, 210 °C.

The HDI based polyurethane shows a similar decrease in intensity of the peak at 1633 cm^{-1} of crystalline amide carbonyl and a simultaneous increase of the peak at 1670 cm^{-1} of amorphous amide carbonyl groups (Figure 8.6b). Upon heating, the peak of monodentate crystalline urea groups at 1680 cm^{-1} also decreases with increasing temperature and with that the peak at 1730 cm^{-1} increases (Figure 8.6b). Upon cooling of the sample the peaks at 1633 cm^{-1} and 1680 cm^{-1} of crystalline groups almost completely return to their starting values. This indicates that crystallisation of HDI based rigid segments is easier than crystallisation of MDI and 2,4-TDI based rigid segments.

The ratio of crystalline and amorphous amide peaks gives an indication of the degree of crystallinity of the 6A6 segment in the polymer. The degree of crystallinity of the 6A6 segment in PTMO-MDI-6A6-MDI and PTMO-TDI-6A6-TDI was 70% at room temperature and remained high until the melting temperature (Figure 8.7a). Just before the melting temperature, a sharp decrease in crystallinity was observed. Upon cooling from the melt, the degree of crystallinity of the 6A6 segments only returns to 40%. Crystallisation is incomplete and slow which is probably due to steric hindrance of the isocyanate residues in the rigid segment.
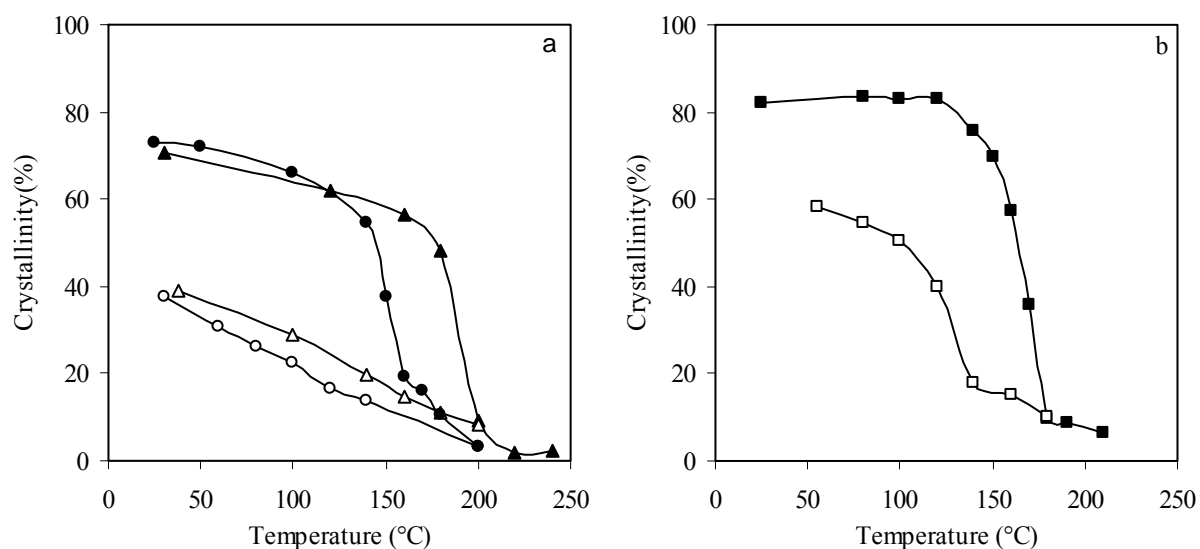

Figure 8.7: Crystallinity of the amide segments in the rigid segments of the polyurethanes as a function of temperature a) ▲, Δ, *PTMO$_{2209}$-MDI-6A6-MDI;* ●, ○, *PTMO$_{1886}$-TDI-6A6-TDI; b) PTMO$_{2000}$-HDI-6A6-HDI: closed symbols, heating curve; open symbols, cooling curve.*

The degree of crystallinity of the amide segments as a function of temperature for the HDI based polyurethane starts at 80%, is constant up to 130 °C, decreases sharply at 160 °C and approaches zero at 180 °C (Figure 8.7b). Upon cooling, the degree of crystallinity of the amide groups increases with decreasing temperature, to approximately 60%. The crystallinity of the 6A6 groups in the rigid segments based on HDI is higher than the crystallinity of these groups in rigid segments based on MDI and TDI. Moreover, after melting and subsequent cooling the crystallinity of 6A6 groups in HDI based rigid segments at room temperature recovers to a higher degree than for the 6A6 groups in the MDI and TDI based rigid segments.

Normally, the absorption bands of crystalline amide carbonyl groups at 1633 cm^{-1} decrease just before the melting temperature as was observed in the case of MDI and TDI based polyurethanes (Figure 8.7a) and also for the PEEA's from chapter 3 (Figures 3.5 and 3.6). However, for the polyurethane based on HDI-6A6-HDI a sharp decrease of the absorption band of crystalline amide carbonyl groups was observed at 180 °C, which is at a lower temperature than the melting temperature determined with DSC (232 °C) or DMTA (225 °C). The reason for this is as yet not clear.

Rigid segment packing

The hydrogen bonding possibilities of the rigid segments TDI-6A6-TDI and HDI-6A6-HDI are given in Figure 8.8. In these structures the 6A6 groups are extended and ideally hydrogen bonded.

The urea groups are monodentate bonded and this is in agreement with the FT-IR results. Obviously, the packing of 2,4-TDI is sterically hindered by the methyl groups (Figure 8.8a). The methyl groups are expected to be in the 4-position with respect to isocyanate groups which has reacted with PTMO, because the reactivity of the C$_4$-positioned isocyanate group is much higher than the C$_2$-positioned isocyanate group[17,18]. The methyl groups hinder the urea hydrogen bonding. The 2,4-TDI group might have turned out of plane to allow urea hydrogen bonding but then probably also the urethane hydrogen bonding is lowered. This packing difficulty of the 2,4-TDI (and the MDI groups) lowers the degree of crystallinity of the rigid segments and possibly also the aspect ratio of the crystallites. The aliphatic HDI does not sterically hinder the urea hydrogen bonding (Figure 8.8b). As a result the crystallinity of the amide groups is higher and the urea groups of the HDI will participate in crystallisation.
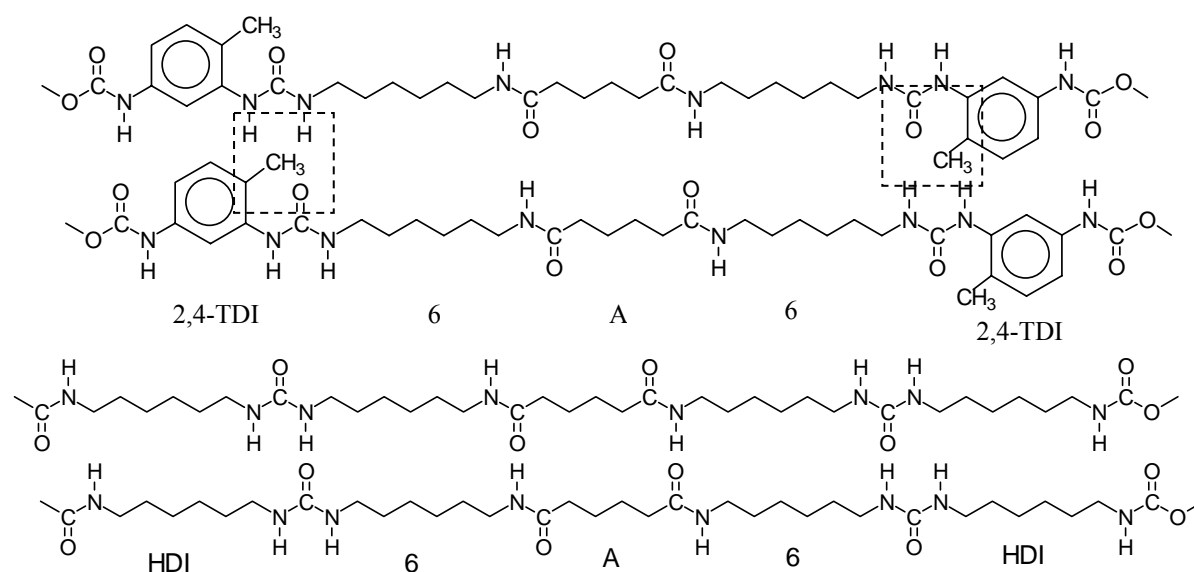
Figure 8.8: Packing of PEUUA copolymers: above, 2,4-TDI-6A6-2,4-TDI; below, HDI-6A6-HDI.

DSC

The melting and crystallisation behaviour of the segmented polyurethanes was evaluated using DSC. Three endotherm transitions were observed for these polymers. The first transition is due the crystalline PTMO phase (Table 8.2). The PTMO length of the prepolymers is slightly different. Increasing the PTMO segment length results in an increase in melting enthalpy and melting temperature. The second transition is related to a change in crystalline structure of the amide phase, as is observed more often for polyamides[19-21].

The third transition is due to melting of the rigid segments. The MDI and HDI based polyurethanes have high melting temperatures of 212 and 231 °C respectively. The 2,4-TDI based polymer has a lower melting temperature of 155 °C. For the 2,4-TDI based polyurethane no crystallisation peak and second melting of the hard phase was observed, indicating that crystallisation is slow and that the crystallinity is low. Therefore, the melting temperature and enthalpy of the first heating run of the 2,4-TDI based polyurethane are given in Table 8.2. For the MDI and HDI based polyurethanes a crystallisation and a melting transition in the second heating run were observed. The HDI copolymers have a higher melting temperature than the copolymers with MDI although the aliphatic nature of HDI. The HDI polyurethanes also have a higher melting enthalpy than the MDI based polyurethane, so the degree of crystallinity of the HDI based polyurethanes is higher. The undercooling (T_m - T_c) is 35 - 55 °C, which is relatively high compared to PEEA with uniform rigid segments

$(PTMO_x-T6A6T)^{[22]}$, indicating the difficult crystallisation of these monodisperse polyurethane segments.
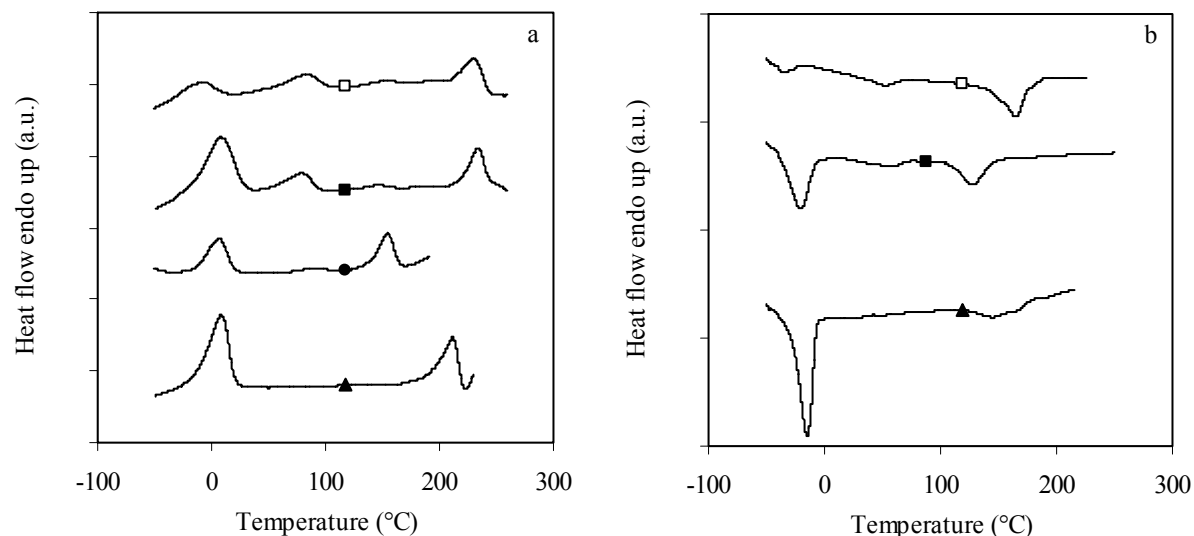
Figure 8.9: a) DSC heating run b) DSC cooling run of PTMO based segmented polyurethanes with different isocyanate endcappers: □, $PTMO_{1270}$-HDI-6A6-HDI; ■, $PTMO_{2000}$-HDI-6A6-HDI; ▲, $PTMO_{2209}$-MDI-6A6-MDI; ●, $PTMO_{1886}$-TDI-6A6-TDI.

Table 8.2: Thermal transitions of polyurethanes.

	Polymer		Rigid segment				
	RS^a (%)	η_{inh} (dl/g)	T_m (°C)	T_c (°C)	T_m-T_c (°C)	ΔH_m (J/g)	ΔH_m (J/g RS)
$PTMO_{1886}$-TDI-6A6-TDI	26.8	1.4	151	-	-	9^b	-
$PTMO_{2209}$-MDI-6A6-MDI	27.6	1.3	211	176	36	7	25
$PTMO_{2000}$-HDI-6A6-HDI	25.3	1.6	234	181	54	9	36
$PTMO_{1270}$-HDI-6A6-HDI	34.8	1.4	231	176	53	16	46

[a] RS = rigid segment based on DI-6A6-DI segment, so including the MDI, TDI or HDI residues; [b] from first heating run.

DMTA

The thermal mechanical properties of the polymers were determined by means of DMTA (Figure 8.10). It has to be realised that the polyurethanes are thermally instable above 180 °C and the DMTA results may be influenced by possible degradation of the polyurethanes. The storage and loss modulus of PEUUA's based on different isocyanate endcappers are plotted as a function of temperature.
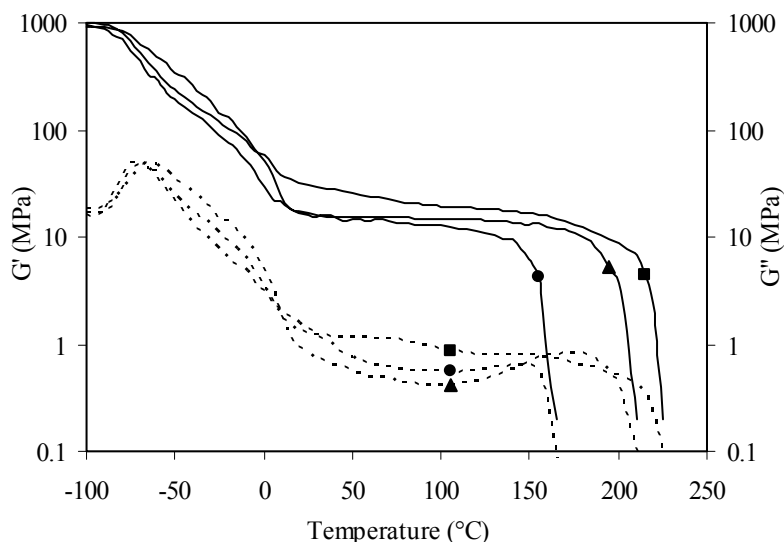
Figure 8.10: DMA spectrum of PEUUA: ■, PTMO$_{2000}$-HDI-6A6-HDI; ▲,PTMO$_{2209}$-MDI-6A6-MDI; ●, PTMO$_{1886}$-TDI-6A6-TDI.

The T_g of the polymers is remarkably low, suggesting good phase separation (Table 8.3). PTMO segments with a length of 2000 g·mol^{-1} can crystallise[23]. This crystalline phase will melt at approximately ~0 °C, giving a shoulder after the T_g and increasing the T_{flex} to 5 - 10 °C. The rubber modulus is almost temperature independent, the $\Delta G'$ values are low and the melting transition is sharp due to the presence of the monodisperse rigid segments. This indicates that the uniformity of the rigid segments is maintained during the polymerisation and processing of the materials.

Table 8.3: DMA properties of polyurethanes.

Polymer	RS[a] (%)	η_{inh} (dl/g)	T_g (°C)	T_{flex} (°C)	$G'_{25 °C}$ (MPa)	T_{flow} (°C)	$\Delta G'$ *10^{-3} (°C^{-1})	CS (%)
PTMO$_{1886}$-TDI-6A6-TDI	26.8	1.4	-72	5	16	165	5.9	12
PTMO$_{2209}$-MDI-6A6-MDI	27.6	1.3	-63	15	16	205	4.8	18
PTMO$_{2000}$-HDI-6A6-HDI	25.3	1.6	-65	15	32	225	2.4	18
PTMO$_{1270}$-HDI-6A6-HDI	34.8	1.4	-67	-15	50	230	4.6	25

[a] RS = rigid segment

The segmented polyurethane based on HDI has a storage modulus at 25 °C ($G'_{25°C}$) of 32 MPa, which is a factor two higher than of polyurethanes based on MDI or 2,4-TDI. The storage modulus at room temperature is dependent on the crystalline content and the aspect

ratio of the crystallites[24]. The crystalline content depends on the amount of rigid segments and their crystallinities. We hypothesise that the difference of the $G'_{25°C}$ between the different copolymers is mainly due to the different degree of crystallinity as was measured with infrared. Decreasing the PTMO length to 1270 g·mol^{-1} for the HDI based polymer does not change the T_g and T_m much but increases $G'_{25°C}$. Decreasing the PTMO length increases the rigid segment content and thereby increases the crystalline content. The loss moduli at room temperature are also low 0.5 - 1 MPa and with that the values for the loss factor tan δ are below 0.1. These low values suggest a good damping behaviour in dynamic loading.

Compression set

The polymers have a CS value varying from 12 - 25%. The TDI based polyurethane has a lower compression set compared to the HDI and MDI based polyurethanes. The HDI based polymer has a somewhat higher compression set but also has a higher rubber modulus than the TDI based polymer. This behaviour is expected as in general the compression set values are lower for polymers with lower moduli. For the same reason the compression set of the HDI based polymer increased with increasing rigid segment content.

Tensile properties

Tensile properties of PEUUA based on different isocyanate endcappers were studied. Compression moulded bars, cut to dumbbell shaped tensile bars (ISO 37 s2), were used for the tensile tests (Figure 8.11, Table 8.4). The stress-strain curves correspond with that of thermoplastic elastomer materials. The stress increases linearly with strain at small deformations (Hooke's Law)[25]. The Young's moduli of the MDI and 2,4-TDI based polymers were 45 MPa. For the HDI based polyurethane with the same rigid segment content the Young's modulus was 73 MPa. This higher value for the HDI copolymers indicates a higher degree of crystallinity and/or a higher aspect ratio of the crystallites compared to the MDI and 2,4-TDI based polyurethanes.

The Young's modulus of the HDI copolymer with $PTMO_{1270}$ was 140 MPa. Thus, increasing the rigid segment content in the copolymer from 25 wt% to 35 wt% strongly increased the modulus. Polyurethanes with higher concentrations than 35 wt% rigid segment were not studied but probably polyurethanes with even higher Young's moduli can be obtained.

The yield point was determined using the Considère construction[26]. The yield stress and yield strain are related to the crystallinity or modulus of a material[27]. With increasing modulus, the yield stress increases and yield strain decreases. The polymer with the highest modulus has the highest yield stress and lowest yield strain. After the yield point the stress increases due to strain hardening of the PTMO phase. These segmented polyurethanes have high strain breaks, indicating that the molecular weight of the polymers was relatively high. Only for the MDI based polymer a relatively low strain break of 200% was observed. This is due to some degradation during processing at high temperatures as the inherent viscosity due to processing decreased from 1.3 to 0.9 dl/g.
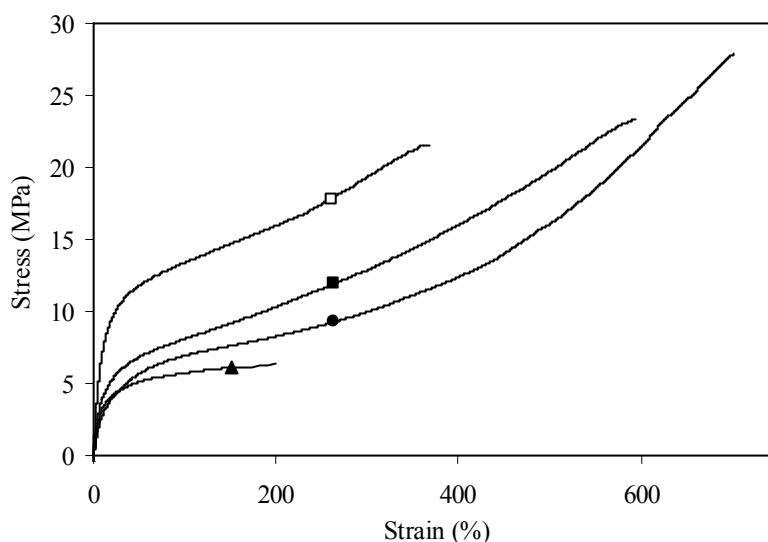
Figure 8.11: Tensile curve for PEUUA's: □, PTMO$_{1270}$-HDI-6A6; ■, PTMO$_{2000}$-HDI-6A6; ▲,PTMO$_{2209}$- MDI-6A6; ●, PTMO$_{1886}$-TDI-6A6.

Table 8.4: Tensile properties of PEUUA's.

Polymer	RS[a] (%)	E-modulus (MPa)	ε_{yield} (%)	σ_{yield} (MPa)	ε_b (%)	σ_b (MPa)
PTMO$_{1886}$-TDI-6A6-TDI	26.8	45	52	6	702	28
PTMO$_{2209}$-MDI-6A6-MDI	27.6	45	36	5	200	8
PTMO$_{2000}$-HDI-6A6-HDI	25.3	73	43	7	594	23
PTMO$_{1270}$-HDI-6A6-HDI	34.8	140	30	11	368	22

[a] *RS = rigid segment*

Comparison of PEUUA's with PEEA's

Properties of the PEUUA's (PTMO-DI-6A6-DI) presented in this chapter can be compared to those of the PEEA's (PTMO-T6A6T) discussed in Chapter 3. The only difference in structure between these polymers is that the PEUUA have an MDI, TDI or HDI group instead of a terephthalic group at the sides of the rigid segment. The concentrations of rigid segment in the polymers are almost the same. Both the PEUUA's and PEEA's have a PTMO flexible segment and a monodisperse crystallisable segment based on 6A6.

The amide groups in the rigid segments in the PEEA's had a high degree of crystallinity of about 90% (based on DSC and FT-IR measurements) compared to 60% for the MDI and TDI based PEUUA's and 80% for the HDI based PEUUA (FT-IR measurements). The degree of crystallinity of the amide groups for the MDI and TDI based polymer was low due to steric hindrance or irregular packing of the rigid segments. Temperature dependent FT-IR showed that the degree of crystallinity of the rigid segments in both PEEA's and PEUUA's is constant to just before the melting temperature and than suddenly decreases. This is a result of the presence of monodisperse rigid segments. Upon cooling, the degree of crystallinity of the rigid segments in the PEEA's recovered completely to their starting values whereas the crystallinity of the PEUUA only partially recovered. The lower degree of crystallinity and lower recovery of crystallinity of the rigid segments in PEUUA's are indications that the crystallisation of the rigid segments is more difficult compared to the rigid segment in PEEA's. This is also confirmed by the higher undercooling values of the PEUUA's compared to PEEA's determined with DSC measurements.

The storage moduli at 25 °C of PEEA's and PEUUA's as a function of rigid segment content can be compared (Figure 8.12).
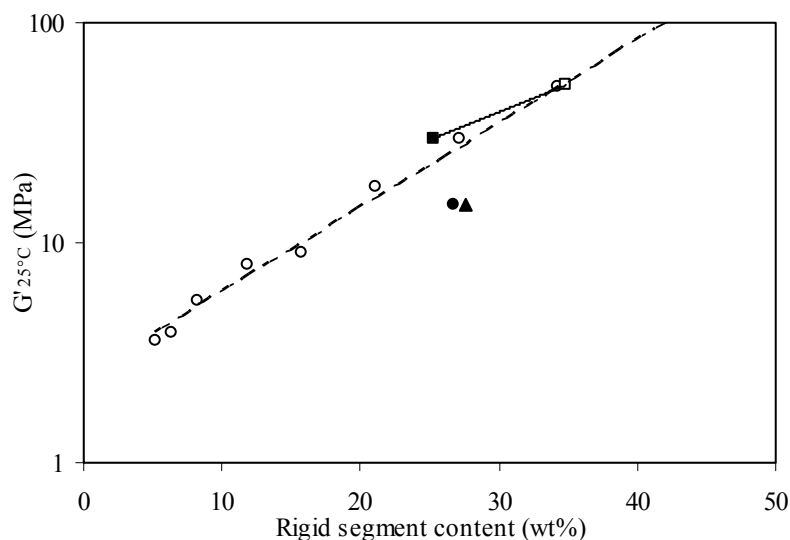
Figure 8.12: Storage modulus at 25 °C as a function of rigid segment content wt%: □, PTMO$_{1270}$-HDI-6A6-HDI; ■, PTMO$_{2000}$-HDI-6A6-HDI; ▲,PTMO$_{2209}$- MDI-6A6-MDI; ●, PTMO$_{1886}$-TDI-6A6-TDI; o, PTMO$_x$-T6A6T$^{[22]}$.

It is expected that the MDI, TDI or HDI residues in the rigid segment also crystallise and therefore the wt% rigid segment is based on DI-6A6-DI. It is assumed that the aspect ratio of the crystallites of PEEA's and PEUUA's are the same. The rubber moduli at 25 °C of the 2,4-TDI and MDI based polyurethanes are lower than for the PEEA's. This is a result of a lower degree of crystallinity. However, the two HDI based polyurethanes have a rubber modulus at room temperature that is comparable to the moduli of PEEA's indicating a high degree of crystallinity.

Conclusions

Polyether(bisurethane-bisurea-bisamide)s (PEUUA's) were made from PTMO endcapped with diisocyanate, with a low free diisocyanate content and uniform 6A6-diamine-diamide extender units. The diisocyanates (DI) used were HDI, MDI and 2,4-TDI. The concentration of the rigid segment (DI-6A6-DI) was about 25 wt%. The resulting polyurethanes were transparent, elastic materials and were colourless or slightly yellowish coloured.

The amide groups in the rigid segments of polyurethanes based on HDI, MDI and TDI are crystalline as determined by FTIR. The crystallinity of the amide groups were relatively high (70 - 80%), but were lower after cooling from the melt (40 - 60%). Infrared spectra showed

that the polyurethanes based on HDI also had crystalline urea groups. The rigid segments based on MDI and TDI showed next to crystalline amide segments a small amount of crystalline urethane groups.

The melting temperatures of the $PTMO_{2000}$-DI-6A6-DI were in the range of 165 - 225 °C. The melting temperatures of polymers based on HDI ($PTMO_x$-HDI-6A6-HDI) were high considering its aliphatic nature, indicating a good packing of the rigid segment. All the PTMO-DI-6A6-DI copolymers had very low T_g values (-72 to -63 °C). This suggests that in the PTMO phase only a very low content of rigid segment is dissolved.

-PTMO-DI-6A6-DI- polyurethanes had an almost temperature independent rubber modulus in the plateau region and a sharp melting transition due to the presence of monodisperse rigid segments. This also indicates that during polymerisation and processing the monodispersity of the rigid segments was maintained. The copolymers had low compression set values (12 - 25%) and fracture strains of 400 - 600%.

The Young's moduli and storage moduli were relatively high for polyurethanes with monodisperse rigid segments. The HDI based polyurethanes had higher moduli than the MDI and 2,4-TDI based polyurethanes. The HDI based polymer has a rigid segment that has a regular structure and no steric hindrance resulting in a high degree of crystallinity of the HDI-6A6-HDI segment.

Increasing the concentration of the HDI-6A6-HDI segment in the polymer from 25 to 35 wt% increased the storage modulus from 32 to 50 MPa and the tensile modulus from 72 to 140 MPa. The storage moduli at room temperature of polyurethanes having HDI-6A6-HDI rigid segments are approximately the same compared to $PTMO_x$-T6A6T, which have the same content of rigid segment and a degree of crystallinity of ~90%.

References

1. Holden, G., Legge, N.R., Quirk, R.,.Schroeder, H.E., *'Thermoplastic elastomers'*, Hanser Publisher, Second Ed. Munich (1996).
2. Szycher, M., *'Szycher's handbook of polyurethanes'*, Boca Raton: CRC Press LLC, (1999).
3. Schuur van der, J.M., *'Poly(propylene oxide) based segmented block copolymers'*, Ph.D. Thesis, University of Twente (2004).

4.   Martin, D.J., Meijs, G.F., Renwick, G.M., Guanatillake, P.A., McCarthy, S.J., *J. Appl. Polym. Sci.* **64**, 803 (1997).

5.   Allegrezza, A.E., Seymour, R.W., Ng, H.N., Cooper, S.L., *Polymer* **15**, 433-440 (1974).

6.   Eisenbach, C.D., Stadler, E., Enkelmann, V., *Macromol. Chem. Phys.* **196**, 833-856 (1995).

7.   Harrel, L.L., *Macromolecules* **2**, 607-612 (1969).

8.   Heijkants, R.G.J.C. *et al.*, *J. Mater. Sci. -Mater. in Medicine* **15**, 423-427 (2004).

9.   Versteegen, R.M., *'Well-defined Thermoplastic Elastomers'*, Ph.D. Thesis, University of Eindhoven (2003).

10. Lattimer, R.P., Williams, R.C., *J. Analyt. Appl. Pyrol.* **63**, 85-104 (2002).

11. Heijkants, R.G.J.C., *'Polyurethane scaffolds as meniscus reconstruction materials'*, Ph.D. Thesis, University of Groningen (2004).

12. Chapter 2 of this thesis

13. Heijkants, R.G.J.C. *et al.*, *Biomaterials* **26**, 4219-4228 (2005).

14. Luo, N., Wang, D.N., Ying, S.K., *Macromolecules* **30**, 4405-4409 (1997).

15. Mallakpour, S.E., Sheikholeslami, B., *Polymer International* **48**, 41-46 (1999).

16. Socrates, G., *'Infrared and Raman Characteristic Group Frequencies: Tables and Charts'*, Wiley, 3rd (2001).

17. Aneja, A., Wilkes, G.L., Rightor, E.G., *J. Polym. Sci. Part B-Polym. Phy.* **41**, 258-268 (2003).

18. Buist, J.N., Gudgeon, H.,.Johnson, P.C., *'Advances in polyurethane technology'*, MacLaren, London (1968).

19. Hirschinger, J., Miura, H., Gardner, K.H., English, A.D., *Macromolecules* **23**, 2153-2169 (1990).

20. Todoki, M., Kawaguchi, T., *Journal of Polymer Science, Polymer Physics Edition* **15**, 1067-1075 (1977).

21. Krijgsman, J., Husken, D., Gaymans, R.J., *Polymer* **44**, 7573-7588 (2003).

22. Chapter 3 of this thesis

23. Dreyfuss, P. *et al.*, *'Encyclopedia of Polymer Science and Engineering'*, New York (1989).

24. Schuur van der, J.M., Feijen, J., Gaymans, R.J., *Abstr. Papers ACS* **222**, U314 (2001).

25. Hertzberg, R.W., *'Deformation and fracture mechanics of engineering materials'*, John Wiley, 3rd edition New York (1989).

26. McCrum, N.G., Buckley, C.P.,.Bucknall, C.B., *'Principles of polymer engineering'*, Oxford university press, 2nd edition New York (2001).

27. Mark, J., Mandelkern, L. *'Physical properties of polymers'*. Cambridge University Press,(2004).

CHAPTER 9

SEGMENTED POLYURETHANES WITH MONODISPERSE RIGID SEGMENTS BASED ON HDI ENDCAPPED PTMO AND DIFFERENT CHAIN EXTENDERS

Abstract

Poly(tetramethylene oxide) based segmented polyurethanes were synthesised by chain extension of PTMO with a length of 1270 g·mol^{-1}, endcapped with 1,6-hexane diisocyanate (HDI), with a uniform chain extender. The starting prepolymer (HDI-PTMO$_{1270}$-HDI) had a low free diisocyanate content (<0.1 wt%). Three different types of uniform crystallisable chain extenders were used; diamine-diamide, diol-diamide and diol-diester. In this way segmented polyurethanes were made with monodisperse rigid segments with a concentration of about 32 wt%. The polyurethanes were tough, transparent and colourless to lightly yellow coloured.

The polyurethanes were characterised by DSC, DMTA and compression set. Polyurethanes with monodisperse rigid segments have a low glass transition temperature, an almost temperature independent rubbery plateau and a sharp melting temperature. The undercooling (T_m - T_c) was moderately low (36 - 54 °C).

The melting temperature of the polyurethanes depends on the type of chain extender used. Amide groups compared to ester groups and urea groups compared to urethane groups in the chain extender increased the melting temperature of the polymer. The melting temperature was also dependent on the structure of the chain extender and the number of methylene groups in the chain extender. The compression set of these polyurethanes was 14 - 42%. Polyurethanes with diamine-diamide chain extenders had the lowest compression set. The storage modulus at room temperature ($G'_{25°C}$) was dependent on the ease of packing of the rigid segments and only little on the number of H-bonding groups in the rigid segment. Interesting combination of properties had the polyurethane with a diol-diamide, namely; a melting temperature of 165 °C and a $G'_{25°C}$ of 56 MPa.

Introduction

Thermoplastic polyurethanes (TPU's) are linear copolymers that can be synthesised using a long-chain diol, a diisocyanate and a chain extender. Often used diisocyanates are 4,4'-diphenylmethane diisocyanate (MDI), toluene diisocyanate (TDI) and 1,6-hexane diisocyante (HDI). The rigid segments usually consist of alternating isocyanate residues and extender units. The content of rigid segment in polyurethanes controls the mechanical properties such as modulus and tensile strength. Increasing the rigid segment content in polyurethanes increases the modulus and tensile strength, but due to incomplete phase separation the T_g increases[1-3]. Chain extenders are low molecular weight reactants (60 - 400 g·mol^{-1}) and the structural regularity of the rigid segment has a strong effect on the physical properties of a TPU, like melting temperature, modulus, fracture strength and elasticity. The chain extender can be either hydroxyl or amine terminated.

The most important chain extenders for commercial TPU's are lineair diols such as ethylene glycol, 1,4-butanediol and hydroquinone bis(2-hydroxylethyl)ether[4]. Primary alcohols react vigorously with diisocyanates, forming a urethane linkage. Non linear diols are not suitable to use in TPU's due to the gelling effect and the decrease in crystallinity. The length of the diol chain extender has an influence on the polymer properties[5-9]. Polyurethanes based on PTMO and MDI (MDI-PTMO-MDI) and different length of diol chain extenders from 1,3-propanediol to 1,8-octanediol (C_3-C_8) have been studied[6,7]. The T_g of the polymers slightly decreases (5 °C) with increasing length of diol extender and this was attributed to a lower polarity and to additional flexibility of the rigid segments. The polymers with even number of methylene groups in the chain extenders had the highest modulus, probably due to a better packing of the rigid segment as was confirmed by X-ray diffraction measurements[7,10]. For polyethers, endcapped with TDI, and different length of diol extenders the same trend was observed[9].

Diamine chain extenders can also be used in polyurethanes and reaction of the diamine with an isocyanate leads to urea groups in the polymer chain. Polyurethanes with diamine extenders have high melting temperatures, sometimes too high to melt synthesise and melt process without degradation. Polyurethanes with different length of aliphatic diamine extenders (C_1 - C_8) have been studied[11-14]. The tensile strength and elongation at break

oscillated with the number of methylene groups in the diamine[11,13]. The polyurethanes with diamines having even number of methylene groups have a higher modulus, higher melting temperature, lower T_g's and had a higher stress at 300% strain compared to the polyurethanes with uneven chain extenders[11-15]. This effect was also attributed to a better phase separation of the rigid segments with even diamine chain extenders.

The rigid segments in commercially available TPU's consist of multiple diisocyanate and extender units and often have a random length distribution, which results in incomplete phase separation. The short rigid segments can dissolve in the polyether soft phase, thereby increasing the T_g of the polyether phase. Longer blocks can precipitate during the polymerisation and not participate in the further reaction, leading to low molecular weight polymers. Polyurethanes can also be made with monodisperse rigid segments. With monodisperse segments the polymers have a high and almost temperature independent rubber modulus and high tensile strength[2,3,16-19].

In some studies the extender unit contained amide groups[3,20,21]. Polyurethanes with amide groups are capable of forming additional hydrogen bonds. Van der Schuur studied polyurethanes based on poly(propylene oxide) (PPO) and TDI and uniform amide chain extenders[3]. He varied the length of the chain extender from diamine to diamine-diamide and diamine tetra-amide. The polyurethanes with a diamine-diamide extender had an interesting combination of properties; enhanced modulus, improved elasticity and good thermal stability. Upon increasing the length of the rigid segments and the number of H-bonding groups per rigid segment, the melting temperature, rubber modulus and crystallisation rate increased and the compression set decreased.

Interesting are TPU's with a high modulus combined with good low temperature properties. It is expected that polyurethanes with monodisperse rigid segments can have a high and temperature independent rubber modulus and also have good low temperature behaviour. Polyurethanes with hexamethylene diisocyanate (HDI) and uniform diamine-diamide extenders and as described in chapter 8 of this thesis, have a high modulus but also a very high melting temperature ($T_m > 200$ °C)[22]. It would be interesting to study the effect of the type of uniform extender on the thermal and dynamical properties of polyurethanes with monodisperse rigid segments.

Research aim

Polyurethanes with monodisperse rigid segments based on 1,6-hexamethylene diisocyanate endcapped PTMO (HDI-PTMO$_{1270}$-HDI) and uniform chain extenders are studied. HDI-PTMO$_{1270}$-HDI with a PTMO length of 1270 g·mol^{-1} and low free diisocyanate content (<0.1 wt%) is used as a prepolymer. This prepolymer was chain extended with three types of chain extenders, namely diamine-diamide, diol-diamide and diol-diester (Figure 9.1).
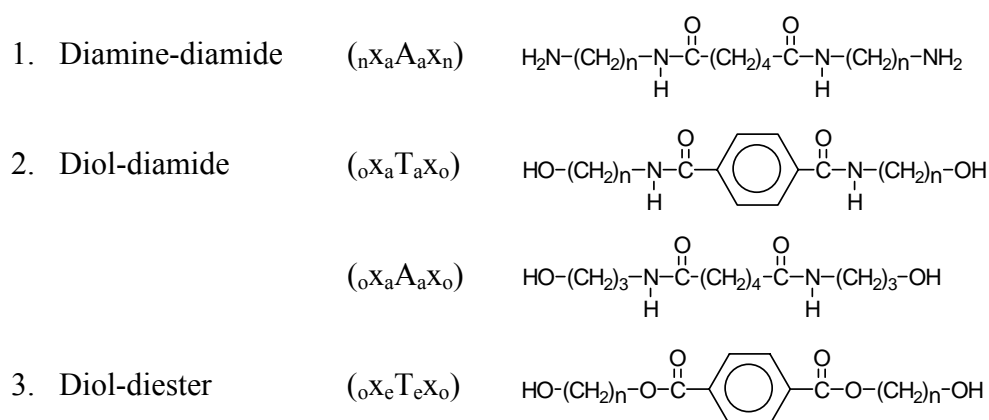
1. Diamine-diamide   ($_nx_aA_ax_n$) $H_2N-(CH_2)_n-N\underset{H}{-}\overset{\overset{O}{\|}}{C}-(CH_2)_4-\overset{\overset{O}{\|}}{C}-N\underset{H}{-}(CH_2)_n-NH_2$

2. Diol-diamide   ($_ox_aT_ax_o$) $HO-(CH_2)_n-N\underset{H}{-}\overset{\overset{O}{\|}}{C}-\bigcirc-\overset{\overset{O}{\|}}{C}-N\underset{H}{-}(CH_2)_n-OH$

                ($_ox_aA_ax_o$) $HO-(CH_2)_3-N\underset{H}{-}\overset{\overset{O}{\|}}{C}-(CH_2)_4-\overset{\overset{O}{\|}}{C}-N\underset{H}{-}(CH_2)_3-OH$

3. Diol-diester   ($_ox_eT_ex_o$) $HO\text{-}(CH_2)_n-O-\overset{\overset{O}{\|}}{C}-\bigcirc-\overset{\overset{O}{\|}}{C}-O-(CH_2)_n-OH$

Figure 9.1: Type of chain extenders: 1, diamine-diamide; 2, diol-diamide; 3, diol-diester with x = (CH$_2$)$_n$, A = adipic residue, T = terephthalic residue, a = amide, n = amine, e = ester and o = hydroxyl group.

The diamine-diamide is based on adipic ester (A) and aliphatic diamines. The diol-diamide is based on adipic and terephthalic esters (T) and amino alcohols. The diol-diester is based on terephthalic ester and aliphatic diols. The subscript letters correspond with the different groups in the chain extender.

The uniformity of the extenders is an important parameter as only uniform chain extenders can result in polyurethanes with monodisperse rigid segments. The influence of the structure of the uniform chain extender on the polymer properties is studied. The thermal properties of the polyurethanes are studied using DSC, the thermal mechanical behaviour with DMTA and the elastic behaviour with compression set measurements.

Experimental

Materials: 1,3-diaminopropane, 1,4-diaminobutane, 1,6-diaminohexane, 1,12-diaminododecane dimethyl adipate, anhydrous N,N-dimethyl acetamide (DMAc), 2-amino-ethanol, 3-amino-1-propanol, 1,3-propanediol, 1,4-butanediol, 1-6-hexanediol, zinc acetate and titanium butoxide were purchased from Aldrich and used as

received. Dimethyl terephthalate and 1,4-dioxane were purchased from Across. Butyl acetate was purchased from Fluka. These chemicals were used as received. Poly(tetramethylene oxide) endcapped with HDI (M_w 1270 g·mol^{-1}, LFH520), was a gift from Crompton Corporation. This prepolymer had a low free isocyanate content (<0.1 wt% diisocyanate). The prepolymer was dried in vacuo at 80 °C overnight before use.

Synthesis of diamine-diamide ($_nx_aA_ax_n$): The synthesis of 4A4 and 6A6-diamine-diamide was performed as described before[23]. The synthesis of 12A12-diamine-diamide was similar to the synthesis of 6A6-diamine-diamide. The synthesis of 3A3-diamine-diamide was similar to the synthesis of 4A4-diamine-diamide.

Synthesis of diol-diamide ($_ox_aA_ax_o$ and $_ox_aT_ax_o$): The diol-diamide extenders were all synthesised in the same way. The synthesis of 2T2-diol-diamide is given as an example. 1-Amino-2-ethanol (200 g, 3.3 mol) and DMT (105 g, 0.5 mol) were added to a round bottomed flask with a reflux condenser, calcium chloride tube, magnetically coupled stirrer and nitrogen inlet. The reaction was carried out for 16 h at 120 °C and during the reaction the product partially precipitated. To the cooled reaction mixture ethanol was added and the precipitate was collected by filtration with a glass filter (no.4). The product was three times washed with diethyl ether. ^{1}H-NMR (DMSO-*d*) 7.9 (s, 4H, terephthalate H), 4.67 (t, 2H, hydroxyl group), 3.50 (q, 4H, CH$_2$ amide *x*), 3.33 (q, 4H, CH$_2$ hydroxy *x*), 3.26 (s, 2H, amide)

Synthesis of diol-diester[24-26]:

3T3-diol-diester ($_o3_eT_e3_o$): 1,3-Propanediol (72.3 ml, 1.0 mol) and DMT (19.4 g, 0.1 mol) were added to a round bottomed flask with a reflux condenser, calcium chloride tube, magnetically coupled stirrer and nitrogen inlet. Zinc acetate (0.05 g) was added as a catalyst. The reaction was carried out for 5 h at 160 °C, distilling off the methanol using a Dean-Stark trap. The temperature was increased to 210 °C for 30 min to distil off the excess 1,3-propanediol. The product was cooled to 100 °C and added to 1 l water of 50 °C and the precipitate (the longer blocks) filtered over a no.3 glass filter. Upon further cooling to 7 °C, the $_o3_eT_e3_o$-diol-diester crystallised and was collected by filtration over a glass filter (no.4). The precipitate was recrystallised from water (100 °C, 20 g/l). ^{1}H-NMR (CDCl$_3$) δ 8.10 (s, 4H, terephthalate H), δ 4.52 (m, 4H, CH$_2$ hydroxy *x*), δ 3.81 (m, 4H, 2nd CH$_2$), δ 2.05 (m, 4H, CH$_2$ ester *x*), δ 1.84 (t, 2H, hydroxyl group).

4T4-diol-diester ($_o4_eT_e4_o$): 1,4-butanediol (355 ml, 3.95 mol) and DMT (39 g, 0.2 mol) were added to a round bottomed flask with a reflux condenser, calcium chloride tube, magnetically coupled stirrer and nitrogen inlet. Titanium butoxide (0.08 g) was added as a catalyst. The reaction was carried out for 5 h at 160 °C and methanol was distilled off using a Dean-Stark trap. The temperature was increased to 210 °C to distil off the excess 1,4-butanediol. To the cooled reaction mixture diethyl ether (3 l) was added and the formed precipitate collected by filtration over a glass filter (no.4). The product was heated in water (100 °C, 20 g/l) and filtered over a hot glass filter (100 °C) and the filtrate was cooled. The formed white needle shaped crystals were collected by filtration over a glass filter (no.4). ^{1}H-NMR (DMSO-*d*) 8.09 (s, 4H, terephthalate H), 4.45 (t, 2H, hydroxyl group), 4.32 (t, 4H, CH$_2$ ester *x*), 3.45 (t, 4H, CH$_2$ hydroxy *x*), 1.75 (m, 4H, 2nd CH$_2$ ester *x*), 1.55 (m, 4H, 2nd CH$_2$ hydroxy *x*).

6T6-diol-diester ($_o6_eT_e6_o$): 1,6-hexanediol (236 g, 2.0 mol) and DMT (39 g, 0.2 mol) were added to a round bottomed flask with a reflux condenser, calcium chloride tube, magnetically coupled stirrer and nitrogen inlet.

Titanium butoxide was used as a catalyst (0.08 g). The reaction was carried out for 5 h at 175 °C. After cooling, the precipitate was filtered over a glass filter (no.3) and washed twice with diethyl ether. The product was recrystallised from water (20 g/l). ^{1}H-NMR (DMSO-*d*) 8.09 (s, 4H, terephthalate H), 4.36 (t, 2H, hydroxyl group), 4.30 (t, 4H, CH_2 ester *x*), 3.41 (t, 4H, CH_2 hydroxy *x*), 1.70 (m, 4H, 2nd CH_2 ester *x*), 1.55 (m, 12H, 2nd - 4th CH_2 hydroxy *x*).

Copolymerisation: The polymerisation -$PTMO_{1270}$-HDI-$_n6_aA_a6_n$-HDI- is given as an example. A dried 250 ml stainless steel reactor with a nitrogen inlet and magnetically coupled stirrer was charged with HDI-$PTMO_{1270}$-HDI (30 g, 0.019 mol) and a solution of 6A6-diamine-diamide (6.39 g, 0.019 mol) in 100 ml anhydrous N,N-dimethylacetamide (DMAc). The stirred reaction mixture was heated to 140 °C and reacted for 5 h under nitrogen flow. Subsequently, the pressure was carefully reduced (P<20 mbar) to distil off the DMAc and then further reduced (P<0.3 mbar) for 60 min. After that, the reactor was slowly cooled, maintaining the low pressure. The synthesised copolymer was transparent, slightly yellowish and tough.

^{1}H-NMR: NMR spectra were recorded on a Bruker AC 300 spectrometer at 300 MHz. Deuterated trifluoro acid (TFA-*d*), dimethyl sulfoxide (DMSO-*d*) and chloroform (CDCl$_3$) were used as solvents.

Viscometry: The inherent viscosity was measured at a concentration of 0.1 g/dl in a mixture of phenol/1,1,2,2-tetrachloroethane (1:1 molar ratio) at 25 ºC using a capillary Ubbelohde type 1B.

Compression moulding: Test samples for DMTA and compression set measurements were made by compression moulding with the use of a 40 ton Lauffer 40 press. The TPU (2.1 g), cut in small pieces and dried overnight, was spread into a bar-shaped mould (8x1.8x0.2 cm) with press plates. The temperature of the press was set at 20 degrees above the melting temperature with a maximum of 230 °C. First, air was removed from the polymer in the mould by quickly pressurising the sample followed by depressurising. This procedure was repeated three times before actually pressing the samples at 10 MP (≈ 8.5 MPa) for 2 minutes. After this, the press was cooled and the test bars were removed from the mould.

DSC: DSC spectra were recorded on a Perkin Elmer DSC apparatus, equipped with a PE7700 computer and TAS-7 software. Dried compression moulded samples of 5 - 10 mg were heated to approximately 20 °C above the melting temperature and subsequently cooled, both at a rate of 20 °C/min. The maximum of the peak in de heating scan is taken as the melting temperature. The second heating scan was used to determine the melting peak and enthalpy of the sample. The first cooling curve was used to determine the crystallisation temperature, which was taken as the onset of crystallisation.

DMTA: The compression moulded test samples (70x9x2 mm) were dried in vacuum at 50 °C for 24 h before use. DMTA spectra were recorded with a Myrenne ATM3 torsion pendulum at a frequency of 1 Hz and 0.1% strain. The storage modulus G' and the loss modulus G'' were measured as a function of temperature. The samples were cooled to -100 °C and subsequently heated at a rate of 1 °C/min. The glass transition was determined as the peak in the loss modulus. The flow temperature (T_{flow}) is defined as the temperature where the

storage modulus reaches 1 MPa. The start of the rubbery plateau, the intercept of the tangents, is called the flex temperature (T_{flex}). The decrease in storage modulus of the rubbery plateau with increasing temperature is quantified by $\Delta G'$, which is calculated from:

$$\Delta G' = \frac{G'_{(Tflex)} - G'_{(Tflow-50°C)}}{G'_{25°C}} \times \frac{1}{\Delta T} \qquad (°C^{-1}) \qquad\qquad (Equation\ 9.1)$$

ΔT is described as the temperature range: (T_{flow}-50 °C) - T_{flex}.

Compression set: Samples for compression set were cut from injection moulded bars. The compression set was measured at room temperature according to ASTM 395 B standard. After 24 h the compression was released at room temperature. After relaxation for half an hour, the thickness of the samples was measured. The compression set was taken as the average of four measurements. The compression set is defined as:

$$Compression\ set = \frac{d_0 - d_2}{d_0 - d_1} \times 100\% \qquad (\%) \qquad\qquad (Equation\ 9.2)$$

With: d_0 = thickness before compression (mm)

d_1 = thickness during compression (mm)

d_2 = thickness after 0.5 h relaxation (mm)

Results and discussion

Polyurethanes with monodisperse rigid segments were synthesised from prepolymers based on poly(tetramethylene oxide) (PTMO) endcapped with 1,6-hexane diisocyanate (HDI) and a uniform chain extender (Figure 9.1). The polyurethanes have all about the same length of the rigid segment but differ in H-bonding groups and structural regularity (Figure 9.2). The effect of the chain extenders on the polymer properties was studied. Chain extenders with amine groups reacting with the isocyanate groups of the prepolymer will lead to urea bonds in the polyurethanes (Figure 9.2a). Reaction of the hydroxyl groups with the isocyanate groups results in urethane groups in the polymer (Figure 9.2b and c).
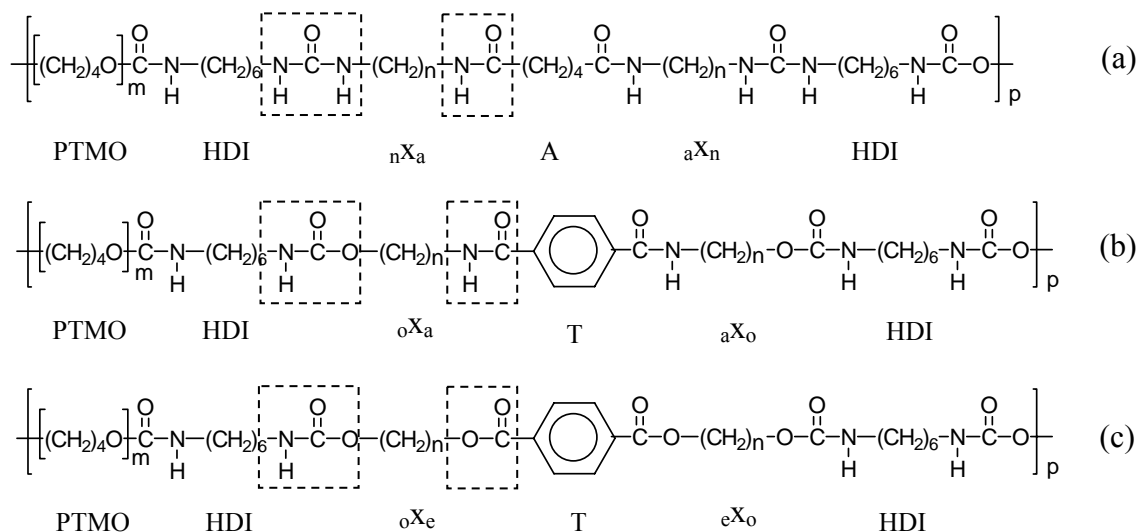
Figure 9.2: Polyurethanes based on PTMO endcapped with HDI and different chain extenders; (a), diamine-diamide, (b), diol-diamide; (c), diol-diester with x = (CH$_2$)$_n$, A = adipic residue, T = terephthalic residue, a = amide, e = ester, n = urea and o = urethane group.

The polymers with diamine-diamide chain extenders ($_n x_a A_a x_n$) have two amide, two urea and two urethane groups in the rigid segment. The length of $x = ((CH_2)_n)$ was varied from 3 to 12. The polymers with the diol-diamide chain extenders ($_o x_a A_a x_o$ and $_o x_a T_a x_o$), have two amide and four urethane groups in the rigid segment and the length of x was varied from 2 to 3. The polymers with the diol-diester chain extender ($_o x_e T_e x_o$), have four urethane groups in the rigid segment and x was varied from 3 to 6.

Chain extenders

Three types of uniform chain extenders were synthesised; diamine-diamide, diol-diamide and diol-diester (Figure 9.1). The diamine-diamide extenders were prepared from adipic ester and aliphatic diamines and the length of the diamine (x) was varied from 3 - 12 (Table 9.1). With increasing x, the molecular weight of the extender increased. After recrystallisation the purity of the compound was ranging from 97 - 100%.

Table 9.1: Properties of chain extenders: n = diamine, a = amide, o = hydroxyl and e = ester group.

Extender	M_w (g/mol)	Purity (%)	T_m (°C)	T_c (°C)	T_m-T_c (°C)	ΔH_m (J/g)
Diamine-diamide						
$_n3_aA_a3_n$	258	99	181	-	-	220[a] / -
$_n4_aA_a4_n$	286	98	180	153	27	330[a] / 42
$_n6_aA_a6_n$	342	98	183	162	21	290[a] / 33
$_n12_aA_a12_n$	510	100	164	149	15	210[a] / 36
Diol-diamide						
$_o2_aT_a2_o$	254	98	234	172	62	115
$_o3_aT_a3_o$	280	98	207	100	107	114
$_o3_aA_a3_o$	284	97	186	136	50	115
Diol-Diester						
$_o3_eT_e3_o$	282	99	91	42	49	130
$_o4_eT_e4_o$	310	99	81	25	56	129
$_o6_eT_e6_o$	366	97	82	40	42	132

[a] *melting enthalpy of the 1st heating run*

The diol-diamide chain extenders are prepared from amino-alcohols with dimethyl adipate or dimethyl terephthalate and have two amide groups and two hydroxyl endgroups. Recrystallisation of the diol-diamide compounds was not necessary as the amine groups compared to hydroxyl groups are more reactive with the ester groups.

The diol-diesters chain extenders had two terephthalate ester and two hydroxyl groups. Here, a terephthalate was used instead of adipate, to increase the melting temperatures of the segment. The length of the diol (*x*) was varied from 3 to 6.

The uniformity of the extenders is an important parameter as only uniform chain extenders can result in polyurethanes with monodisperse rigid segments. The purity of the chain extenders was estimated with ^{1}H-NMR[27]. To ensure the uniformity of the chain extenders the diamine-diamide and diol-diester chain extenders were recrystallised. The synthesised chain extenders all had a high purity.

DSC

The melting temperature of the chain extender depends on the number of amide groups and the flexibility of the extender. The flexibility of the chain extender was varied in two ways; the centre group was either a terephthalic (T) or an adipic group (A) and the number of

methylene groups (*x)* was changed from 3 - 12. Chain extenders with a terephthalic (T) compared to an adipic residue (A) had a 20 °C higher melting temperature ($_o3_aT_a3_o$ vs $_o3_aA_a3_o$). Increasing the number of methylene groups (*x*) only slightly decreases the melting temperature of the chain extender. The biggest influence on the melting temperature of the chain extenders is caused by the number of amide groups (a). The melting temperature of chain extenders having two amide groups compared to two ester groups (e) is 100 °C higher (diamine-diamide / diol-diamide vs diol-diester). The diamine-diamide extenders showed a second transition upon heating and cooling and this is probably caused by a crystalline transition as was reported before[28-31].

Upon cooling, the chain extender units crystallise. The undercooling ($T_m - T_c$) of the diamine-diamide extenders with even *x* values is remarkably low, indicating that crystallisation of these units is fast. For the diol-diamide and diol-diester extenders the undercooling is approximately 50 °C. The melting enthalpy for diol-diamide and diol-diester extenders is high but the melting enthalpy of the diamine-diamide extenders is low. For 3A3-diamine-diamide no crystallisation peak was observed.

Stability of the chain extenders

The diamine-diamide extenders have a very high melting enthalpy at the first heating run but the crystallisation enthalpy and melting enthalpy of the second heating run are low. This difference is probably due to degradation or transreactions that occur in the first heating run. The diamine-diamide extenders do not appear to be stable in their melts. The diol-diamide and diol-diester have a melting enthalpy in the first heating run that is comparable to the melting enthalpy in the second heating run and also the crystallisation enthalpy is similar. This suggests that the diol-diamide and diol-diesters are stable to temperatures well above their melting temperature.

Synthesis of polyurethane copolymers

Segmented polyurethanes were synthesised from a prepolymer based on $PTMO_{1270}$, endcapped with HDI (HDI-$PTMO_{1270}$-HDI), and a uniform chain extender. All polyurethanes were made with the same HDI-$PTMO_{1270}$-HDI prepolymer and only the chain extender was varied. The rigid segment of the polyurethanes is formed during the reaction and consists of the HDI residues from the prepolymer and the chain extender (HDI-chain extender-HDI) (Figure 9.2).

The prepolymer, extender and polymerisation set-up were dried overnight at 80 °C in vacuo. The prepolymer was weighed into the reactor, after which a solution of the chain extender in 100 ml DMAc was added. The polymerisation of these systems is fast and takes place at relatively low temperatures due to the highly reactive isocyanate functional groups. The reaction was carried out for five hours at 140 °C to ensure completion of the polymerisation reaction. The resulting polymers are non-sticky, transparent and colourless to lightly yellowish materials (Table 9.2).

Table 9.2: Thermal properties of polyurethanes with different chain extenders (PTMO$_{1270}$-HDI-extender-HDI).

	η_{inh}	RS[a]	H-groups[b]			T_m	T_c	T_m-T_c	ΔH_m	Colour
	(dl/g)	(%)	am	urea	ureth	(°C)	(°C)	(°C)	(J/g)	
Diamine-diamide										
-$_n3_aA_a3_n$-	1.6	31.9	2	2	2	222	143	79	5[c]	yellow
-$_n4_aA_a4_n$-	1.2	32.9	2	2	2	251	209	42	8[c]	yellow
-$_n6_aA_a6_n$-	1.4	34.8	2	2	2	231	176	55	8[c]	yellow
-$_n12_aA_a12_n$-	1.3	40	2	2	2	186	142	44	7[c]	yellow
Diol-diamide										
-$_o2_aT_a2_o$-	1.2	31.8	2	0	4	156	105	51	19	colourless
-$_o3_aT_a3_o$-	1.1	32.8	2	0	4	155	121	34	17	colourless
-$_o3_aA_a3_o$-	1.0	32.7	2	0	4	142	98	44	19	colourless
Diol-diester										
-$_o3_eT_e3_o$-	1.8	32.7	0	0	4	106	39	67	13	colourless
-$_o4_eT_e4_o$-	1.2	33.7	0	0	4	99	33	66	24	colourless
-$_o6_eT_e6_o$-	1.1	35.6	0	0	4	87	23	64	23	colourless

[a] RS = rigid segment content based on HDI-$_n6_aA_a6_n$-HDI, so including the HDI residue; [b] possible hydrogen bonded groups per rigid segment: amide, urea, urethane; [c] low due to degradation or transreactions that possibly occurred at first heating run of the polymer

The polyurethanes based on chain extenders with hydroxyl groups (diol-diamide and diol-diester) were all transparent and colourless. The inherent viscosity of the polyurethanes after polymerisation varied from 1.0 to 1.8 dl/g. These values are moderate compared to poly(ether-ester-amides) from chapter 3 or 5. The type of extender has no effect on the inherent viscosities.

The wt% of rigid segment in the copolymers is based on the chain extender and the isocyanate residues and varies from 32 to 40 wt%. This difference is mainly due to the

varying length of *x* in the chain extenders. Depending on the type of extender, the rigid segments have different groups that can form H-bonds. The H-bonding groups in the segments are amide, urea and urethane (Figure 9.2 and Table 9.2). The H-bonds have a strong influence on the melting temperature of the polymers. Whether they form H-bonds also depends on the structural regularity of the extender.

Processing of the polyurethanes

Polyurethanes are known to be unstable at high temperatures. Processing these polymers at high temperature for a long time leads to polymer samples with a yellow colour and the polymer will lose its transparency. Especially the polyurethanes with diamine-diamide extenders had to be processed at high temperatures and are therefore slightly yellow coloured. To measure possible degradation the inherent viscosity of the polyurethanes was measured before and after compression moulding of the materials. The polyurethanes with diol-diamide and diol-diesters were processed at temperatures below 200 °C and their inherent viscosity was unchanged, implying that degradation did not take place. The polyurethanes with diamine-diamide have melting temperatures in the range of 186 - 251 °C and were compression moulded at 230 °C for 1 min. The inherent viscosity of the compression moulded samples of $PTMO_{1270}$-HDI-$_n3_aA_a3_n$-HDI and $PTMO_{1270}$-HDI-$_n4_aA_a4_n$-HDI increased to high values of 3.7 and 4.0 dl/g respectively. These samples were difficult to dissolve and showed swelling of the polymer samples. These very high inherent viscosities after pressing at 230 °C are probably due to some network formation during processing at 230 °C. Higher processing temperatures (>230 °C) were not possible due to a strong decrease of inherent viscosity. For example, $PTMO_{1270}$-HDI-$_n3_aA_a3_n$-HDI compression moulded at 240 °C (1 min) was white coloured and the inherent viscosity decreased from 1.6 to 0.7 dl/g. The degradation of the polyurethanes is due to the instability of the urea or urethane group at higher temperatures[4,32]. The inherent viscosity first seems to increase due to some network forming in the polymers followed by a decrease in inherent viscosity due to degradation. The degradation in these polyurethanes is not specific due to the type of isocyanate used as a similar decrease in inherent viscosity was observed for MDI based polyurethanes and diamine-diamide extenders[22].

DSC

The thermal properties of compression moulded polymer samples were studied using DSC. In the heating cycle a peak was observed from the melting of the rigid segment. The melting

temperature of the copolymers depends on the type and number of H-bonding groups and flexibility and structural regularity of the rigid segments. As the concentration of rigid segment in the copolymers is approximately the same for these series, the melting temperature is only influenced by the structure of the rigid segment. The polyurethanes with rigid segments based on diamine-diamide chain extenders have two amide, two urea and two urethane groups and had melting temperatures of 190 to 250 °C. The polymers with diamine-diamide also had a second endotherm and exothermic transition as was also observed for the extender units. This is probably a crystalline transition as is more often observed for (poly)amides[28-31]. Polymers with diamine-diamides extenders have a lower melting temperature of the polymer with uneven x compared to even x. This can be a result of processing the materials. Compression moulded samples used for the DSC were processed at high temperatures were degradation takes places but still below the melting temperature of the polymer.

The polyurethanes with diol-diamide extenders have two amide and four urethane groups in the rigid segments and have melting temperatures of approximately 155 °C. Changing the urea to urethane groups ($_n3_aA_a3_n$ vs $_o3_aA_a3_o$) decreased the melting temperature of the copolymers by 80 °C. The polyurethanes with diol-diester extenders have only four urethane groups and have melting temperatures of about 100 °C. Leaving out the two amide groups in the rigid segments ($_o3_aT_a3_o$ vs $_o3_eT_e3_o$) lowered the melting temperature of the polymer by about 50 °C. Using a terephthalic instead of an adipic residue in the rigid segment ($_o3_aT_a3_o$ vs $_o3_aA_a3_o$) increased the melting temperature of the polyurethane by 13 °C. Increasing the length of (even) x in the extender from 4 to 12 ($_n4_aA_a4_n$ vs $_n12_aA_a12_n$) decreased the melting temperature of the polymer by 65 °C. Changing x from even to uneven has little effect on the melting temperature of the polymers with diol-diamide and diol-diester extenders. The melting enthalpy of the rigid segments in the polymers were determined in the second heating run and varied from 5 to 24 J/g and were particularly low for the diamide-diamide extenders. This can be due to degradation or transreactions of the polymer with diamine-diamide extenders occurring in the first heating run.

Upon cooling, the monodisperse rigid segments in the polymer crystallise. The crystallisation of the rigid segment is 34 to 79 °C below the melting temperature of the polymer. The rigid segments based on diol-diester had higher undercooling values than the rigid segments with diol-diamide and diamine-diamide extenders. More hydrogen bonding groups in the rigid

segment seem to increase the crystallisation rate. It is not yet clear whether the value of *x* has an effect on the crystallisation rate of the polymer.

DMTA

Thermal mechanical properties of the copolymers were determined by means of DMTA. The DMTA analysis was performed on compression moulded samples processed at 20 °C above their melting temperature but never above 230 °C. At temperatures higher than 230 °C serious degradation during melt processing is observed. What the effect is of compression moulding at or below the melting temperatures of these polyurethanes, as is the case for the polymers with $_n4_aA_a4_n$ and $_n6_aA_a6_n$, is as yet not clear. The storage and loss modulus of the polyurethanes with different chain extenders have been plotted as a function of temperature (Figure 9.3, 9.5 and 9.7) and the results are summarised in Table 9.3.

Table 9.3: DMA properties of polyurethanes with different chain extenders (PTMO$_{1270}$-HDI-extender-HDI).

Extender	RS[a]	η_{inh}	NH groups[b]			T_g	$G'_{25°C}$	tan δ 25 °C	T_{flow}	$\Delta G'$ *10^{-3}	CS
	(%)	(dl/g)	am.	urea	ureth	(°C)	(MPa)	(-)	(°C)	(°C^{-1})	(%)
Diamine-diamide											
$_n3_aA_a3_n$-	31.9	1.6	2	2	2	-68	22	0.05	175	8	18
$_n4_aA_a4_n$-	32.9	1.2	2	2	2	-67	49	0.05	245	4	21
$_n6_aA_a6_n$-	34.8	1.4	2	2	2	-67	49	0.04	225	5	25
$_n12_aA_a12_n$-	40.0	1.3	2	2	2	-65	47	0.05	195	10	14
Diol-diamide											
$_o2_aT_a2_o$-	31.7	1.2	2	0	4	-67	44	0.04	155	7	42
$_o3_aT_a3_o$-	32.8	1.1	2	0	4	-65	56	0.03	160	7	37
$_o3_aA_a3_o$-	32.7	1.0	2	0	4	-66	34	0.03	140	8	26
Diol-diester											
$_o3_eT_e3_o$-	32.7	1.8	0	0	4	-65	39	0.05	100	2	26
$_o4_eT_e4_o$-	33.7	1.2	0	0	4	-66	31	0.05	95	3	26
$_o6_eT_e6_o$-	35.6	1.1	0	0	4	-67	23	0.05	80	3	30

[a] *RS = rigid segment content based on HDI-extender-HDI, so including the HDI residues;* [b] *possible hydrogen bonded groups per rigid segment: amide, urea, urethane*

TPU's with diamine-diamide chain extenders

It has to be realised that the polyurethanes are thermally unstable above 180 °C and the DMTA results may be influenced by degradation of the polymer. Polyurethanes with

diamine-diamides extenders have a low T_g, a storage modulus that is almost temperature independent and a relatively sharp flow temperature (melting) (Figure 9.3).
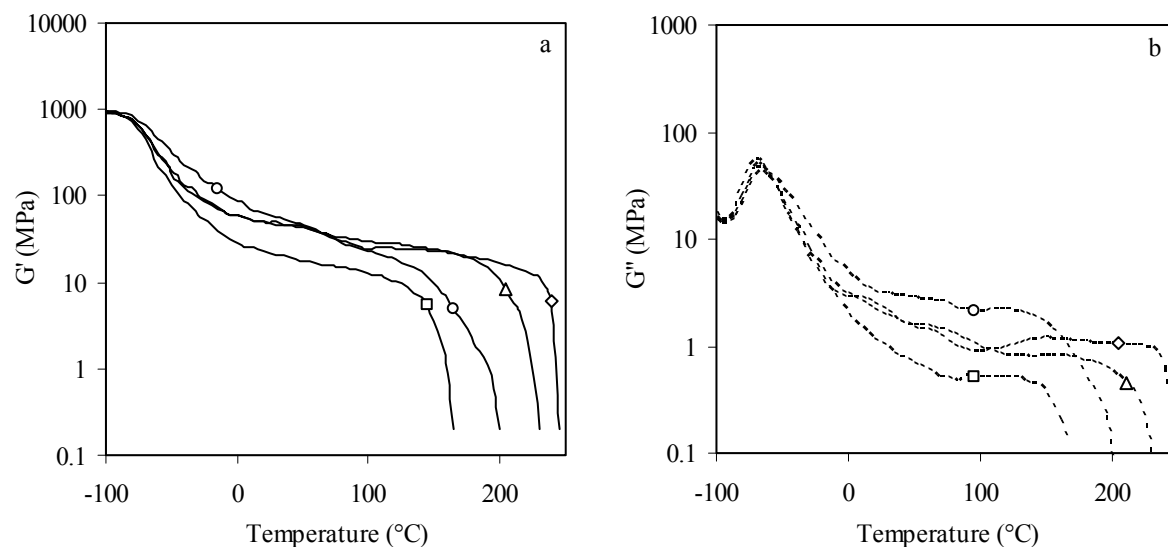

Figure 9.3: a) Storage and b) loss modulus of segmented polyurethanes with diamine-diamide chain extenders: □, PTMO$_{1270}$-HDI-$_n$3$_a$A$_a$3$_n$-HDI; ◊, PTMO$_{1270}$-HDI-$_n$4$_a$A$_a$4$_n$-HDI; Δ, PTMO$_{1270}$-HDI-$_n$6$_a$A$_a$6$_n$-HDI; o, PTMO$_{1270}$-HDI-$_n$12$_a$A$_a$12$_n$-HDI..

The glass transition temperature of this series of polymers is low (-68 °C) indicating good phase separation. The T_g of PTMO$_{1270}$-HDI-$_n$12$_a$A$_a$12$_n$-HDI is somewhat broader than the T_g of the other polymers. The storage moduli at 25 °C for the polymers with an even number of *x* are approximately 50 MPa, which is higher than the modulus of the polyurethane with a chain extender with *x* is 3, which was 22 MPa. The high storage modulus obtained for the polymers with the even diamine-diamide extenders is probably a result of a high degree of crystallinity of the rigid segment. The tan δ (G'/G") is for all these polyurethanes low (0.05) suggesting a low mechanical damping behaviour. These polymers have an almost temperature independent storage modulus (low ΔG' value) from room temperature to about the flow temperature. This behaviour is typical for segmented block copolymers with monodisperse rigid segments. However, the polymer with *x* is 12 has a modulus that is more temperature dependent and has a higher ΔG' value. This effect may be explained by possible folding of the long -(CH$_2$)$_{12}$- units. In polyamides folding of the chain in the crystallite surface readily takes place if the methylene length is minimal 6 units[33]. Folding of the diamine means that the crystallite has variations in its thickness.

The flow temperature of the polyurethanes decreases with increasing even x values and corresponds reasonable well with melting temperatures measured by DSC (Table 9.2). This decrease is a result of the more aliphatic structure for longer chain extenders. The flow temperature of PTMO$_{1270}$-HDI-$_n3_aA_a3_n$-HDI (175 °C) does not coincide with the melting temperature measured with DSC in the second heating run (222 °C) (Table 9.2). However, in the first heating run of the polymer an extra melting/crystallisation peak was observed at about 175 °C. In the second heating run only a small melting peak at 222 °C was present. This indicates that for fast cooled samples the crystallisation of the rigid segments was not complete which may lead to a low flow temperature and a low modulus at room temperature. Probably, the processing temperature to prepare the DMTA samples was not high enough for this polymer to properly melt the rigid segments in the polymer. Processing temperatures of 235 °C have been tried for compression moulding but at this temperature the polymer sample degraded.

Rigid segments from diamine-diamide extenders have two amide, two urea and two urethane groups. The packing of rigid segments (H-bonding) is dependent on whether x has an even or uneven number of methylene groups in the x chains (Figure 9.4).
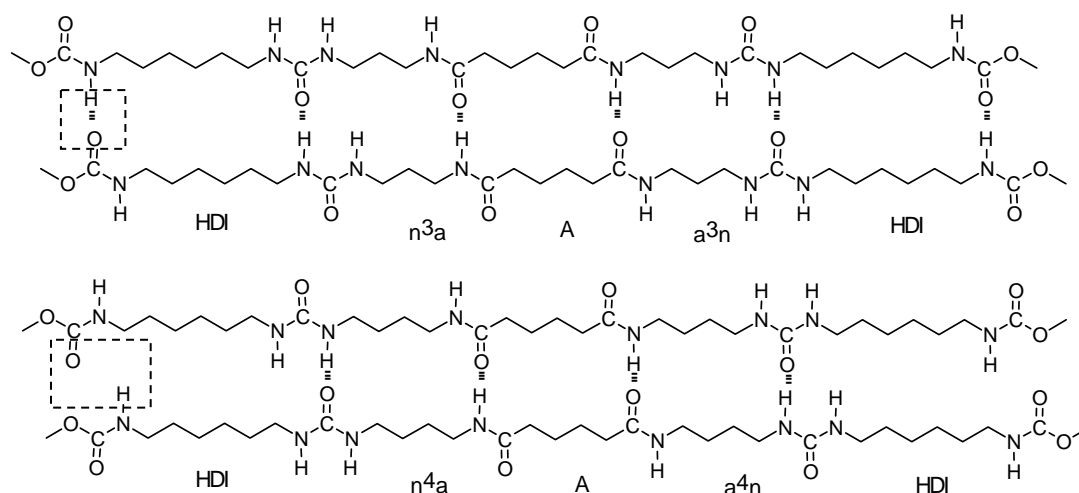

Figure 9.4: Packing of the rigid segment with uneven and even diamine-diamide chain extenders.

With x is uneven (HDI-$_n3_aA_a3_n$-HDI) the segment has six possible hydrogen bonds, while with x is even (HDI-$_n4_aA_a4_n$-HDI, HDI-$_n6_aA_a6_n$-HDI and HDI-$_n12_aA_a12_n$-HDI) only four hydrogen bonds seems to be possible. The planar extended structure of the rigid segment with even x shows that either the urethane or the amide groups cannot form H-bonds. According to

FTIR measurements, the amide groups in $_n6_aA_a6_n$ rigid segments are highly crystalline[22]. Thus it would be expected that in rigid segments with even x the urethane groups have difficulty to form H-bonding in the crystal. However, the polyurethanes with x is even (4, 6, 12) have a high rubber modulus at room temperature, despite the non optimal H-bonding. Based on the packings of the rigid segments (Figure 9.4) it was expected that the rigid segments in the polyurethanes with uneven x chains in the chain extender would have a higher degree of crystallinity than rigid segments with even number of methylene groups. Surprisingly, the polymer with x is uneven (3) packs well but has a low modulus. We had difficulty in processing this polymer and the inherent viscosity decreased during processing. This may have played a role in the determination of the properties.

TPU's with diol-diamide extenders

The DMTA properties of polyurethanes with three diol-diamide extenders have been studied, namely; $_o2_aT_a2_o$, $_o3_aT_a3_o$ and $_o3_aA_a3_o$ (Figure 9.5). The polymers were transparent, colourless and tough. These polymers could be easily melt processed by injection moulding. The inherent viscosity of the polymers did not decrease during injection moulding and therefore degradation did not occur.
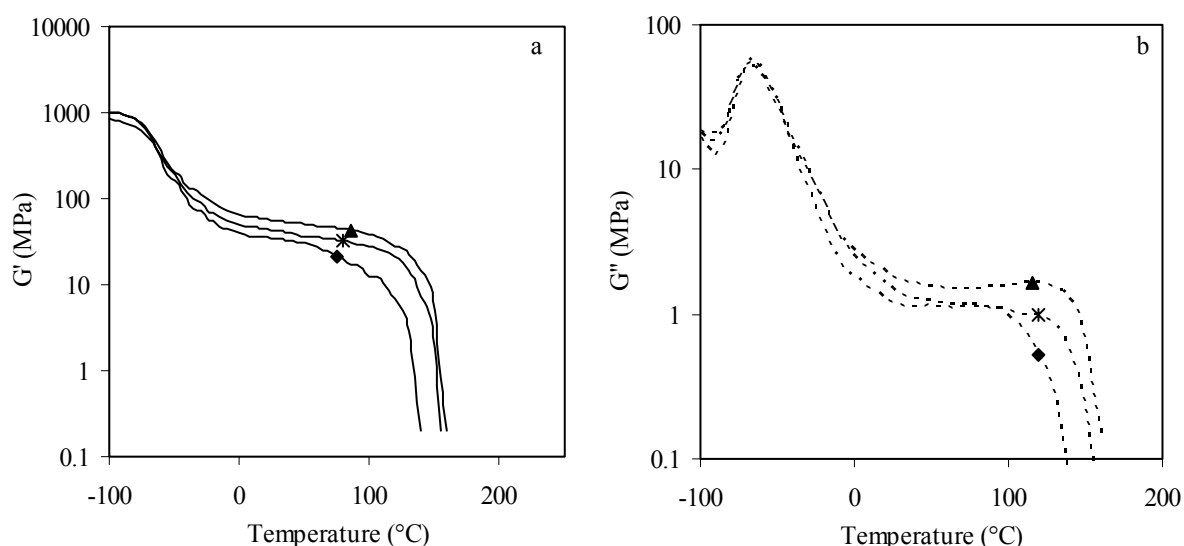

*Figure 9.5: a) Storage and b) loss modulus of segmented polyurethanes with diol-diamide extenders: *, PTMO$_{1270}$-HDI-$_o2_aT_a2_o$-HDI; ▲, PTMO$_{1270}$-HDI-$_o3_aT_a3_o$-HDI; ♦, PTMO$_{1270}$-HDI-$_o3_aA_a3_o$-HDI.*

TPU's with diol-diamide extenders have two amide and four urethane groups in the rigid segment. The melting temperatures of these polyurethanes are appreciable lower than that of

corresponding diamine-diamide. Thus changing the two urea groups for two urethane groups lowers the melting temperature (Table 9.3).

The T_g of the polyurethanes with diol-diamide extenders is low (-68 °C) indicating good phase separation. The storage moduli at 25 °C for the polymers with 2T2, 3T3 and 3A3-diol-diamide are 44, 56 and 34 MPa respectively. The rubber moduli of the polymers with 2T2 and 3T3-diol-diamide are high and thus the degree of crystallinity must be high for these polymers. The rubber modulus of $PTMO_{1270}$-HDI-$_o3_aA_a3_o$-HDI is somewhat lower. Having a terephthalic instead of an adipic group in the extender ($_o3_aT_a3_o$ vs $_o3_aA_a3_o$) increases the modulus of the polymer. These polyurethanes have an almost temperature independent rubber modulus due to the presence of monodisperse rigid segments. The flow temperatures of the polymers were 140 - 160 °C, which is close to the melting temperatures as measured by DSC. A terephthalic compared to the adipic group in the rigid segments ($_o3_aT_a3_o$ vs $_o3_aA_a3_o$) increases the flow temperature of the polymer with 20 °C. The polymer with x is 2 compared to x is 3 has a somewhat lower modulus and lower melting and flow temperature. This might be due to the even/uneven effect of x and/or that with ethylene extenders the crystallisation is often not fast and complete (PET vs PBT). The planar extended rigid segment packing of diol-diamide with even x shows that hydrogen bonds are possible for the four urethanes groups but not for the two amide groups (Figure 9.6). The packing of the rigid segment with the uneven x in the chain extender shows the possibility of H-bonding in the four urethane groups as well as in the two amide groups.
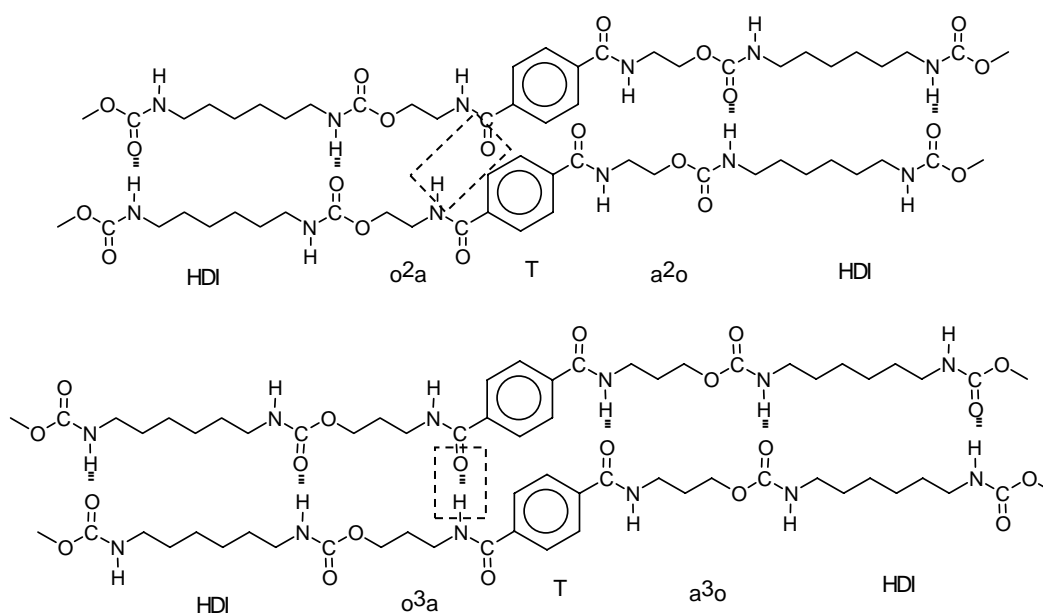

Figure 9.6: Packing of rigid segment with uneven and even diol-diamide chain extenders.

The modulus at room temperature of the polyurethanes with 3A3-diol-diamide ($-_o3_aA_a3_o-$) is higher than for the 3A3-diamine-diamide ($-_n3_aA_a3_n-$), but this might have been due to the poor processability of the $PTMO_{1270}$-HDI-$_n3_aA_a3_n$-HDI copolymer.

TPU's with diol-diester chain extenders

The extenders with diol-diester groups have four urethane groups in the rigid segment. For this series of polymers the T_g's are approximately -66 °C (Figure 9.7)
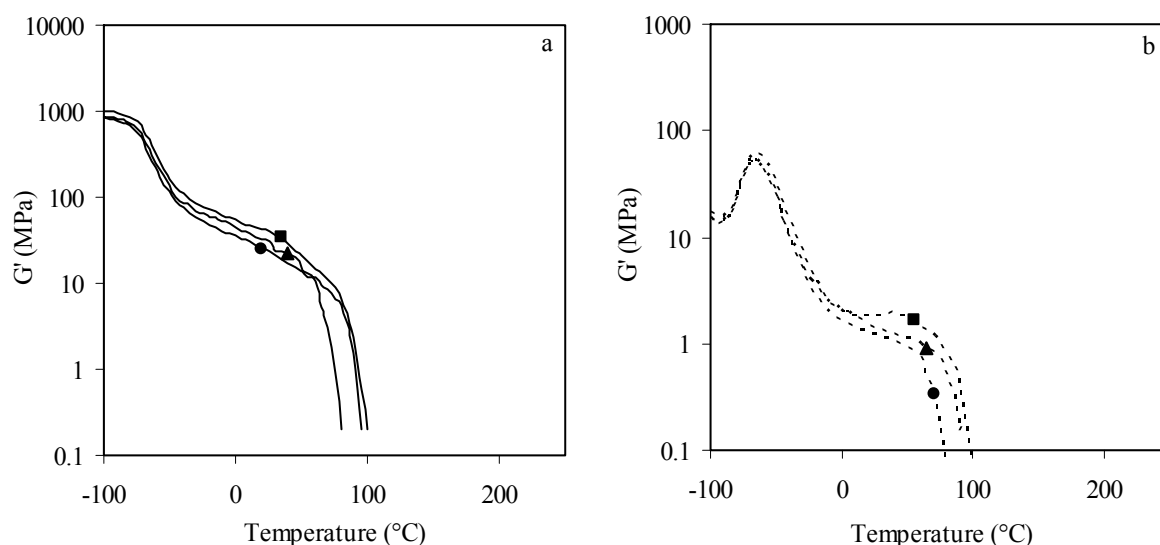

Figure 9.7: a) Storage and b) loss modulus of segmented polyurethanes with diol-diester extenders: ■, $PTMO_{1270}$-HDI-$_o3_eT_e3_o$-HDI; ▲, $PTMO_{1270}$-HDI-$_o4_eT_e4_o$-HDI; ●, $PTMO_{1270}$-HDI-$_o6_eT_e6_o$-HDI.

The low glass transition temperature indicates a good phase separation for the copolymers with diol-diester extenders. The rubber modulus in the plateau region is not temperature independent although the diol-diester units were uniform. This is probably due to the low melting temperature creating only a small temperature window (25 - 90 °C) to form a rubbery plateau. The flow temperature of these polyurethanes decreases with increasing length of *x* in the chain extender, as was also observed by DSC measurements (Table 9.2). This effect of length *x* was also observed for the diamine-diamide series and is due to a more flexible structure. The rubber modulus at 25 °C for the polyurethane with the uneven *x* in the diol-diester extender is relatively high (39 MPa) but somewhat lower than for uneven *x* is 3 with the diol-diamide. A diester instead of a diamide in the chain extender lowers the melting temperature and also the modulus of the polymer. The polyurethanes with even *x* in the diol-diester extender compared to the uneven *x*, have lower moduli and lower melting

temperatures. The rigid segments with uneven x seem to pack better than rigid segments with even x (Figure 9.8). The packing of the rigid segments with even ($x = 4$ and 6) diol-diester extenders is sterically hindered by the terephthalate ring.
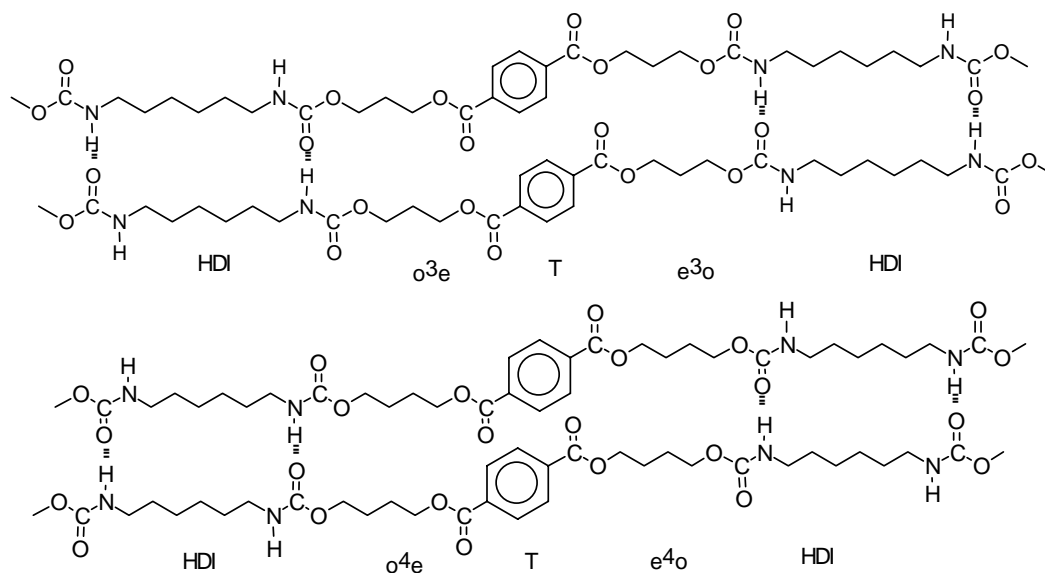

Figure 9.8: Packing of rigid segment with uneven and even diol-diester chain extenders.

The overall picture of the DMTA results is that the polyether phase T_g is in all these systems low. The flow (melting) temperature of the polymers increases from four urethane < four urethane + two amide < two urethane + two urea + two amide groups in the rigid segment. A terephthalic group compared to an adipic group in the rigid segment gives a 20 °C higher melting temperature of the polymer. The uneven length x compared to an even length in the rigid segments seem to give a higher melting temperature of the polymer too, though this picture is not completely clear. The moduli at room temperature are higher if x is uneven and terephthalic residues instead of adipic residues are used. The presence of amide groups (compare $-_o3_eT_e3_o-$ and $-_o3_nT_n3o-$) enhances the moduli. The length of x does not seem to have a strong effect on the moduli.

Compression set

A standard measurement to test the elastic behaviour of a polymer is a compression test. A lower compression set value means a more elastic behaviour of the polymer. In Chapter 3 and Chapter 5 it was shown that the compression set values for copolymers with uniform amide segments are low. The compression set of these polyurethanes with monodisperse rigid

segments are between 18 and 42% (Table 9.3). The polyurethanes based on diamine-diamide chain extenders have a somewhat lower compression set than the polyurethanes based on diol-diamide or diol-diester chain extenders. The length of x in the diamine-diamide extenders does not seem to have a clear effect.

Conclusions

Polyurethanes with monodisperse rigid segments were synthesised from prepolymers based on poly(tetramethylene oxide) (PTMO) with a length of 1270 g·mol^{-1}, endcapped with 1,6-hexane diisocyanate (HDI), and a uniform chain extender. Three types of chain extenders, diamine-diamide ($-_ax_nA_nx_a-$), diol-diamide ($-_ox_nA_nx_o-$ and $-_ox_nT_nx_o-$) and diol-diester ($-_ox_eT_ex_o-$), were used for the chain extension of the prepolymer resulting in polyurethanes with monodisperse rigid segments. The concentration of the rigid segment (HDI-chain extender-HDI) in the polymers was about 32 wt%. The resulting polyurethanes were elastic, transparent and colourless to slightly yellow materials. The crystallisation was studied with DSC and the thermal mechanical behaviour was evaluated with DMTA and the elastic behaviour with CS.

These polyurethanes with monodisperse rigid segments had a low T_g ($\sim$ -67 °C), indicating good phase separation. The rubber modulus of the polymers was almost temperature independent and the melting transitions were sharp due to the presence of monodisperse rigid segments. This indicates that during polymerisation and processing the monodispersity of the rigid segments was maintained.

Using diamine-diamide as chain extenders leads to polyurethanes with 2 urea, 2 urethane and 2 amide groups in the rigid segment. The resulting polyurethanes had high melting temperatures (186 - 251 °C) high moduli at room temperature and low compression set values. Increasing the length x of the chain extender resulted in polymers with a lower melting temperature. Using a chain extender with uneven x was expected to have a better packing of the rigid segment but for this polymer the processing was difficult.

Using diol-diamide chain extenders gives polyurethanes with four urethane and two amide groups in each rigid segment. The polymers had melting temperatures of 140 - 160 °C. The

polyurethane with uneven x in the chain extender had a higher modulus compared to the polymer with even x due to a better packing of the rigid segment. Incorporating a terephthalic instead of an adipic group increased the rubber modulus and T_m of the polymer. The CS-values of the polymers were moderately high. The polyurethane with monodisperse HDI-$_o3_aT_a3_o$-HDI rigid segment had an interesting combination of properties: a transparent colourless material with a melting temperature of 165 °C, a storage modulus at room temperature of 56 MPa and the material can be easily melt processed.

Polyurethanes with diol-diester chain extenders have four urethane groups in the rigid segment. The resulting polymers have low melting temperatures (80 - 100 °C) due to the low number of hydrogen bonding possibilities. The rigid segment packing was better for polyurethanes with uneven x and as a result the rubber modulus at room temperature was higher compared to polyurethanes with even x in the extender.

References

1. Garrett, J.T., Xu, R., Cho, J., Runt, J., *Polymer* **44**, 2711-2719 (2003).

2. Heijkants, R.G.J.C. *et al.*, *Biomaterials* **26**, 4219-4228 (2005).

3. Schuur van der, J.M., *'Poly(propylene oxide) based segmented block copolymers'*, Ph.D. Thesis, University of Twente (2004).

4. Holden, G., Legge, N.R., Quirk, R.,.Schroeder, H.E., *'Thermoplastic elastomers'*, Hanser Publisher, Second Ed. Munich (1996).

5. Born, L., Hespe, H., Crone, J., *Colloid Polym. Sci.* **260**, 819 (1982).

6. Bae, J.Y., Chung, J., An, J.H., Shin, D.H., *J. Mat. Sci.* **34**, 2523 (1999).

7. Blackwell, J., Nagarajan, M.R., Hoitink, T.B., *Polymer* **23**, 950-956 (1982).

8. Hong, J.L., Lillya, C.P., Chien, J.C.W., *Polymer* **33**, 4347-4351 (1992).

9. Pandya, M.V., Deshpande, D.D., Hundiwale, D.G., *J. Appl. Polym. Sci.* **35**, 1803-1815 (1988).

10. Blackwell, J., Nagarajan, M.R., Hoitink, T.B., *Polymer* **22**, 1534-1539 (1981).

11. Bonart, R., Morbitzer, L., Rinke, H., *Kolloid-Z. Z. Polymere* **240**, 807-819 (1970).

12. Gisselfalt, K., Helgee, B., *Macromol. Mat. Engin.* **288**, 265-271 (2003).

13. Heikens, D., Meijers, P., Reth von P.H., *Polymer* **9**, 15 (1968).

14. Takahara, A., Tashita, J.i., Kajiyama, T., Takayanagi, M., MacKnight, W.J., *Polymer* **26**, 978-986 (1985).

15. Takahara, A., Tashita, J.i., Kajiyama, T., Takayanagi, M., MacKnight, W.J., *Polymer* **26**, 987-996 (1985).

16. Allegrezza, A.E., Seymour, R.W., Ng, H.N., Cooper, S.L., *Polymer* **15**, 433-440 (1974).

17. Harrel, L.L., *Macromolecules* **2**, 607-612 (1969).

18. Miller, A.M., Cooper, S.L., *Macromolecules* **18**, 32 (1985).

19. Versteegen, R.M., *'Well-defined Thermoplastic Elastomers'*, Ph.D. Thesis, University of Eindhoven (2003).

20. Cohn, D., Aronhime, M., Stern, T., *Polymer* **41**, 6519-6526 (2000).

21. Yui, N., Nojima, K., Sanui, K., Ogata, N., *Polymer journal* **17**, 969-975 (1985).

22. Chapter 8 of this thesis

23. Chapter 2 of this thesis

24. Sivaram, S., Upadhyay, V.K., Bhardwardwaj, I.S., *Polymer Bulletin* **5**, 159-166 (1981).

25. Tomita, K., *Polymer* **17**, 221-224 (1976).

26. Kim, J.H., Prak, J.H., Kwon, C.H., Lyoo, W.S., *J. Polym. Sci. Part A-Polym. Chem.* **40**, 2435-2441 (2002).

27. Krijgsman, J., Husken, D., Gaymans, R.J., *Polymer* **44**, 7043-7053 (2003).

28. Stapert, H.R., *'Environmentally degradable polyesters, poly(ester-amide)s and poly(ester-urethane)s'*, Ph.D. Thesis, University of Twente (1998).

29. Hirschinger, J., Miura, H., Gardner, K.H., English, A.D., *Macromolecules* **23**, 2153-2169 (1990).

30. Todoki, M., Kawaguchi, T., *Journal of Polymer Science, Polymer Physics Edition* **15**, 1067-1075 (1977).

31. Krijgsman, J., Husken, D., Gaymans, R.J., *Polymer* **44**, 7573-7588 (2003).

32. Szycher, M., *'Szycher's handbook of polyurethanes'*, Boca Raton: CRC Press LLC, (1999).

33. Cooper, S.J., Atkins, E.D.T., Hill, M.J., *Macromolecules* **31**, 5032-5042 (1998).

SUMMARY

Poly(tetramethylene oxide) (PTMO) based segmented block copolymers containing alternating amorphous flexible segments (PTMO) and crystallisable rigid segments are thermoplastic elastomers (TPE's). The flexible segments form the continuous amorphous phase with a low T_g and give the material low temperature flexibility. The rigid segments can crystallise and form lamellae in the low T_g phase, acting as thermo-reversible physical crosslinks, giving the material dimensional stability and solvent resistance.

The **aim** of the research described in this thesis is to study the structure-property relations of PTMO based segmented polyether(ester-amide)s (PEEA) with tetra-amide rigid segments. The influence of the rigid segment structure on the polymer properties is intensively studied. The rigid segment structure can be varied by the number of methylene groups, aliphatic or aromatic character and the number of hydrogen bonding groups.

The synthesis of the tetra-amide rigid segments is described in **Chapter 2**. The bisester tetra-amide units were prepared from aliphatic diamines with x = $(CH_2)_n$ (n = 4 - 10), dimethyl terephthalate (T) and or dimethyl adipate (A). The first step was the synthesis of the diamine-diamide xTx or xAx. The second step was the reaction of the diamine-diamide with methyl phenyl terephthalate (MPT) to TxTxT- and TxAxT-dimethyl. The structure of the tetra-amide units was confirmed with NMR. The melting temperature of these units increases with decreasing x and the melting temperature of TxTxT are 50 °C higher than the corresponding TxAxT units.

In **Chapter 3** poly(tetramethylene oxide) based polyether(ester-amide)s (PEEA) having uniform tetra-amide segments are described. PEEA's with uniform crystallisable tetra-amide segments are transparent semi-crystalline TPE's with a low T_g, temperature independent rubbery plateau and sharp melting temperature. The tetra-amide segment (T6A6T) is based on adipic acid (A), terephthalic acid (T) and hexamethylene diamine (6). The rigid amide segments form crystalline ribbons with a thickness of 3.5 nm in the polyether matrix. The

crystallinity of the tetra-amide segments in the copolymers was about 80 - 90%. With increasing content of crystallisable segment in the copolymer (3 – 44 wt%), the G'-modulus at room temperature increases from 1 to 102 MPa. This strong increase in modulus with amide content can be approximated using a model for fibre reinforced polymers. The melting temperatures of the copolymers decrease with increasing ether content and this can be explained by the solvent effect proposed by Flory.

In **Chapter 4** the tensile and elastic properties of the polymers from chapter 3 with emphasis on $PTMO_{2000}$-T6A6T were studied as a function of temperature and relaxation time. Temperature has a strong influence on the tensile properties of these PEEA copolymers. The yield stress, yield strain, fracture stress and fracture strain decrease with increasing temperature. However, the E-modulus was temperature independent in the range of 20 – 110 °C, which implies that the morphology of the polymers does not change within this temperature range. The yield stress as a function of temperature could be fitted with the Eyring relationship. At room temperature, strain hardening due to the crystallisation of $PTMO_{2000}$ segments takes place, thereby increasing the ultimate tensile properties. The elastic properties of these polymers decrease with increasing temperature. At strains below the yield strain the tensile set deformation was almost completely viscoelastic in nature. Stress relaxation measurements showed two processes, a fast initial decay in the first 10 seconds and a second slower relaxation process. The normalised stress relaxation values of this second process were independent of strain and modulus of the system.

Chapter 5 describes the solution/melt route and melt polymerisation synthesis of copolymers based on PTMO and tetra-amide units. Solution/melt polymerisation resulted in higher molecular weights but the melt synthesised copolymers were less coloured. Melt polymerisation is well possible if the melting temperature of the used bisester tetra-amide was less than 260 °C. All the copolymers had a low T_g, an almost temperature independent rubbery plateau and a sharp melting transition. These segmented copolymers have a two-phase structure: a continuous polyether phase with a low T_g and a dispersed crystalline amide phase. The degree of crystallinity of the rigid segments in these copolymers as determined by DCS and FT-IR was very high, on average 80 - 90%.

The type of tetra-amide had an effect on the T_m of the copolymer and somewhat on the rubber modulus. A more aliphatic character of the rigid segment decreased the T_m and the rubber modulus of the polymer. The start of the rubbery plateau (T_{flex}) is influenced by the length of

the PTMO segment. The copolymers with $PTMO_{1000}$ have the lowest T_{flex} of -15 °C. Longer blocks than $PTMO_{1000}$ can crystallise and thereby increasing the T_{flex}, while $PTMO_{650}$ copolymers have a small extra phase at 0 °C.

In **Chapter 6** the influence of the polydispersity of the rigid segment on the polymer properties is studied. Polyether(ester-amides) (PEEA) based on $PTMO_{2000}$ and uniform T6A6T were compared with PEAA's having polydisperse amide segments. The polymer with uniform crystallisable segments crystallises fast, has an almost temperature independent rubbery plateau, a low compression set and a low tensile set. Polymers with polydisperse amide segments crystallise slower, have a lower rubber modulus and a higher T_{flex} compared to the polymer with uniform amide segments. Also the elastic properties of the copolymers decrease with increasing polydispersity of the rigid segments. One copolymer was made via a one pot polymerisation and this copolymer had a "random" distribution of amide sequence length. In general, the copolymers with random amide segments have inferior properties compared with the properties of copolymers with mixtures of uniform amide segments.

The synthesis and characterisation of segmented copolymers based on non hydrogen bonding crystallisable amide based segments of uniform length and poly(tetramethylene oxide) segments is reported in **Chapter 7**. The non hydrogen bonding segments are based on alternating terephthalic acid and piperazine units connected through amide bonds which are not able to form hydrogen bonds (TPTPT). Poly(tetramethylene oxide) with a segment length of 1000 and 2000 g·mol^{-1} were reacted with pre-synthesised TPTPT. The resulting segmented copolymers had a low glass transition temperature (T_g, -70 °C), moderate modulus (G', 10 - 33 MPa) and high melting temperatures (185 - 220 °C). The rubber modulus of the plateau region of the segmented copolymers is almost temperature independent due to the presence of uniform crystallisable segments. The rubber moduli, yield stress and elasticity of these copolymers are lower compared to those of segmented copolymers which are able to form hydrogen bonds.

Polyether(urethane-urea-amide)s elastomers with monodisperse rigid segments are described in **Chapter 8**. The polyurethanes were synthesised from PTMO, a uniform diamine-diamide (6A6) extender and a diisocyanate (DI). The diisocyanate was either 4,4'-diphenylmethane diisocyanate (MDI), 2,4-toluene diisocyanate (2,4-TDI) or 1,6-hexanediisocyanate (HDI). Polyurethanes with monodisperse rigid segments (DI-6A6-DI) have a low glass transition

temperature, an almost temperature independent rubbery plateau and a sharp melting temperature. The degrees of crystallinity of the amide groups in the rigid segment determined by FTIR were 70 - 80% before heating and 40 - 60% after cooling. The rate of crystallisation (T_m - T_c) was moderately fast (36 - 54 °C). The polyurethanes based on HDI have a much higher rubber modulus compared to the MDI and 2,4-TDI based polymers due to a higher degree of crystallinity and/or higher aspect ratio of the crystallites.

In **Chapter 9** the influence of different chain extenders in polyurethanes is studied. Polyurethanes with monodisperse rigid segment were synthesised form PTMO$_{1270}$, endcapped with 1,6-hexanediisocyanates (HDI), and a uniform chain extender. Three different types of uniform crystallisable chain extenders were used; -diamine-diamide, -diol-diamine and -diol-diester. The polyurethanes were tough, transparent and colourless to lightly yellow coloured. Polyurethanes with monodisperse rigid segments have a low glass transition temperature, an almost temperature independent rubbery plateau and a sharp melting temperature. The T_m of the polyurethanes decreased with the number of hydrogen bonding groups in the rigid segments (diamine-diamide > diol-diamide > diol-diester) and with a higher aliphatic character of the chain extender. The compression set of these polyurethanes was 14 - 42% and the polyurethanes with diamine-diamide chain extenders had the lowest compression set. The storage modulus at room temperature was dependent on the ease of packing of the rigid segments and only little on the amount of hydrogen bonding groups.

SAMENVATTING

Gesegmenteerde blokcopolymeren gebaseerd op poly(tetramethylene oxide) (PTMO) amorfe flexibele segmenten en gekristalliseerde stijve segmenten zijn thermoplastische elastomeren (TPE's). De flexibele segmenten vormen de continue amorfe fase met een lage T_g zodat het materiaal ook flexibel is bij lage temperaturen. De stijve segmenten kunnen kristalliseren en vormen daarbij linten in de lage T_g fase. Deze lamellen zijn zogeheten thermisch-reversibele fysische knooppunten die het materiaal dimensionele stabiliteit en oplosmiddelbestendigheid geven.

Het doel van het onderzoek beschreven in dit proefschrift is om de structuur-eigenschappen relatie te bestuderen van polyether(ester-amide)s gebaseerd op PTMO en tetra-amide segmenten. De invloed van de structuur van het stijve segment op de polymeer eigenschappen is intensief onderzocht. De structuur van het stijve segment is gevarieerd door; het aantal methyleen groepen te variëren, het karakter van het segment alifatisch of meer aromatisch en het aantal waterstofbrug vormende groepen te veranderen.

De synthese van het stijve tetra-amide eenheid is beschreven in **Hoofdstuk 2**. De bisester tetra-amide eenheden zijn opgebouwd uit alifatische diamines met $x = (CH_2)_n$ (n = 4 - 10), dimethyl tereftalaat (T) en/of dimethyl adipaat (A). Eerst wordt het diamine-diamide xTx of xAx eenheid gesynthetiseerd. Vervolgens wordt de diamine-diamide met methyl phenyl tereftalaat (MPT) gereageerd tot TxTxT- and TxAxT-dimethyl. De structuur van de tetra-amide eenheden is bevestigd met behulp van NMR metingen. Het smeltpunt van de tetra-amide neemt toe met afnemende x en de smelttemperatuur van TxTxT is 50 °C hoger dan die van TxAxT eenheden.

In **Hoofdstuk 3** zijn de synthese en de eigenschappen van poly(tetramethylene oxide) gebaseerde polyether(ester-amide)s (PEEA) met uniforme tetra-amide segmenten beschreven. PEEA's met uniforme kristalliseerbare segmenten zijn transparante semi-kristallijne TPE's en hebben een lage T_g, temperatuursonafhankelijk rubberplateau en een scherpe

smelttemperatuur. De tetra-amide (T6A6T) is gebaseerd op adipine zuur (A), tereftaal zuur (T) en hexamethyleen diamine (6). De stijve amide segmenten vormen kristallijne linten met een dikte van 3.5 nm in de polyether matrix. De kristalliniteit van het tetra-amide segment in de copolymeren is ongeveer 80 - 90%. Met toenemend gehalte kristalliseerbaar segment in het copolymeer (3 – 44 wt%), neemt de G'-modulus bij kamertemperatuur toe van 1 tot 102 MPa. Deze sterke toename van de modulus kan benaderd worden met een model voor vezelversterkte polymeren. De smelttemperatuur van de polymeren neemt af met toenemend ether gehalte van het copolymeer. Dit effect kan verklaard worden met de oplosmiddel-effect theorie van Flory.

In **Hoofdstuk 4** zijn de trek-rek en elastische eigenschappen bestudeerd van de polymeren uit Hoofdstuk 3, in het bijzonder van $PTMO_{2000}$-T6A6T. Deze eigenschappen zijn als functie van de temperatuur en relaxatie tijd bestudeerd. Temperatuur heeft een sterke invloed op de trek-rek eigenschappen van deze PEEA copolymeren. De vloeikracht, vloeirek, breukkracht en breukrek nemen af met toenemende temperatuur. De E-modulus was echter wel temperatuursonafhankelijk in het gemeten gebied van 20 tot 110 °C, wat suggereert dat de morfologie van het polymeer niet verandert binnen dit temperatuursgebied. De vloeikracht als functie van de temperatuur kan met de Eyring relatie beschreven worden. Bij kamertemperatuur kan strain hardening door rekkristallisatie van $PTMO_{2000}$ segmenten optreden, waarbij de ultieme rek eigenschappen toenemen. De elastische eigenschappen van deze polymeren nemen af met toenemende temperatuur. Bij rekken beneden de vloeirek is de deformatie die optreedt bij tensile set metingen bijna compleet viscoelastisch. Stress relaxatie metingen laten zien dat twee processen optreden, een snel verval in de eerste 10 seconden en een tweede langzamer relaxatie proces. De genormaliseerde stress relaxatie waarden van dit tweede proces zijn onafhankelijk van de opgelegde rek en van de modulus van de polymeren.

Hoofdstuk 5 beschrijft de oplossing/smelt route en de smelt polymerisatie synthese van copolymeren gebaseerd op PTMO en tetra-amide eenheden. Oplossing/smelt polymerisatie resulteert in polymeren met een hoger molgewicht maar de polymeren gemaakt in de smelt zijn minder verkleurd. Smelt polymerisatie is goed mogelijk wanneer de smelttemperatuur van de bisester tetra-amide eenheid beneden 260 °C is. Alle copolymeren hebben een lage T_g, een bijna temperatuursonafhankelijk rubber gebied en een scherpe smelt overgang. Deze copolymeren hebben een twee-fase structuur: een continue polyether fase met een lage T_g en een gedispergeerde kristallijne amide fase. De graad van kristallinieit van de stijve segmenten

in deze copolymeren, bepaald met DSC en FT-IR metingen, was zeer hoog (80 - 90%). Het type tetra-amide had een effect op de T_m van het copolymeer en een klein effect op de rubber modulus. Een meer alifatisch karakter van het stijve segment zorgde voor een afname van de T_m en de rubber modulus van het polymeer. De start van het rubbergebied (T_{flex}) wordt beïnvloed door de lengte van het PTMO segment. De copolymeren met $PTMO_{1000}$ hebben de laagste T_{flex} (-15 °C). Langere segmenten dan $PTMO_{1000}$ kunnen kristalliseren en daarbij neemt de T_{flex} toe, terwijl $PTMO_{650}$ copolymeren een kleine extra fase hebben bij 0 °C.

In **Hoofdstuk 6** is de invloed van de polydispersiteit van het stijve segment in het copolymeer op de polymeereigenschappen bestudeerd. Polyether(ester-amides) (PEEA) gebaseerd op $PTMO_{2000}$ en uniforme T6A6T segmenten worden vergeleken met PEAA's die polydisperse amide segmenten hebben. Het polymeer met uniforme kristalliseerbare segmenten kristalliseren snel, hebben een bijna temperatuursonafhankelijk rubber gebied, een lage compressie- en tensile set. Polymeren met een polydisperse verdeling van amide segmenten kristalliseren langzamer, hebben een lagere rubber modulus en een hogere T_{flex} vergeleken met polymeren met uniforme amide segmenten. Ook de elastische eigenschappen van de copolymeren nemen af met toenemende polydispersiteit van de stijve segmenten. Eén polymeer was gemaakt via een één-pot polymerisatie en dit polymeer had een "random" verdeling van de amide lengte. In het algemeen hebben de copolymeren met een random amide segment verdeling inferieure eigenschappen vergeleken met copolymeren met een menging van uniforme amide segmenten.

De synthese en karakterisering van gesegmenteerde copolymeren gebaseerd op niet waterstofbrug vormende kristalliseerbare segmenten met een uniforme lengte en poly(tetramethylene oxide) segmenten zijn beschreven in **Hoofdstuk 7**. De niet waterstofbrug vormende segmenten zijn gebaseerd op alternerende tereftaal zuur en piperazine eenheden (TPTPT). De tertiaire amide bindingen kunnen geen waterstofbruggen vormen. Poly(tetramethylene oxide) met een segment lengte van 1000 en 2000 g·mol^{-1} zijn gereageerd met van tevoren gesynthetiseerde TPTPT. De resulterende gesegmenteerde copolymeren hebben een lage glasovergangstemperatuur (T_g, -70 °C), matige rubber modulus (G', 10 - 33 MPa) en hoge smelt temperatuur (185 - 220 °C). De rubber modulus in het rubber gebied van de gesegmenteerde copolymeren is bijna temperatuursonafhankelijk door de uniforme kristalliseerbare segmenten. De rubber moduli, vloeikracht en elasticiteit van

deze copolymeren zijn lager vergeleken met die van gesegmenteerde copolymeren die in staat zijn om waterstofbruggen te vormen.

Polyether(urethane-urea-amide)s elastomeren met monodisperse stijve segmenten zijn beschreven in **Hoofdstuk 8**. De polyurethanen zijn gesynthetiseerd van PTMO, een uniform diamine-diamide (6A6) verlenger en een diisocyanaat (DI). De diisocyanaat was of 4,4'-difenylmethaan diisocyanaat (MDI), 2,4-toluene diisocyanaat (2,4-TDI) of 1,6-hexaandiisocyanaat (HDI). Polyurethanen met monodisperse stijve segmenten (DI-6A6-DI) hebben een lage glasovergangstemperatuur, een bijna temperatuursonafhankelijk rubber gebied en een scherpe smelttemperatuur. De kristallisatiegraad van de amide groepen in het stijve segmenten is met temperatuursafhankelijke FT-IR bepaald en is 70 - 80% voor verwarmen en 40 - 60% na afkoelen. De snelheid van kristallisatie (T_m - T_c) was gemiddeld snel (36 - 54 °C). De polyurethanen gebaseerd op HDI groepen hebben een veel hogere rubber modulus vergeleken met MDI en 2,4-TDI gebaseerde polymeren door een hogere kristallisatiegraad en/of een hogere aspect ratio van de kristallijne linten.

In **Hoofdstuk 9** is de invloed van verschillende keten verlengers in polyurethanen onderzocht op de polymeereigenschappen. Polyurethanen met monodisperse stijve segmenten zijn gesynthetiseerd van PTMO$_{1270}$ met 1,6-hexaandiisocyanaat (HDI) eindgroepen, en uniforme keten verlengers. Drie verschillende type uniforme kristalliseerbare keten verlengers zijn gebruikt; -diamine-diamide, -diol-diamine en -diol-diester. De polyurethanen zijn taai, transparant en kleurloos. Polyurethanen met monodisperse stijve segmenten hebben een lage glasovergangstemperatuur, een bijna temperatuursonafhankelijk rubber gebied en een scherpe smelt temperatuur. De T_m van de polyurethanen neemt af met het aantal waterstofbrug vormende groepen in het stijve segment (diamine-diamide > diol-diamide > diol-diester) en met een hoger alifatisch karakter van de keten verlenger. De compressie set van deze polyurethanen was 14 - 42% en de polyurethanen met diamine-diamide keten verlengers hadden de laagste compressie set. De rubber modulus bij kamertemperatuur is afhankelijk van hoe makkelijk de stijve segmenten pakken en niet zozeer van het aantal brugvormende groepen.

CURRICULUM VITAE

Edwin Biemond is geboren op 30 juli 1976 te Zevenaar. Na de lagere school "Albert Schweizer" heeft hij het atheneum aan het Liemers College te Zevenaar gevolgd. Hij heeft in 1995 eindexamen gedaan en begon in datzelfde jaar aan de studie Chemische Tenchnologie aan de Universiteit Twente. Zijn stage werd uitgevoerd bij het Forschungsinstitute van Daimler Chrysler in Ulm aan het onderwerp "LCP phase behaviour materials". Zijn afstudeeropdracht met de titel "PPE segmented copolymers having uniform tetra-amide units" is uitgevoerd bij de vakgroep Synthese en Technologie van Engineering Plastics (STEP) van Dr. R.J. Gaymans. In oktober 2001 studeerde hij af en begon 1 november 2001 met zijn promotieonderzoek in dezelfde STEP groep. Het onderzoek getiteld "Hydrogen bonding in segmented block copolymers" is uitgevoerd onder begeleiding van Dr. R.J. Gaymans en Prof. J. Feijen als promotor. Het promotie onderzoek was gericht om de invloed van waterstofbrug vorming tussen kristallijne segmenten in gesegmenteerde blokcopolymeren te onderzoeken.